

# **Development of Unidirectional Abrasive Flow Machine for Internal Finishing of Price Sensitive Industrial Components**

**Ph.D. Thesis**

**JAI KISHAN**  
**(2012RME9553)**



**DEPARTMENT OF MECHANICAL ENGINEERING**  
**MALAVIYA NATIONAL INSTITUTE OF TECHNOLOGY**  
**JLN MARG, JAIPUR-302017, INDIA**

**September, 2017**

# **Development of Unidirectional Abrasive Flow Machine for Internal Finishing of Price Sensitive Industrial Components**

A Thesis Submitted

in Partial Fulfilment of the Requirements for the Degree of

**DOCTOR OF PHILOSOPHY**  
in  
**MECHANICAL ENGINEERING**

by

**JAI KISHAN**

**(2012RME9553)**

Under the guidance of

**Dr. Harlal Singh Mali**



to the

**DEPARTMENT OF MECHANICAL ENGINEERING  
MALAVIYA NATIONAL INSTITUTE OF TECHNOLOGY  
JLN MARG, JAIPUR-302017, INDIA**

© Copyright by Jai Kishan 2017. All Rights Reserved



**Malaviya National Institute of Technology, Jaipur**

## **CANDIDATE'S DECLARATION**

I hereby certify that the thesis entitled “**Development of Unidirectional Abrasive Flow Machine for Internal Finishing of Price Sensitive Industrial Components**” submitted in partial fulfillment of the requirements for the award of **Doctor of Philosophy in Mechanical Engineering** to the **Malaviya National Institute of Technology, Jaipur** is an authentic record of research work carried out by me under supervision and guidance of Dr. Harlal Singh Mali. The work incorporated in this thesis has not been submitted elsewhere for the award of any degree.

**Jai Kishan**  
**(2012RME9553)**

This is to certify that the above statement made by the candidate is correct to the best of my knowledge.

**Signature of Supervisor**

**Dr. Harlal Singh Mali**

Assistant Professor

Department of Mechanical Engineering

Malaviya National Institute of Technology Jaipur

Jaipur- 302017, India.

**September-2017**



**Malaviya National Institute of Technology, Jaipur**

## **CERTIFICATE**

This is to certify that the thesis entitled "**Development of Unidirectional Abrasive Flow Machine for Internal Finishing of Price Sensitive Industrial Components**", submitted by **Jai Kishan (2012RME9553)** to **Malaviya National Institute of Technology, Jaipur**, is a record of bona fide research work under my supervision and I consider it worthy of consideration for the award of the degree of **Doctor of Philosophy** of the Institute.

**Signature of Supervisor**

**Dr. Harlal Singh Mali**

The Ph.D. viva voce examination of Mr. Jai Kishan has been conducted by the Oral Defense Committee (ODC) constituted by the Dean (Academic Affairs), as per 9.4.3, vide letter No. F.4(P) PhD/Acad/MNIT/2016/1661 dated 9 Aug 2017 on Friday, 8<sup>th</sup> September, 2017. The ODC declares that the student has successfully defended the thesis in the viva-voce examination.

**Dr. Harlal Singh Mali**

(Supervisor)

Assistant Professor

Department of Mechanical Engineering  
Malaviya National Institute of  
Technology Jaipur.

**Dr. Alakesh Manna**

(External Examiner)

Professor,

Department of Mechanical Engineering,  
PEC University of Technology, Sector-12  
Chandigarh-160012, U.T, India.

## **ACKNOWLEDGEMENT**

---

I take this opportunity to express my deep sense of gratitude to my esteemed thesis supervisor Dr. Harlal Singh Mali, for his discerning and uncompromising help in completing my thesis.

His expert guidance on subject, constructive criticism, encouragement and inspiring advices allow me to think different dimensions of research and realize value of hard work and investigating approach. The technical and personal lesson that I learned by working under him are now foundation pillars for my rest of life.

I am thankful to my parents for giving me freedom to choose my carrier path and support my thinking. I am indebted to them for their constant encouragement to pursue my dreams.

I thankfully acknowledge the financial aid provided by the Department of Science & Technology, Govt. of India, for DST Project No. SR/FTP/ETA-0078/2011 Dated 17/09/2012 entitled Design & development of low cost one way Abrasive Flow Machine (AFM) utilising pulp & fullers' earth based media has been invaluable, for which I am grateful to Govt. of India.

I am also thankfully acknowledge Pushup Tools Udyog Ltd, Rohtak, for arranging industrial components for the research work.

I thank the Malaviya National Institute of Technology (MNIT), Jaipur for supporting my research by providing the research scholarship and to the Advanced Manufacturing and Mechatronics Lab and Materials Research Centre for providing the facilities and support, without which the present work would not be possible. I would like to thank Head of the Department of Mechanical Engineering and all faculty, and staff members of the Department

of Mechanical Engineering, Materials Research Centre, and various other departments in MNIT Jaipur for their help and support in the direct or indirect way throughout my time in MNIT Jaipur.

I like to express heartfelt thanks to all my Ph.D. colleagues especially Dr. Deepak Unune, Ajit Singh, Bhargav Prajwal Pathri and Rupali Baghel for their constant support, love, and encouragement, and for all time we spend together here in MNIT Jaipur. I like to thank all my lab mates Nick Lennon, Divyanshu Gupta, Jugal Kishor, Deepa Ram, Jitendra, Jasa Ram, Priyanshu Singh, Vishal Garg, Sandeep Tiwari, Arjun Yadav and Pawan Sahu for their cooperation and support. I would also like to thank lab technicians Sandeep Thakur and Dipak Kumar for their assistance.

Jai Kishan

## **Abstract**

---

Surface finish is very critical factor for deciding the service life of a wide variety of components. Surface finish influences the fatigue strength because the uneven and rough surfaces usually lead to inferior fatigue properties resulting in early failure of the component. Uneven and rough surfaces develop stress concentration at mating parts and may lead to crack development over the surfaces. High surface quality of the components is also important to ensure interchangeability of components. Therefore, finishing is a vital processing technique for enhancing the surface qualities of components to ensure their desired performance. Various traditional finishing processes such as grinding, honing, lapping, etc. are being used for finishing of components. In these processes, a very small amount of material is removed by loose or bonded abrasives to smoothen the surface with close tolerances. However, each of the traditional finishing processes has a major limitation about the shape and size of a part that they can finish. For example in grinding, the generation of large amount of heat results in defects such as micro-cracks, heat affected zone, thermal residual stresses, etc. Honing is useful for cylindrical surfaces, while lapping is suitable mainly for flat surfaces. Though, Abrasive Flow Finishing (AFF) processes have wide range of applications and could be used in most of the shop floors for finishing of components leading to their better performance but its usage are limited owing to high running costs associated with them. Therefore, currently available AFF processes are uneconomical in small scale industries (SSIs), finishing price sensitive components in developing countries. Hence, these SSIs are finishing the components manually which results in non-consistencies, waste of material and difficulty in finishing of complicate/intricate surfaces. Though some industries can afford costly Abrasive Flow Machine (AFM), they face

the pinch of the high recurring cost of media and available AFM media is also not environmentally sustainable. Therefore, a research focusing the development of low-cost alternative environmentally sustainable media and low cost AFM setup meeting SSIs needs is very essential.

The media in AFM process acts as a flexible grinding tool during the finishing processes. AFM media generally consists of two main constituents – the carrier (a viscoelastic base material, e.g. polymers, gels and oils) and the solid parts (abrasives and additives to support the abrasives). As efforts were made in improving the performance of AFF processes, research is also being done to synthesize better AFM media. The physical (appearance), chemical (ingredients and their quantity in the base carrier, inertness, etc.) and rheological properties (apparent viscosity, shear stress, yield stress, thixotropic, critical strain, critical temperature, etc.) of AFM media considerably affects the overall performance of the AFF process.

The present research work attempts the improvement in environ-friendly AFM media and development of low cost AFM setup for finishing complicated price sensitive industrial components. Rheological and other characterization of AFM media with different base and additive gels, along with their effect on precision finishing in AFM are studied during rheological experiments. The rheological properties of synthesized media are studied and characterized using FTIR, TGA, and SEM. The major ingredients of Polymer Abrasive Gel (PAG) based AFM media used here are abrasives, polymer base and liquid synthesizer.

Fourier transform infrared spectroscopy (FTIR) is used for detecting functional groups and characterizing C-H bonding information of PAG media. In PAG media, Alkenes, Esters, amines and aromatic groups are more dominating which provides the elastic nature, thermal



stability and tensile strength to the media. Thermogravimetric analysis (TGA) is measured as a function of increasing temperature (with constant heating rate), or as a function of time (with constant temperature and/or constant mass loss). TGA results signify that the PAG media can be used in AFM for finishing for temperature rise up to critical limit of media. SEM images of PAG media samples shows that polymeric chains along with liquid synthesizer molecules holds the abrasive grain and assists in finishing process. Abrasives grains have sharp cutting edges which helps in material removal of work piece surface which is to be finished. For study of rheological properties of viscoelastic fluids mainly Power Law, Bingham Plastic and Herschel–Bulkley model have extensive use in the analysis of the flow behavior and simulation. The model values are derived for all samples of PAG media for its rheology properties. The correlation coefficient ( $R^2$ ) was derived to find the usefulness of these fluid models. The rheological properties of commercially available media (streamer) were also evaluated to compare it with PAG media. For development of unidirectional abrasive flow machine, initially, the mechanism and concept of computer aided design was realised by a 3D printed AFM setup referred as micro unidirectional abrasive flow machine (MUAFM). After successive results it was revealed that, MUAFM setup can be used as replacement of hand polishing method of finishing in price sensitive industry. After successful trial on MUAFM, a production grade unidirectional abrasive flow machine (UAFM) was designed and fabricated for finishing internal surfaces.

The same mechanism of MUAFM was used in design and development of UAFM setup. After successful fabrication of designed UAFM setup, trial experiments are performed to observe the effect of finishing variables [extrusion pressure (A), finishing time (B) and viscosity (C)] on finishing performance variables [improvement in surface roughness ( $\Delta Ra$ )

and material removal (MR)].

For detailed experimentations, response surface methodology was used to observe the effect of finishing variables i.e. extrusion pressure, finishing time and viscosity on performance variables i.e. improvement in surface roughness ( $\Delta Ra$ ) and material removal during finishing of price sensitive industrial components (Trim die and Stamping die). After experimentation, analysis of variance (ANOVA) is executed to statistically investigate the results of the selected model. Significant control factors were recognized and interaction effects of these control factors on performance measures were studied using response surface graphs. SEM analysis is used to observe the surface condition before and after finishing the trim die surface and results show the enhancement in surface quality after finishing with UAFM setup and PAG media. For validation of experimental outcomes, mathematical model results were compared with the experimental results for material removal (MR). Two additional studies are also performed for component specific finishing consultancy for tool & die industry using the developed UAFM setup and PAG media.

Experimentation results of 3D printer nozzle shows that the maximum improvement in surface roughness achieved and material removal is 0.92  $\mu m$  and 136 mg respectively. UAFM setup and PAG media is utilized for improvement of glass mold internal surface at low cost. After experiments, lowest surface roughness value obtained after finishing is 0.61  $\mu m$  and maximum material removal was 4 gm.

# Table of Contents

|  |      |
|--|------|
| <b>ACKNOWLEDGEMENT</b> .....   | i    |
| <b>Abstract</b> .....  | iii  |
| <b>List of figures</b> .....   | xi   |
| <b>List of tables</b> .....  | xv   |
| <b>Nomenclature</b> .....  | xvii |
| <b>Chapter 1 Introduction</b> .....  | 1    |
| 1.1 Conventional finishing process .....   | 1    |
| 1.1.1 Grinding .....   | 1    |
| 1.1.2 Honing.....  | 2    |
| 1.1.3 Lapping .....  | 2    |
| 1.2 Need and importance of advanced finishing processes .....                              | 2    |
| 1.3 Challenges in abrasive flow finishing of components.....                               | 3    |
| 1.3.1 Cost effectiveness of consumables.....   | 3    |
| 1.3.2 Acceptance across industries.....  | 4    |
| 1.3.3 Tooling design.....  | 4    |
| 1.3.4 Environmental issues .....   | 5    |
| 1.4 Organization of thesis .....   | 5    |
| <b>Chapter 2 Literature Review</b> .....   | 7    |
| 2.1 Overview.....  | 7    |
| 2.1.1 Introduction to AFM .....  | 7    |
| 2.1.2 Classification of AFM processes .....  | 7    |
| 2.1.3 Mechanism of material removal.....   | 9    |
| 2.2 Literature survey .....  | 10   |
| 2.2.1 Process parameters and their influence on quality characteristics .....              | 10   |
| 2.2.2 Process modelling and optimization in abrasive flow finishing process.....           | 15   |
| 2.2.3 Developments in abrasive flow finishing media .....                                  | 23   |
| 2.2.4 Advancements in AFF processes through hybridizing it with other processes.....       | 30   |
| 2.2.5 Recent advances in abrasive flow finishing processes.....                            | 34   |
| 2.2.6 Development on finishing of hard materials and different work piece geometries:..... | 39   |
| 2.3 Research gap .....   | 41   |
| 2.4 Objective and scope of present work.....   | 42   |
| <b>Chapter 3 Characterization and Rheological Study of PAG</b> .....                       | 43   |
| 3.1 Introduction.....  | 43   |
| 3.1.1 Importance of rheology.....  | 46   |

|  |            |
|--|------------|
| 3.1.2 Test equipment.....  | 47         |
| 3.2 Synthesization of PAG.....   | 48         |
| 3.3 Characterization of PAG.....   | 49         |
| 3.3.1 FESEM analysis.....  | 49         |
| 3.3.2 FTIR analysis.....   | 52         |
| 3.3.3 TGA.....   | 54         |
| 3.4 Rheological study.....   | 58         |
| 3.4.1 Power law fluid:.....  | 58         |
| 3.4.2 Bingham plastic model:.....  | 59         |
| 3.4.3 Hershel bulkley model:.....  | 60         |
| 3.4.4 Correlation coefficient of fluid models:.....                                  | 60         |
| 3.4.5 Optimization of media variables for rheology control.....                      | 62         |
| 3.5 Comparative study of PAG and streamer for characterization.....                  | 70         |
| 3.5.1 Characterization of AFM Media.....   | 71         |
| 3.5.2 PAG media preparation.....   | 71         |
| 3.5.3 Rheological analysis.....  | 71         |
| 3.5.4 TGA.....   | 72         |
| 3.5.5 FTIR Analysis.....   | 73         |
| 3.6 Performance study of PAG and streamer.....                                       | 75         |
| 3.6.1 Design of experiment.....  | 75         |
| 3.6.2 Results and discussion.....  | 77         |
| <b>Chapter 4 Design and Development of Unidirectional Abrasive Flow Machine.....</b> | <b>83</b>  |
| 4.1 Introduction.....  | 83         |
| 4.2 Design & development of MUAFM.....   | 84         |
| 4.2.1 Major components of MUAFM:.....  | 84         |
| 4.2.2 Fabrication of MUAFM.....  | 88         |
| 4.3 Design & development of UAFM.....  | 90         |
| 4.3.1 Major Components of UAFM.....  | 90         |
| 4.3.2 Development of UAFM.....   | 100        |
| 4.3.3 Summary of raw material used for developed UAFM setup.....                     | 102        |
| <b>Chapter 5 Experiment Methodology.....</b>   | <b>103</b> |
| 5.1 Machine tools.....   | 103        |
| 5.1.1 Unidirectional abrasive flow machine (UAFM).....                               | 103        |
| 5.1.2 Bidirectional abrasive flow machine (Micro Technica BL 100 D).....             | 104        |
| 5.1.3 Workpiece material.....  | 105        |

|                       |  |            |
|-----------------------|--|------------|
| 5.1.4                 | AFM media .....  | 106        |
| 5.2                   | Measuring instruments .....                              | 106        |
| 5.3                   | Design of experiment .....                               | 107        |
| 5.4                   | Scheme of experimentation .....                          | 107        |
| 5.5                   | Preliminary study .....                                  | 108        |
| 5.5.1                 | Control factors and their range.....                     | 108        |
| 5.5.2                 | Taguchi based experimental design .....                  | 109        |
| 5.6                   | Detailed experiments.....                                | 110        |
| 5.6.1                 | Control factors and their range.....                     | 111        |
| 5.6.2                 | Response surface method based experimental design.....   | 112        |
| <b>Chapter 6</b>      | <b>Experimentation, Results and Discussion .....</b>     | <b>115</b> |
| 6.1                   | Preliminary experiments.....                             | 115        |
| 6.1.1                 | Preliminary experimental results.....                    | 115        |
| 6.1.2                 | Discussion on preliminary results .....                  | 116        |
| 6.1.3                 | Parametric effect on response variables .....            | 119        |
| 6.2                   | Detailed experimentations .....                          | 125        |
| 6.2.1                 | Abrasive flow finishing of trim die components.....      | 125        |
| 6.2.2                 | Abrasive flow finishing of stamping die components.....  | 139        |
| <b>Chapter 7</b>      | <b>Mathematical Modelling and Validation .....</b>       | <b>154</b> |
| 7.1                   | Introduction.....  | 154        |
| 7.2                   | Modelling of material removal.....                       | 155        |
| 7.2.1                 | Material Removal.....                                    | 157        |
| 7.3                   | Control factors and their range.....                     | 162        |
| 7.4                   | Comparison of theoretical and experimental results ..... | 162        |
| 7.4.1                 | Effect of extrusion pressure on material removal.....    | 163        |
| 7.4.2                 | Effect of finishing time on material removal .....       | 165        |
| 7.4.3                 | Effect of viscosity on material removal .....            | 166        |
| <b>Chapter 8</b>      | <b>Conclusions and Future Scope.....</b>                 | <b>169</b> |
| 8.1                   | Conclusion .....   | 169        |
| 8.1.1                 | Contribution in AFF technology .....                     | 172        |
| 8.2                   | Future work .....  | 173        |
| 8.2.1                 | Glass mold finishing .....                               | 173        |
| 8.2.2                 | 3D Printer nozzle finishing .....                        | 177        |
| <b>References</b>     | .....  | <b>185</b> |
| <b>Appendix-A (1)</b> | <b>Extruding element .....</b>                           | <b>199</b> |

|  |     |
|--|-----|
| <b>Appendix-A (2) Screw feeder</b> .....                     | 200 |
| <b>Appendix-A (3) Rotor</b> .....                            | 201 |
| <b>Appendix-A (4) Split tooling</b> .....                    | 202 |
| <b>Appendix-A (5) Tooling washer</b> .....                   | 203 |
| <b>Appendix-B (1) UAFM-Screw feeder</b> .....                | 205 |
| <b>Appendix-B (2) Flange -Tooling</b> .....                  | 206 |
| <b>Appendix-B (3) Flange-Reducer</b> .....                   | 207 |
| <b>Appendix-B (4) Extruding element</b> .....                | 208 |
| <b>Appendix-B (5) Recycling pipe</b> .....                   | 209 |
| <b>Appendix-B (6) Reducer</b> .....                          | 210 |
| <b>Appendix-B (7) Rotor</b> .....                            | 211 |
| <b>Appendix-B (8) Stator</b> .....                           | 212 |
| <b>Appendix-C Design specification of UAFM system</b> .....  | 213 |
| <b>Appendix-D Viscosity grade and cost comparison</b> .....  | 215 |
| <b>Appendix-E TGA graphs for PAG samples</b> .....           | 217 |
| <b>Appendix-F SEM images of PAG samples</b> .....            | 227 |
| <b>Appendix-G Experiments on MUAFM</b> .....                 | 233 |
| <b>Appendix H Results for Modelling and Validation</b> ..... | 241 |
| <b>List of the publications based on this research</b> ..... | 243 |

## List of figures

---

|   |    |
|---|----|
| Figure 2.1 (a) Schematic of one way AFF (b) Working principle of two way AFF (c) Orbital AFF .....                              | 8  |
| Figure 2.2 Recent development in abrasive flow finishing media .....  | 23 |
| Figure 2.3 Recent development in abrasive flow finishing process .....  | 34 |
| Figure 3.1 Rotational Rheometer with temperature control.....   | 47 |
| Figure 3.2 Nomenclature of developed Polymer Abrasive Gel (PAG).....  | 48 |
| Figure 3.3 SiC abrasive 120 Mesh Size .....   | 50 |
| Figure 3.4 SiC abrasive 220 Mesh size .....   | 50 |
| Figure 3.5 SiC abrasive 320 Mesh Size .....   | 50 |
| Figure 3.6 FESEM Images of developed PAG showing interference of abrasives and base.....  | 51 |
| Figure 3.7 FTIR analysis of developed alternative Polymer Abrasive Gel.....   | 53 |
| Figure 3.8 TGA graphs of different PAG sample .....   | 55 |
| Figure 3.9 SN ratio for critical temperature .....  | 58 |
| Figure 3.10 Fitting the constitutive model equations to actual experimental data (run. 15).....                                 | 62 |
| Figure 3.11 SN ratio for yield stress .....   | 66 |
| Figure 3.12 SN ratio graph for viscosity .....  | 66 |
| Figure 3.13 Effect of polymer abrasive gel variables on viscosity .....   | 67 |
| Figure 3.14 Rheological behaviour of PAG and commercial media (streamer) .....  | 72 |
| Figure 3.15 TGA graphs between weight loss % and temperature for both AFM media .....   | 73 |
| Figure 3.16 FTIR for streamer and PAG media.....  | 74 |
| Figure 3.17 Bidirectional abrasive flow machine for finishing workpiece .....   | 76 |
| Figure 3.18 Tooling of holding stamping die component .....   | 76 |
| Figure 3.19 Effects of extrusion pressure on surface roughness improvement. (Finishing time 35 min and medium viscosity).....   | 77 |
| Figure 3.20 Effects of extrusion pressure on material removal. (Finishing time 35 min and medium viscosity).....                | 78 |
| Figure 3.21 Effects of finishing time on surface roughness improvement (extrusion pressure 30 bar and medium viscosity).....    | 79 |
| Figure 3.22 Effects of finishing time on material removal (extrusion pressure 30 bar and medium viscosity).....                 | 79 |
| Figure 3.23 Effects of viscosity on surface roughness improvement (finishing time 35 minute and extrusion pressure 40 bar)..... | 80 |
| Figure 3.24 Effects of viscosity on material removal (finishing time 35 minute and extrusion pressure 40 bar).....              | 80 |
| Figure 4.1 Extruder with hopper .....   | 85 |
| Figure 4.2 Sectional view of rotor and stator design.....   | 85 |
| Figure 4.3 Geometry of displacement element .....   | 86 |
| Figure 4.4 Fabricated rotor and stator parts of MUAFM .....   | 86 |
| Figure 4.5 Sectional view of tooling for holding the workpiece (i.e. wire drawing die) .....                                    | 87 |
| Figure 4.6 Fabricated tooling unit for holding the workpiece (i.e. wire drawing die) .....                                      | 88 |
| Figure 4.7 2D Sketch with dimension (in mm) of MUAFM.....   | 89 |
| Figure 4.8 Fabricated micro unidirectional abrasive flow machine (MUAFM) .....  | 89 |
| Figure 4.9 Sectional view of hopper and screw feeder .....  | 90 |
| Figure 4.10 Dimensions (in mm) of hopper and screw feeder.....  | 91 |

|  |     |
|--|-----|
| Figure 4.11 Dimensions of rotor and stator in UAFM.....  | 91  |
| Figure 4.12 Sectional view of flange for recycling unit with dimensions .....  | 92  |
| Figure 4.13 CAD model of flange for UAFM .....   | 92  |
| Figure 4.14 Cad model of Reducer (with dimensions) .....   | 92  |
| Figure 4.15 Recycling unit for flow of media in hopper.....  | 93  |
| Figure 4.16 Electric motor with gear unit .....  | 93  |
| Figure 4.17 Variable frequency drive .....   | 94  |
| Figure 4.18 Strain gauge based pressure sensor and data logger.....  | 95  |
| Figure 4.19 Sketch with dimension (in mm) of mounting base.....  | 95  |
| Figure 4.20 (a) HSS trim die (b) Tooling scheme (c) Dimensions of tooling (Left and right part).....   | 96  |
| Figure 4.21 Sectional view of tooling for trim die.....  | 96  |
| Figure 4.22 (a) UAFM without nylon tooling (b) Tooling fixed with trim die (c) Left and right part of tooling .....                          | 97  |
| Figure 4.23 (a) HSS stamping die (mm) (b) Tooling scheme (c) Dimensions of tooling (Left and right part) .....                               | 98  |
| Figure 4.24 Sectional view of tooling for stamping die.....  | 98  |
| Figure 4.25 (a) Tooling fixed with stamping die (b) Left and right part of tooling.....  | 98  |
| Figure 4.26 CAD model of designed tooling.....   | 99  |
| Figure 4.27 Nylon tooling for holding the stamping die in commercial AFM .....   | 100 |
| Figure 4.28 Assembled cad model of unidirectional abrasive flow machine .....  | 100 |
| Figure 4.29 2D sketch with dimension (in mm) of UAFM.....  | 101 |
| Figure 4.30 Images of fabricated unidirectional abrasive flow machine (UAFM) setup.....  | 101 |
| Figure 5.1 Fabricated unidirectional abrasive flow machine setup.....  | 103 |
| Figure 5.2 Bidirectional abrasive flow machine (Micro Technica BL100D) .....   | 105 |
| Figure 6.1 Signal to Noise ratio graphs for improvement in surface roughness ( $\Delta Ra$ ).....  | 117 |
| Figure 6.2 Signal to Noise ratio graphs for material removal (MR).....   | 118 |
| Figure 6.3 Effect of extrusion pressure.....   | 119 |
| Figure 6.4 Effect of finishing time.....   | 120 |
| Figure 6.5 Effect of viscosity on improvement in surface roughness .....   | 121 |
| Figure 6.6 Effect of extrusion pressure on material removal.....   | 122 |
| Figure 6.7 Effect of finishing time on material removal.....   | 123 |
| Figure 6.8 Effect of viscosity on material removal.....  | 124 |
| Figure 6.9 Predicted and actual responses for improvement in surface roughness and material removal. ....                                    | 129 |
| Figure 6.10 Perturbation plots for $\Delta Ra$ .....   | 131 |
| Figure 6.11 Response 3D surface plot demonstrating the interactive influence of finishing time and extrusion pressure for $\Delta Ra$ . .... | 131 |
| Figure 6.12 Response 3D surface plot demonstrating the interactive influence of finishing time and viscosity for $\Delta Ra$ .....           | 132 |
| Figure 6.13 Perturbation graph for MR .....  | 133 |
| Figure 6.14 Response 3D surface plot demonstrating the interactive influence of finishing time and extrusion pressure for MR .....           | 133 |
| Figure 6.15 Response 3D surface plot demonstrating the interactive influence of viscosity and extrusion pressure for MR .....                | 134 |
| Figure 6.16 Response 3D surface plot demonstrating the interactive influence of viscosity and finishing time for MR .....                    | 134 |
| Figure 6.17 Percentage contribution of AFM variables on MR and $\Delta Ra$ .....   | 136 |



|  |     |
|--|-----|
| Figure 6.18 SEM images of trim die before and after finishing.....   | 138 |
| Figure 6.19 XRD results of finished workpiece.....   | 139 |
| Figure 6.20 Predicted and actual responses for improvement in surface roughness and material removal.....                                      | 143 |
| Figure 6.21 Perturbation plots for $\Delta Ra$ .....   | 145 |
| Figure 6.22 Response 3D surface plot demonstrating the interactive influence of finishing time and extrusion pressure for $\Delta Ra$ .....    | 145 |
| Figure 6.23 Response 3D surface plot demonstrating the interactive influence of extrusion pressure and viscosity for $\Delta Ra$ .....         | 146 |
| Figure 6.24 Response 3D surface plot demonstrating the interactive influence of extrusion pressure and viscosity for $\Delta Ra$ .....         | 146 |
| Figure 6.25 Perturbation graph for MR.....   | 148 |
| Figure 6.26 Response 3D surface plot demonstrating the interactive influence of finishing time and extrusion pressure for MR.....              | 148 |
| Figure 6.27 Response 3D surface plot demonstrating the interactive influence of viscosity and extrusion pressure for MR .....                  | 149 |
| Figure 6.28 Response 3D surface plot demonstrating the interactive influence of viscosity and finishing time for MR.....                       | 149 |
| Figure 6.29 Percentage contribution of AFM variables on MR and $\Delta Ra$ .....   | 151 |
| Figure 6.30 SEM images of stamping die surface before and after finishing .....  | 152 |
| Figure 6.31 XRD results of finished stamping die surface .....   | 153 |
| Figure 7.1 Schematic diagram of spherical geometry of abrasive grit during material removal process in AFM.....                                | 155 |
| Figure 7.2 Cylindrical shape work piece.....   | 158 |
| Figure 7.3 Flow chart for Material Removal.....  | 161 |
| Figure 7.4 Comparison of theoretical and experimental material removal with extrusion pressure at finishing time constant (40 minute) .....    | 164 |
| Figure 7.5 Comparison of theoretical and experimental material removal with extrusion pressure keeping viscosity constant (Medium Grade) ..... | 164 |
| Figure 7.6 Comparison of theoretical and experimental material removal with finishing time keeping extrusion pressure constant (22 bar). ..... | 165 |
| Figure 7.7 Comparison of theoretical and experimental material removal with finishing time keeping viscosity constant (medium grade).....      | 166 |
| Figure 7.8 Comparison of theoretical and experimental material removal with viscosity keeping finishing time constant (40 minute). .....       | 166 |
| Figure 7.9 Comparison of theoretical and experimental material removal with viscosity keeping extrusion pressure constant (22 bar) .....       | 167 |
| Figure 8.1 Steps for tooling design and fabrication .....  | 174 |
| Figure 8.2 Actual photograph and schematic view .....  | 174 |
| Figure 8.3 Photograph of UAFM setup with tooling holding the glass mold .....  | 175 |
| Figure 8.4 Images of glass mold M1 before AFM and after AFM .....  | 177 |
| Figure 8.5 Images of glass mold M2 before AFM and after AFM .....  | 178 |
| Figure 8.6 Steps for tooling design and fabrication .....  | 178 |
| Figure 8.7 3D printer nozzle component.....  | 179 |
| Figure 8.8 Sectional view of CAD model for tooling .....   | 179 |
| Figure 8.9 Signal to noise ratio for improvement in surface roughness ( $\Delta Ra$ ) .....  | 181 |
| Figure 8.10 Signal to noise ratio for material removal (MR).....   | 182 |

Figure 8.11 Images of nozzle surfaces..... 183

## List of tables

---

|   |     |
|---|-----|
| Table 2.1 Summary of experimental work on AFF process parameters and their influence on output response.....                    | 13  |
| Table 2.2 Physical AFF models in mathematical equations for abrasive flow finishing process .....                               | 17  |
| Table 2.3 Optimization of process variables of abrasive flow finishing process .....  | 21  |
| Table 2.4 Cost comparison of alternative developed polymer abrasive gel with commercial available AFM media.....                | 28  |
| Table 2.5 Physical properties of commercial AFM media [47]. .....   | 30  |
| Table 2.6 Advancements in AFF processes through hybridizing it with other processes .....                                       | 31  |
| Table 3.1 Technical Specifications .....  | 48  |
| Table 3.2 Different weight percentage of constitutes of polymer abrasive gel .....  | 49  |
| Table 3.3 Coded levels and corresponding actual values of control factors .....   | 54  |
| Table 3.4 Critical temperature for different PAG .....  | 56  |
| Table 3.5 ANOVA results after experimentation.....  | 57  |
| Table 3.6 Rheological variable for three selected model .....   | 61  |
| Table 3.7 Experimental design.....  | 63  |
| Table 3.8 Plan of experiment and experimental results for viscosity and yield stress of polymer abrasive gel.....               | 64  |
| Table 3.9 ANOVA table after model reduction for viscosity. ....   | 65  |
| Table 3.10 ANOVA table after model reduction for yield stress.....  | 69  |
| Table 3.11 Experimental setting .....   | 75  |
| Table 5.1 Specifications of UAFM .....  | 104 |
| Table 5.2 Specifications of Bidirectional AFM-BL 100 D.....   | 104 |
| Table 5.3 Percentage proportions of basic elements in trim die workpiece material .....   | 105 |
| Table 5.4 Percentage proportions of basic elements in stamping die workpiece material.....                                      | 105 |
| Table 5.5 Experimental control factors and their levels.....  | 108 |
| Table 5.6 Taguchi experimental design of L <sub>9</sub> orthogonal array.....   | 110 |
| Table 5.7 Input variables and their levels .....  | 111 |
| Table 5.8 Experimental design matrix and observed performance measures in .....   | 113 |
| Table 6.1 Parametric level setting as per L <sub>9</sub> orthogonal array with experimental outcomes .....                      | 116 |
| Table 6.2 Rank of AFM variable for improvement in surface roughness ( $\Delta Ra$ ). .....                                      | 117 |
| Table 6.3 Rank of AFM variable for Material removal (MR) .....  | 118 |
| Table 6.4 Experimental design matrix and observed performance measures in AFM of trim die.....                                  | 125 |
| Table 6.5 ANOVA outcomes for fitted RSM model for improvement in surface roughness .....  | 127 |
| Table 6.6 ANOVA outcomes for fitted RSM model for material removal.....   | 128 |
| Table 6.7 Regression relations for improvement in surface roughness and material removal.....                                   | 130 |
| Table 6.8 Single factor and multi-factor optimization and comparative study of optimized outcomes and experimental facts .....  | 137 |
| Table 6.9 Experimental design matrix and observed performance measures in AFM of stamping die.....                              | 140 |
| Table 6.10 ANOVA outcomes for fitted RSM model for improvement in surface roughness .....                                       | 141 |
| Table 6.11 ANOVA outcomes for fitted RSM model for material removal.....  | 142 |
| Table 6.12 Regression relations for improvement in surface roughness and material removal.....                                  | 143 |
| Table 6.13 Single factor and multi-factor optimization and comparative study of optimized outcomes and experimental facts ..... | 151 |

|  |     |
|--|-----|
| Table 7.1 Coded levels and corresponding actual values of process parameters.....                          | 162 |
| Table 8.1 Weight and dimensional changes.....  | 175 |
| Table 8.2 Improvement in surface roughness value for Mold (M1) and Mold (M2).....                          | 176 |
| Table 8.3 Design of experiment.....  | 179 |
| Table 8.4 Parametric level setting as per L <sub>9</sub> orthogonal array with experimental outcomes ..... | 180 |
| Table 8.5 Rank of AFM variable for material removal (MR).....  | 182 |
| Table 8.6 Rank of AFM variable for improvement in surface roughness ( $\Delta Ra$ ). .....                 | 182 |

## Nomenclature

---

### Roman symbols

|          |  |
|----------|--|
| $a_i$    | Acceleration of particle $i^{\text{th}}$                       |
| $A'$     | Cross section area of groove generated.                        |
| $A_m$    | Area to be finished  |
| $b$      | Radius of projected area of indentation                        |
| $C$      | Weight of abrasives/weight of medium                           |
| $C$      | Clearance,   |
| $d_{ij}$ | Distance between particle $i$ and $j$                          |
| $d_a$    | Grit diameter  |
| $D_H$    | Hydraulic diameter,  |
| $e$      | Eccentricity,  |
| $E_m$    | Modulus of elasticity of workpiece material, N/mm <sup>2</sup> |
| $f$      | Friction factor  |
| $F_{ij}$ | Force on particle $i$ by particle $j$                          |
| $F_n$    | Normal force acting on the grain                               |
| $F_{ng}$ | Normal force applied to abrasive grain                         |
| $F_t$    | Tangential force   |
| $H_w$    | Brinell hardness of the workpiece                              |
| $i_d$    | Depth of indentation   |
| $L$      | Sampling length  |
| $L_i$    | Actual contact length in $i^{\text{th}}$ stroke, m             |
| $l_t$    | Base length of this equilateral triangle                       |
| $L_C$    | Actual length of contact                                       |

|            |  |
|------------|--|
| $L_s, l_s$ | Stroke length  |
| $L_w$      | Workpiece length   |
| $n$        | Active grain density   |
| $n_s$      | Total number of abrasive contacts  |
| $N_a$      | Number of active grits per unit machining area                                       |
| $N$        | Total number of active grits   |
| $P_R$      | Pitch of rotor   |
| $P_S$      | Pitch of stator  |
| $R$        | Magnitude of the force   |
| $R_a$      | Mean surface roughness value   |
| $R_d$      | Rotor diameter   |
| $r_{eff}$  | Effective radius   |
| $r_i$      | Radius of particle $i^{th}$  |
| $R_q$      | Root mean square average of the roughness profile                                    |
| $R_w$      | Radius of work-piece   |
| $R_z$      | Arithmetic mean value of the single roughness depths of consecutive sampling lengths |
| $S$        | Slip flow  |
| $S_d$      | Stator diameter,   |
| $t$        | Depth of indentation   |
| $t^*$      | Time of machining  |
| $u$        | Velocity   |
| $V_F$      | Volume of all free cavities  |
| $v_f$      | Flow velocity  |
| $V_f$      | Velocity of the medium near the workpiece  |

|                  |  |
|------------------|--|
| $V_i$            | Volume of material removed in $i^{\text{th}}$ stroke, $\text{m}^3$ |
| $V_p$            | Piston velocity  |
| $V_t$            | Volume removal rate  |
| $\dot{V}_{grit}$ | Volumetric removal rate by each abrasive grit                      |
| $V_{grit}$       | Average grit velocity  |
| $\dot{V}$        | Overall material removal rate                                      |
| $W$              | Effective hydraulic power  |
| $W_F$            | Effective hydraulic power due to friction loss                     |
| $W_S$            | Width of stator  |
| $W_S$            | Effective hydraulic power due to internal slip                     |
| $W_U$            | Effective hydraulic power due to load                              |
| $W_{u,th}$       | Geometrically determined power consumption                         |
| $Y$              | Young's modulus  |

### **Greek Symbols**

|               |  |
|---------------|--|
| $\alpha$      | Angle of surface asperity                  |
| $\nabla A$    | Projected area of indentation              |
| $\delta_{ij}$ | Deformation between particle $i$ and $j$   |
| $\Delta Ra$   | Improvement in surface roughness           |
| $\mu$         | Co-efficient of friction                   |
| $\vartheta$   | Poisson's ratio                            |
| $\omega$      | Rotational speed of rotor (rpm)            |
| $\rho$        | Density of work-piece material             |
| $\rho_a$      | Density of the medium around the workpiece |

|            |  |
|------------|--|
| $\rho_c$   | Carrier density                            |
| $\rho_m$   | Density of the medium                      |
| $\sigma_n$ | Normal stress acting on the abrasive grit. |

### **Acronyms**

|         |   |
|---------|---|
| AFM     | Abrasive flow machine                                   |
| AJM     | Abrasive jet machining                                  |
| AWJM    | Abrasive water jet machining                            |
| AE      | Acoustic emission                                       |
| AM      | Additive manufacturing                                  |
| ANOVA   | Analysis of variance                                    |
| ANN     | Artificial neural networks                              |
| AFM     | Atomic force microscopy                                 |
| BEMRF   | Ball end magnetorheological finishing tool              |
| C/Cs    | Carbon-carbon composites                                |
| CIPs    | Carbonyl iron particles                                 |
| CFAAFM  | Centrifugal-force-assisted abrasive flow machining      |
| CFD     | Computational fluid dynamics                            |
| C-EMAM  | Cylindrical electrochemical magnetic abrasive machining |
| DDS     | Data dependent systems                                  |
| DBG-AFF | Dill bit guided abrasive flow finishing                 |
| EEM     | Elastic emission machining                              |
| ECAFM   | Electrochemical assisted abrasive flow machine          |
| ECM     | Electrochemical machining                               |
| EC-MAF  | Electrochemical magnetic abrasive finishing             |
| ECP     | Electro-chemical polishing                              |
| EDM     | Electric discharge machining                            |
| FEM     | Finite element modelling                                |
| FTIR    | Fourier transform infrared spectroscopy                 |
| GA      | Genetic algorithm                                       |
| HMP     | Hybrid machining process                                |



|         |  |
|---------|--|
| HSS     | High speed steel                                       |
| MAF     | Magnetic abrasive finishing                            |
| MAM     | Magnetic abrasive machining                            |
| MFGA    | Magnetic finishing with abrasive gel                   |
| MFP     | Magnetic float polishing                               |
| MAFM    | Magneto abrasive flow machining process                |
| M-RAFF  | Magneto-rheological abrasive flow finishing            |
| MR      | Magneto rheological                                    |
| MRF     | Magneto-rheological finishing                          |
| MRP     | Magneto rheological polishing                          |
| MR      | Material removal                                       |
| MRR     | Material removal rate                                  |
| MMCs    | Metal matrix composite                                 |
| MUAFM   | Micro unidirectional abrasive flow machine             |
| MVRA    | Multivariable regression analysis                      |
| OOR     | Out-of-roundness                                       |
| PBS     | Polyborosiloxane                                       |
| PEG     | Polyethylene glycol                                    |
| PAG     | Polymer abrasive gel                                   |
| PEL     | Profiled edge laminae                                  |
| RP      | Rapid prototyping                                      |
| RT      | Rapid tooling  |
| RSM     | Response surface method                                |
| R-AFF   | Rotational abrasive flow finishing                     |
| R-MRAFF | Rotational magneto rheological abrasive flow finishing |
| RIR     | Roughness improvement rates                            |
| SEM     | Scanning electron microscopy                           |
| SSR     | Scatter of surface roughness                           |
| S/N     | Signal to noise  |
| SOD     | Stand-off distance                                     |
| SBR     | Styrene butadiene rubber                               |

|        |   |
|--------|---|
| TGA    | Thermo gravimetric analysis                 |
| UAAFMM | Ultrasonic assisted abrasive flow machining |
| UFP    | Ultrasonic flow polishing                   |
| USM    | Ultrasonic machining                        |
| UTM    | Universal testing machine                   |
| WEDM   | Wire electric discharge machining           |
| WEDM'd | Wire electro discharge machined             |
| XRD    | X-Ray diffraction technique                 |

## **Chapter 1 Introduction**

---

### **1.1 Conventional finishing process**

High surface qualities for manufacturing industries are very important to improve interchangeability of component, quality and longer wear/fatigue life. So before discussing the advanced finishing process, it is very important to know the commonly used traditional finishing processes. The process known for good surface finishing are grinding, honing, lapping and super finishing. In these processes, a very small amount of material is removed by loose abrasives or bonded abrasives to make the smooth surface with close tolerance. Hardness of abrasive particles compared to workpiece material is an important aspect for generation of high surface quality.

#### **1.1.1 Grinding**

Grinding process uses grinding wheel made of large multipoint abrasive particles retained by bonding material. Grinding is more efficient for removing material than other finishing methods, due to random distribution of protrusion of abrasive particles. Finishing of intricate parts by grinding process is difficult, and requires expensive shaped grinding wheels. The projecting particles of a grinding wheel cut or abrade a layer of material from the workpiece in form of tiny chips [1]. The application of grinding is mainly available for simple geometries like cylindrical or plane surface where size is limited by grinding wheel movement.

### **1.1.2 Honing**

Honing is a different abrasive finishing process commonly used to finish internal cylindrical surfaces. The abrasives in the form of stones or sticks carried in an expanding and oscillating mandrel are used to create random cross-marked surface with good finish. The stick pressure on workpiece surface is comparatively more than lapping. The surface produced after honing process has self-lubricating behaviour due to oil retaining capability in cross-hatched pattern.

### **1.1.3 Lapping**

Lapping is loose abrasive finishing process to improve surface finish and accuracy of component. Lapping removes subsurface damage caused by grinding or similar other processes. It works on the principle of three body abrasive wear in which finishing action takes place through abrasion by abrasive particles trapped between workpiece surface and a relatively softer polishing pad called lap. The workpiece is held against the lap and the lap is moved in random direction under pressure after introducing abrasive slurry between the workpiece and the lap surface. This process is generally used for finishing the flat surfaces due to flexibility of the lap. However, simple and well defined curved surfaces (concave, convex etc.) can be finished to some extent by proper designing of lap.

## **1.2 Need and importance of advanced finishing processes**

Traditional finishing processes are suitable only for certain type of workpieces such as flat or cylindrical and have a low degree of control on the achieved surface finish. There are some critical issues associated with traditional finishing processes, like in grinding, the generation of large amounts of heat and defects such as micro-cracks, thermal residual stresses, etc. The traditional finishing processes cannot finish complex and miniaturized workpieces such as 3-

dimensional components and cooling holes in automobile components and in turbine blades having diameters less than 2 mm. Hand polishing or deburring could also result in inconsistent results, and is impossible to perform on complicated or internal surface [2].

Finishing is widely used technique for improvement in the surface quality of the work piece. Uneven surface generates stress concentration at the mating elements and also results in cracks over the surface at varying situations. For estimation of fatigue life of the component, surface quality in terms of surface roughness play an important role in manufacturing process. Experimental outcomes showed that finished profile have more fatigue lifespan as related to partially finished or rougher profile. Hence finishing or polishing of the component is very important to improved component lifespan. So the technique of providing extremely effective and precise methods for finishing has become an essential research focus. Various methods for finishing have been invented by researchers over a period of stage. The most widely used technique by academics as well as in manufacturing industry is abrasive flow machining (AFM).

To overcome difficulties like finishing of intricate shapes and finishing surfaces with high surface quality, advanced finishing processes have been proposed by Extrude Hone Co. in the 1960s. AFF is one of the newest nonconventional finishing processes in which a deformable viscoelastic abrasive laden (AFF media) is extruded over the surfaces to be finished.

### **1.3 Challenges in abrasive flow finishing of components**

#### **1.3.1 Cost effectiveness of consumables**

For a small scale industry, especially in developing countries cost factor is very important for finishing the components because they have not enough purchasing power for currently

available AFM as compared to availability of cheaper labour. Thus, people are finishing the components manually, hence getting non-consistent results, waste of material and non-finishing of complicated surface. Even major industries who purchase the costly AFM machine face the pinch of the high recurring cost of media for not having a low-cost media for finishing the components which are also environmentally sustainable. Some industries are facing the problems related to media to extend that they are not able to utilize their machines to the full extent. Today main competition in industries is technology at an affordable price.

### **1.3.2 Acceptance across industries**

Due to many difficulties associated with development, technology takes up numerous years to transfer from the research originations to become a common exercise in manufacturing industry. After development of a new technology or improved method, Industries use numerous inspective techniques before implementing a new technology. As deliberated earlier, cost usefulness is an important characteristic which is considered by manufacturing industry.

An industrial-oriented study should be made on the AFF process for find the suitable finishing condition and required quality of finish. More research on industrialized application of abrasive flow finishing processes is mandatory to be accomplished.

### **1.3.3 Tooling design**

Many researchers worked on the development of tooling and fixture for the components which are different in geometrically shape and size. But still there are many requirements in the development of tooling and fixture for multiple components and for complex shape and size components, so that the mass production can be increased and cost of surface finishing

can be reduced. Also more work is required in the design of tooling and fixture of abrasive flow finishing and in its other variants to improve surface roughness and increases in material removal rate.

#### **1.3.4 Environmental issues**

In the current age, environmental footprints of any commercial activity cannot be ignored. Due to commercial PBS based media presently AFM produces bio-non-degradable recurring waste. Efforts are to be put in to make this process environmentally friendly. Many researchers developed AFM media, but still, there is need of AFM media that should be environmental friendly. Another competition in industries is technology at an affordable price and at environmentally sustainable scale explaining why research for low cost environmentally sustainable media is needed.

### **1.4 Organization of thesis**

The thesis is organized in eight chapters with references and appendices. First chapter describes the need and importance of finishing processes with classification of AFM process.

The present research work attempt the development of an environ-friendly AFM media and low cost AFM setup for finishing complicated price sensitive industrial components.

Chapter 1 briefly presents importance of finishing processes along with challenges in finishing in today's manufacturing industries. In the end significance of research is discussed.

Chapter 2 presents the literature review of abrasive flow machining process along with mechanism of material removal. Based on literature survey, research gaps are identified and objectives for the present work are defined.

Chapter 3 discusses the rheological studies and characterization of developed polymer

abrasive gel (PAG) using scanning electron microscopy (SEM), thermogravimetric analysis (TGA) and Fourier transform infrared spectroscopy (FTIR).

Chapter 4 explains the development of micro unidirectional abrasive flow machine (MUAFM) and unidirectional abrasive flow machine (UAFM). Design and fabrication of tooling and fixture for holding the components are also discussed.

Chapter 5 elaborates the experimentation details and methodology adopted during experimentation on UAFM setup. Equipment used for measurement and analysis are also discussed at the end.

Chapter 6 explains the results in terms of improvement in surface roughness and material removal. Surface characterization of finished components is also discussed.

Chapter 7 discusses the validation of experimental results for material removal with theoretically derived models by MATLAB software. The conclusions, contributions and guidelines for future work are presented in Chapter 8.



## **Chapter 2 Literature Review**

---

### **2.1 Overview**

#### **2.1.1 Introduction to AFM**

To overcome difficulties like finishing of intricate shapes and finishing surfaces with high surface quality, advanced finishing processes have been proposed by Extrude Hone Co. in the 1960s. AFF is one of the newest nonconventional finishing processes in which a deformable viscoelastic abrasive laden (AFF media) is extruded over the surface to be finished. The major components of the AFF are the machine parts, tooling and fixtures, types of abrasives, AFM media composition and process variables [3]. AFF process is used for deburring, polishing, and radiusing in difficult-to-machine materials and workpieces having difficult-to-reach profile such as intricate shape and edges. Many research studies claim that high surface finish quality can be obtained over a wide range of geometrically different components like fuel injector nozzles and heading dies, rapid tooling, turbine blades, knee joints, etc., using AFF technique. High end industries such as aerospace, medical tools, electronics, automobiles and high precision moulds & dies manufacturing etc. are widely using AFF process as a part of their industrialized activities. For example, AFF technique is used to finish automotive engine components like nozzle, gears, camshafts and bearings etc. and thus improved air and fluid flow over high finished components results in lower emissions, high cycle fatigue strength and increased performance of the engine.

#### **2.1.2 Classification of AFM processes**

The finishing processes which involves in improvement of finishing levels of surfaces are broadly classified as either traditional surface finishing processes like lapping, honing, polishing and grinding or into advanced finishing techniques like abrasive flow finishing

(AFF), magnetic abrasive finishing (MAF), magnetic float polishing (MFP), magneto-rheological finishing (MRF), etc.

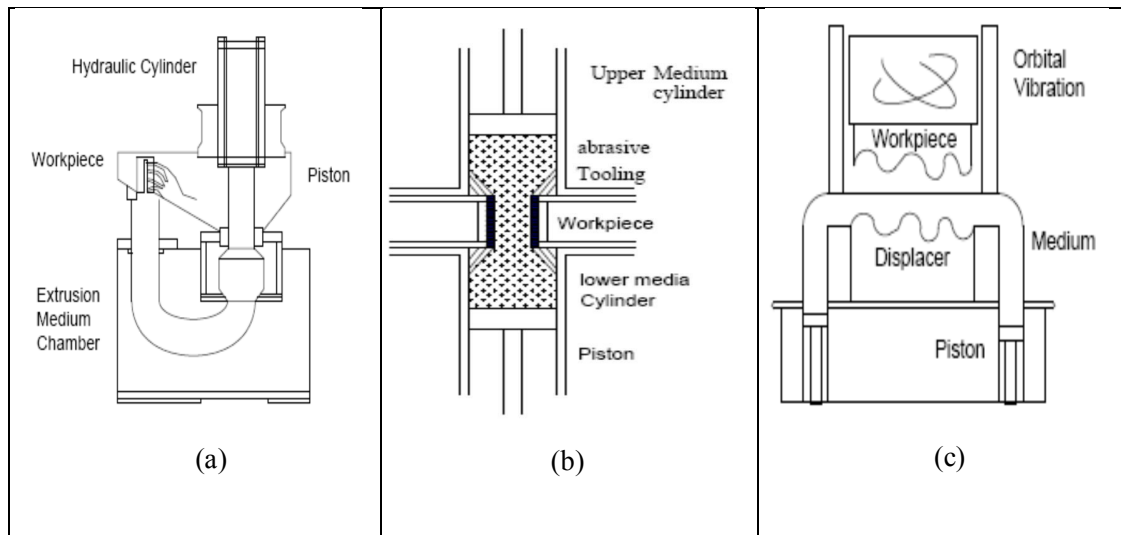


**Figure 2.1 (a) Schematic of one way AFF (b) Working principle of two way AFF (c) Orbital AFF**

Further, the main configuration of AFF setup has been classified as i) one way AFF, ii) two way AFF, and iii) orbital AFF as shown in Figure 2.1 (a), (b), (C). In one way AFF process (Figure 2.1 (a)), hydraulically operated reciprocating piston cylinder and AFM media cylinder arranged in such a way that the AFF media flow unidirectional over the internal surfaces of the workpiece. In two-way AFF system, two vertically arranged media chambers extrude the AFF media backward and forward [4] over the workpiece surfaces (see, Figure 2.1 (b)). While in orbital AFF, the workpiece is specifically oscillated in two or three proportions inside a slow flowing pad of acquiescent elastic or plastic AFF media (Figure 2.1 (c)). The special features of this process are more suitable for three dimensional complex forms/shapes [5] . Besides these conventional configurations of AFF, the different hybrid configurations of AFF with different machining processes, which have superior performance than that of AFF, can be found in literature, e.g. magnetic abrasive finishing (MAF), magnetic float polishing

(MFP), magneto rheological finishing (MRF), drill bit guided abrasive flow finishing (DBG-AFF), centrifugal-force-assisted abrasive flow machining (CFAAFM) and elastic emission machining (EEM).

### **2.1.3 Mechanism of material removal**

Sliding action of random abrasives of different composition in unidirectional cause material removal from the workpiece geometry, process called abrasion in AFM. Many researchers worked on basic mechanism of abrasion in common. Khrushchov and Bavichov [1] observed two processes when abrasive grits comes in contact with the wearing surface.

- 1) The development of physical surface indentation which did not affect material removal.
- 2) The partition of material grains in the terms of microchips.

Shape of indenting particle is major factor for chip cutting and rubbing speed [2]. Micro ploughing and micro cutting are two basic processes to understand the mechanism between abrasives and finished surface profile in abrasive flow finishing. Micro ploughing action of one time flow of single abrasive is not responsible for impartiality of material from the work piece surface. During finishing process in projecting part of abrading element, the material is constantly evacuated sidelong to make edges next to channel formed.

The continual action of single abrasive or due to action of several abrasives results in volumetric losses in material removal of AFM process.

Material may be removed by constant action of flowing abrasives and may breakdown by micro fatigue. Volume of channel formed equivalent to volume loss occurred in terms of chip

formed during pure micro cutting process. In brittle material, micro cutting is dominant but for ductile material micro ploughing and micro-cutting are the key processes.

## **2.2 Literature survey**

### **2.2.1 Process parameters and their influence on quality characteristics**

There are numerous variables that affect the feature characteristics of the AFF process, such as media extrusion pressure, abrasive grain size, number of finishing cycles, media flow volume, abrasive media rheology, etc. Many researchers worked on the abrasive flow finishing process to finish different shape and size of workpieces. Jain and Adsul [6] stated that MR and improvement in surface roughness is greater for the soft workpiece material as related to hard workpiece material. They reported that the most important process variables are percentage abrasive concentration followed by abrasive grain size, and number of finishing cycles. Rhoades [7] stated that the media flow rate is one of the key variable which affects the homogeneity of the material removal and development of an edge radiusing. Williams and Rajurkar [8] studied the performance parameters, surface characterization and process modelling in abrasive flow finishing process. A new modelling and analysis method called Data Dependent Systems (DDS) has been applied to study the finished surface generated by AFM process. After the experimental study, they concluded that media viscosity majorly affects the material removal and surface finish. The ratio  $R_{max}$  to  $R_a$  was found by DDS methodology between 1.4 and 2.2 for the AFM process.

Gorana et al. [9] observed the collective influences of media extrusion pressure, percentage abrasive concentration, and abrasive grain size with produced cutting forces (axial and radial forces) during the finishing process. Experimental results show that a decrease in surface

roughness value ( $R_a$ ) was found to be linearly proportionate to the force ratio. For improvement of surface finishing quality, the kind of machining process used to fabricate the workpiece earlier to AFF is a very essential parameter in performance measure. The volumes of material removal from the WEDM'd process and milled process is ominously diverse from that of turning and grinding operations because these machining processes generate dissimilar micro surface contours[10].

Fang et al.[11] studied the particle movement arrangements of ellipsoidal elements to find the influence of particle movement arrangements in AFM. An analytical model of ellipsoidal geometry was anticipated with abrasive particle ellipticity, normal load, particle grain size and material hardness. They reported that sharper particles are easy to groove; additionally, grooving configuration will be major if particle ellipticity is below 0.8. Gov et al. [12] investigated the influence of different hard components on AFM process performance for finishing AISI D2 tool steel material of hardness 31, 45 and 55 HRC. They reported that white layer generated during WEDM process can be detached by AFM process in few cycles that results in abolishing surface cracks and increased fatigue strength.

Finishing of spring collets of chrome molybdenum material were performed by Kim and Kim [13] on abrasive flow machining for removing burrs. Abrasive AFM media has been synthesized by mixing a silicon polymer with abrasive grits for effective removal of edges and burrs through the interior and micro-grooves of the spring collet. They also concluded that high viscosity media give higher deburring effects related to medium viscosity media or low viscosity media. Gov and Eyercioglu [14] analysed the effects of abrasives in media on abrasive flow machining process. From experimental results, it is observed that AFM media

synthesized with B<sub>4</sub>C and SiC abrasives have better surface improvement than the Al<sub>2</sub>O<sub>3</sub> and Garnet abrasives.

Table 2.1 explains the brief summary of work done for process parameters and its influence on output response in AFF.

**Table 2.1 Summary of experimental work on AFF process parameters and their influence on output response**

| Author                  | Title  | Workpiece material and size  | Abrasive media                              | Abrasive  | No. of cycle / Extrusion pressure  | MRR And Ra   | Other   | Remarks  |
|-------------------------|--|--|---|---|--|--|---|--|
| Gorana et al.[15]       | Forces prediction during material deformation in abrasive flow machining   | Mild steel and aluminium workpiece with hardness 187 BHN   | Plain silly putty                           | Silicon carbide 80,180,220 mesh size  | 40,50,60,70, 80 Bar  | AFM exp. 0.7–0.9<br>Scratching exp.-0.5–0.6  | -   | Variables like Axial force, radial force, active grain density and depth of indentation all have a substantial influence on the scale of material deformation.   |
| Ravishankar et al. [16] | Experimental investigation and mechanism of material removal in nano finishing of MMCs using abrasive flow finishing (AFF) process | Al alloy, Al alloy/SiC MMCs with 10% SiC and 15% SiC volume element                                      | SBR, hydraulic oil                          | SiC abrasives of mesh size 220  | Finishing Cycles 200,400,600, 800,1000 & extrusion pressure 4, 5, 6, 7, 8 MPa                            | MR 1.25 ,2.0,2.5,2.9 and 3.25 mg at 200,400,600,800, 100 cycles and ΔRa for Al alloy, Al alloy/SiC (10%) and Al alloy/SiC (15%) at 400, 600 and 800 cycles | -   | MR increases with increase in medium extrusion pressure and number of cycles, but decreases as weight percentage of oil in the AFM media increases.  |
| Yin et al.[17]          | Surface characterization of 6H-SiC (0001) substrates in indentation and abrasive machining   | 6H-SiC (0001) of 8 mm diameter, 10 mm thickness substrates polished with 15, 6, 3 and 1 μm diamond paste | 3 μm and 0.05 μm diamond grit for polishing | Diamond cup wheel of diameter -7.1 mm, grit sizes of 25, 15 and 7 μm used in grinding | peak load of 400 MN in indentation and polished for 8 minutes, contacting force SiC sample and cloth-50N | Ra=2.35 μm, 1.89 μm for grit size=3 μm, 0.05 μm for polished 6H SiC substrate.<br>Ra=0.050,0.062 μm for feed rate of 0.05 and 0.2 mm/min.                  | Grinding wheel speed 10 m/s, spindle rotation-26913 rpm, vertical feed rate-0.05,0.1,0.2 mm/min, flow rate-6.6 l/min, in polishing disc rotation-40,150 rpm | Nano-hardness value for single crystal 6H-SiC 32.05 +- 0.60 GPa<br>In polishing, a decrease of abrasive grain size of diamond suspensions from 3 to 0.05 μ<br><br>no substantial improvement in surface roughness value (2–3 |

| Author            | Title   | Workpiece material and size  | Abrasive media                         | Abrasive  | No. of cycle / Extrusion pressure                             | MRR And Ra  | Other  | Remarks  |
|-------------------|---|--|--|---|---|---|--|--|
|                   |   |  |  |   |   |   |  | nm Rq).  |
| Kenda et al. [18] | Surface Integrity in Abrasive Flow Machining of hardened tool steel AISI D2         | Tool steel AISI D2, 59 HRC, 35 mm long passage, 14 mm width and 10 mm high, Ra=1.69µm, Rz=10.66 µm | Polishing Media viscosity 2650 Pa-sec. | SiC abrasive with 80 mesh size, 57% concentration | Extrusion pressure 3.5 MPa, 6.0 MPa, 1800 sec. machining time | Ra=1.68 µm surface generated AFM - 0.94 – 0.23 µm, High tensile stress in EDM-550 MPa, Compressive stress in AFM for media pressure 6.0 MPa, -350 MPa and for 3.5 MPa, 200 MPa.   | Volume flow =109247*10 <sup>11</sup> m <sup>3</sup> /s, 355053*10 <sup>11</sup> m <sup>3</sup> /s, for measuring residual stress, 20kV tension, 4 mA current using Cr Kα tube and angle of Bragg 156.1°. | Surface integrity produces by EDM process can be ominously enhanced by AFM, AFM media pressure increase with increase in compressive stresses.   |
| Wang et al. [19]  | Enhancing the surface precision for helical passageways in abrasive flow machining. | circular holes of SKD-11 steel material<br><br>Diameter-61mm length =30mm                          | polymer gels                           | SiC abrasive mesh size100 With 50% concentration  | extrusion pressure= 402 MPa, Back Pressure= 2.1 MPa           | Ra initial= 0.65 µm, roughness improvement rates (RIR) 70%, 76% and 76% for 3,4,5 helical grooves ,in 25 cycle, For 1.5,1.0,0.5 mm Gap RIR 52,59, and 76 % after 25 cycle, 0.5 mm gap is a most appropriate.<br><br>RIR of 0.5 helical turn can touch closely 62%, RIR comes to 65% in 0.7 helical turn | Helical core dia. =15mm, Working temp. 27°C, thickness of helical slot= 0.5 mm, 0.5 mm gap   | Material Removal (MR) and RIR can be increased based on the length of the path traveled by a distinct abrasive grain is increased in the same finishing cycle, greater number of helical grooves performs more quantity of material removal. |



### **2.2.2 Process modelling and optimization in abrasive flow finishing process.**

The physical AFF models present the relationship between AFF performance and control parameters that assists in emerging an effective control mechanism for automation of a finishing process. The AFF process is not absolutely implicit as there is a lack of quantitative interactions between finishing parameters (extrusion pressure, abrasive mesh size, abrasive concentration) and output variables (improvement in surface finishing quality and material removal rate), specially for exterior surface finishing. The process modelling and analysis benefits in understanding the effects of various finishing parameters on the finishing process mechanism and material removal. To enhance the capability of the multifaceted process, it is essential to create a modest model in which process parameters can be varied in random order to examine their effects on performance measure variables can be analysed.

In analysing the influence of AFM process variables on MRR and surface finish quality, many researchers worked on developing the mathematical models and compared with the experimental outcomes. Table 2.2 represents the different mathematical model developed for material removal and surface roughness predictions.

Dong et al.[20] studied the machining mechanism of high viscoelastic AFM and developed theoretical model of the normal pressure on the work surface and the wall sliding velocity based on rheology theory. They performed the numerical simulations using proposed model at various machining conditions and confirmed the outcomes with actual experimental results. Jain and Jain[21] anticipated a model for the calculation of specific energy and tangential forces in the AFM process and reported that specific energy remains almost persistent with a change in abrasive grain size, but it will be more for

higher hardness of the component material. Jain et al.[22] established a surface roughness method to compute the centreline average surface roughness (Ra) in MAF process. After checking the validity of the developed surface roughness method with experimental results they observed that average surface roughness value of the finished specimen surface decrease with increase in magnetic flux density, the size of magnetic abrasive grains and the rotating speed of flexible magnetic abrasive brush.

**Table 2.2 Physical AFF models in mathematical equations for abrasive flow finishing process**

| Name of author and year                                      | Mechanism of material removal   | Proposed physical mathematical model  | Assumptions  | Conclusion   |
|--|---|---|--|--|
| V. K. Jain, R. Kumar, P. M. Dixit, and A. Sidpara (2009)[23] | Indentation (caused due to normal force) of the abrasive particle in the workpiece surface followed by its linear movement  | Total volumetric material removal after ‘n’ number of cycles<br>$V = \frac{6K_n C \rho_m L_s V_f (D_1 L_1 + (D_1 + D_2) L_2)}{\pi \rho_a d_g^3 V_p L_w} \left( \frac{F_n}{H_w} \right)^2$ Where $K = K_1 K_2^{-2}$<br>Where $K_2 = 1$ for brittle materials and $K_2 > 1$ for ductile materials (for steel, $K_2 = 3.1$ ) | 1. Material removed by each abrasive grits in each cycle is assumed same and constant.<br>2. Abrasive particle shapes are considered as spherical and same size.<br>3. Normal force acting on each abrasive particle is assumed to be same and equal.<br>4. Abrasive particles are uniformly distributed in the media.   | Theoretical model developed for material removal is compared with experimental outcomes and observed the same behaviour but some deviation in both.  |
| Rajendra K. Jain, Vijay K. Jain and P.M. Dixit (1999)[24]    | Sliding action accomplished by abrasive particles and normal force applied by the spherical abrasive particle cause it to penetrate in the workpiece surface and produces a groove on the surface and translated action of abrasive grains cause the material removal from the workpiece surface. | Volumetric material removal $i^{th}$ stroke ( $V_i$ )<br>$V_i = 2 \Pi N l_s \frac{R_c^2}{R_w} \left[ \frac{d_g^2}{4} \sin^{-1} \frac{2 \sqrt{t(d_g - t)}}{d_g} - \sqrt{t(d_g - t)} \left( \frac{d_g}{2} - t \right) \right] L_i$  | For material removal<br>1. All abrasive particles are blocky crystals that may be assumed as spherical in Shape.<br>2. Each abrasive particles contains of a single active cutting edge.<br>3. Load on each abrasive particle is constant and equal to the average load.<br>4. Every abrasive particle is assumed to achieve the same penetration depth depending upon the applied force.<br>For surface roughness<br>1. Workpiece surfaces have uniform profile and initial surface roughness $R_a^i$ ,<br>2. Abrasives move in the length direction of the scratches | Model for the flow of AFM media through cylindrical work piece is developed and solved by finite element method. Normal stress, achieved from the flow model, is used for the estimation of material removal and surface finish. Further model can be developed for three dimensional shape and consideration of change in machining conditions of AFM process |
| Rajendra K. Jain and V.K. Jain (2004)[25]·[26]               | Statistically estimates the interaction between spherical abrasive particles and workpiece surface that will help in prediction of abrasive grain density at any  | Total volume of abrasive grains ( $V_a$ ) in $V_m$ volume of media $= \frac{C \rho_c r_c^2 l_s}{C \rho_c + (100 - C) \rho_a}$<br>for a spherical grain of diameter $d_g$ , the maximum depth of indentation $t$ of a grain in workpiece material  | 1. Each abrasive particle travel in a straight path.<br>2. Abrasive particle is spherical in shape.<br>3. Distribution of abrasives’ radii is assumed to be normal and symmetric about the mean grain radius.  | Utilized microscope techniques for quantitatively characterizing the topography of AFM media, also this technique can be extended for simulation of surface  |

|   |  |   |  |  |
|---|--|---|--|--|
|   | concentration and mesh size.   | $t = \frac{d_g}{2} - \frac{d_g}{2} \sqrt{1 - \frac{\sigma_n}{H_w}}$   |  | generation in abrasive flow machining.   |
| V.K. Gorana, V. K. Jain and G. K. Lal (2006) [27] | Mathematical simulation is used for prediction of material removal and surface roughness by considering the interaction of a single grain with assumed single equilateral triangular profile of the workpiece surface. | <p>material removal from the workpiece by each grain is calculated using depth of indentation 'd' of an abrasive grain <math>d' = 1.550 \sqrt[3]{\frac{F_{ng}^2}{2R E_m^2}}</math></p> <p>force acting on a single grain</p> $F_{ng} = \sigma * \pi * \left(\frac{b}{2}\right)^2$ $R_a = \frac{1}{L} \int_0^L  Y  dx = \frac{A_3 + A_4 + A_5 + \dots + A_n}{L}$ <p>initial center line average (Ra) value = Ra</p> $= \frac{t_t \sqrt{3}}{8}$ | <ol style="list-style-type: none"> <li>1. Diameter of all the abrasive grains is the same.</li> <li>2. The shape of an abrasive grain is approximated as a sphere, and not composed of acute cutting edges.</li> <li>3. Path traced by an individual grain is a straight line.</li> <li>4. Material removal is assumed as 100 % ploughing.</li> <li>5. All active abrasive grains are achieving the same depth of indentation.</li> <li>6. Initial workpiece surface profile is considered as an equilateral triangular in shape.</li> </ol> | Active abrasive grain density during the finishing process increases with an increase in extrusion pressure and percent abrasive concentration in the AFM media, results in increase in reduction in $R_a$ . |

Some researchers [28][29][30][31] worked on CFD simulations to understand the flow characteristics and relation to performance measure variables of abrasive flow finishing process. For understanding the mechanism of reduction of material removal proficiency with temperature, Fang et al.[29] used CFD methodology to calculate the abrasive grains movement propensity. Howard and Cheng [32] proposed industrial feasibility approach to confirm an integrated optimum configuration of machine, media, and geometry can be achieved by abrasive flow machining process optimization. They incorporated the CFD simulations on AFM fluid behavior with output results composed from thoroughly organized and proved machining experiments. Uhlmann et al.[33] developed a process model using modern simulation techniques by determining the basic principles of AFM on ceramic materials such as a relationship between flow processes, surface development, and edge rounding. With the help of CFD analysis at constant pressure, Wang et al.[30] reported the velocities, strain rates and shear forces of the AFM media acting on the finishing profile could be evaluated. In analysing the influence of AFM process variables on MRR and surface finish quality, Jain et al.[34] used artificial neural network and MVRA technique in AFM process. After assessment of outcomes, they concluded that percentage error in estimation of untrained data by artificial neural network model was from 0.25% to 8.95%, while it was from 0.09% to 25% in outcomes anticipated by MVRA. Mali and Manna[35] also compared ANN model with MVRA for modelling and simulation of output parameters during finishing of Al/SiCp MMCs components. Petri et al.[36] developed the process modelling method, by combining a heuristic search algorithm with artificial neural network methods that calculates surface finish quality and dimensional variation for abrasive flow machining.

Generally, advance machining processes (AMPs) are categorized by low values of MRR and greater specific energy depletion. AMPs are significant only when no other traditional machining method can meet the essential necessities, proficiently and economically because most of the AMPs are linked with comparatively greater preliminary asset cost, power depletion and functioning cost, tooling and fixture cost, and maintenance cost. Therefore, effective, proficient, and economic deployment of abilities of AMPs demands selection of optimum process constraints. Generally, values of process constraints of AMPs are designated either based on the skill, capability, and acquaintance of the machinist or from the propriety machining handbooks. Assortment of process constraints based on the machinist knowledge does not entirely fulfil the necessities of high effectiveness and good superiority. So by using different optimization and simulation technique, the influence of various process variables on output characteristics can be achieved. Some research study on various optimization techniques used in AFF process are summarized in Table 2.3

**Table 2.3 Optimization of process variables of abrasive flow finishing process**

| Researcher year           | Technique used                                  | Decision variable  | Objective function  | Constraints and variable   | Remarks and limitation  |
|---------------------------|---|--|---|--|---|
| Jain et al. (2007) [37]   | Genetic algorithm (GA)                          | WJM-Water Jet Pressure, Dia. of nozzle, Stand-off Distance (SOD)<br>AJM-Mass flow Rate, Mean radius<br>AWJM-Water jet pressure, Jet transverse rate, abrasive flow rate<br>USM-Amplitude and frequency of vibration, Abrasive size and concentration | Maximize MRR  | Power consumption, wearing of nozzle or tool, limiting value of surface roughness value.   | Single objective optimization formulated objective function and constraints are very complex and imply to decision variables.   |
| Mali and Manna (2010)[38] | Taguchi Technique and SEM                       | Abrasive grain size, number of finishing cycles, media extrusion pressure, percentage of abrasive concentration, and abrasive media viscosity grade  | MRR and surface roughness   | Stroke length: 50 mm<br>Volume of media: 400,000 mm <sup>3</sup> (400 ml)<br>Average volume flow rate: 600 mm/min<br>Room temperature: 22±0.5°C.           | Maximum ΔR <sub>a</sub> is attained within primary 10 cycles and at 3MPa extrusion pressure, % of abrasive concentration and abrasive grain size are supreme important variables for min. R <sub>a</sub> (max Δ R <sub>a</sub> and max MRR respectively). |
| Jain and Jain (2000) [39] | Generalized back propagation neural network, GA | Media flow speed, percentage concentration and mesh size of abrasive, no. of cycles  | Max. MRR and low Surface roughness  | $R_a \leq R_a \text{ max}$<br>$x_i^l \leq x_i \leq X_i^u$  | Process optimization can be achieved in nonexistence of process model and by observation.<br>Can be applied to other machining abrasive process for improving the machining efficiency  |
| Jain et al.(2007) [40]    | Genetic Algorithm                               | AFM:<br>1. Abrasive concentration of by volume<br>2. Abrasive grain size 'Ma'<br>3. Number of strokes 'Ns'<br>4. Extrusion pressure 'Ph' (MPa or N/mm <sup>2</sup> )   | Minimize final surface roughness value (Ra), minimize size and shape incorrectness<br>MAF:<br>Maximize the difference between | $0.05 \leq Cav \leq 0.5$<br>$8 \leq Ma \leq 1000$<br>$1 \leq Ns \leq 100$ (cycles)<br>$0.7 \leq Ph \leq 25.0$ Mpa<br>MAF:<br>$0.015 \leq dma \leq 0.15$ mm | Process parameter optimization can also be done on different geometry/ surface  |

| Researcher year        | Technique used    | Decision variable  | Objective function   | Constraints and variable  | Remarks and limitation  |
|------------------------|-------------------|--|--|---|---|
|                        |                   | MAF:<br>1. Mean diameter of the magnetic abrasive particles 'dma' (mm)<br>2. Relative velocity between magnetic abrasive particles and workpiece<br>3. Volume ratio of ferromagnetic $W_f$<br>4. Input current 'I' (A)<br>5. Finishing time 'tf' (s) | initial and final surface roughness values                     | $500 \leq V_{ma} \leq 5000$ mm/sec.<br>$0.3 \leq wf \leq 0.8$<br>$1 \leq I \leq 10$ (Amp)<br>$1 \leq tf \leq 1200$ (s)  |   |
| Walia et al. 2006[41]  | Taguchi Technique | Rotational speed of rectangular rod, extrusion pressure and abrasive mesh size.  | MRR and scatter of surface roughness (SSR) Value               | Surface Roughness $0.950 \pm 0.050$ $\mu$ m, Extrusion pressure <60 bar, Mesh Size-100,150,200<br>Polymer to gel ratio: 4:3; abrasive concentration: 1:2;<br>Number of cycles: 3; temperature: $32 \pm 2$ °C. | SSR (mm) 0.023–0.097<br>MR is $37.53 < MR$ (mg) <42.51<br>Effect of other process parameter can be find on MR and SSR   |
| Singh et al., 2004[42] | Taguchi Technique | Voltage (DC) applied to electromagnet, working gap, rotational speed of magnet, abrasive mesh size.  | Change in surface roughness ( $\Delta Ra$ ), finishing process | Magnetic flux density of 0–0.44 T, working gap of 1.00–2.00 mm<br>voltage=11.5V; working gap=1.25 mm; RPM=180;<br>mesh size=800; time=20 min  | MR effects on different process can also be studied. By changing the values of process parameters further their effects on both MR and surface roughness can be done. |



### 2.2.3 Developments in abrasive flow finishing media

The media in AFM process acts as a flexible grinding polishing tool during the finishing process. AFM Media generally consists of two main constituents – the carrier (a viscoelastic base material, e.g. polymer gels and oils) and the solid part (abrasives and elements to support the abrasive). As efforts were made for improving the performance of AFF, research was also done to synthesize better AFM media. The physical (appearance), chemical (ingredients and their quantity in the base carrier, inertness, etc.) and rheological properties (apparent viscosity, shear stress, yield stress, thixotropic, critical strain and critical temperature etc.) considerably affect the overall performance of the AFF process. The most extensively used AFF media are classified as shown in Figure 2.2.

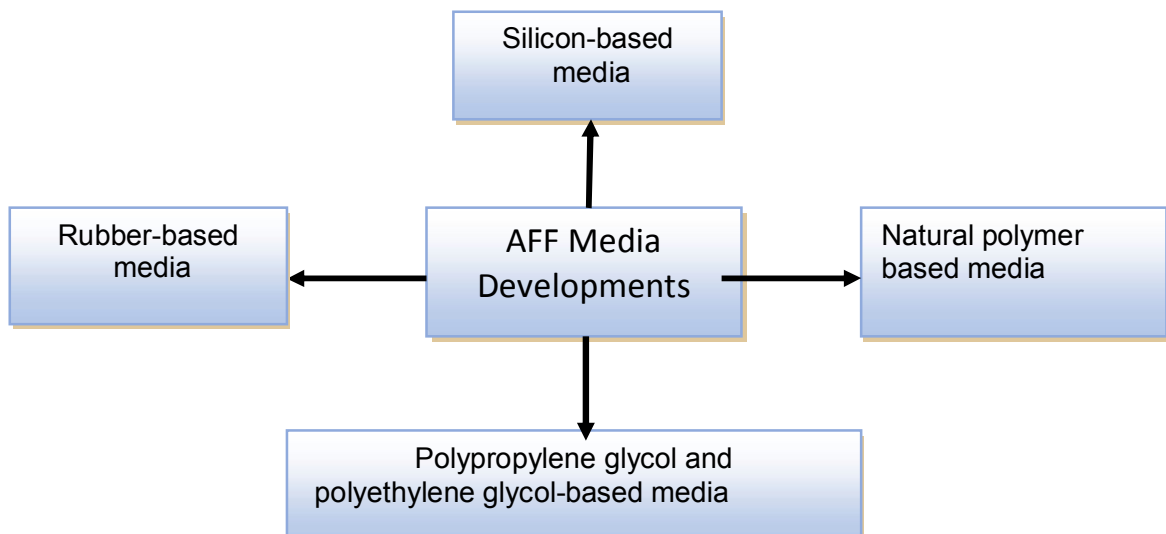


Figure 2.2 Recent development in abrasive flow finishing media

In the next section, research work done in the development of abrasive flow finishing media is discussed as classified in Figure 2.2.

### **2.2.3.1 Silicon based AFF media:**

In 1990, Larry Rhoades [7] studied a viscoelastic AFF medium to observe the effect of viscosity, abrasive grain size, abrasive type and abrasive concentration on finishing performance. The study showed that low viscosity of media is more suitable for radiusing edges and short passage geometry workpieces and stiffer media are more suitable for finishing of large passage workpieces. Davies and Fletcher [43] studied the influence of rheological variables on response variables (improvement in surface roughness and MRR) on Polyborosiloxane (PBS) based AFM media. From experimental analysis, they observed that rate of temperature rise, decrease with increase in viscosity of the medium. They also reported that no. of cycles, temperature, and pressure drop are majorly affected by media type and abrasive- PBS ratio.

### **2.2.3.2 Rubber based AFF media:**

To achieve more flexibility in media, Wang and Weng[44] used abrasive particles and silicone rubber for the development of new type of media (polymer abrasive gels). To observe the performance of developed alternative polymer abrasive gel, they performed some experiments for eliminating recast layers on the surface machined using EDM process by AFF method at persistent temperature. Ravishankar et al.[45] developed an alternative AFM media using a polymer of co-polymeric soft styrene butadiene, plasticizer, and abrasives. They study the effect of storage modulus, stress relaxation, creep recovery and shear viscosity, on material removal rate and surface finishing quality through finishing of Al based MMCs using R-AFF. After experimental analysis, they found the major impact of AFM media, medium temperature, shearing rate and creeping time on rheological nature and percentage constituents in AFM medium. Kar et al.[46]

developed and characterized an alternative AFM media using butyl rubber as a viscoelastic base carrier for finishing the workpiece in AFM process.

After experimental analysis they found that frequency, creeping time, temperature and shear rate had the main influence on rheological characteristics. They also observed that more oil loading degrade the surface quality improvement. They observed the abrasive mesh size 220 better related to abrasive mesh size 800 and abrasive mesh size 1200 for enhanced improvement of surface roughness. Kar et al.[47] developed styrene butadiene rubber (SBR) based AFM media and used thermogravimetric analysis (TGA) technique for observation of weight loss with an increase in temperature of media. They performed mechanical characterization technique as well as rheological using a UTM and a Rheometer device. During the rheological study, they found the effects of cyclic loading, strain, shear rate, temperature and time of applied constant stress on mechanical and rheological characteristics. They observed 88% enhancement in surface finishing quality SBR based AFM media.

### **2.2.3.3 Polypropylene glycol- and polyethylene glycol-based AFF media**

Dabrowski et al.[48] developed AFM media for ECAFM process using the mixture of polymeric electrolytes such as gelated polymers (polypropylene glycol) and water-gels (sodium iodide salt and polyethylene glycol with potassium cyanide) as base material. During finishing process, reduction in no. of the finishing cycles was observed with developed media as compared to other abrasive media. But the major limitation of this process is that it is applicable only for electrically conductive materials.

#### **2.2.3.4 Natural polymer based AFF media**

Rajasha et al.[49] synthesized an alternative AFM media using the natural polymer of easter group and naphthenic based oil for varying the viscosity of the AFM media. They used TGA and FTIR techniques for characterization of AFM media. From experimental results, they found the major impact of escalation in percentage abrasive concentration and extrusion media pressure on surface roughness improvement and MRR. Sambharia and Mali [50] developed a low cost and environmentally sustainable alternative AFM media using base polymers, additives, and liquid synthesizer. From rheology study, they found the effects of the percentage abrasive concentration, percentage of liquid synthesizer, temperature and abrasive grain size on the viscosity of polymer abrasive gel. During the experimental study they observed 0.6-1.3 mg of material removal on high-speed steel material trim dies using various viscosity ratings of synthesized polymer abrasive gel AFM media. Wang et al.[28] developed power law to study the relation of shear rates and viscosities on various abrasive gels in CFD-ACE+ software. After simulation, they found full deformation for the highly viscous gel in the complex hole. They also found that high viscosity abrasive gel produced a higher shear force compared to low viscosity abrasive gel. Jain et al.[51] developed an AFF media by mixing abrasive particles and varnish oil in commercial grade putty and conducted rheological experiments to observe the influence of abrasive grain size, media temperature and percentage of abrasive concentration on viscosity of media using a fabricated capillary viscometer. The results show that AFM media viscosity drops with enlarged shear rate and wall shear stress, and also observed that percentage of abrasive concentration, media temperature, and abrasive grain size had the main impact on media viscosity. After experimentation,

they observed the improvement in material removal and reduction in the surface roughness value with increase in viscosity of AFM media.

Tzeng et al.[52] synthesized an AFM media which has the self-modulating properties like viscosity and fluidity that could be controlled during the finishing process. They finished the micro channel cavity generated on stainless steel material with WEDM process. They stated that at high abrasive concentration and media viscosity, the surface roughness value of the micro channel surface with rough abrasive grain size will be lesser compared to an AFM media with fine abrasive mesh size. They also observed the enhancement in surface quality of micro channel with an increase in media extrusion pressure and the finishing time. Mali and Sambharia [53] developed a low-cost alternative polymer abrasive gel and rheological study was performed to find the influence of rheological variables on finishing quality. After internal finishing of Trim Dies with developed polymer abrasive gel, they observed the  $R_a$  value improved from 3.5 to 0.60  $\mu\text{m}$  after 50 numbers of finishing cycles and 60 percentage abrasive concentration by weight.

Sidpara et al. [54] used Bingham Plastic flow model, Herschel–Bulkley model, and Casson fluid models to illustrate the rheological properties (yield stress and viscosity) of MR fluid under the effect of the magnetic field. Using Analysis of Variance (ANOVA) analysis, they perceived that magnetic field has the maximum influence on the yield stress i.e. 92.72% and viscosity i.e. 49.95%. Optimization results show that maximum yield stress and viscosity was observed at 38% CIPs, 4% abrasive, 52% deionized water and 0.6 T magnetic field. Saraswathamma et al.[55] designed and fabricated a parallel-plate magneto-rheometer to study the role of CIP size on the rheological characteristics (field-induced yield stress and shear viscosity) of MR polishing fluid under various magnetic

flux densities. From rheology results, they concluded that field-induced yield stress of the MR polishing fluid was influenced by the surface roughness of shearing plate and observed higher shear thinning in the case of CIP-OS (coated with SiO<sub>2</sub>) with and without exterior magnetic flux density.

Finishing media used in AFF is the main component that dominates the finishing performance of AFF. However, commercially available AFM media are very costly and environmentally not sustainable and not every user can afford the expenses of the high prices. Therefore, low-cost and environmental friendly abrasive media is needed to be developed. Sambharia and Mali[50] synthesized alternative low cost polymer abrasive gel and compared the cost with commercially available AFM media as shown in Table 2.4

**Table 2.4 Cost comparison of alternative developed polymer abrasive gel with commercial available AFM media**

| Cost of Media                                  |                         |   |
|--|-------------------------|---|
| Polymer abrasive gel                           |                         | Commercial available AFM media (STUTZ Company, USA) |
| Media ingredients                              | Cost                    | Media ingredients                                   |
| Abrasive (50%) aluminium oxide of 24 grit size | \$42                    | For 24 grit aluminium oxide in a polymer slurry     |
| Additive polymer base (50%)                    | \$23                    |   |
| Liquid synthesizer (3%)                        | \$2                     |   |
| Total cost (For 10 gallons media)              | \$67 (approximate cost) | \$200   |

During finishing process, the same type of AFM media could be re-used on different geometry components. In industries, the same batch of AFM media is used on different shape of components without changing the media. After losing the capability of media, they usually add more unused media to increase the performances of finishing process. Also, the re-usability life of AFM media is very important and it majorly depends on

abrasives cutting edges, hardness, and geometry of workpiece. During finishing operations, number of cycles, the finishing quality, and material removal rate increases but after some time its starts decreasing; at that time there is need to change the AFM media for next finishing cycles.

Also, temperature rise during finishing operation has major effect on the efficiency of the media. Due to constant shearing of the surface peaks and friction in finishing surface, the media temperature rises. As the temperature of media increases, the long chains of polymer presented in media collapse into small sections as well as the polymer molecules attains energy and try to move separately. So, with rise in temperature, the shear viscosity of media progressively decreases and the AFM media losses its finishing abilities [56]. So, during finishing process, the temperature control device is very essential to increase the life cycle as well for increasing the performance of process.

Literature shows a number of studies on finishing quality of various abrasive media with varying rheological properties. Zhang et al. [57] fabricated a new iron-based SiC spherical composite magnetic abrasive and compared the service life. During assortment of the media it was found important that the media should be mechanically steady. During finishing process, with flow of media the induced shear stress degrade the media and media loses its binding capability of abrasives. Kar et al.[47] characterized the commercial AFM media through mechanical properties such as modulus, tear strength and hysteresis loss. The results of study are shown in Table 2.5.

**Table 2.5 Physical properties of commercial AFM media [47].**

| Physical properties   |                       |
|---|-----------------------|
| Modulus at 25% strain and at 25° C (MPa)  | 0.04                  |
| Modulus at 25% strain and at 35° C (MPa)  | 0.03                  |
| Tear modulus at 25° C and 25% strain (kN/m)   | 0.03                  |
| Hysteresis loss at 25° C and 50% strain (J/m <sup>2</sup> )                                     | 474                   |
| Instantaneous viscosity/shear viscosity at 27° C and shear rate of 100.0 s <sup>-1</sup> (Pa s) | 2400                  |
| Creep compliance at 27° C and creep time of 100 s (1/Pa)  | 5.63*10 <sup>-4</sup> |
| Complex viscosity at 27° C and frequency of 20 Hz (Pa s)  | 3.82*10 <sup>4</sup>  |

#### **2.2.4 Advancements in AFF processes through hybridizing it with other processes.**

The hybrid machining process (HMP) engage synchronized action of more than one machining methods or take assistance of some energy support in material removal to improve benefits and reduce possible drawbacks originating in different material removal methods [58]. Based on working principals, specific features and response parameters like material removal rate and surface roughness, some hybrid variants of AFF process are presented in Table.2.6.



**Table 2.6 Advancements in AFF processes through hybridizing it with other processes**

| Process   | Author             | Working principle  | Hybridizing parameters         | Abrasive (type/size)   | Media carrier  | Workpiece (size/material)   | Extrusion pressure | Material removal rate                                 | Change in surface roughness ( $\Delta Ra$ )   | Remarks   |
|---|--------------------|--|--------------------------------|--|--|---|--------------------|---|---|---|
| Rotational Abrasive Flow Finishing (R-AFF)          | Shankar et al.[59] | Media reciprocated up and down with piston & Workpiece with tooling rotated                      | Rotating speed of workpiece    | SiC 220 mesh size  | Soft polymer base (soft styrene-based polymer), processing oil (hydrocarbon oil) | Al alloy, Al alloy/SiC (10%), Al alloy/SiC (15%) MMC, Abrasive particle size in MMC- 6.07+- 0.5 mm. | 40–80 bar          | MR 0.5,0.7,0.10 mg with workpiece speed at 2,6,10 rpm | Percentage change in Ra -15,37,45 at 2,6,10 rpm   | As the percentage of composition in MMC increases in Al Alloy more surface roughness is obtained. |
| Magneto-Rheological Abrasive Flow Finishing (MRAFF) | Jha & Jain[60]     | Abrasion by extrusion of magnetically reinforced MRP-fluid through workpiece surface and fixture | Magnetic flux density, current | Cubic boron carbide (CBN), silicon carbide (SiC) & diamond with 1000 mesh size | Mixture of 20 wt% of AP3 grease and 80 wt% paraffin liquid                       | silicon nitride of size $10 \times 10 \times 5$ mm  | 37.8 bar           | –   | With SiC abrasives mesh size 2000,500 cycles-0.18 $\mu$ m, diamond abrasive 1000 mesh size cycle-0.15 $\mu$ m | Surface roughness improvements rate decreases with increases in no. cycles                        |

| Process   | Author             | Working principle  | Hybridizing parameters            | Abrasive (type/size)   | Media carrier   | Workpiece (size/material)                                    | Extrusion pressure | Material removal rate                         | Change in surface roughness ( $\Delta Ra$ )             | Remarks  |
|---|--------------------|--|-----------------------------------|--|---|--|--------------------|---|---|--|
| Magnetic Abrasive Flow Machining (MAFM)               | Singh & Shan [61]  | Application of rotated magnetized abrasive around the ferromagnetic material workpiece   | Magnetic flux density             | Brown super emery consists of 45% $Al_2O_3$ , 35% $Fe_2O_3$ , 15% $Si_2O_3$ , 5% $TiO_2$ | Silicon-based polymer, hydrocarbon gel                    | Brass, aluminium, mild steel                                 | 15 bar             | 12, 22, 33, and 38 (mg)                       | 50, 65, 80, and 75%                                     | Surface Roughness ( $\mu m$ ) 0.11, 0.16, 0.18, and 0.12   |
| Centrifugal Assisted abrasive Flow Machining (CFAAFM) | Walia et al.[62]   | Using rotating centrifugal force generating (CFG) rod on abrasive media inside the passageway of flowing media inside workpiece. | Geometry and speed of CFG rod     | $Al_2O_3$ , 150 micron   | Silicon-based polymer (polyborosiloxane), hydrocarbon gel | Brass Material size $\Phi 8 \text{ mm} \times 16 \text{ mm}$ | 40 Bar             | Avg. increase in Material Removal (MR)= 69.4% | Avg. increase in surface roughness $\Delta R_a=64.45\%$ | 62% average increase in number of dynamic active grains per unit cross sectional area ( $C_d$ ) values is perceived for samples at low abrasive media viscosity. |
| Drill Bit Guided Abrasive Flow                        | Shankar et al.[63] | Helical fluted drill placed between the specimen, whi  | Drill diameter, oil concentration | SiC abrasives of mesh size 220   | Soft polymercarrier (softstyrene polymer),                | AISI1040, AISI 4340  | –                  | MR for AISI 4340& AISI 1040-0.55 & 0.65 mg    | Percentage change in Ra =40 & 45 for AISI 4340          | Surface roughness value of workpiece increase with increase in oil percentage in media and MR decrease with  |

| Process   | Author               | Working principle                                   | Hybridizing parameters  | Abrasive (type/size) | Media carrier   | Workpiece (size/material) | Extrusion pressure | Material removal rate | Change in surface roughness ( $\Delta R_a$ ) | Remarks  |
|---|----------------------|---|---|----------------------|---|---------------------------|--------------------|-----------------------|--|--|
| Finishing (DBG-AFF)                                   |                      | ch reorganizes the abrasives particles in AFM media |   |                      | processing oil (hydrocarbon oil)  |                           |                    |                       | and AISI1040                                 | increase in abrasive mesh size and oil percentage in media.  |
| Electrochemical Aided Abrasive Flow Machining (ECAFM) | Dabrowski et al.[48] | Polymeric electrolyte carries abrasive particles    | Abrasive concentration, media flow speed, Voltage, current and intensity. | $Al_2O_3$ and SiC    | Abrasive media synthesized by mixing polypropylene glycol and polyethylene glycol | Stainless steel           | 20-50 bar          |                       | $\Delta R_a=0.37\mu m$                       | Finishing on electrochemical assistance process depends on the selection of the appropriate abrasive paste |

## 2.2.5 Recent advances in abrasive flow finishing processes.

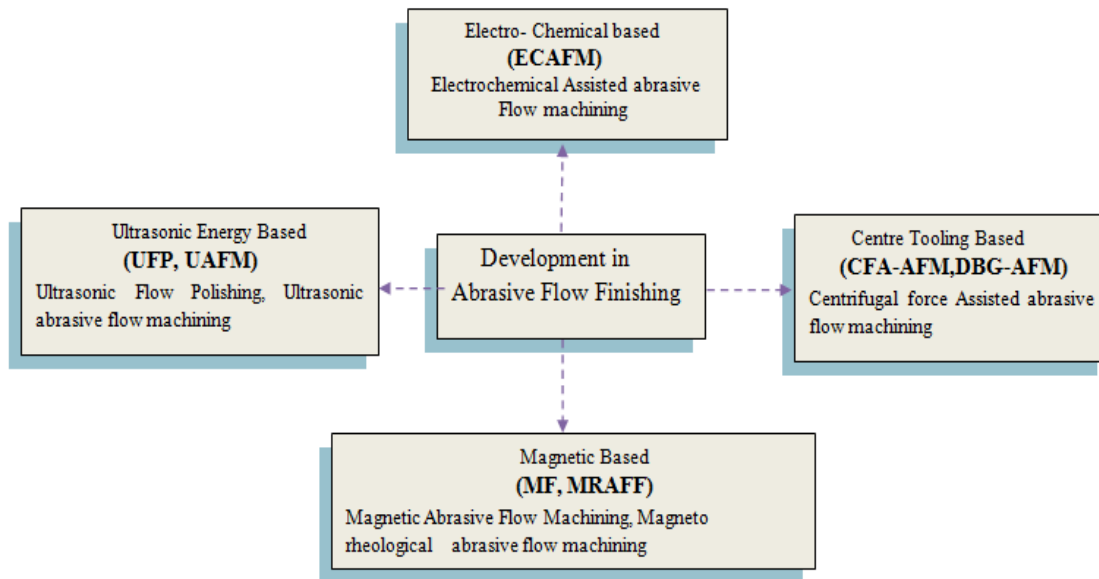


Figure 2.3 Recent development in abrasive flow finishing process

Many researchers are working to overcome the limitations, such as low surface finishing rate, and inability to correct the custom geometry, and at the same time to improve the surface quality, surface reliability and compressive residual stresses formed on the component surface profile. So to study the recent developments in AFF, abrasive flow finishing process has been classified as shown in Figure 2.3, based on different forces and energy.

### 2.2.5.1 Magnetic force assisted AFF

Major limitations of the Abrasive flow finishing process is the low material removal rate (MRR) and low surface quality, so for improvement in material removal rate (MRR), Singh and Shan [64] established a novel process called Magnetic abrasive flow machining process (MAFM) by incorporating magnetic energy with abrasive flow machining process. It was observed that using a magnetic energy and magnetic charged abrasive grits instead of regular abrasives in MAFF process will increase MRR and change in surface roughness value. Due to magnetic energy, abrasive particles are fascinated near

the inside surface integrity so abrasive concentration increased near the finishing surface which results in less no. of cycles are required for finishing the components. MRAFF technique is suitable for nano finishing of workpieces with complex surface profile for various industrial applications. From experimental study, they reported that improvement in surface roughness reduces with increase in magnetic energy at constant number of finishing cycles. After finishing, average surface roughness ( $R_a$ ) values of 30 nm were achieved for stainless steel and silicon nitride material workpieces [60]. Jha and Jain[65] developed a new finishing technique for complicated internal profiles utilizing magnetorheological polishing media. They reported that MRAFF gives better results (mechanism) over the rheological behavior of abrasive-suspended magnetorheological (MR) finishing fluid. MR fluid consists of carbonyl iron particles (CIPs) and silicon carbide abrasives suspended in a mixture of grease and mineral oil which is viscoplastic behavior, and shows a change in rheological property with an external applied magnetic field. Jha and Jain [66] developed a model for MRAFF technique for calculation of forces on abrasive grits for improvement in surface roughness value. They reported that degree of finishing force was influenced by the radial and tangential forces applied on abrasive grits due to CIPs organized in a columnar configuration in the existence of peripheral magnetic energy. During MRAFF, final surface roughness was mainly affected by mesh size of the CIPs abrasives in comparison with the regular abrasive size. In MRAFF process, Jha et al.[67] performed some experiments to study the influence of number of machining cycles and extrusion pressure on the improvement of surface roughness value of finished workpieces. At 3.75 MPa extrusion pressure, they found highest finishing quality of the surface and also found that actual finishing was acting after 200 finishing cycles while all loosely bonded burrs left from the finishing surface.

### 2.2.5.2 Centre tooling assisted AFF

Centrifugal-force-assisted abrasive flow machining (CFAAFM) process was introduced by Walia et al. [68] in which a revolving centrifugal force generating (CFG) rod was used inside the component flow path with abrasive media. They achieved the reduction in 70 to 80% finishing time by using the triangular-shaped CFG rod inside the workpiece finishing passage. The placing of CFG rod in the center and providing rotation to it increase the finishing rate by 70-80%.[69][70][71][72].

For improvement of surface finishing rate ( $\Delta Ra$ ) and MRR, Ravi Shankar et al.[59] developed a Rotational Abrasive Flow Finishing (R-AFF) setup by providing the rotatory motion to workpiece so that more active abrasive particles come into contact with workpiece finishing region. From experimental observation, they concluded that the resultant force that shears the workpiece surface peaks is greater in R-AFF process related to AFF process that results in higher material removal. They also concluded that as the number of machining cycles increase, change in surface roughness ( $\Delta Ra$ ) increases and also  $\Delta Ra$  increases as extrusion pressure and processing oil content increase till 6.5MPa and 10%, respectively, and then it starts decreasing gradually.

Ravi Shankar et al. [73] conducted some experiments for finishing Aluminium (Al) alloy and Al/SiC metal matrix composite material workpieces at various extrusion pressure and utilizing the different media composition to find the optimum conditions for higher change in roughness ( $\Delta Ra$ ). They concluded that R-AFF can finish 44% better in improvement in surface roughness ( $\Delta Ra$ ) and 81.8% more Material Removal related to the AFF technique and also R-AFF finished surfaces produced micro cross hatch arrays that help in increase in lubricant accumulating ability on the workpiece.

### 2.2.5.3 Ultrasonic force assisted AFF

Ultrasonic Flow Polishing (UFP) process [74] was developed in 1998, by combining the abrasive flow machining process and ultrasonic machining process to achieve a superior finishing surface with slight disintegrate to its shape or dimensional incorrectness. In this process significant improvement in surface finishing was achieved using 0.25 kw, 40 kHz ultrasonic power for finishing of Aluminium material workpieces.

A new hybrid finishing process called ultrasonic assisted magnetic abrasive finishing (UAMAF) developed by Muilk and Pandey [75] by integrating the ultrasonic vibrations and magnetic abrasive finishing (MAF) process to achieve surface roughness up to nanometric level. They achieved better finishing results than MAF process for AISI 52100 steel workpiece. In another work Muilk and Pandey [76] highlighted the mechanism of surface finishing in UAMAF. They studied the microscopic effects on surface quality ensuing from the interaction of abrasives with workpiece profile. For studying the material removal and wear behavior during finishing, they used surface roughness measurement, scanning electron and atomic force microscopy. In UAMAF process, during finishing action mainly two forces act namely normal force and finishing torque [77]. During finishing process, the supply voltage to the electromagnet and finishing gap have been found to be the important factors affecting the finishing quality of the surface.

In another studies by Venkatesh et al.[78], the ultrasonic assisted abrasive flow machining (UAAFMM) process was used for finishing to EN8 steel bevel gears. In UAAFMM, ultrasonic vibrations influence the abrasives to interrelate with the finishing profile to an angular shift ' $\theta$ '. They used Computational Fluid dynamics (CFD) simulation technique for velocity and pressure profiles to observe the finishing media properties in UAAFMM process and compared to the traditional AFF. Kala and Pandey[79] studied the finishing

performance of ultrasonic-assisted double-disk magnetic abrasive finishing process for two different paramagnetic materials (copper alloy and stainless steel) with different mechanical properties such as flow stress, hardness and shear modulus.

#### **2.2.5.4 Electrochemical-based AFF**

Dabrowski et al.[80] developed an electrochemical-assisted abrasive flow machine (ECAFM), using the mixture of water-gels (sodium iodide salt and polyethylene glycol with potassium cyanide) and polymeric electrolytes such as gelled polymers (polypropylene glycol) as base material. During finishing process polymeric electrolyte abrasive media is enforced through the slight inter-electrode opening that resulted in superior flow convection of the polymer electrolyte media, which proceeds like a semi-liquid paste. Dabrowski et al.[48] performed experiments for finishing flat geometry workpieces using the polymer electrolytes as gelled polymers and water-gels based on acrylamide. From this study, they concluded that finishing time can be reduced by using the electrochemical assistance in finishing process.

Brar et al.[81] also developed a hybrid form of electrochemical machining (ECM) and abrasive flow machining (AFM) process, for the fine finishing of internal holes or prismatic respites. In fabricated electrochemical-aided abrasive flow machining (ECA<sup>2</sup>FM) setup, higher material removal was perceived due to the synergetic consequence of ECM and AFM processes. Also, this process was found beneficial for the industries which have thin/delicate and hard alloy workpieces. In another work, Brar et al.[82] performed experiments for internal surface finishing of hollow cylindrical brass components using electro-chemical aided abrasive flow machining (ECA<sup>2</sup>FM) process. During finishing process it was found that higher material removal was observed in the ECA<sup>2</sup>FM process over AFM process, due to simultaneous material abrasion and erosion due to AFM and ECM machining actions.



## **2.2.6 Development on finishing of hard materials and different work piece**

### **geometries:**

In current manufacturing industries, demand for this process is increasing continuously because of development of a wide variety of hard materials and requirements of high precision components with superior surface quality. So many researchers are working for finishing different types of materials and complex geometrical shape workpieces.

Williams et al.[83] used abrasive flow machining (AFM) process to finish conformal cooling/heating channels in profiled edge laminae (PEL) rapid tooling (RT) component. They fabricated and assembled PEL tools of both material aluminium and steel for finishing by AFM. After finishing, they found significantly enhanced finish in the channels for aluminium and steel PEL tooling.

Finishing of Carbon-carbon composites (C/Cs) are very challenging because of their non-homogeneity, anisotropy, hardness and inherent brittleness properties. Some experimental investigations were carried out by Ravikumar et al. [84] for finishing initially finished manually 3-D C/Cs workpieces using SBR based finishing media. So after finishing they observed finest surface finish at a media extrusion pressure of 6 MPa and 150 finishing cycles by a finishing media having 70wt% SiC abrasive of 220 grain size and 12wt% processing oil.

Mali and Manna[38] conducted experiments for finishing the metal matrix composite (MMCs) of Al/15 wt% SiCp material. Scanning electron micrograph (SEM) technique was used to investigate the effectiveness of finishing performance. They reported the abrasive mesh size as a supreme important factor for metal removal and an improvement in surface roughness height ( $\Delta Re$ ). They also reported that percentage of abrasive concentration in AFM media as supreme important factor for average surface roughness ( $R_a$ ), MR and  $\Delta Re$ .

For finishing workpieces of composite materials with a high percentage of SiC (e.g., 20–60%SiC in Al/SiC composites) Sushil et al. [85] used abrasive flow finishing process with liquid silicone (carrier) based abrasive media. From the ANOVA analysis, media extrusion pressure was found the supreme important variable for MRR and  $\Delta R_a$ . After experimenting they found the Optimal MRR rendering to the confirmation experiment as  $8.81 \times 10^{-6}$  g/s, and anticipated value as  $8.59 \times 10^{-6}$  g/s.

Finishing of complex freeform surfaces is very challenging in current manufacturing industries. For overcoming the difficulty of finishing the freeform surface Sidpara and Jain [86] developed magneto-rheological fluid-based finishing method for finishing knee joint implant, which has intricate freeform planes. They developed water-based MR fluid by addition of the chemicals that react with titanium material, such as hydrofluoric acid (HF) and nitric acid (HNO<sub>3</sub>). After finishing the knee joint implant of titanium material the best final finishing value attained was 28 nm.

For finishing nonmagnetic stainless steel cylindrical work pieces Judal and Yadava [87] developed a cylindrical electrochemical magnetic abrasive machining (C-EMAM) setup and compared the outcomes with magnetic abrasive machining (MAM) process. After an experimental investigation on the C-EMAM process, they observed MR increases by 500–1,800%, and  $R_a$  decreases by 40–50% as compared to MAM at 0.298 T.

Abrasive flow finishing process has also been used for finishing plastic gears which is a significant invention for injection molding tools industries. Kenda et al.[88] used abrasive flow machining technique to finish the plastic gear and improved the surface roughness value from  $R_a=0.68 \mu\text{m}$  to  $R_a=0.08 \mu\text{m}$  in 120 sec.

Finishing of Ti alloy is very challenging for current industries. So for finishing the Ti alloy Howard and Cheng [89] conducted some experiments on AFM process to observe the effect of machining variable on surface quality. After finishing they achieved up to

1.5 mm the edge rounding in finishing of titanium alloy 6Al4V using media with abrasive grit size 700mm.

### **2.3 Research gap**

The literature review on rheological evaluation and abrasive flow machining process reveals the following knowledge gap, through which the objectives of present work can be set.

- There is a need of low cost and environmental friendly alternative media for machining the components.
- Only few researchers focused on the property evaluation of base consumables with different additive gels, and how these gels affect the polish precision in AFF.
- Environmental sustainable and affordable media is extensively required for the finishing industries
- There is an essential need to develop adjustable fixtures (tooling) for different geometries so as to increase productivity and decrease the overall cost of the design and manufacture in AFM.
- Necessity of low cost abrasive flow machine is required for small scale industries which can be integrated with other shop floor equipment's for batch production.
- For better utility of the AFF process there is a need for Industry-oriented practices for better understanding of performance measure parameters
- Very few researchers worked on finishing hard materials like carbides, ceramics etc. on abrasive flow machine.
- Only few focused on hybrid-Abrasive Flow Machining to improve MRR and finishing rate but still there is a need to explore this process.

## **2.4 Objective and scope of present work**

The detailed objectives of my research work according to research gap are as following

1. To synthesize different grades of polymer abrasive gels as a low cost environmental friendly media.
2. To characterize and evaluate the rheology of developed abrasive polymer gel.
3. Design and fabrication of the tooling for finishing internal passage of standard industrial components in Abrasive Flow Machining setup using the synthesized polymer abrasive gel.
4. Design and fabrication of low cost one way Abrasive Flow Machining Setup for finishing the internal passages of industrial components.
5. Experimental investigation on developed AFM setup for finishing internal passage of industrial components.
6. Optimization of process parameters of abrasive flow machining.

## **Chapter 3 Characterization and Rheological Study of PAG**

---

### **3.1 Introduction**

Abrasive media plays a major role in finishing because of its ability to precisely finish the selected surfaces along the media flow passage. A polymer abrasive gel (PAG) based alternative media for Abrasive Flow Machining (AFM) was developed keeping in view the properties like adhesiveness, self-deformability, viscoelasticity, porosity and permeability (using natural polymer base, additives, and abrasives of different mesh sizes and concentration). In this study, characterization of developed polymer abrasive gels (PAGs) were done by using Field Emission Scanning Electron Microscopy (FESEM), Thermogravimetric Analysis (TGA) and Fourier Transform Infrared Spectroscopy (FTIR). The Power law, Bingham plastic, and Herschel–bulkley fluid models were used to illustrate the rheological nature of developed PAGs. Experimental analyses were carried out using statistical design of experiments (DOE) to characterize rheological properties of developed PAGs. The effects of the control variables on viscosity of PAGs were analysed using Taguchi technique. Analysis of variance (ANOVA) was used to determine contribution of each control variable on yield stress and viscosity of polymer abrasive gels.

Researchers have attempted to enhance the performance capabilities of AFM and also to develop a superior alternative to commercially available media. Media usually contains two major components as the carrier (a viscoelastic material, e.g. gels and oils) and the solid phase (abrasives and other particles to assist the abrasion). The physical (appearance), chemical (constituents and their proportion in the carrier, inertness, etc.) and rheological (viscosity, shear stress, yield stress, thixotropy, critical strain, critical

temperature, etc.) characteristics significantly influence the overall performance of the AFM process.

A polymer based media was developed containing ester group and naphthanic based processing oil for varying the viscosity of media. FTIR and TGA tests were carried out for characterization of the developed media. After experimentation, it was concluded that average surface roughness ( $R_a$ ) and material removal rate (MRR) improves with increase in abrasive concentration and extrusion pressure [49].

An alternative media has also been developed using co-polymeric soft styrene butadiene based polymer, plasticizer and abrasives. Rheological characterization of media was done to study the effect of creep recovery, shear viscosity, stress relaxation and storage modulus on the MRR and the  $R_a$  during finishing of Al alloy as well as its metal matrix composites using rotational abrasive flow finishing (R-AFF). It was found that in butyl-based rubber media, temperature, shear rate and creeping time had a significant impact on rheological properties and percentage ingredients in the media [45].

AFM media was developed using abrasive particles and silicone rubber to perform experiments for removing recast layers on the electro discharge machined (EDM) surfaces. After experimentation high efficiency in AFM was observed with silicon media of high viscosity at constant temperature [44].

A butyl rubber viscoelastic carrier based AFM media was developed and characterized. During rheological observation, temperature, shear rate, creeping time and frequency were found to be mainly impacting the rheological properties. It was also investigated that the oil loading beyond 12% reduced the surface quality while using abrasive mesh size of 220 [46].

Studies have been made to create the power law in CFD-ACE+ software using relations of viscosities and shear rates of different abrasive media. The flow model of abrasive

media was set up by the power law and the comparisons between the simulated and experimental results were made. The simulated results indicated that the media with high viscosity could fully deform in the complex hole than the media with low viscosity because media with high viscosity generated a better shear force than the media with low viscosity in the similar area [28].

To study effects of abrasive concentration, mesh size and temperature of media on its viscosity some experiments were done using a capillary viscometer. Their results indicated that the viscosity of the media increases with increase in the abrasive concentration and decreases with the increase in abrasive mesh size and media temperature. During finishing with the developed media, an increase in material removal and decrease in surface roughness value was observed with increase in viscosity [51].

Viscosity and fluidity could be adjusted during the processing period in self-modulating abrasive media. Experiments were made on a fabricated complex micro channel of stainless steel (SUS304) using developed abrasive media. During experimentation in AFM, results proved that, at high viscosity and abrasive concentration the surface roughness of the micro channel with coarse particle size is lower than that of a media with fine particle size. Machining quality of the micro channel also improves as the extrusion pressure and the machining time increase due to increase in the fluidity of the media [52].

Styrene butadiene rubber (SBR) based media was developed and studies were made using TGA and characterized by mechanical, as well as rheological properties with the help of a universal testing machine and a rheometer. After rheological investigation, it was found parameters; namely, strain, temperature, shear rate, time of applied constant stress, cyclic loading mainly impacted on mechanical and rheological properties of the developed media. After finishing on AFM setup, 88% improvement in surface finish was found using the SBR based media[47].

Natural polymer based environmental friendly AFM media synthesis was done to form polymer abrasive gels (PAGs) of various grades and upon trial on a developed AFM setup the results were encouraging. Taguchi technique was used to analyze the effect of AFM process variables on surface finish and material removal. Based on experimental study [38], it was observed that abrasive mesh size and percentage of abrasive concentration in media are the most significant parameters for material removal and improvement in surface roughness. Also viscosity of media was found as significant parameter for material removal for the considered size and shape of the work-piece. Looking at the multiple variables affecting the output of the system, artificial neural network (ANN) technique was used to simulate the machining variables during the finishing of Al/SiC<sub>p</sub> metal matrix composites (MMCs) components by abrasive flow machining [35].

This chapter explains the study of rheological properties like yield stress and viscosity of the developed polymer abrasive gels (PAGs) based AFM media under the influence of the shear rate that help in understanding of mechanism and modelling of finishing process. To study the thermal stability and nature of compounds present in media, TGA and FTIR tests were used. For characterizing the rheological properties of developed PAG, the media compositions have been varied at different shear rate. Effect of temperature change on rheological properties of developed PAG was also studied.

### **3.1.1 Importance of rheology**

Since most of polymers are amorphous in nature, their rheological characterization is a challenge. Polymer's rheological nature depends on polymer molecules shape, structure and interaction. A polymer consists of a large number of molecular chains and these chains can bend, coil and twist, leading to extensive entanglement and intertwining with neighbouring chains. These complex molecular entanglements of chains contribute to a large extent in determining important mechanical and thermal properties of polymers.



Normally AFM medium is complex viscoelastic material in which different viscous and elastic properties under varying condition of shear rate, stress, strain, time and temperature. This viscoelastic medium when left at rest, with the effect of natural gravitational force, it slowly flows like a fluid. When rolled into a ball and bounced, it behaves like an elastic solid ball as well as when stretched rapidly; it breaks as a solid plastic piece. These unique properties demonstrate the importance of evaluation of rheology properties to understand its behavior during finishing process.

Study of static and dynamic rheological properties helps in understanding the pattern and aggressiveness of abrasive action. Abrasion is high where the medium flow experiences high restriction and travel with high velocity [51]. In this study, shear rate, yield stress are controlled to measure various properties such as apparent viscosity.

### **3.1.2 Test equipment**

Complete rheological experiments are carried out using a commercial available rotational Rheometer with temperature control (Anton Paar Rheolab QC) (Figure 3.1). The technical specifications of Rheometer are shown in Table 3.1.



**Figure 3.1 Rotational Rheometer with temperature control.**

**Table 3.1 Technical Specifications**

|                              |                              |
|------------------------------|------------------------------|
| Speed :                      | 0.01 to 1200***1/min         |
| Torque :                     | 0.25 to 75 m Nm              |
| Shear stress* :              | 0.5 to 30000 Pa              |
| Shear rate*:                 | 10 <sup>-2</sup> to 4000 1/s |
| Viscosity measuring range* : | 1 to 109 m Pas               |
| Temperature range ** :       | -20 to 180 °C                |
| Dimensions : W x H x D       | 300 x 720 x 350 mm.          |

\*Depends on the measuring system used

\*\* Depends on the temperature control device used

\*\*\* Max. speed with torque derating

### 3.2 Synthesization of PAG

Major constituents of PAG are polymer carrier, liquid synthesizer and abrasive particles. PAG is prepared by thoroughly mixing abrasives of various mesh sizes in the semisolid polymer carrier prepared in bulk with different weight percentages whose viscosity could be controlled by the amount of liquid synthesizer. Similarly PAG of 25 different viscosity grades were prepared as shown in Table 3.2 based on the percentage of liquid synthesizer added into the abrasive mixed polymer carrier. 11 to 27 % of liquid synthesizer is added into the abrasive mixed polymer to obtain various media viscosity grades. Different mesh sizes of silicon carbon (SiC) abrasive are used in synthesization of AFM media. The prepared PAG samples are given nomenclature and a method of nomenclature for a sample is as shown in Figure 3.2.

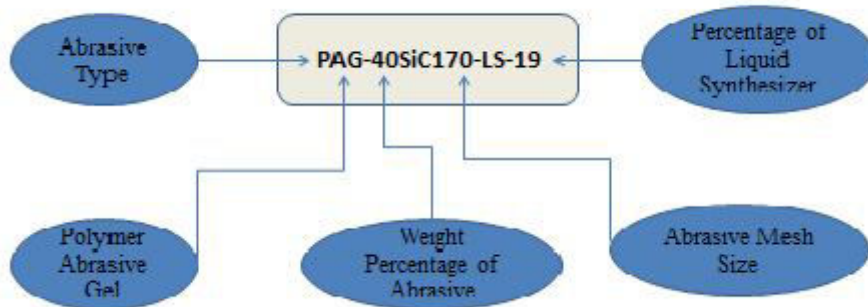


**Figure 3.2 Nomenclature of developed Polymer Abrasive Gel (PAG)**

**Table 3.2 Different weight percentage of constituents of polymer abrasive gel**

| Sr.No. | Ab. Conc. | Mesh Size | LS % | Nomenclature        |
|--------|-----------|-----------|------|---------------------|
| 1      | 30        | 120       | 11   | PAG 30SiC120-LS-11  |
| 2      | 30        | 170       | 15   | PAG 30SiC170-LS-15  |
| 3      | 30        | 220       | 19   | PAG 30SiC220-LS-19  |
| 4      | 30        | 270       | 23   | PAG 30SiC270-LS-23  |
| 5      | 30        | 320       | 27   | PAG 30SiC320-LS-27  |
| 6      | 40        | 120       | 15   | PAG 40SiC120-LS-15  |
| 7      | 40        | 170       | 19   | PAG 40SiC170-LS-19  |
| 8      | 40        | 220       | 23   | PAG 40SiC220-LS-23  |
| 9      | 40        | 270       | 27   | PAG 40SiC270-LS-27  |
| 10     | 40        | 320       | 11   | PAG 40SiC320-LS-11  |
| 11     | 50        | 120       | 19   | PAG 50SiC120-LS-19  |
| 12     | 50        | 170       | 23   | PAG 50SiC170-LS-23  |
| 13     | 50        | 220       | 27   | PAG 50SiC220-LS-27  |
| 14     | 50        | 270       | 11   | PAG 50SiC270-LS-11  |
| 15     | 50        | 320       | 15   | PAG 50SiC320-LS-15  |
| 16     | 60        | 120       | 23   | PAG 60SiC120-LS-23  |
| 17     | 60        | 170       | 27   | PAG 60SiC170-LS-27  |
| 18     | 60        | 220       | 11   | PAG 60SiC220-LS-11  |
| 19     | 60        | 270       | 15   | PAG 60SiC270-LS-15  |
| 20     | 60        | 320       | 19   | PAG 60SiC320-LS-19  |
| 21     | 70        | 120       | 27   | PAG 70SiC120-LS-27  |
| 22     | 70        | 170       | 11   | PAG 70SiC170-LS-11  |
| 23     | 70        | 220       | 15   | PAG 70SiC220-LS-15  |
| 24     | 70        | 270       | 19   | PAG 70SiC270-LS-19  |
| 25     | 70        | 320       | 23   | PAG 70SiC320-LS-23. |

### 3.3 Characterization of PAG

#### 3.3.1 FESEM analysis

To check abrasive geometry and bonding with polymeric gel, randomly selected samples of PAG were tested by field emission scanning electron microscope (FESEM) for determination of the orientation of its constituents. Experiments were carried out on NOVA Nano SEM 450 instrument. FESEM images shows that the abrasives have sharp cutting edges which helps in material removal of work piece surface which is to be finished. The average sizes of abrasives were observed to be 31 to 102 micron ( $\mu\text{m}$ ) (Figure 3.2 to 3.4).

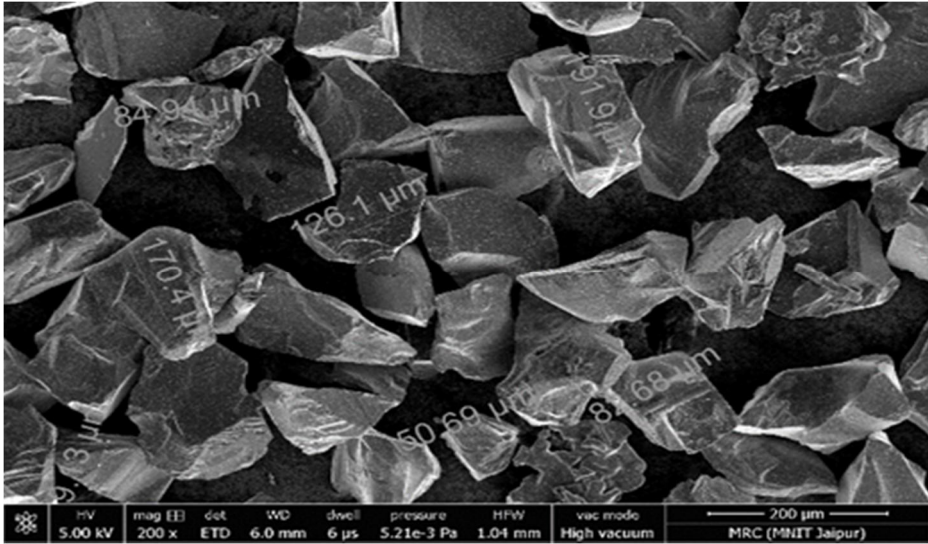


Figure 3.3 SiC abrasive 120 Mesh Size

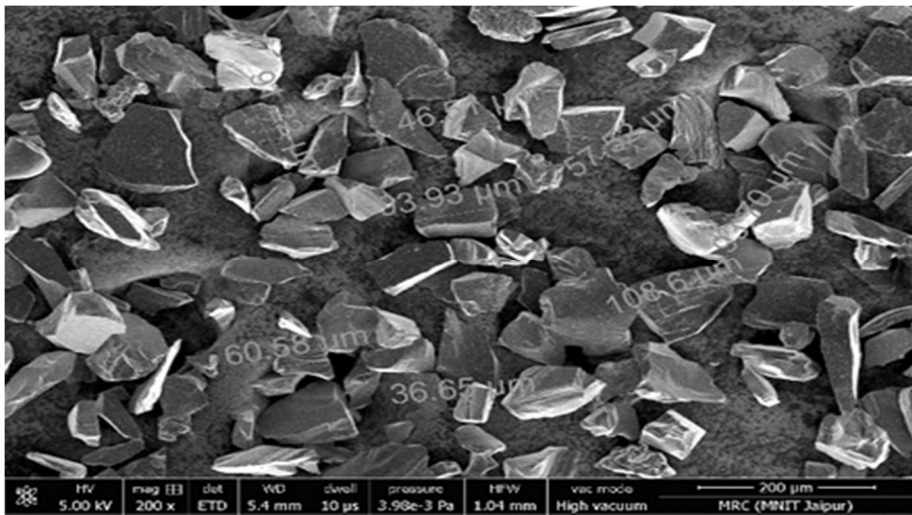


Figure 3.4 SiC abrasive 220 Mesh size

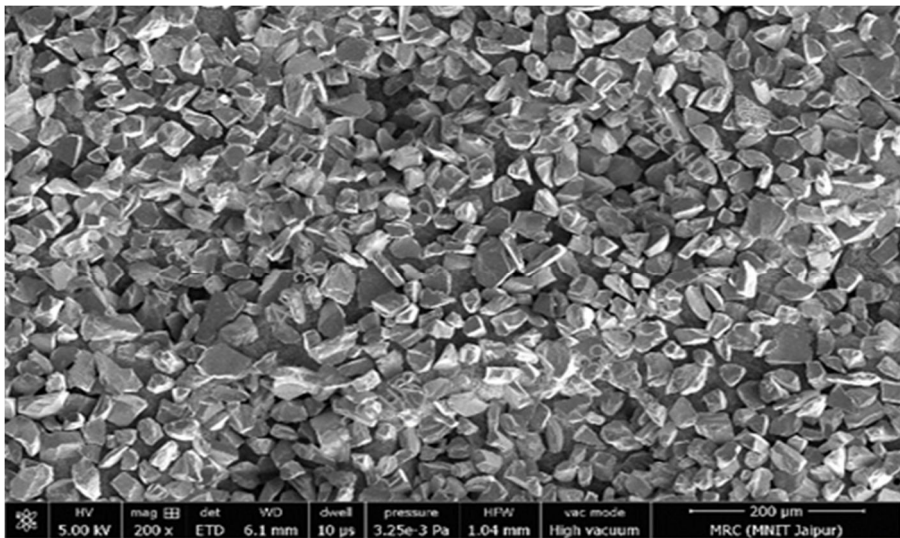


Figure 3.5 SiC abrasive 320 Mesh Size

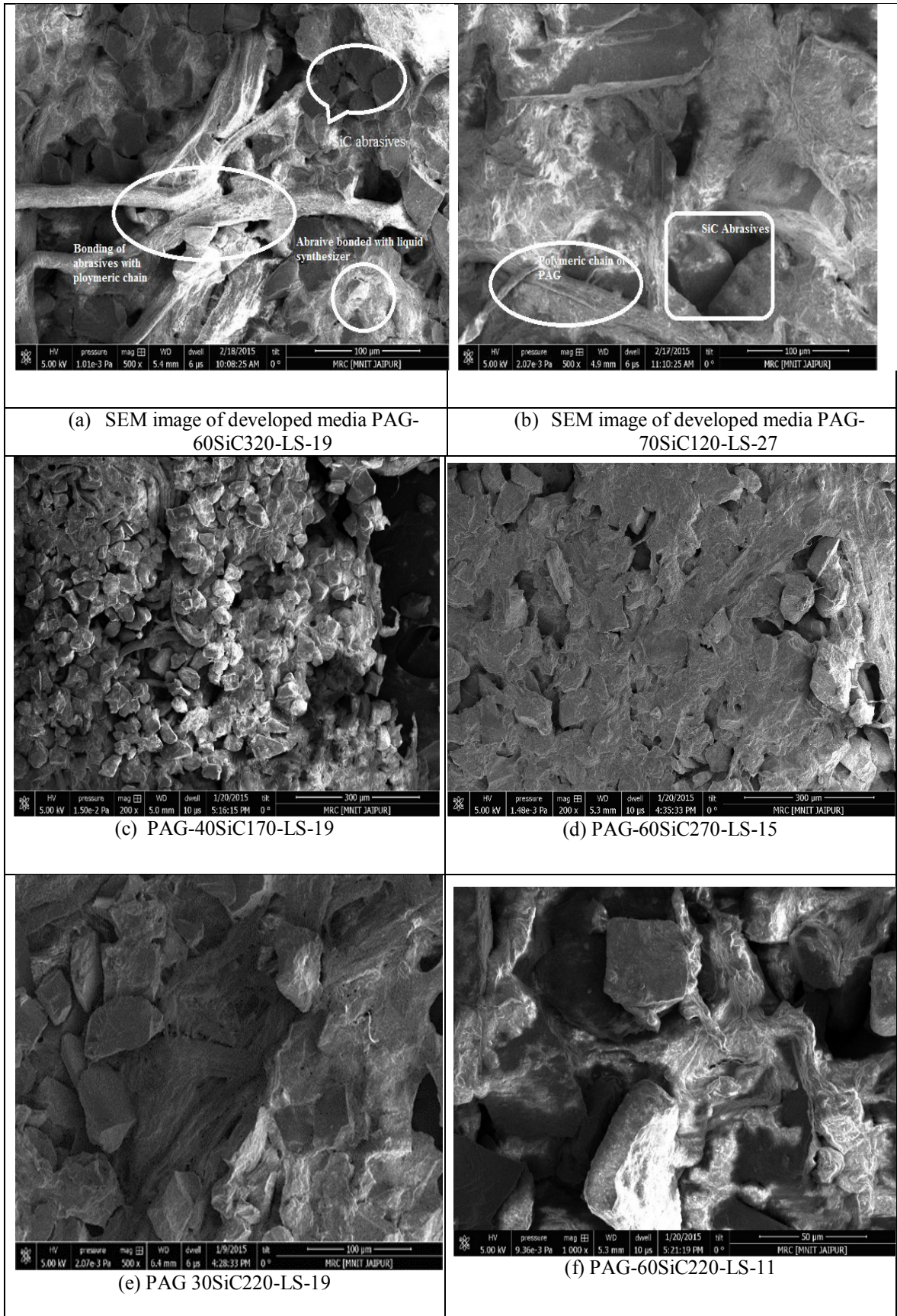


Figure 3.6 FESEM Images of developed PAG showing interference of abrasives and base

Figure 3.5 shows the interface between the constituents of the additives polymeric base and abrasive particles. The polymeric constituents are activated by the additives which generate enough adhesive force to hold the abrasive particles in place even after continuous use in AFM. Figure 3.5 (a) to (f) shows abrasives surrounded by the adhesive forces of the base material in increasing magnification. It is clearly visible in Figure 3.5 (a) and Figure 3.5 (b) that the reason of abrasives bonding in the media is the polymeric chains activated by the additives. SEM images for all 25 PAG samples are shown in annexure F.

### 3.3.2 FTIR analysis

FTIR identifies chemical bonds in a molecule by producing an infrared absorption spectrum. The spectra produce a profile of the sample, a distinctive molecular fingerprint that can be used to screen and scan samples for many different components. FTIR is an effective analytical instrument for detecting functional groups and characterizing covalent bonding information.

FTIR spectrometer operates on a different principle called Fourier transform. The mathematical expression of Fourier transform can be expressed as,

$$f(x) = \frac{1}{2\pi} \int_{-\infty}^{+\infty} F(\omega) e^{-i\omega x} d\omega \quad \dots(3.1)$$

Where  $\omega$  is angular frequency and  $x$  is the optical path difference in our case.  $F(\omega)$  is the spectrum and  $f(x)$  is called the interferogram. It is clear that if the interferogram  $f(x)$ , is determined experimentally, the spectrum  $F(\omega)$  can be obtained by using Fourier transform.

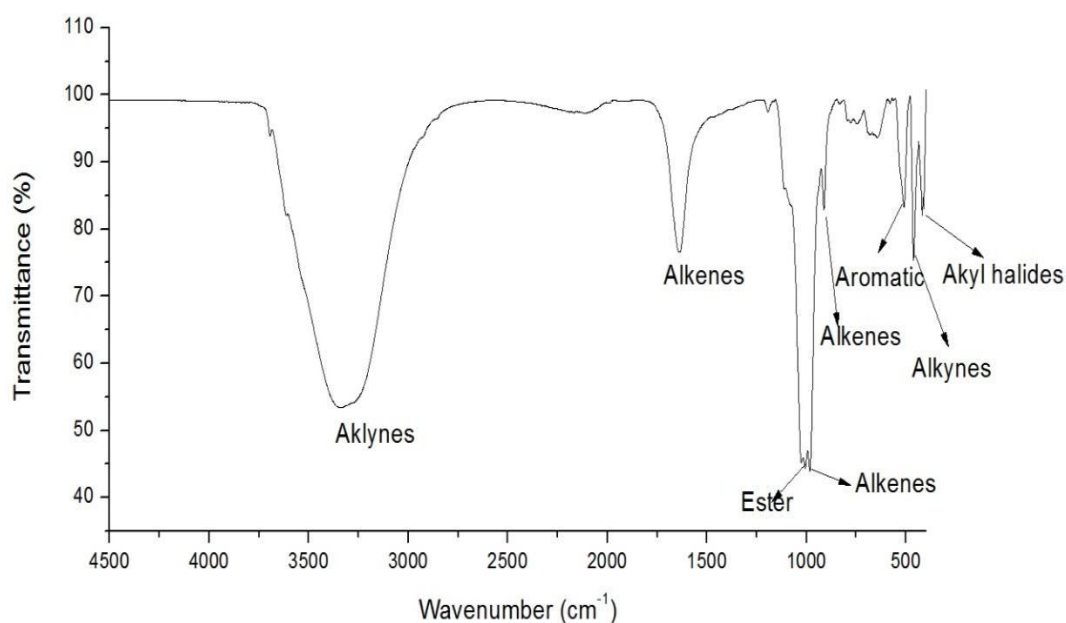


**Figure 3.7 FTIR analysis of developed alternative Polymer Abrasive Gel**

For developing the new alternative carrier, it is very important to know the details of structure of compound that is used for synthesizing the abrasive polymer gel. So FTIR analysis is used to identify the structure and type of compounds presented in carrier. Perkin Elmer Frontier FT-IR/FIR Spectrometer is used for FTIR analysis. Figure 3.6 shows the FTIR analysis of developed media. The functional groups are identified using IR chart, at different wave number. During FTIR analysis alkenes, alkynes, esters, aromatic and alkyl halides groups are found to be present in PAG. It was observed that alkenes, esters, amines and aromatic are more dominating which provides the elastic nature, thermal stability and tensile strength to the PAG. But major alkenes and alkynes present in PAG that shows presence of these groups are more dominating which provided elastic nature to media.

### 3.3.3 TGA

TGA is a method of thermal analysis in which changes in physical and chemical properties of materials are measured as a function of increasing temperature (with constant heating rate) or as a function of time (with constant temperature and/or constant mass loss). TGA experiments were carried out on Simultaneous Thermal Analysers (Make Perkin Elmer) under dynamic N<sub>2</sub> gas atmosphere of 200 ml/min flow rate, with heating rate of 10° C cover a range of 20° C to 300° C.

Total 25 samples have been prepared and analysed according to experimental design Taguchi L<sub>25</sub> orthogonal array as shown in Table 3.3.

**Table 3.3 Coded levels and corresponding actual values of control factors**

| <b>Factor</b>            | <b>Level 1</b> | <b>Level 2</b> | <b>Level 3</b> | <b>Level 4</b> | <b>Level 5</b> |
|--------------------------|----------------|----------------|----------------|----------------|----------------|
| Mesh size                | 120            | 170            | 220            | 270            | 320            |
| % abrasive concentration | 30             | 40             | 50             | 60             | 70             |
| % liquid synthesizer     | 11             | 15             | 19             | 23             | 27             |

In Figure 3.7 (a), (b), (c), TGA graphs for three random samples were shown representing the critical temperature limit. Figure 3.7 (a) shows, TGA analysis of developed PAG at different abrasive concentration, abrasive mesh size and percentage of liquid synthesizer, where the effect of temperature on derivative weight loss during heating of media is presented.

Analysis of variance is used to know variables which have most significant effect on the critical temperature of PAG. Table 3.4 shows summary of experiments done at different media composition and response variable i.e. critical temperature. TGA graphs for all PAG 25 sample are shown in Annexure E.



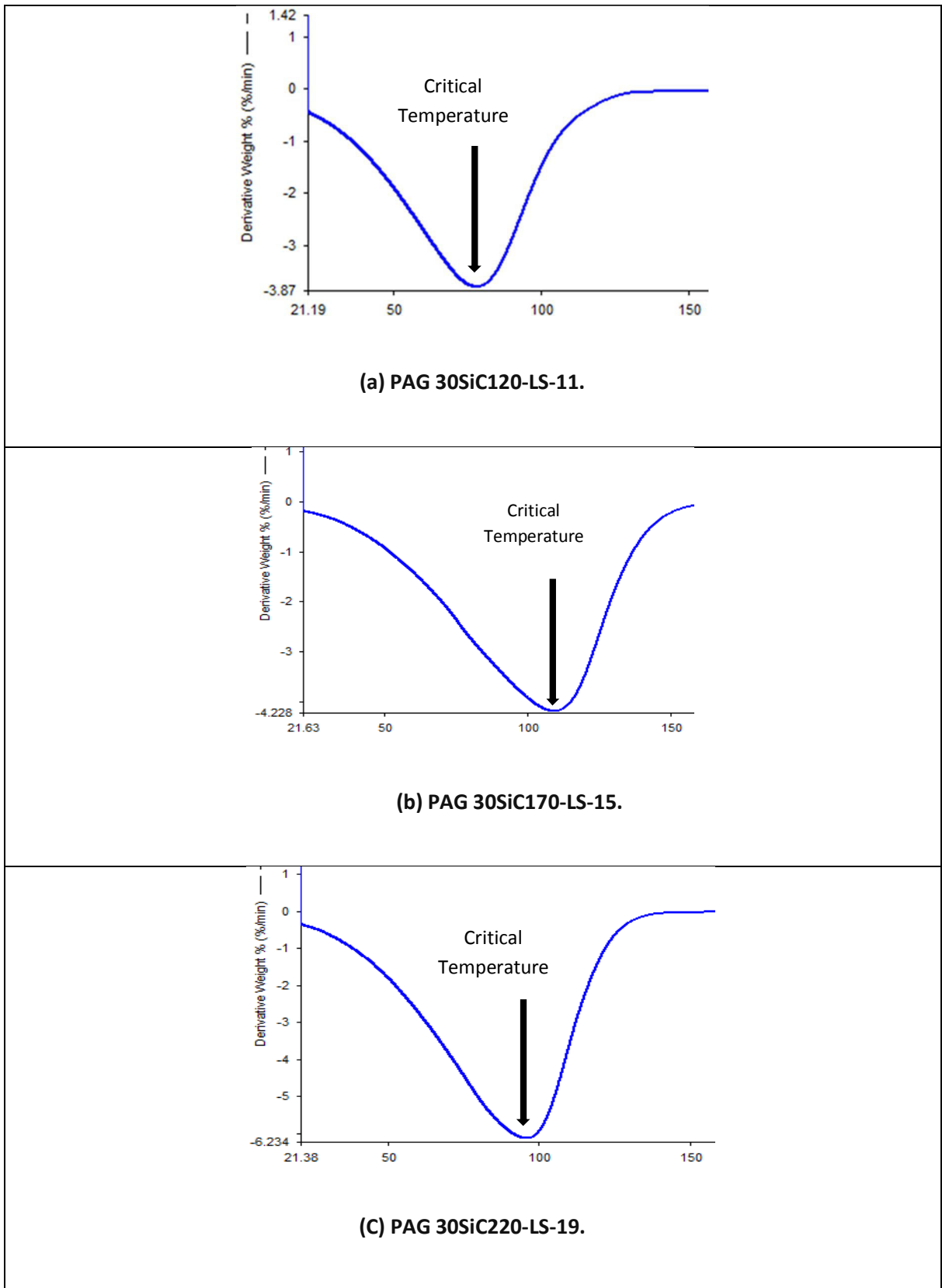


Figure 3.8 TGA graphs of different PAG sample

**Table 3.4 Critical temperature for different PAG**

| <b>Sr. No.</b> | <b>Ab Conc. (%)</b> | <b>Mesh Size</b> | <b>LS %</b> | <b>Critical Temp.(°C)</b> |
|----------------|---------------------|------------------|-------------|---------------------------|
| 1              | 30                  | 120              | 11          | 78.43                     |
| 2              | 30                  | 170              | 15          | 109.59                    |
| 3              | 30                  | 220              | 19          | 95.99                     |
| 4              | 30                  | 270              | 23          | 114.18                    |
| 5              | 30                  | 320              | 27          | 99.14                     |
| 6              | 40                  | 120              | 15          | 115.28                    |
| 7              | 40                  | 170              | 19          | 91.85                     |
| 8              | 40                  | 220              | 23          | 117.55                    |
| 9              | 40                  | 270              | 27          | 126.37                    |
| 10             | 40                  | 320              | 11          | 91.26                     |
| 11             | 50                  | 120              | 19          | 81.14                     |
| 12             | 50                  | 170              | 23          | 107.35                    |
| 13             | 50                  | 220              | 27          | 101.71                    |
| 14             | 50                  | 270              | 11          | 103.96                    |
| 15             | 50                  | 320              | 15          | 108.88                    |
| 16             | 60                  | 120              | 23          | 87.25                     |
| 17             | 60                  | 170              | 27          | 102.90                    |
| 18             | 60                  | 220              | 11          | 95.09                     |
| 19             | 60                  | 270              | 15          | 108.58                    |
| 20             | 60                  | 320              | 19          | 103.11                    |
| 21             | 70                  | 120              | 27          | 91.84                     |
| 22             | 70                  | 170              | 11          | 73.82                     |
| 23             | 70                  | 220              | 15          | 94.44                     |
| 24             | 70                  | 270              | 19          | 83.47                     |
| 25             | 70                  | 320              | 23          | 90.20                     |

### 3.3.3.1 ANOVA for critical temperature

The analysis of variance (ANOVA) of experimental results after neglecting contribution of all the insignificant variables is given in Table 3.5.

**Table 3.5 ANOVA results after experimentation**

| Source        | Sum of Square | D.O.F. | Mean Square | F    | Prob>F  | Percentage contribution |
|---------------|---------------|--------|-------------|------|---------|-------------------------|
| Ab. Conc. (%) | 1212.12       | 4      | 303.031     | 5.32 | 0.0106* | 29.82                   |
| L.S.(%)       | 1448.01       | 4      | 362.003     | 6.36 | 0.0055* | 35.62                   |
| M.S.          | 720.83        | 4      | 180.207     | 3.17 | 0.0542  | 17.73                   |
| Error         | 683.21        | 12     | 56.934      |      |         | 16.80                   |
| Total         | 4064.17       | 24     |             |      |         |                         |

\*Significant

For removing the insignificant variables, model reduction techniques can be used for improvement of model [90]. It is important to check the model hierarchy before reducing insignificant terms. According to hierarchy principle if a model contains a higher order term, it should also contain all of the lower-order terms that comprise it. The model F value 6.36 implies that liquid synthesizer percentage in liquid is most significant for thermal stability of developed media. If the values of 'Prob >F' is less than 0.05 (significance level), then it indicates that the model term is significant. From ANOVA, abrasive concentration and liquid synthesizer (LS) are only significant parameters which affect the critical temperature of TGA analysis. Percentage contribution for LS and abrasive concentration is found 35.62% and 29.82% respectively.

Final equation in term of actual variables is given as:-

$$\text{Critical Temp.} = 91.7272 + 0.6928 \text{ LS} + 0.05134 \text{ M.S.} - 0.345 \text{ Ab. Conc} \quad \dots(3.2)$$

Figure 3.8 shows the signal to noise ratio for critical temperature, and optimum level is observed as 40 abrasive concentrations, 270 mesh size and 15% liquid synthesizer.

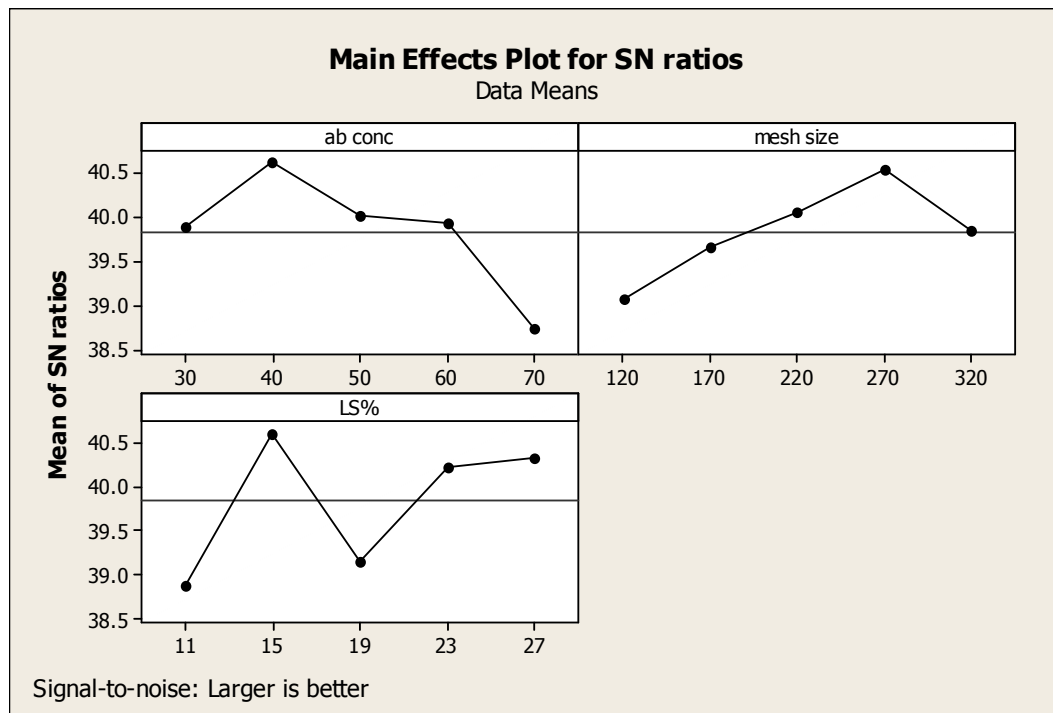


Figure 3.9 SN ratio for critical temperature

### 3.4 Rheological study

Characterization of rheological properties such as yield stress and viscosity are very important for finishing performance. The Power law, Bingham plastic and Herschel–bulkley are major models used to define the behavior of viscoplastic fluid. Different variables of rheology were characterized using the data obtained from rheometer in terms of shear yield stress, apparent viscosity and shear rate.

#### 3.4.1 Power law fluid:

Power law model is used mainly to defines the shear-thinning and shear thickening behavior of fluids [91].

$$\sigma = K\dot{\gamma}^n \quad \dots (3.3)$$

Where,  $K$  is consistency coefficient

Exponent  $n$  is the flow behavior index

For Newtonian fluid ( $n = 1$ ), the consistency index  $K$  is identically equal to the viscosity of the fluid,  $\eta$ .

When the magnitude of  $n < 1$  the fluid is shear-thinning and when  $n > 1$  the fluid is shear-thickening in nature.

Taking logarithmic of equation (3.3)

$$\log \sigma = \log K + n \log \dot{\gamma} \quad (3.4)$$

The parameters  $K$  and  $n$  are determined from a plot of  $\log \sigma$  versus  $\log \dot{\gamma}$ , and the resulting straight line's intercept is  $\log K$  and the slope is  $n$ .

#### 3.4.2 Bingham plastic model:

This model shows that developed polymer abrasive gel acts like rigid fluid before a critical shear stress value is achieved, known as yield stress ( $\sigma_y$ ). Polymer abrasive gel beyond value of yield stress behaves as a Newtonian fluid [91].

Bingham plastic fluid with yield stress ( $\sigma_y$ ) is represented by

$$\sigma - \sigma_y = \eta' \dot{\gamma} \quad \dots (3.5)$$

$\eta'$  is called the Bingham plastic viscosity. Bingham plastic model can be described by straight lines in terms of shear rate and shear stress. Major two parameters  $\eta'$  and  $\sigma$  used to describe the Bingham plastic fluid behavior.

### 3.4.3 Hershel bulkley model:

Herschel–bulkley model is used to illustrate the rheological behavior of a Non-Newtonian fluid with shear thinning properties. Shear thinning properties of fluid shows decreased in apparent viscosity as shear rate increases [91].

Equation for Herschel bulkley Model

$$\sigma = \sigma_y + K\dot{\gamma}^n \quad \text{for } \sigma > \sigma_y \quad \dots(3.6)$$

Where  $K$  is the consistency index

$n$  is the power-law index if  $n < 1$  the fluid is shear-thinning behavior.

$\dot{\gamma}$  is shear rate ( $S^{-1}$ ),  $\sigma$  is shear stress (Pa),  $\sigma_y$  is yield stress

If the yield stress of a sample is known from an independent experiment values of  $K$  and  $n$  can be determined from graph of  $\log(\sigma - \sigma_y)$  and  $\log\dot{\gamma}$ .

Experimental results were fitted with Power law, Bingham plastic and Herschel–bulkley model. The values of their rheological parameters ( $\sigma_y$  - yield stress,  $K$ -consistency index, Exponent  $n$ -flow behavior index and  $\eta'$  - Bingham plastic viscosity) are shown in Table 3.6. Polymer abrasive gels of 25 samples have been synthesized according to detailed composition shown in design of experiment (Table 3.3).

### 3.4.4 Correlation coefficient of fluid models:

To study rheological properties of viscoelastic fluids majorly Power law, Bingham plastic and Herschel–bulkley model are found to have extensive use in the analysis of the flow behavior and simulation. The Correlation coefficient is derived to find the usefulness of these fluid models. It signifies the proportion of the variance in the dependent variable that is predictable from the independent variable derived from regression analysis. Figure

3.9 shows graphically fitting of model equations for above fluid models with actual experimental data (run no. 15).

**Table 3.6 Rheological variable for three selected model**

| Run no. | Power law<br>( $\sigma = K \dot{\gamma}^n$ ) |           | Bingham plastic model<br>( $\sigma - \sigma_y = \eta' \dot{\gamma}$ ) |                      | Herschel–bulkley<br>( $\sigma = \sigma_y + K \dot{\gamma}^n$ ) |            |         |
|---------|--|-----------|---|----------------------|--|------------|---------|
|         | $K$  | $n$       | $\sigma_y (Pa)$   | $\eta' (Pa \cdot s)$ | $\sigma_y (Pa)$  | $K$        | $n$     |
| 1       | 577.68                                       | -0.0805   | 447   | -0.6                 | 424.00   | -0.71175   | 0.88285 |
| 2       | 1,098.3                                      | 0.027427  | 1,157   | 1.41                 | 1206.30  | 0.00021458 | 3.7148  |
| 3       | 482.76                                       | 0.14736   | 632.89  | 4.2784               | 1160.00  | 7,097      | 0.01    |
| 4       | 297.83                                       | 0.12425   | 142.17  | 6.891                | 314.66   | 0.0068464  | 3.001   |
| 5       | 408.22                                       | 0.1421    | 545.14  | 3.4109               | 1220.50  | 9934.9     | 0.01    |
| 6       | 440.62                                       | 0.16236   | 497.04  | 5.7569               | 316.87   | 75.395     | 0.46053 |
| 7       | 625.55                                       | 0.14668   | 948.38  | 2.0671               | 943.00   | 1.1152     | 1.1916  |
| 8       | 467.92                                       | -0.001084 | 441.86  | -0.11                | 400.58   | 0.34673    | 1.3248  |
| 9       | 254.75                                       | 0.10468   | 228.39  | 2.7278               | 247.82   | 0.55431    | 1.3769  |
| 10      | 21,320                                       | -0.20268  | 12,610  | -65.8                | 250.00   | -185,350   | 0.01    |
| 11      | 393.47                                       | -0.034654 | 281.11  | 1.4219               | 302.88   | 0.0035905  | 2.4769  |
| 12      | 769.36                                       | -0.06045  | 663.62  | -1.21                | 4295.90  | -3,548.7   | 0.01    |
| 13      | 1,365.4                                      | -0.022009 | 1,260   | -0.255               | 1243.40  | 2,289.8    | 0.01    |
| 14      | 956.69                                       | 0.11819   | 1,184.7   | 6.156                | 1432.40  | 19,446     | 0.01    |
| 15      | 792.15                                       | 0.0006648 | 744.07  | 1.3769               | 4.75   | 896.25     | 0.50755 |
| 16      | 956.56                                       | -0.049598 | 813.83  | -0.514               | 892.45   | 0.0098983  | 2.1685  |
| 17      | 320.44                                       | 0.038228  | 240.86  | 2.4989               | 272.02   | 0.051482   | 1.9456  |
| 18      | 939.49                                       | 0.027747  | 411.2   | 12.067               | 430.99   | 1.8646     | 1.5065  |
| 19      | 679.16                                       | 0.081854  | 774.79  | 3.2699               | 2950.00  | 3,813.1    | 0.01    |
| 20      | 514.61                                       | 0.042159  | 533.23  | 1.448                | 3810.90  | -3,016.6   | 0.01    |
| 21      | 223.5  | 0.057142  | 275.24  | -0.404               | 4224.20  | -3,583.3   | 0.01    |
| 22      | 886.63                                       | -0.33047  | 290.75  | -1.27                | 4087.10  | -3,709.1   | 0.01    |
| 23      | 2,134.8                                      | 0.038841  | 2,329   | 3.1603               | 7450.00  | 9,554.4    | 0.01    |
| 24      | 1,925.8                                      | 0.014174  | 1,740.8   | 2.3503               | 3260.00  | 4,909.3    | 0.01    |
| 25      | 210.99                                       | -0.002295 | 202.74  | 0.16823              | 927.16   | -616.25    | 0.01    |

It reveals that  $R^2$  values of Bingham plastic ( $R^2=0.9997$ ) was highest as compared to Herschel–bulkley model ( $R^2=0.9587$ ) and Power law model ( $R^2=0.1765$ ). Viscoelastic fluid behaves mainly shear-thinning (pseudoplastic) or shear-thickening (dilatant behavior) at high shear rate which is mainly represented by Herschel–bulkley model as compared to other fluid models. So viscosity and yield stress are calculated from Bingham plastic model.

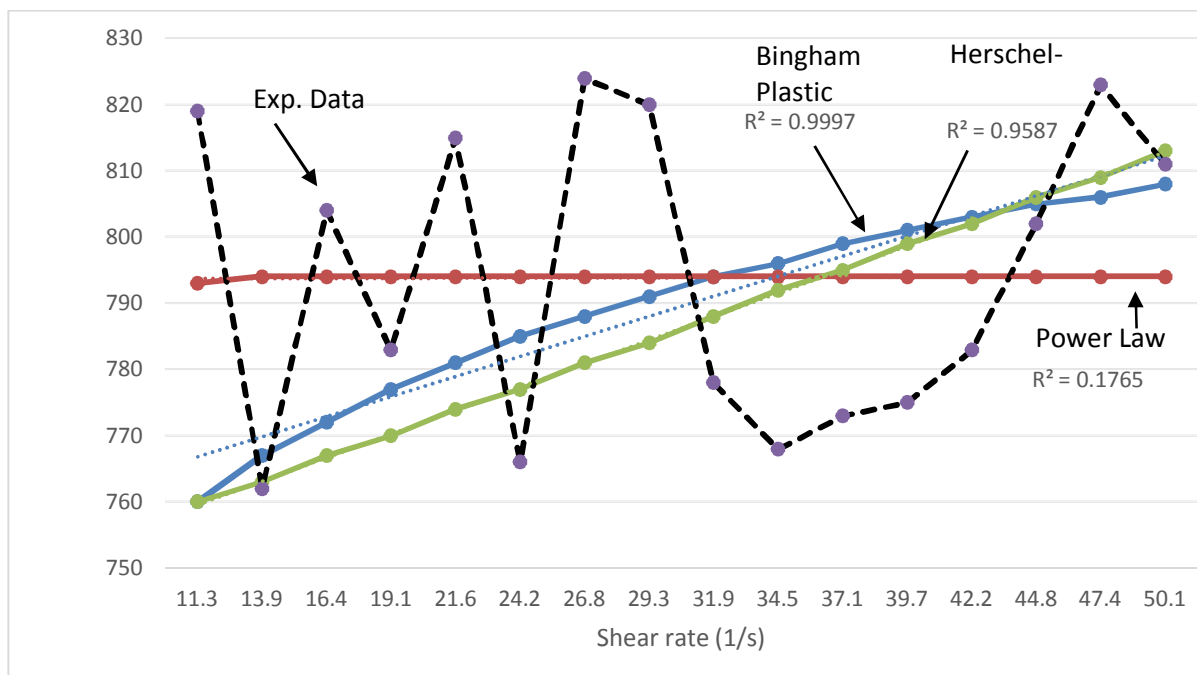


**Figure 3.10 Fitting the constitutive model equations to actual experimental data (run. 15)**

### 3.4.5 Optimization of media variables for rheology control

#### 3.4.5.1 Design of experiment

Design of experiment is most significant tool for investigation of effect of control variables on output responses. Initially in design of experiment main difficulty is selection of control variables, maximum number of variables is to be included to study the significant variable. Literature review on abrasive media developed shows that variables abrasive mesh size, percentage abrasive concentration, percentage of liquid synthesizer and temperature majorly effect on viscosity and yield stress of polymer



abrasive gel [45] [51]. In current study, four main parameters namely abrasive mesh size, percentage abrasive concentration, percentage liquid synthesizer, and temperature are considered for rheological investigation. Taguchi method-based design of experiment [90] and L<sub>25</sub> orthogonal array is used for parametric design. Table 3.7 represents the various parameters considered with their levels for conducting the rheological experiments.

**Table 3.7 Experimental design**

| Factor                   | Symbol | Level 1 | Level 2 | Level 3 | Level 4 | Level 5 |
|--------------------------|--------|---------|---------|---------|---------|---------|
| % Abrasive Concentration | A      | 30      | 40      | 50      | 60      | 70      |
| Mesh Size                | B      | 120     | 170     | 220     | 270     | 320     |
| % Liquid Synthesizer     | C      | 11      | 15      | 19      | 23      | 27      |
| Temperature (°C)         | D      | 25      | 35      | 45      | 55      | 65      |

The S/N ratio for maximum viscosity can be expressed as “higher is better” characteristic, which is calculated as logarithmic transformation of loss function as shown below

‘Higher is better’ characteristics 
$$\frac{S}{N} = -10 \log \frac{1}{n} \left( \sum \frac{1}{y^2} \right) \quad \dots(3.7)$$

Where ‘n’ is the number of observations, and y is the observed data.

Taguchi analysis was performed to evaluate the effect of individual parameter on response variables viz. yield stress and viscosity of developed PAG using Minitab software.

## Viscosity

Table 3.8 shows the experimental compositions in percentage volume of constituents of polymer abrasive gel and summary of responses of viscosity and yield stress based on Herschel-bulkley Model. Figure 3.10 shows graphically the effect of the four control factors on viscosity.

The percentage of liquid synthesizer was found to be significant parameter of media contributing 35.76 % on viscosity of media.

**Table 3.8 Plan of experiment and experimental results for viscosity and yield stress of polymer abrasive gel**

| Sr. No. | Ab Conc. (%) | Mesh Size | LS % | Temp(°C) | Viscosity (Pa-sec.) | Yield Stress (Pa) |
|---------|--------------|-----------|------|----------|---------------------|-------------------|
| 1       | 30           | 120       | 11   | 25       | 12.00               | 424.00            |
| 2       | 30           | 170       | 15   | 35       | 34.50               | 1206.30           |
| 3       | 30           | 220       | 19   | 45       | 22.60               | 1160.00           |
| 4       | 30           | 270       | 23   | 55       | 11.40               | 314.66            |
| 5       | 30           | 320       | 27   | 65       | 19.20               | 1220.50           |
| 6       | 40           | 120       | 15   | 45       | 20.50               | 316.87            |
| 7       | 40           | 170       | 19   | 55       | 30.30               | 943.00            |
| 8       | 40           | 220       | 23   | 65       | 13.00               | 400.58            |
| 9       | 40           | 270       | 27   | 25       | 9.54                | 247.82            |
| 10      | 40           | 320       | 11   | 35       | 32.90               | 250.00            |
| 11      | 50           | 120       | 19   | 65       | 9.58                | 302.88            |
| 12      | 50           | 170       | 23   | 25       | 17.50               | 4295.90           |
| 13      | 50           | 220       | 27   | 35       | 36.80               | 1243.40           |
| 14      | 50           | 270       | 11   | 45       | 40.20               | 1432.40           |
| 15      | 50           | 320       | 15   | 55       | 23.30               | 4.75              |
| 16      | 60           | 120       | 23   | 35       | 7.20                | 892.45            |
| 17      | 60           | 170       | 27   | 45       | 9.65                | 272.02            |
| 18      | 60           | 220       | 11   | 55       | 25.90               | 430.99            |

| Sr. No. | Ab Conc. (%) | Mesh Size | LS % | Temp(°C) | Viscosity (Pa-sec.) | Yield Stress (Pa) |
|---------|--------------|-----------|------|----------|---------------------|-------------------|
| 19      | 60           | 270       | 15   | 65       | 25.60               | 2950.00           |
| 20      | 60           | 320       | 19   | 25       | 16.70               | 3810.90           |
| 21      | 70           | 120       | 27   | 55       | 7.60                | 4224.20           |
| 22      | 70           | 170       | 11   | 65       | 19.85               | 4087.10           |
| 23      | 70           | 220       | 15   | 25       | 31.60               | 7450.00           |
| 24      | 70           | 270       | 19   | 35       | 32.30               | 3260.00           |
| 25      | 70           | 320       | 23   | 45       | 5.96                | 927.16            |

**Table 3.9 ANOVA table after model reduction for viscosity.**

| Source        | DOF | Seq. SS | Adj. SS | Adj. MS | F    | P      | Percentage Contribution |
|---------------|-----|---------|---------|---------|------|--------|-------------------------|
| Ab. Conc. (%) | 4   | 194.05  | 194.05  | 48.51   | 1.02 | 0.454  | 7.52                    |
| Mesh Size     | 4   | 641.94  | 640.94  | 160.48  | 3.36 | 0.068  | 24.90                   |
| LS (%)        | 4   | 922.08  | 922.08  | 230.52  | 4.83 | 0.028* | 35.76                   |
| Temp (°C)     | 4   | 437.46  | 437.46  | 109.37  | 2.29 | 0.148  | 16.98                   |
| Error         | 8   | 382.18  | 382.18  | 47.77   |      |        | 14.82                   |
| Total         | 24  | 2577.71 |         |         |      |        |                         |

\*Significant

ANOVA has been performed for viscosity to study the most significant variable which affects the response variable. Table 3.9 shows ANOVA for viscosity after model reduction. From the ANOVA analysis (Table 3.9), liquid synthesizer is only significant parameter for viscosity of developed media. It is observed from previous work [51] that with increase in media viscosity, surface roughness decreases. It is due to the fact that stiffer medium has a greater depth of penetration of abrasive particle and would improve the surface finish. Final regression equation in terms of actual value of parameters is

$$\text{Viscosity} = 36.2004 - 0.05194 B + 0.03584 A - 0.8828 C - 0.09084 D \dots (3.8)$$

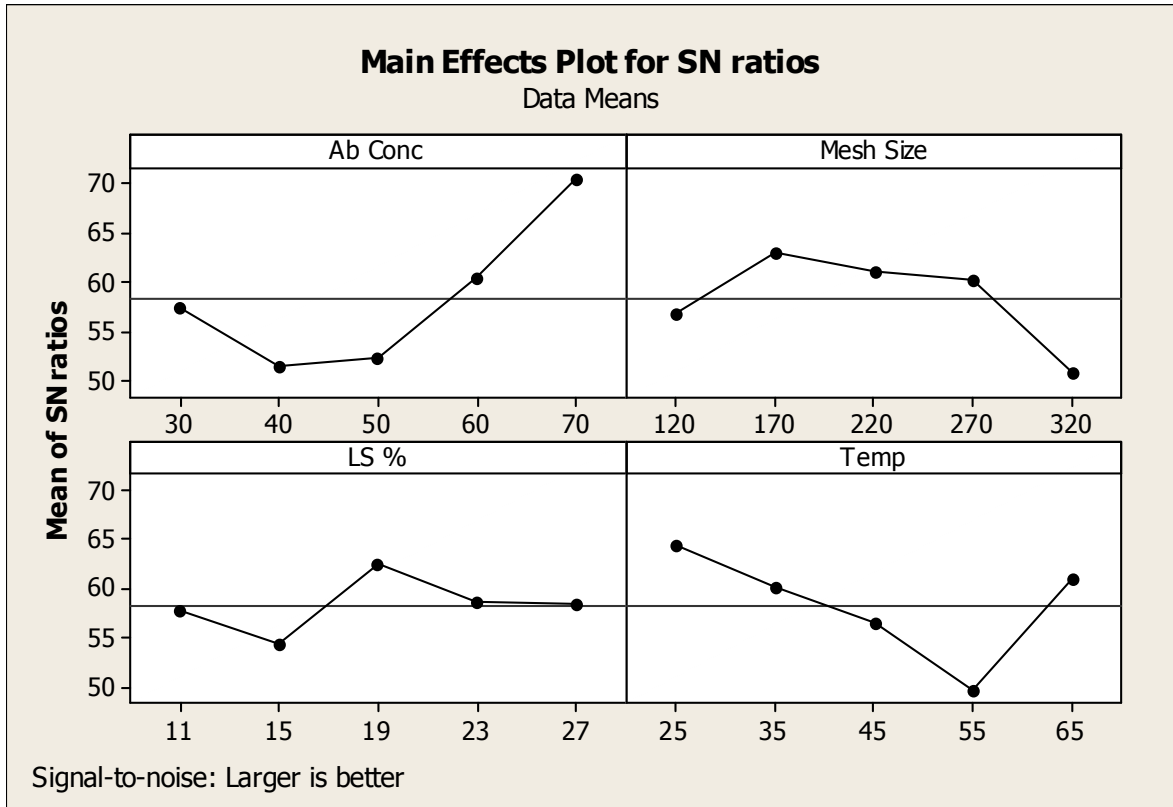


Figure 3.11 SN ratio for yield stress

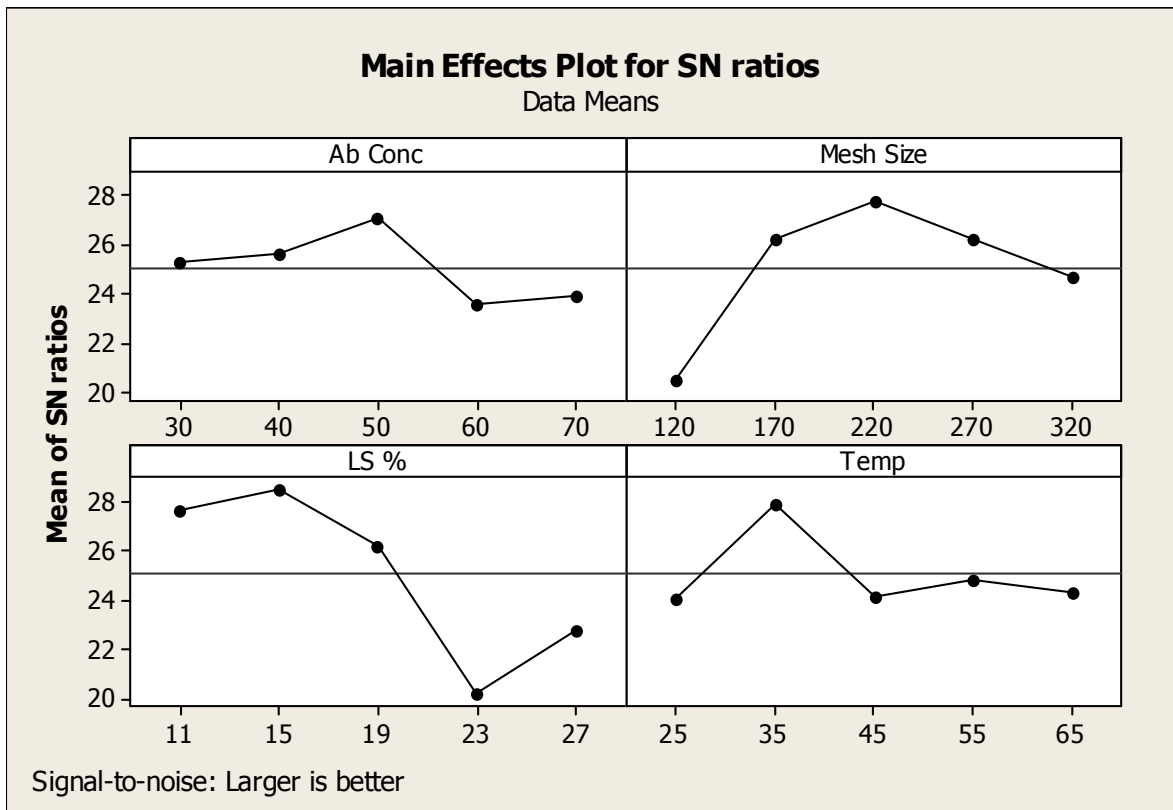


Figure 3.12 SN ratio graph for viscosity

Figure 3.10 shows the SN ratio graph for yield stress of PAG media. The optimum level of variable for larger is better loss function will be 70% abrasive concentration, 170 abrasive mesh size, 19% liquid synthesizer and 25 °C temperature. Figure 3.11 shows the SN ratio graph for viscosity of PAG media. The optimum level of variable for larger the better loss function will be 50% abrasive concentration, 220 abrasive mesh size, 15% liquid synthesizer and 35 °C temperature.

Viscosity of AFM media plays major role in surface finishing improvement, so based on the regression equation [Eqs.(3.8)] obtained after regression analysis, the results in terms of percentage abrasive concentration, abrasive mesh size, percentage of liquid synthesizer and temperature on viscosity have been computed and discussed.

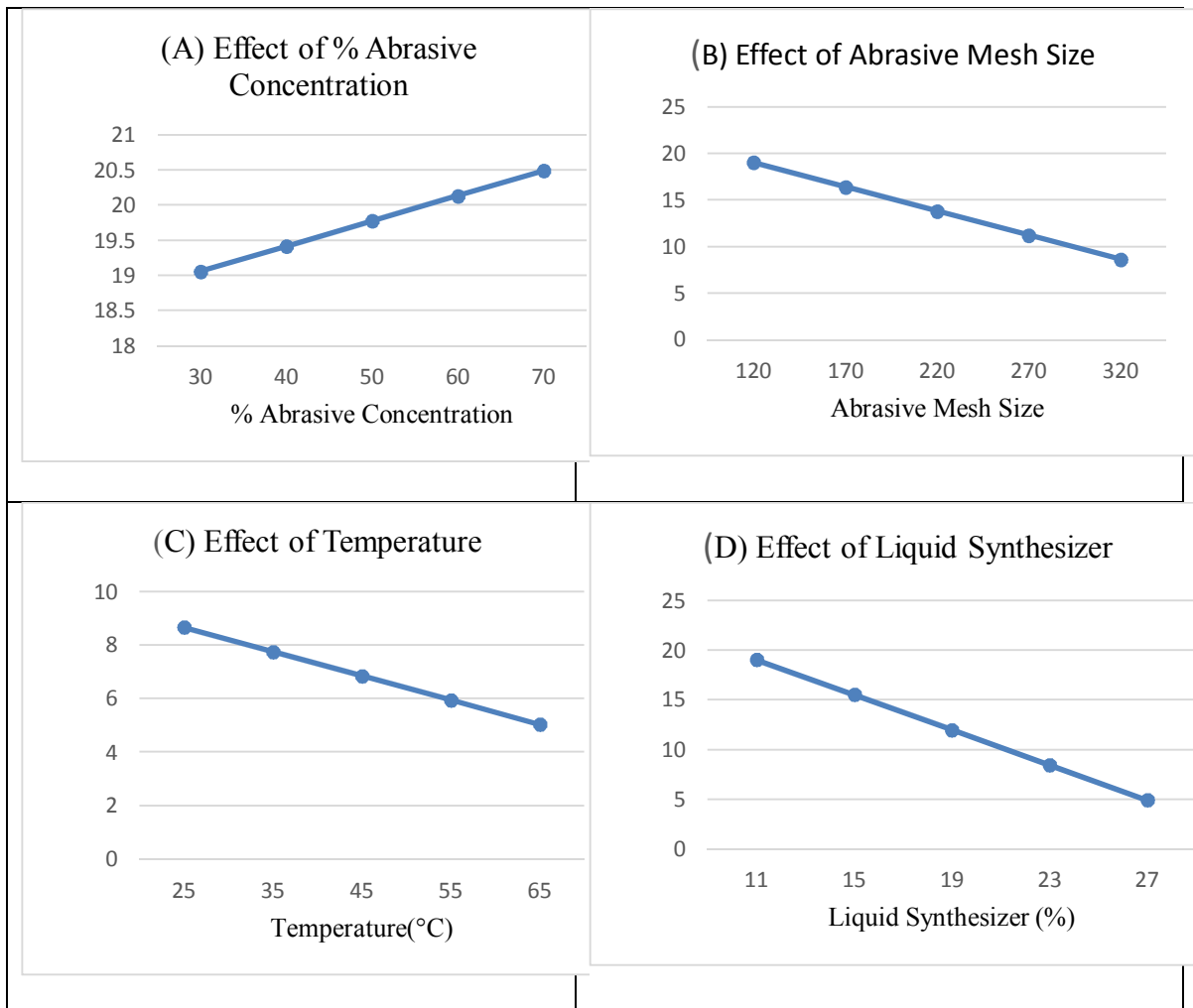


Figure 3.13 Effect of polymer abrasive gel variables on viscosity

### **Effect of abrasive concentration**

Figure 3.12 (A) shows the effects of increase in percentage of abrasive concentration on viscosity of PAG. From Graphs it has been observed that PAG viscosity increases continuously with increase in percentage of abrasive concentration. It is due to higher concentration of abrasive particles which decreases fluidity of PAG and results in decreased in the mobility of particles in the media. As a result, a lower volumetric flow rate is observed and viscosity decreased. Steady state condition for this analysis for different variable is 120 abrasive mesh sizes, 11 % liquid synthesizer and 25 °C temperature.

### **Effect of abrasive mesh size**

Figure 3.12 (B) shows the effect of increase of abrasive mesh size on viscosity of developed PAG. From graphs it is observed that PAG viscosity decreases with increase in abrasive mesh size. It is due to an increase in the abrasive mesh size (i.e. smaller grits) which increases the amount of squeeze out material subsequent in increased pressure gradient and AFM media flow rate. So increasing in shear rate and wall shear stress will result in decrease in viscosity of PAG. Steady state condition for this analysis for different variable was 30% abrasive concentration, 11 % liquid synthesizer and 25 °C temperature.

### **Effect of percentage liquid synthesizer**

Figure 3.12 (C) shows the effect of increase of percentage liquid synthesizer on viscosity of developed PAG. From graphs it is observed that PAG viscosity decreases with increase in percentage liquid synthesizer. An increase in the percentage of liquid synthesizer which results in more fluidity and decreased stiffness of PAG. Steady state condition for

this analysis for different variable was 120 abrasive mesh sizes, 30 % abrasive concentration and 25 °C temperature.

### Effect of temperature

Figure 3.12 (D) shows the effect of increase of Temperature on viscosity of developed PAG. From graphs it was observed that PAG viscosity decreases with increase in temperature. It is due to facts that as the temperature of PAG increases, there exist decrease in flow rate (i.e. decrease in extrude material) which cause decrease in the apparent shear rate and consequentially decreased in the viscosity of PAG. Steady state condition for this analysis for different variable was 320 abrasive mesh sizes, 30 % abrasive concentration and 11% liquid synthesizer.

### Yield stress

Yield stress values obtained from Herschel–bulkley model (Table 3.8) are used for ANOVA analysis to know most significant variable that effecting response of polymer abrasive gel. ANOVA has been performed for yield stress also as procedure explained for viscosity in last section.

**Table 3.10 ANOVA table after model reduction for yield stress**

| Source           | DOF | Seq. SS  | Adj. SS | Adj. MS | F    | P      | Percentage co |
|------------------|-----|----------|---------|---------|------|--------|---------------|
| Ab. Conc.<br>(%) | 4   | 38036978 | 3803697 | 9509244 | 4.01 | 0.045* | 45.81         |
| Mesh Size        | 4   | 4167285  | 4167285 | 1041821 | 0.44 | 0.777  | 5.01          |
| LS (%)           | 4   | 4128145  | 4128145 | 1032036 | 0.44 | 0.780  | 4.97          |
| Temp. (°C)       | 4   | 17715344 | 1771534 | 4428836 | 1.87 | 0.210  | 21.33         |
| Error            | 8   | 18971177 | 1897117 | 2371397 |      |        | 22.85         |
| Total            | 24  | 83018929 |         |         |      |        |               |

\*Significant

Table 3.10 shows ANOVA for yield stress after model reduction. From the ANOVA analysis Abrasive concentration is most significant parameter which effect the yield stress of polymer abrasive gel. The final regression equation in terms of actual value of parameters is:

$$\text{Yield Stress (Pa)} = -76.609 + 74.8882 \text{ Ab Conc.} - 0.99745 \text{ Mesh Size} - 19.6513 \text{ LS \%} - 30.9393 \text{ Temp} \quad \dots (3.9)$$

### **3.5 Comparative study of PAG and streamer for characterization**

In this section, the synthesized alternative polymer abrasive gel (PAG) for AFM is compared with commercial media (streamer) through rheology studies, Thermogravimetric Analysis (TGA) and Fourier Transform Infrared Spectroscopy (FTIR). Finishing experiment are conducted on bidirectional AFM utilizing the PAG media and commercial media using the variables as extrusion pressure, viscosity of media, and finishing time. Many researchers worked on parametric analysis and their influence on material removal and surface finishing quality. Also Jain et al. and some researchers [51][6][35] [92] studied the influence of number of cycles, concentration of abrasive, media flow speed, mesh size, media viscosity and temperature of AFM media on performance measure parameters of AFM process. The AFM variables like media extrusion pressure, flow volume, media viscosity, abrasive mesh size, abrasive concentration and workpiece structure which influence the surface quality and material removal in AFM process have been studied by Rhoades and some researchers [93][94][38][7] with considerations of wide industrial applications. The developed alternative polymer abrasive gel (PAG) media is characterized [50] using the Thermogravimetric analysis (TGA) and FTIR technique and compared with commercial AFM media.



### **3.5.1 Characterization of AFM Media**

As the commercial available media is environmentally unsustainable and costly, so there is essential need for an extensive research for synthesization of alternative media and it is essential to select the appropriate alternative elements compared with those that are used presently. The selected elements should have the same or a close characteristic trend as the current media and the elements must be companionable with each other and suitable for easy synthesization as well as exhibiting low cost. During finishing process, material starts to damage due to shear action, so media cannot acts as binder to hold the abrasives, explaining media should be mechanical stable. During the finishing time, media should not be reacting with workpiece material and with abrasive material, so chemical stability of media is very essential.

### **3.5.2 PAG media preparation**

Three samples of alternative polymer abrasive gels are synthesized and rheological experiments are performed for both streamer and polymer abrasive gel. Polymer abrasive gel is developed using additive polymer base, liquid synthesizer and abrasive particles as the major ingredients. Additives and liquid plasticizers are mixed to regulate the viscosity of the AFM media specific to the workpiece shape, size and materials. The alternative media is prepared by mixing SiC abrasives of 220 mesh sizes in the semisolid polymer base prepared in bulk with 50% weight percentages, whose viscosity could be regulated by proportion of liquid synthesizer (7–32%).

### **3.5.3 Rheological analysis**

Rheological properties of AFM media is main criteria for good finishing quality in AFM process. This study shows the effects of apparent viscosity (ratio of the shear stress and shear rate) on shear rate. Rheological experiments are performed on Rotational

Rheometer (Anton-Par) in dynamic shear conditions at different shear rates ranging from  $10 \text{ sec}^{-1}$  to  $100 \text{ sec}^{-1}$  and at ambient temperature ( $30 \text{ }^\circ\text{C}$ ).

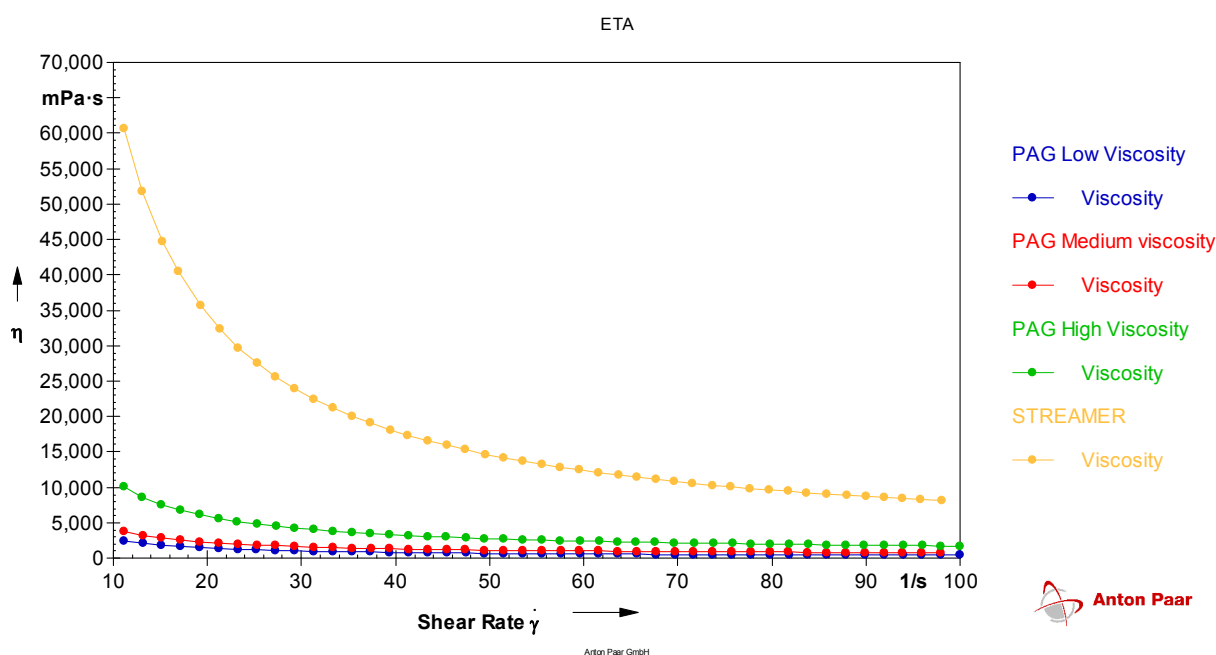


**Figure 3.14 Rheological behaviour of PAG and commercial media (streamer).**

Figure 3.13 shows the comparative relation of apparent viscosity with shear rate for Polymer Abrasive Gel at different viscosity and streamer. From graph it reveals that as apparent viscosity decreases with shear rate, it shows the shear thinning behaviour [95] (Power law) of AFM media. The graphs show the same behaviour of all three samples of PAG of different viscosity and streamer.

### 3.5.4 TGA

Thermogravimetric analysis (TGA) has been performed to investigate the high temperature stability and degradation behaviour of PAG media and streamer. Media samples are heated at heating rate of  $15^\circ \text{C}/\text{min}$  over a range of temperature of  $25\text{-}300^\circ \text{C}$ . The sample weights are kept at  $2.5 \pm 0.2 \text{ mg}$ , for all TGA experiments. Thermal properties of the media samples are analysed by using Perkin Elmer Pyris-7 instrument.

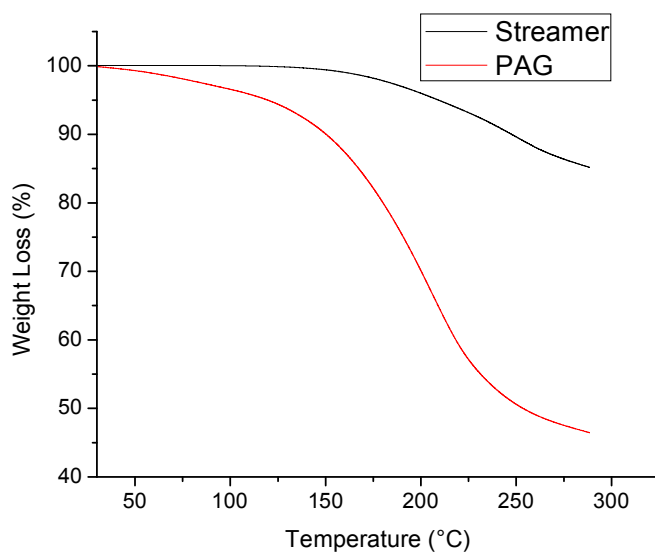


**Figure 3.15 TGA graphs between weight loss % and temperature for both AFM media**

Figure 3.14 shows the TGA curves for streamer and PAG media. It signifies the thermal degradation characteristics of AFM media. It can be observed that two main thermal degradation phases (weight loss) were found in the graph. For Polymer Abrasive Gel, the first step started at low temperatures about 55°C with small degradation rate. In first step, 6% weight loss is observed at 120°C temperature. In second step, highest weight loss (44%) is observed for 120°C-250°C temperature range. At the end of the graph a small weight loss (5%) is observed between 250 to 290°C. For streamer media, in graph till 170°C temperature very small 2% weight loss is observed. After 170°C to 260°C temperature highest weight loss (10%) is observed.

### 3.5.5 FTIR Analysis

Functional groups are identified using Fourier transform infrared spectroscopy for streamer and PAG media. Analysis on Perkin Elmer FT-IR Spectrum-2 is performed in the range between 450 to 3500  $\text{cm}^{-1}$  with 8 scans per analysis at a resolution of 4  $\text{cm}^{-1}$ .

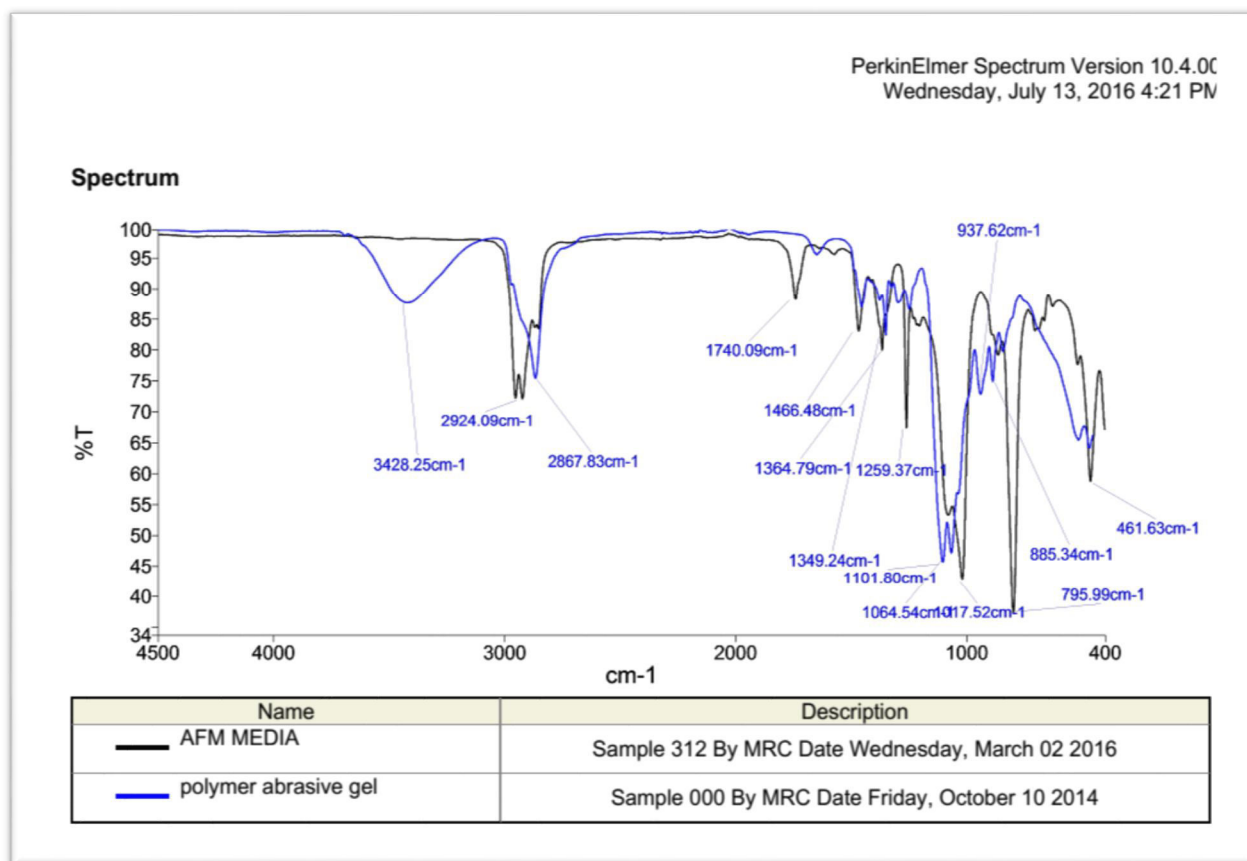


**Figure 3.16 FTIR for streamer and PAG media**

Figure 3.15 shows the infrared spectra recorded for streamer and PAG media. From the graphs major peaks are identified and their corresponding functional group are identified from IR chart. At  $796.01\text{ cm}^{-1}$  wavenumber, the graph indicates the formation of stable and strong alkenes group ( $=\text{C}-\text{H}$  bend) which shows the elastic nature of both AFM media. At  $1017.560\text{ cm}^{-1}$ ,  $1259.38\text{ cm}^{-1}$ ,  $1740.14\text{ cm}^{-1}$  wavenumber,  $\text{C}=\text{O}$  stretch esters group are identified from IR chart which shows the thermal stability of both media. At  $1466.58\text{ cm}^{-1}$ ,  $2954.03\text{ cm}^{-1}$ ,  $2924.09\text{ cm}^{-1}$  wavenumber,  $\text{C}-\text{H}$  bend alkanes functional group are identified from IR chart and shows again elastic behaviour of both AFM media. At  $1364.81\text{ cm}^{-1}$  wavenumber,  $\text{C}-\text{N}$  stretch aromatic amines functional group is found and that shows the tensile strength of the both media.

### 3.6 Performance study of PAG and streamer

For comparative study of PAG and streamer media, the effects of process variables on performance variables are studied on bidirectional abrasive flow machine.

#### 3.6.1 Design of experiment

The performance of streamer and PAG media is accompanied on a commercial bidirectional AFM setup (Micro-Technica) as shown in Figure 3.16. Initially, lower media cylinder is filled with media by keeping upper piston and cylinder at top position. For experimentation on AFM setup using polymer abrasive gel and streamer, stamping die of high speed steel material is used as work-pieces. After filling the media, fixture for holding the workpiece is placed (Figure 3.17) and clamped in between the upper and lower media cylinders. The experiment on AFM setup is run for the certain finishing time and extrusion pressure as given in Table 3.11. After completion of experiments, the workpieces are cleaned with acetone, and surface roughness value is measured using Taylor hobson surface measuring instrument and material removal is calculated by measuring the weight of workpiece before and after finishing process. During the experiment, stroke length of 200 mm and 30°C temperature are kept constant. The measured surface roughness  $R_a$  in terms of surface roughness improvement ( $\Delta R_a$ ) and material removal is calculated by the following equation

$$\text{Surface roughness improvement } (\Delta R_a) = (\text{Initial } R_a - \text{Final } R_a)$$

$$\text{Material Removal (MR)} = (\text{Initial weight} - \text{final weight}) \text{ mg.}$$

**Table 3.11 Experimental setting**

| Sr. No. | Variables          | Levels          |                      |                    |
|---------|--------------------|-----------------|----------------------|--------------------|
|         |                    | 1               | 2                    | 3                  |
| 1       | Extrusion pressure | 30              | 40                   | 50                 |
| 2       | Finishing time     | 35              | 45                   | 55                 |
| 3       | Viscosity          | Low (75Pa-sec.) | Medium (175 Pa-sec.) | High (275 Pa-sec.) |

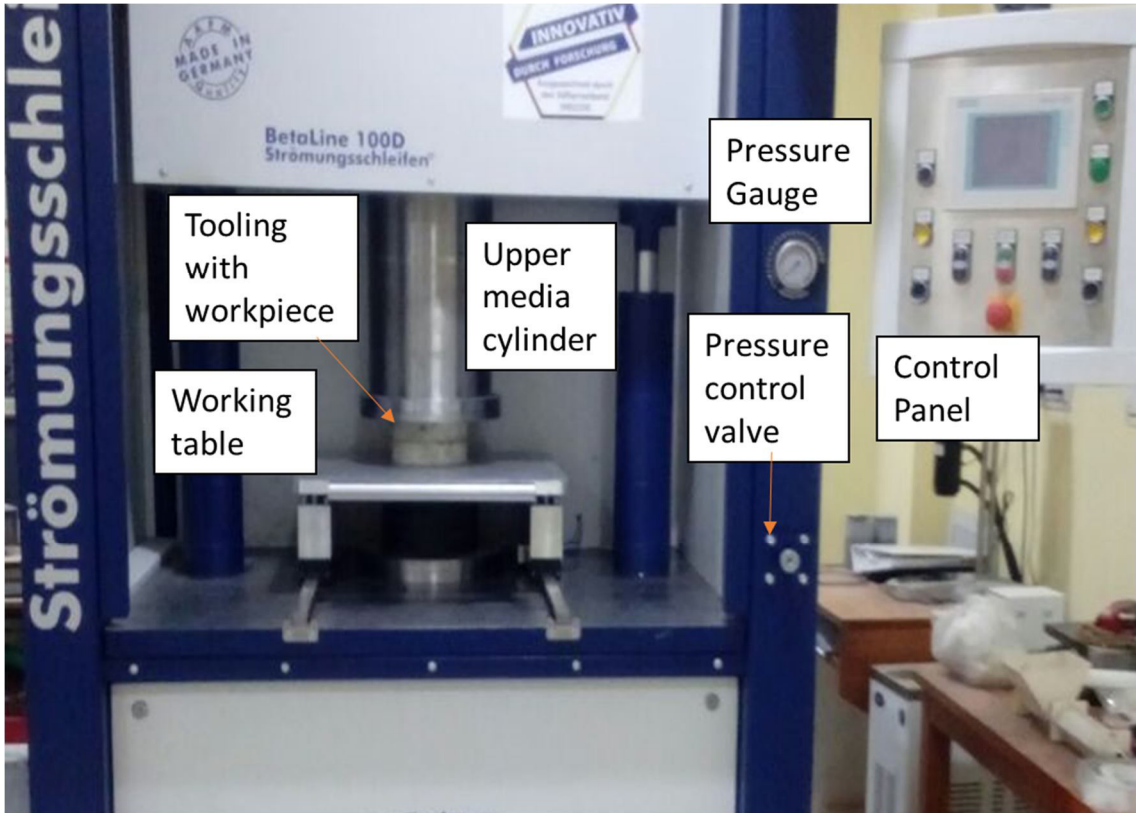


**Figure 3.17 Bidirectional abrasive flow machine for finishing workpiece**



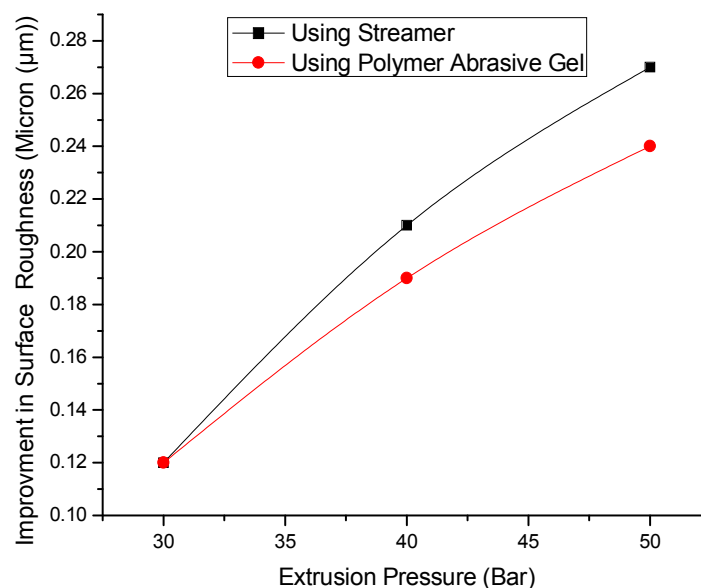
**Figure 3.18 Tooling of holding stamping die component**

### 3.6.2 Results and discussion

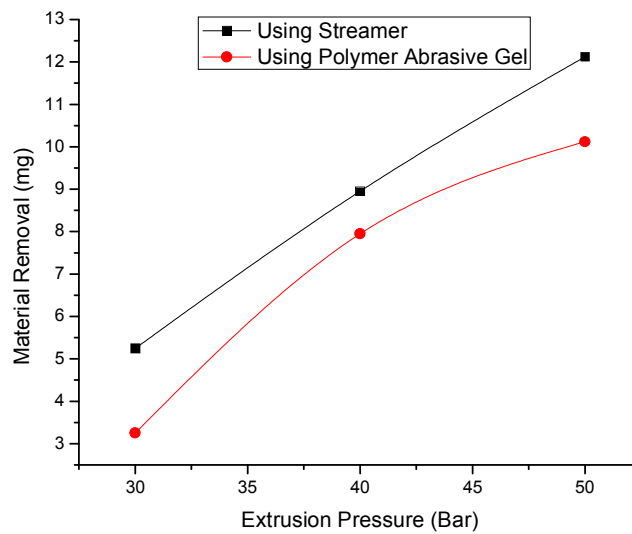
After characterization of polymer abrasive gel and streamer, the same media samples are used for evaluating and comparing the performance by keeping the experimental condition as shown in Table 3.11. This section explains the effects of extrusion pressure, finishing time and viscosity of media on surface roughness improvement and material removal.

#### 3.6.2.1 Effects of extrusion pressure on surface roughness improvement and MR

Figure 3.18 shows comparison of effects of extrusion pressure on surface roughness improvement using PAG media and streamer keeping finishing time (35 minute) and viscosity (medium) constant. From graphs it is clear that as extrusion pressure is increasing surface roughness improvement is increasing. This is due to fact that as the extrusion pressure increases, the axial and radial forces increases which remove the peaks over the workpiece surface.



**Figure 3.19 Effects of extrusion pressure on surface roughness improvement. (Finishing time 35 min and medium viscosity)**



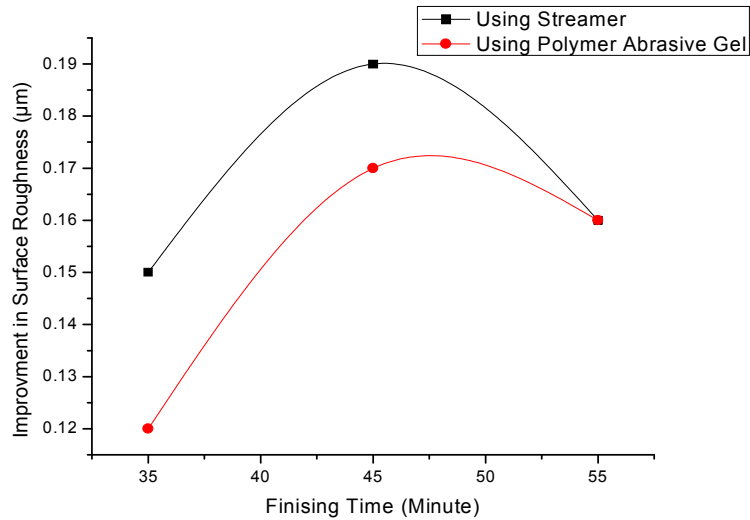
**Figure 3.20 Effects of extrusion pressure on material removal. (Finishing time 35 min and medium viscosity)**

Figure 3.19 shows comparison of effect of extrusion pressure on material removal using PAG media and streamer keeping finishing time (35 minute) and viscosity (medium) constant. From graphs it is clear that material removal is increasing with increase in extrusion pressure. This is due to as the extrusion pressure increases, the axial and radial forces increases which remove the more quantity of material over the workpiece surface.

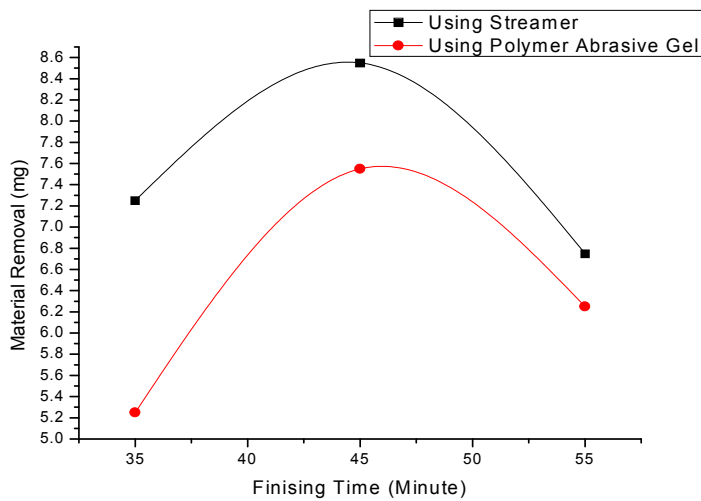
### **3.6.2.2 Effects of finishing time on surface roughness improvement and MR**

Figure 3.20 shows comparison of effect of finishing time on surface roughness improvement using PAG media and streamer keeping extrusion pressure (30 bars) and viscosity (medium) constant. Results in this graphs shows that as the finishing time increases, the surface roughness improvement increases. This is due to fact that increases in time of indentation of abrasives particles on workpiece surface increases results in higher surface roughness improvement.





**Figure 3.21 Effects of finishing time on surface roughness improvement (extrusion pressure 30 bar and medium viscosity)**



**Figure 3.22 Effects of finishing time on material removal (extrusion pressure 30 bar and medium viscosity)**

Figure 3.21 shows comparison of effect of finishing time on material removal using PAG media and streamer keeping extrusion pressure (30 bars) and viscosity (medium) constant. Results in this graphs show that as the finishing time increases, the material removal increases. In initial finishing time the material removal is high due to workpiece surface having large number of peaks and indentation. After some finishing time, the surface become flat (peak height reduces) and at higher finishing time the media just stream over the workpiece surface resulting in decrease in material removal.

### 3.6.2.3 Effects of viscosity on surface roughness improvement and material removal

Figure 3.22 shows the comparison of effect of viscosity on surface roughness improvement using PAG media and streamer (keeping finishing time 35 minutes and extrusion pressure 40 bar constant). Results in graph show the decrease in surface roughness improvement with increase in viscosity of media. Because of stiffer media, higher depth of penetration of abrasive grains is possible which would decrease the surface finish quality.

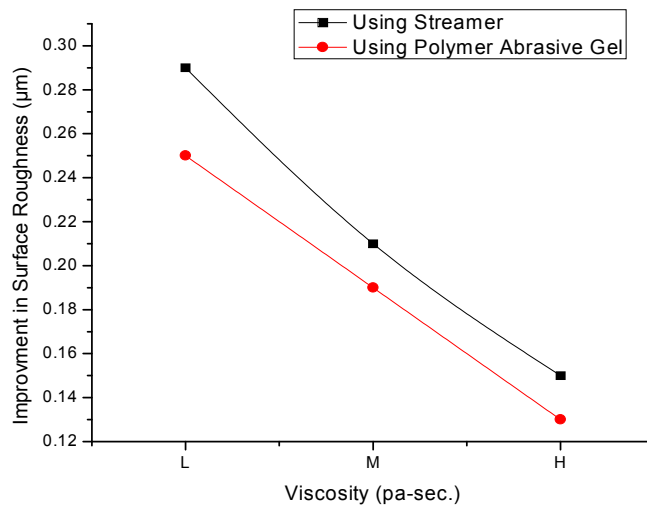


Figure 3.23 Effects of viscosity on surface roughness improvement (finishing time 35 minute and extrusion pressure 40 bar).

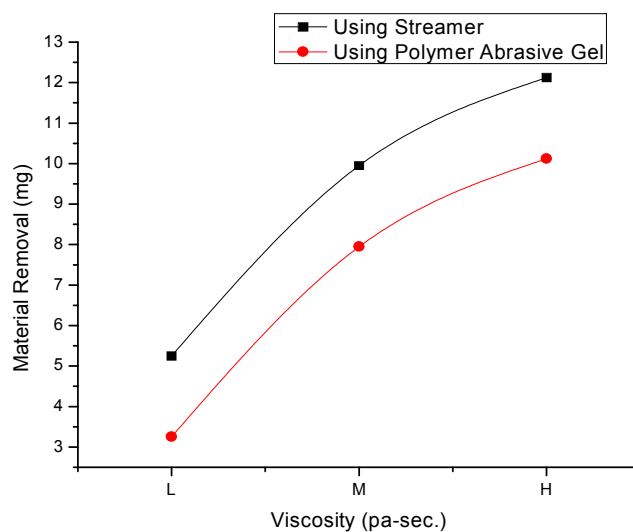


Figure 3.24 Effects of viscosity on material removal (finishing time 35 minute and extrusion pressure 40 bar)

Figure 3.23 shows the comparison of effect of viscosity on material removal using PAG media and streamer keeping finishing time (35 bar) and extrusion pressure (40 bar) constant. Results in graph show the increase in material removal with increase in viscosity of media. As high viscosity media have higher confrontation so more material extrude out from surface which results in high material removal.



## **Chapter 4 Design and Development of Unidirectional Abrasive Flow Machine**

---

### **4.1 Introduction**

Abrasive Flow Machining (AFM) processes, are proving to be one of the important finishing processes mainly used for finishing intricate surfaces, deburring, polishing, removing recast layers and radiusing by flowing abrasive laden viscoelastic carrier. They are however exorbitantly priced due to their consumable, so only high end industries in developed world e.g. aerospace, automobile tool & die and prosthetic etc. use these processes. This invention has the potential to make AFM affordable for every shop floor which is presently limited by its high running cost. Need was also felt to develop an equally efficient and low cost advanced finishing setup with environmentally sustainable consumables to finish components with nano range surface finish which is adaptable to price sensitive small scale industries in India.

Keeping in view, alternative media, cost and modularity first a micro unidirectional abrasive flow machine (MUAFM) has been designed and fabricated for finishing carbide wire drawing dies which were otherwise being finished manually. Most of the parts of the MUAFM are 3D printed using Fused Deposition Modelling (FDM) technique and integrated with alternative media and tooling. Experimental investigation has been carried out to understand the effect of the various machining variables on surface finish quality (explained in Annexure G).

After successful trials of MUAFM showing significant improvement in surface quality, a production grade UAFM has been designed by using same concept and fabricated for finishing industrial component like trim dies. The designed and developed MUAFM setup has capability to finish nano-range quality surfaces on complicated internal as well external surfaces required in many manufacturing applications across industries including

medical implants, tools & dies and automobile & aerospace components affordable by small scale industries.

## **4.2 Design & development of MUAFM**

MUAFM setup has been designed keeping in view the vital mechanism of the MUAFM using the abrasive based material specified in 2369/DEL/2010 [96] and basic useful requirements of different parts. Before the production grade setup was attempted it was natural to design, develop and test a prototype of the mechanism using rapid manufacturing techniques. The same is referred as Micro unidirectional abrasive flow machine with the acronym of MUAFM.

### **4.2.1 Major components of MUAFM:**

The system has the following three major components which use the abrasive laden base material (ABM), namely extruding element, media displacement components, and tooling. The detailed drawings of all components with all dimensions are shown in Appendix B.

#### **4.2.1.1 Extruding element**

In this part, two major parts are designed and fabricated. First is hopper (shown in Figure 4.1 and second is screw feeder. Hopper is designed for feeding the PAG media for finishing process. Basically hopper has been designed for smooth feeding of polymer abrasive gel. Size of hopper depends on flow rate or capacity of setup that can flow or pass the quantity of media.

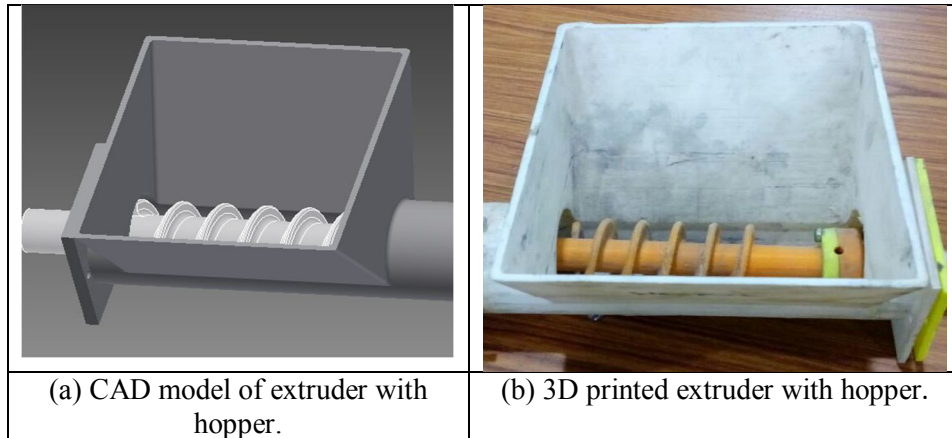


**Figure 4.1 Extruder with hopper**

#### 4.2.1.2 Media displacement components

The hopper is filled with the PAG media which needs to be transferred to the workpiece for finishing; this transfer is ensured through displacement elements which consist of series of rotors (internal) and stators (external) as shown in Figure 4.2. Usually hard rotors operate against a soft elastomer stator. In this process single threaded helical screw or rotor, rotates eccentrically inside a double threaded helical stator as shown in Figure 4.2. The mechanism of the stator and rotor is shown in Figure 4.3. The rapid fabricated rotor and stator parts of MUAFM are shown in Figure 4.4.

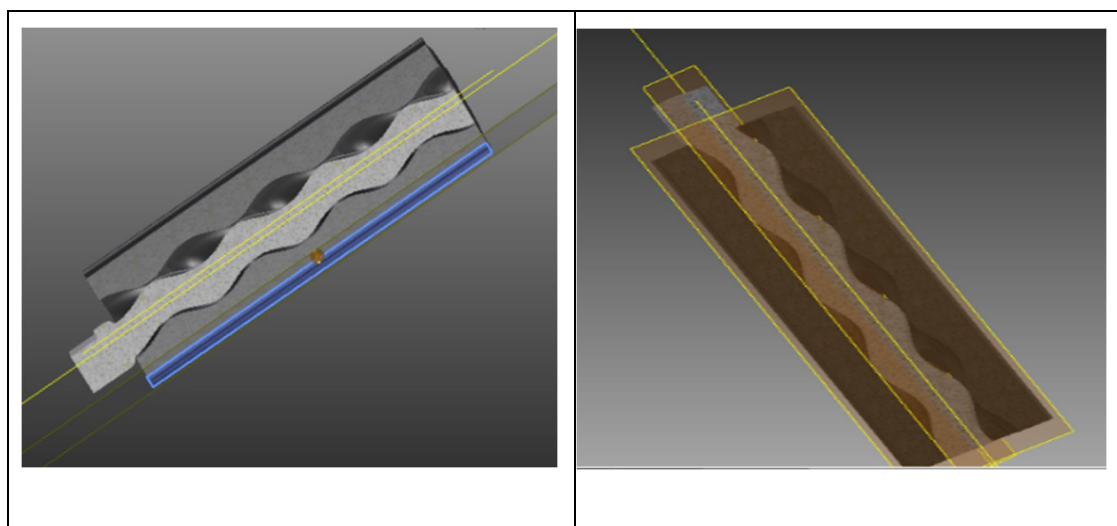


**Figure 4.2 Sectional view of rotor and stator design**

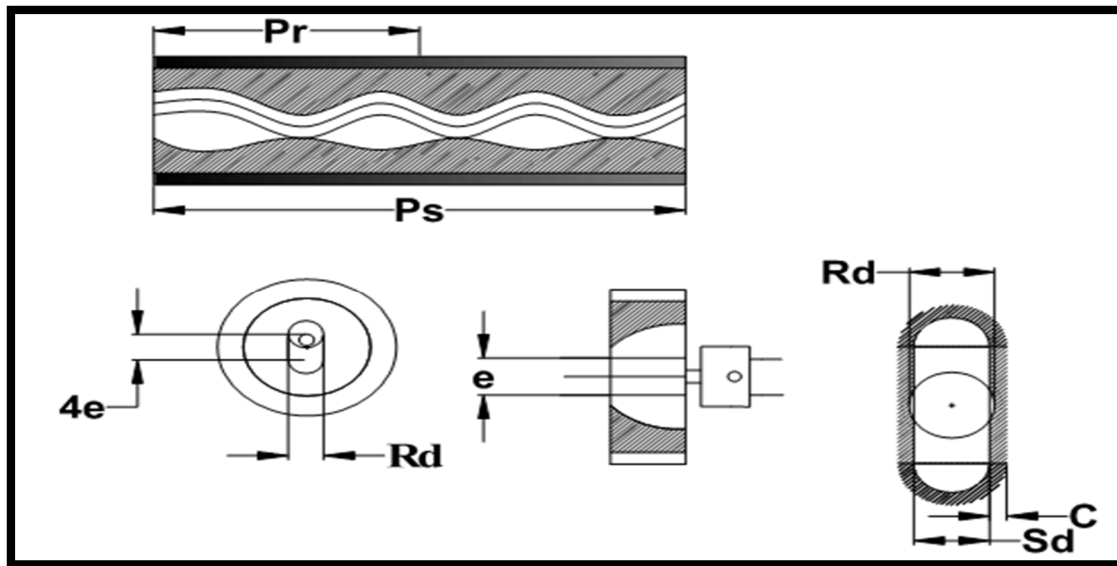


Figure 4.3 Geometry of displacement element

**Legend**

|       |   |                 |          |   |                                 |
|-------|---|-----------------|----------|---|---------------------------------|
| $e$   | - | Eccentricity    | $R_d$    | - | Rotor diameter                  |
| $S_d$ | - | Stator diameter | $\omega$ | - | Rotational speed of rotor (rpm) |
| $P_s$ | - | Pitch of stator | $W_s$    | - | Width of stator                 |
| $P_r$ | - | Pitch of rotor  | $V_f$    | - | Volume of all free cavity       |
| $C$   | - | Clearance       |          |   |                                 |

The details of design calculations for displacement elements i.e. rotor and stator are given in Annexure C at the end of thesis.

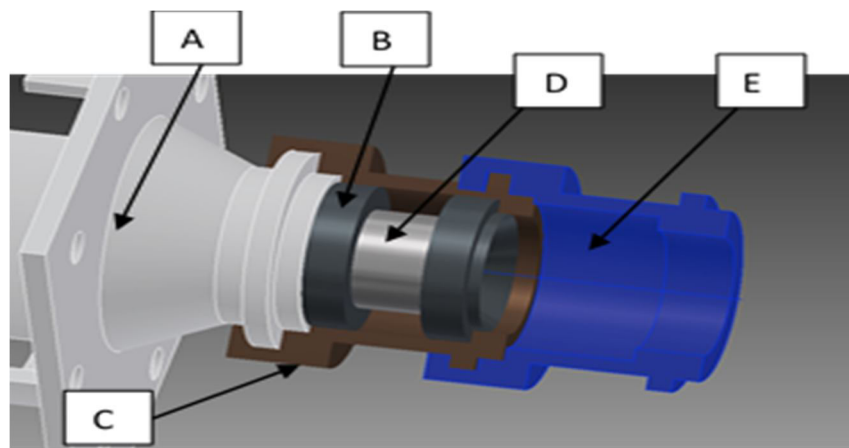


Figure 4.4 Fabricated rotor and stator parts of MUAFM



### 4.2.1.3 Tooling

For holding the workpiece (i.e. wire drawing die); tooling is designed as shown in Figure 4.5. Tooling restrains and guides the media flow to the areas where deburring, radiusing and surface improvements are anticipated [97]. Tooling is designed based on the shape, size and surface of workpiece to be finished. Another criterion for the design of tooling is the easy mounting and removal of the workpiece.



**Figure 4.5** Sectional view of tooling for holding the workpiece (i.e. wire drawing die)

Different parts of tooling as shown in above Figure 4.5 are discussed as:-

- A. Flange for holding displacement components and reducing for directing the ABM to workpiece and supporting the split tooling.
- B. Inner washers to hold the workpiece.
- C. Split tooling for easy fitment and removal of the workpiece.
- D. Workpiece in the first split tooling
- E. Additional split tooling for the successive workpiece.

The designed tooling components are rapid fabricated using FDM 3D printing technique and assembled as shown in Figure 4.6.

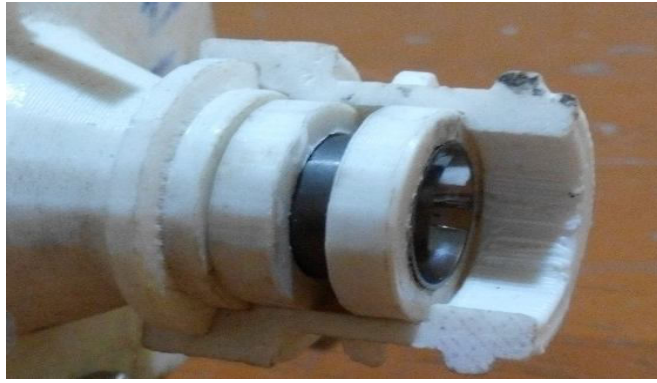


**Figure 4.6 Fabricated tooling unit for holding the workpiece (i.e. wire drawing die)**

#### **4.2.1.4 Powering element**

The series of rotors are coupled to a RPM controlled electrical motor via an extruding element and coupling. Care is taken that the shaft is supported on bearings and leak proof oil seals. The designed setup housing is divided in three places, which are main housing, bearing housing and seal housing. Cardan coupling has been designed for providing the motion between the Cardan shaft and rotor. The drive shaft has been designed and attached with motor that provide motion to Cardan shaft.

#### **4.2.2 Fabrication of MUAFM**

3D printer is used for fabrication of micro unidirectional abrasive flow machine. The setup is designed in different parts and was printed on 3D printer. Material used for fabrication is ABS filament of 1.75 mm diameter. For fabrication of MUAFM setup different parts are designed and each printed parts are assembled using adhesive paste of aerolite. Screw rod and rotor parts were joined using coupling which is flexible in four directions. A ball bearing was used on driving shaft for smooth functioning of setup.

For holding wire drawing die, tooling and fixtures were designed and printed. Tooling was designed in such a way that component can holding and removing time can be reduced. After printing, each part is assembled using joints, coupling and screw nuts and MUAFM setup was developed using FDM technique as shown in Figure 4.8.



### 4.3 Design & development of UAFM

This production grade system has been designed keeping in view the vital mechanism of the UAFM using the abrasive based material specified in 2369/DEL/2010 and successful design, development and testing of the MUAFM. The same is referred as unidirectional abrasive flow machine (UAFM).

#### 4.3.1 Major Components of UAFM

The systems has the following six major components which use the abrasive laden base material (ABM) of 2369/DEL/2010, namely extruding element, media displacement components, reducer, tooling & recycling unit, driving and control element and mounting base. The detailed drawings of all components with all dimensions are shown in Appendix A.

##### 4.3.1.1 Extruding elements

Hopper has been designed for smooth feeding of polymer abrasive gel. Size of hopper depends on flow rate or capacity of setup that can flow or pass the quantity of media. Figure 4.9 shows the sectional view of the hopper and screw feeder. The dimensions of the hopper and screw feeder to push the PAG media forward are shown in Figure 4.10. The main application of screw feeder is to push the AFM media to media displacement unit and also helps in uniform mixing of abrasive in media.

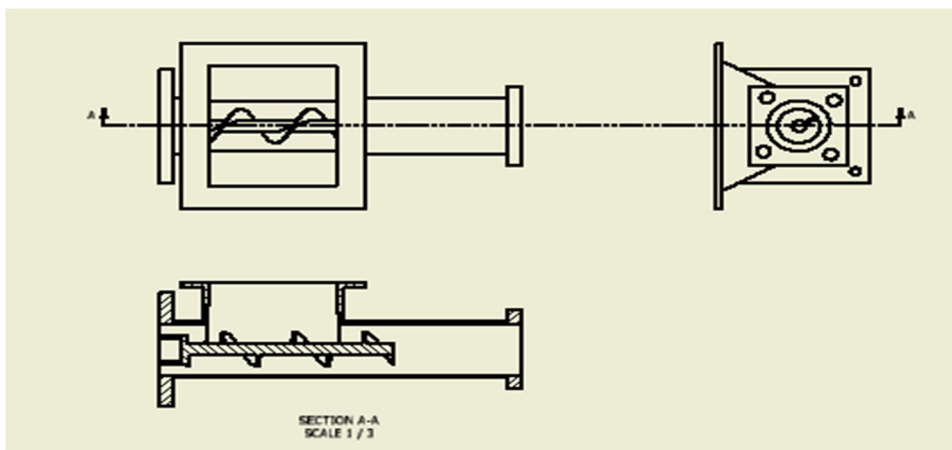
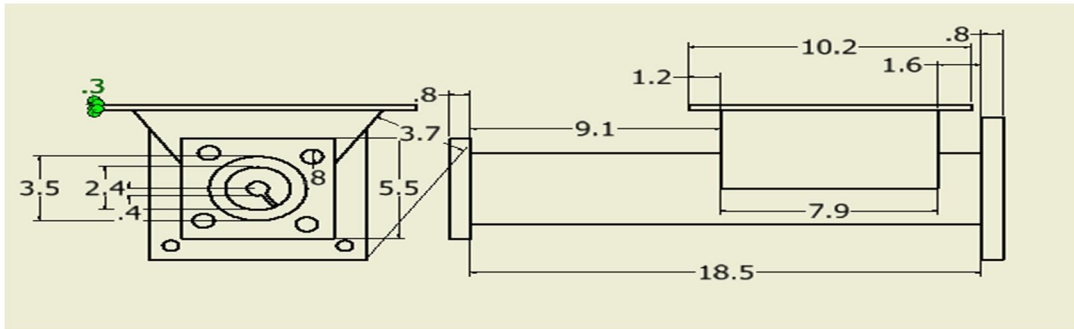


Figure 4.9 Sectional view of hopper and screw feeder



**Figure 4.10 Dimensions (in mm) of hopper and screw feeder**

### 4.3.1.2 Media displacement components

The hopper is filled with the PAG media which needs to be transferred to the workpiece for finishing, this transfer is ensured through displacement elements which consists of series of rotors (internal) and stators (external) as shown in Figure 4.11. Usually hard rotors operate against a soft elastomer stator. In this process single threaded helical screw or rotor, rotates eccentrically inside a double threaded helical stator.

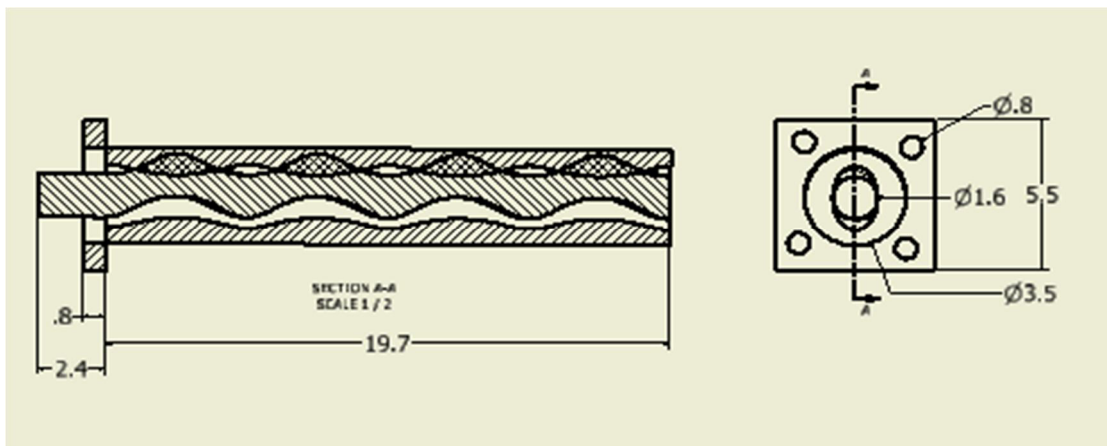


**Figure 4.11 Dimensions of rotor and stator in UAFM**

### 4.3.1.3 Reducer, flange & recycling unit

Flange is fabricated to support the reducer and assembled after the rotor and stator part.

Figure 4.12 shows sectional view of flange for recycling unit with dimensions.

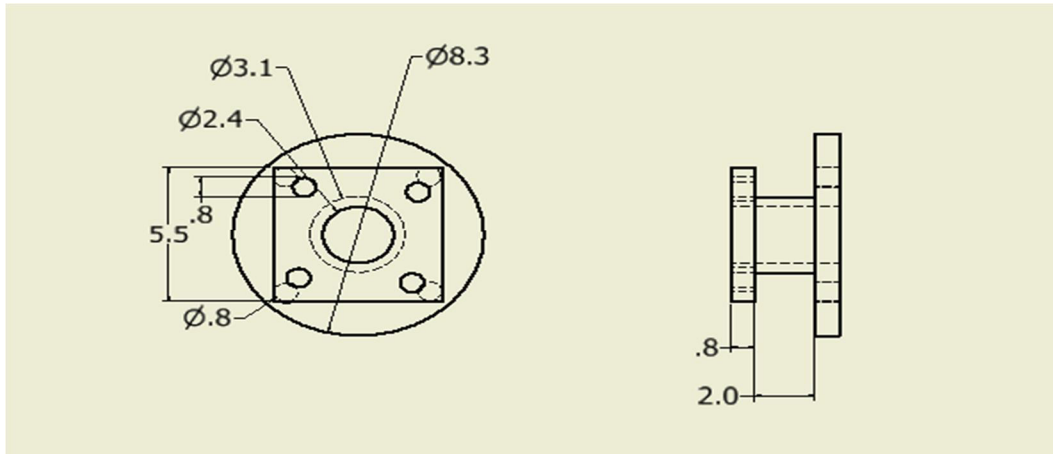


**Figure 4.12** Sectional view of flange for recycling unit with dimensions

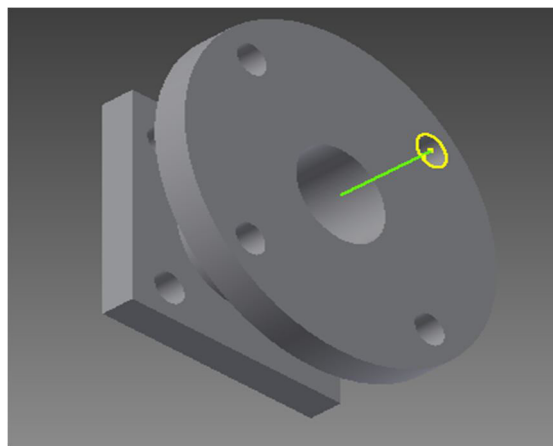


**Figure 4.13** CAD model of flange for UAFM

In this unit reducer is fabricated using the sand casting technique as shown in Figure 4.14. Reducer is mainly used after rotor and stator parts to provide flow at reduced dimensions. Pressure measurement sensor is installed on reducer unit.

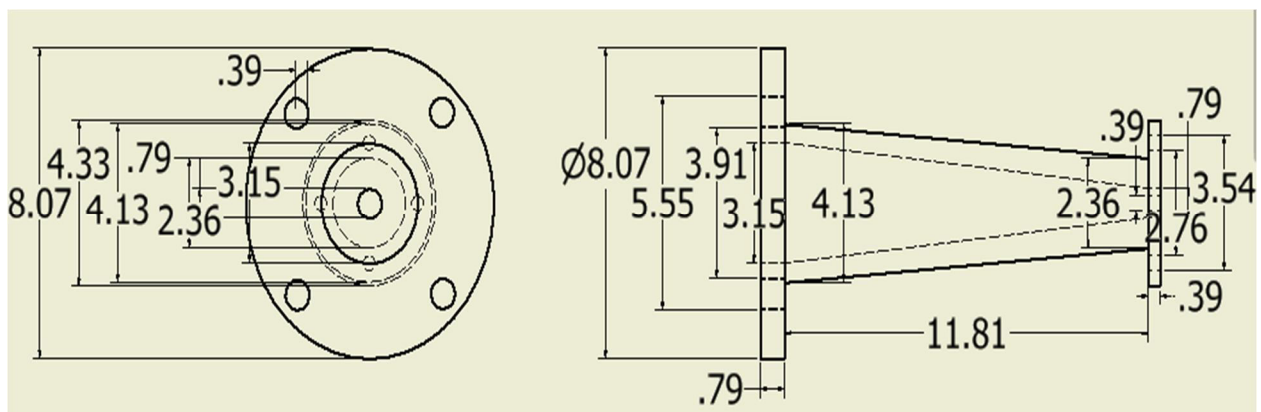


**Figure 4.14** Cad model of Reducer (with dimensions)

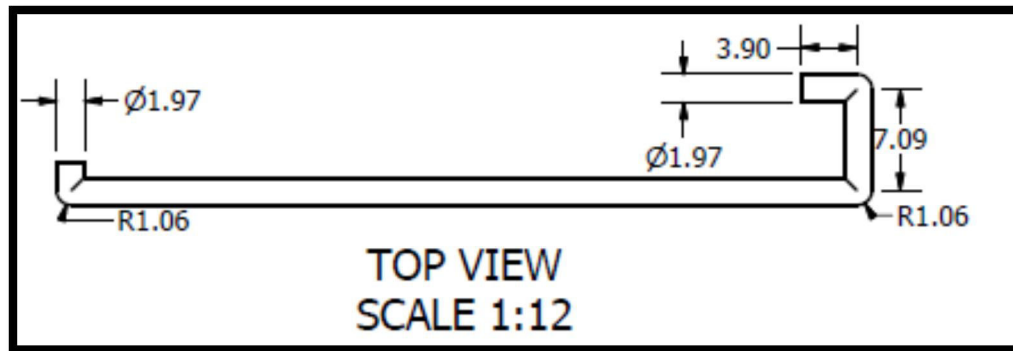


**Figure 4.15 Recycling unit for flow of media in hopper**

Recycling unit is used for flowing of AFM media after finishing in hopper. SS pipes are joined as per dimensions given in above Figure 4.15. This unit is installed after tooling unit in UAFM setup.

#### **4.3.1.4 Driving and control element**

Driving unit consists of 3 phase AC motor (Crompton Greaves Limited) of capacity 5.5 KW as shown in Figure 4.16. Motor is also attached with gear box (gear ratio 5.09) to reduce the rpm of motor. Motor is main driving unit to provide the power to whole AFM setup. The motor is coupled with Oldham coupling to provide rotary motion to media extruding element.



**Figure 4.16 Electric motor with gear unit.**

The series of rotors are coupled to a RPM controlled electrical motor via a extruding element and coupling. Care is taken that the shaft is supported on bearings and leak proof oil seals.

### **Variable frequency drive**

Variable frequency drive is used to control the speed of motor. During experimentation, speed in terms of rpm is controlled by using VFD device. VFD (Crompton Greave Ltd.) is installed (shown in Figure 4.17) to control the rpm of motor. The maximum motor rpm is 1450 rpm. After using the reduction gear, it is further reduced by 285 using gear ratio of 5.09. The controlled rpm is used for setting the UAFM setup at different pressure.



**Figure 4.17 Variable frequency drive**

### **Strain gauge based pressure unit**

Figure 4.18 shows the strain gauge based pressure sensor installed on reducer unit of UAFM setup. Also a single channel data logger is used to read the pressure reading during experimentations. So pressure is changed by varying the flow rate (using VFD) and readings are recorded on display of data logger.





Figure 4.18 Strain gauge based pressure sensor and data logger

#### 4.3.1.5 Mounting base

The UAFM setup is mounted on the work table with the help of steady rests. Mounting base (shown in Figure 4.19) is designed on basis of overall length and weight of the machine. Major important factor is to reduce noise and vibration disturbance.

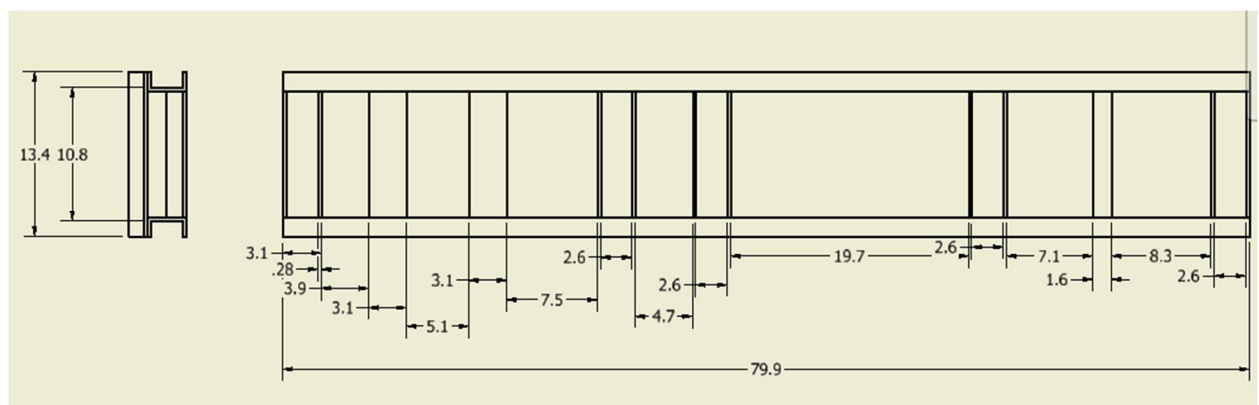


Figure 4.19 Sketch with dimension (in mm) of mounting base

#### 4.3.1.6 Tooling

Tooling play major role to link media displacing unit with workpiece during AFM of Trim die by guiding the AFM media. The inner shape and dimensions of tooling are selected based on principle of slug length of workpiece. The amount of material removal from workpiece is directly related to slug length of the flow. Restriction in passage formed by the combination of workpiece and tooling cause the removal of material from the desired surface [98], [99]. The slug length of flow can be determined from relation of media flow volume divided by cross sectional area of restricting passage [94].

### Tooling for trim die for UAFM

For flowing the PAG media for internal surfaces and holding the workpiece (i.e. trim die), tooling is designed as shown in Figure 4.20 (b). Tooling is designed based on the shape, size and surface to be finished. Another criterion for the design of tooling is the easy mounting and removal of the component. A typical die for which tooling is designed is shown in Figure 4.20 (a).

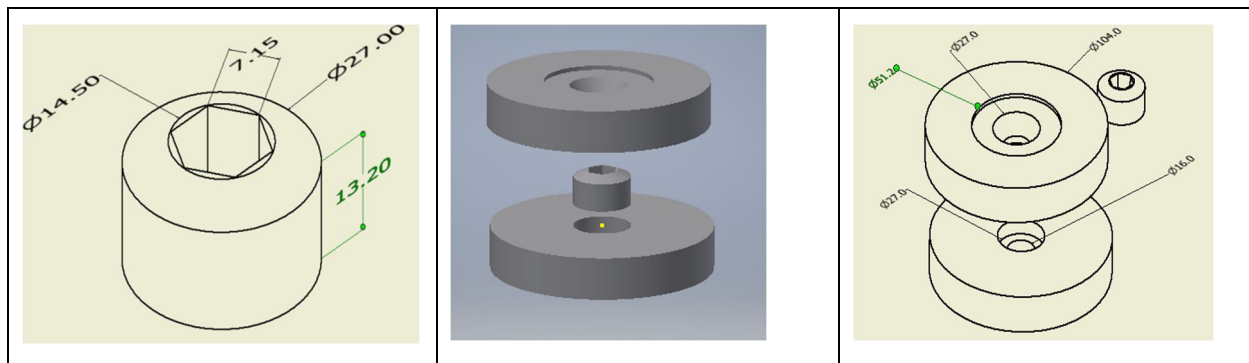


Figure 4.20 (a) HSS trim die (b) Tooling scheme (c) Dimensions of tooling (Left and right part)

Dimensions (in mm) of tooling for flowing the PAG media and holding the workpiece (i.e. Trim die) are shown in Fig. 4.20 (c). Tooling for flowing the PAG media and holding the workpiece 4.22 (a) without nylon tooling 4.22 (b) clamping with nylon tooling.

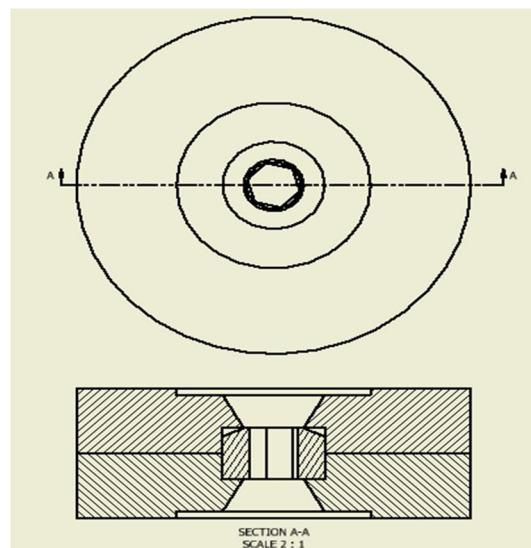
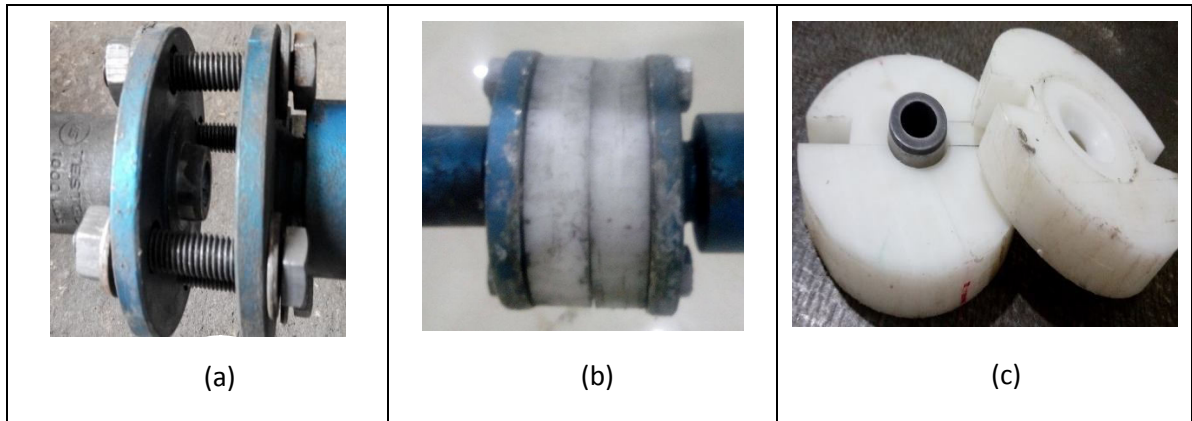


Figure 4.21 Sectional view of tooling for trim die



**Figure 4.22 (a) UAFM without nylon tooling (b) Tooling fixed with trim die (c) Left and right part of tooling**

The designed and fabricated tooling is used for finishing the hexagonal shape trim die of 14.50 mm diameter and 13.20 mm length as shown in Figure 4.20 (a). Nylon is selected as tooling material die to its leak proof fitting with workpiece and good machinability. Figure 4.20 (b) shows the CAD model of left and right part of tooling and Figure 4.20 (c) shows the detailed dimensions of left and right part of tooling. The inner dimensions left part of tooling is designed with matching the workpiece internal dimensions and outer dimensions are selected based on reducer internal diameter. Figure 4.21 shows the CAD model of different section of left and right part of tooling for holding the trim die workpiece and guiding the AFM media.

### **Tooling for Stamping die For UAFM**

For flowing the AFM media for internal surfaces and holding the workpiece (i.e. stamping die), tooling is designed as shown in Figure 4.23 (b). Tooling is designed based on the shape, size and surface to be finished. A typical die for which tooling is designed is shown in Figure 4.23 (a).

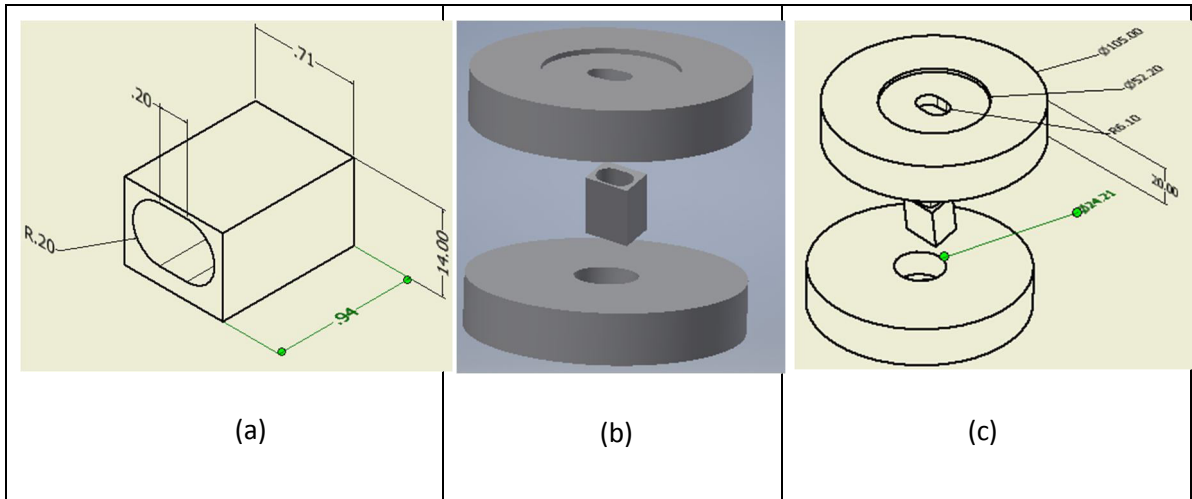


Figure 4.23 (a) HSS stamping die (mm) (b) Tooling scheme (c) Dimensions of tooling (Left and right part)

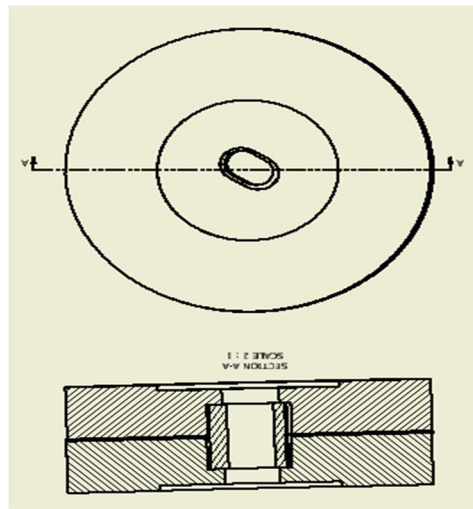


Figure 4.24 Sectional view of tooling for stamping die

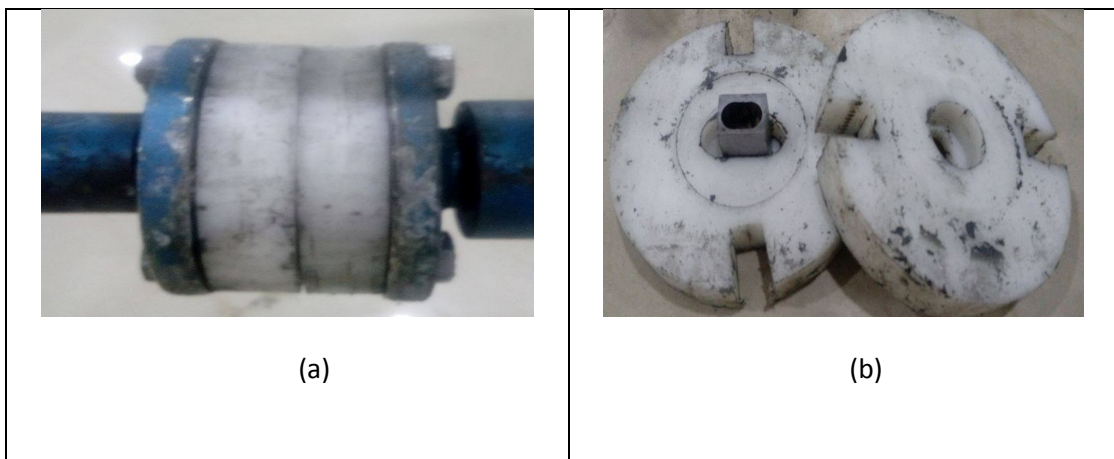


Figure 4.25 (a) Tooling fixed with stamping die (b) Left and right part of tooling

Dimensions (in mm) of tooling for flowing the AFM media and holding the workpiece (i.e. Stamping die) are shown in Fig. 4.23 (c). Figure 4.24 shows tooling for flowing the AFM media and holding the stamping workpiece Figure 4.25 (a) with nylon tooling Figure 4.25 (b) Left and right part of tooling.

The designed and fabricated tooling is used for finishing the stamping die of 10 mm diameter and 14 mm length as shown in figure 4.23 (a). Nylon is selected as tooling material die to its leak proof fitting with workpiece and good machinability. Figure 4.23 (b) shows the CAD model of left and right part of tooling and Figure 4.23 (c) shows the detailed dimensions of left and right part of tooling.

The inner dimensions left part of tooling is designed with matching the workpiece internal dimensions and outer dimensions are selected based on reducer internal diameter. Figure 4.24 shows the CAD model of different section of left and right part of tooling for holding the trim die workpiece and guiding the AFM media.

### **Tooling for stamping die for micro technica AFM**

Figure 4.26 shows the tooling designed for stamping die for commercial available AFM (Micro-Technica). Figure 4.27 shows the fabricated tooling for holding the stamping die.

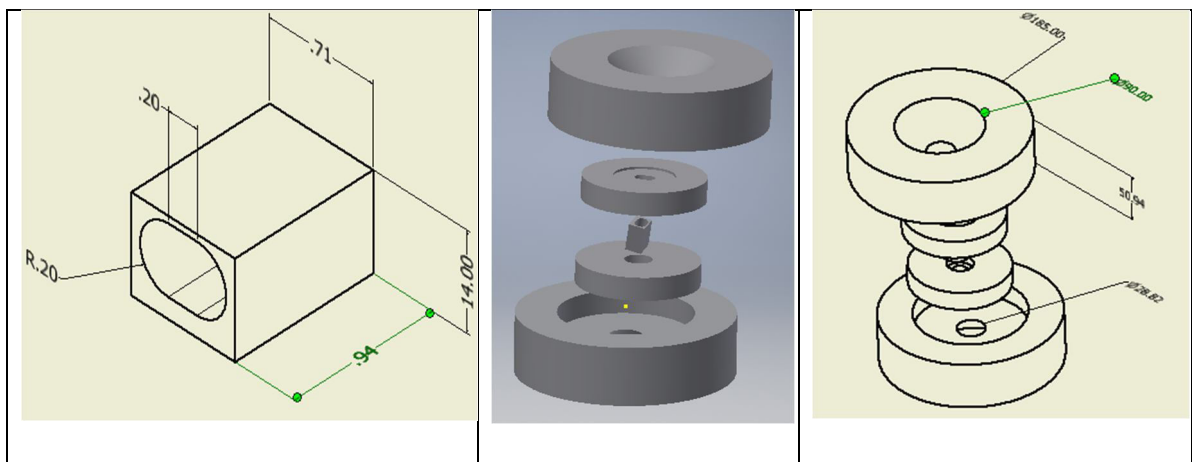


**Figure 4.26 CAD model of designed tooling**



**Figure 4.27 Nylon tooling for holding the stamping die in commercial AFM**

### **4.3.2 Development of UAFM**

During fabrication process the standard parts are procured from different vendor and assembled with fabricated parts. Major parts are media displacement element, extrusion element and reducer, tolling unit. Some parts are casted as per drawings using sand casting technique. For tooling, nylon material is used and machined by CNC milling machine. Screw feeder and rotor parts are joined using oldham coupling which is flexible in four direction. A ball bearing was used on driving shaft for smooth functioning of setup. Tooling is designed and fabricated in such a way that component can be hold and removed in minimum time.

Each designed parts of UAFM setup are assembled as shown in Figure 4.28. The fabricated UAFM setup with label of major parts are shown in Figure 4.30.

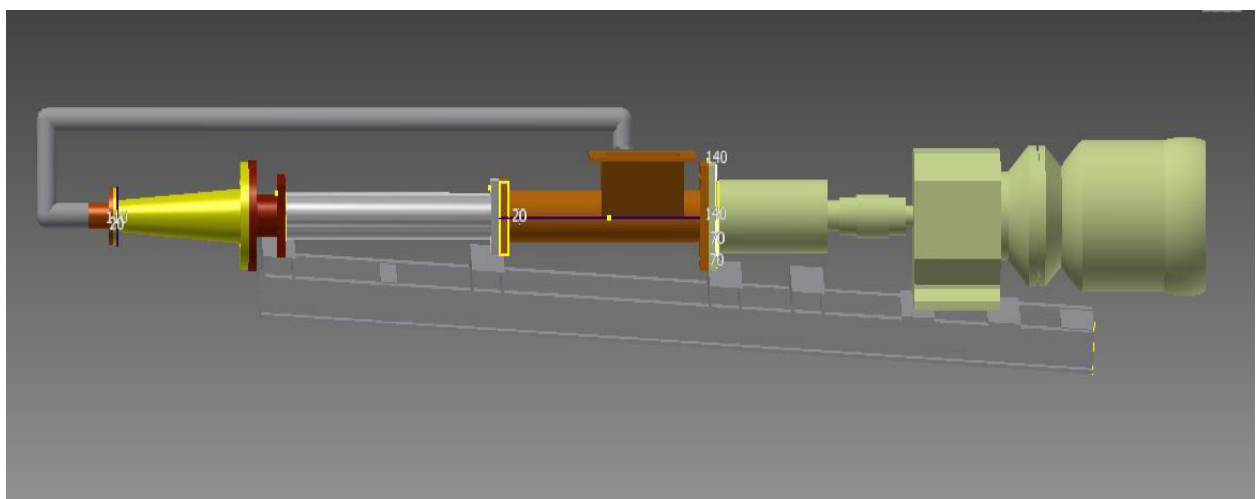


**Figure 4.28 Assembled cad model of unidirectional abrasive flow machine**

The sketch with all dimensions of the UAFM has been shown in Figure 4.29.

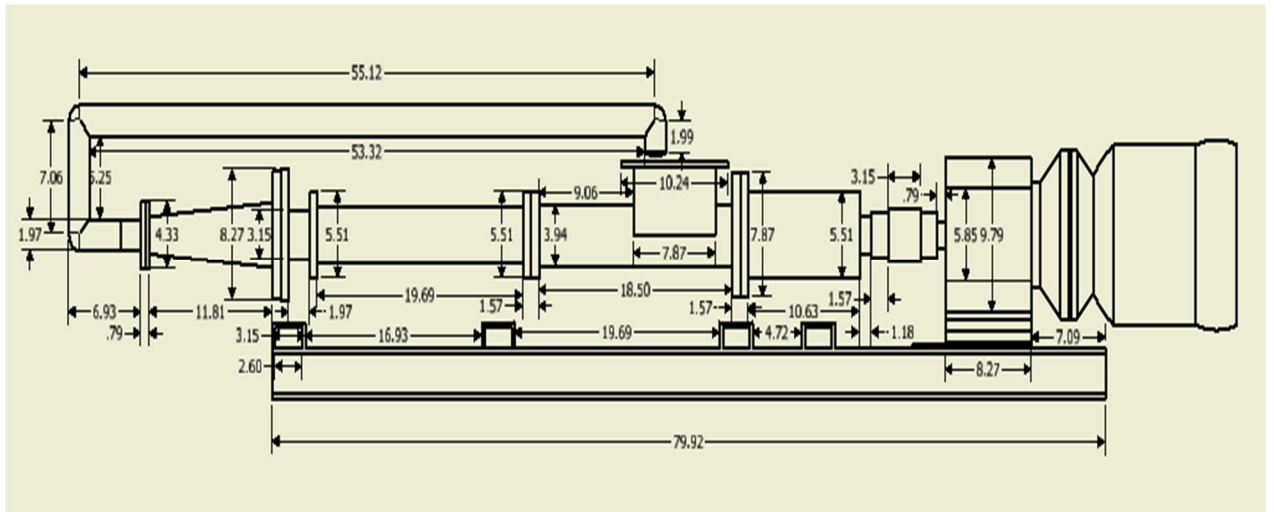


Figure 4.29 2D sketch with dimension (in mm) of UAFM

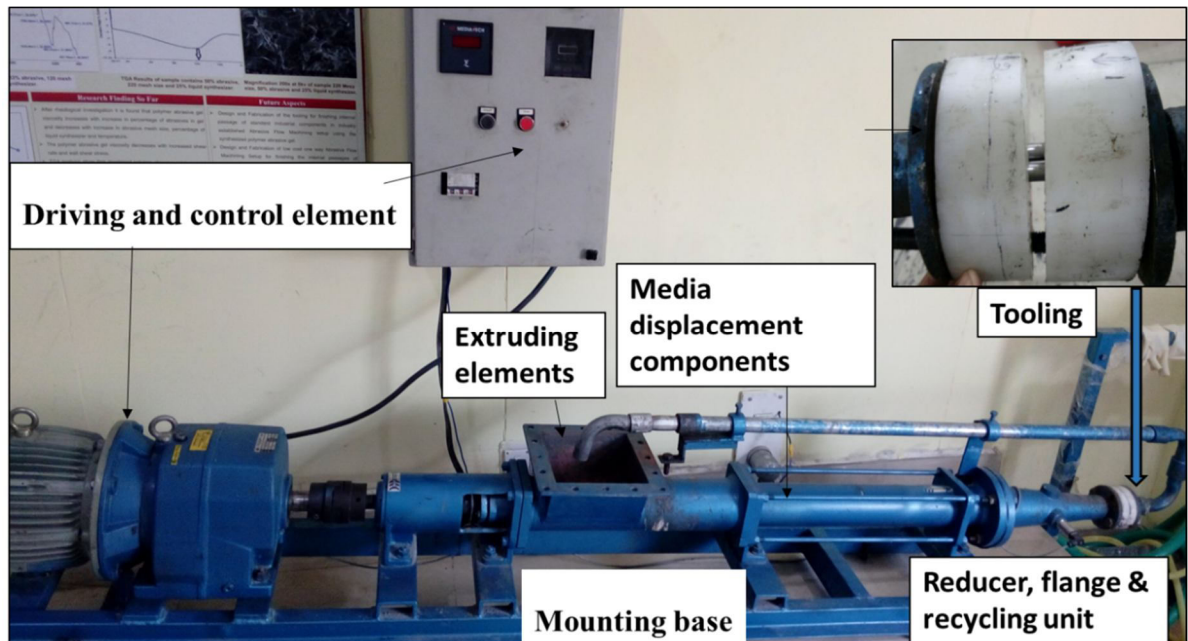


Figure 4.30 Images of fabricated unidirectional abrasive flow machine (UAFM) setup.

All fabricated parts are assembled using joints, coupling and screw nut bolts to form a unidirectional abrasive flow machine setup as shown in Figure 4.30. This setup is capable of work up to maximum extrusion pressure of 3.2 MPa.

### 4.3.3 Summary of raw material used for developed UAFM setup

The following is list of raw material used for various components of developed AFM setup:-

- (1) A. C. Motor- 5.5 kw capacity with gear reduction of 5.09 gear ratio
- (2) Variable frequency derive- Crompton Greaves of 5.5 capacity kw A.C. motor
- (3) Pressure Sensor unit - Strain gauge based sensor, NI single channel data logger
- (4) Extruding element- Screw feeder (Cast iron), Hopper (Cast iron)
- (5) Media displacement components- Stator (Ethylene propylene rubber), Rotor (HSS material).
- (6) Flange, reducer & recycling unit- Flange (CI), Reducer (CI), and Recycling hose pipe (SS).
- (7) Tooling - Nylon material.
- (8) Support base : CI

Appendix C represents detailed raw material specifications, mathematical relation [100] [101] used for design of each components, calculated and designed dimensions considered for the developed UAFM setup.



## Chapter 5 Experiment Methodology

This chapter includes the experimental setups and experimental procedures adopted for experimentation of internal finishing of industrial components. The overview of setup, workpiece, alternative PAG media along with numerous measurement techniques and equipment is also described in the final section.

### 5.1 Machine tools

#### 5.1.1 Unidirectional abrasive flow machine (UAFM)

The unidirectional abrasive flow machining setup is designed using Autodesk inventor professional software. The same designed parts are fabricated, procured and assembled in the laboratory. The fabricated UAFM setup is shown in Figure 5.1. The specifications of BL 100 D are given in Table 5.1 below.

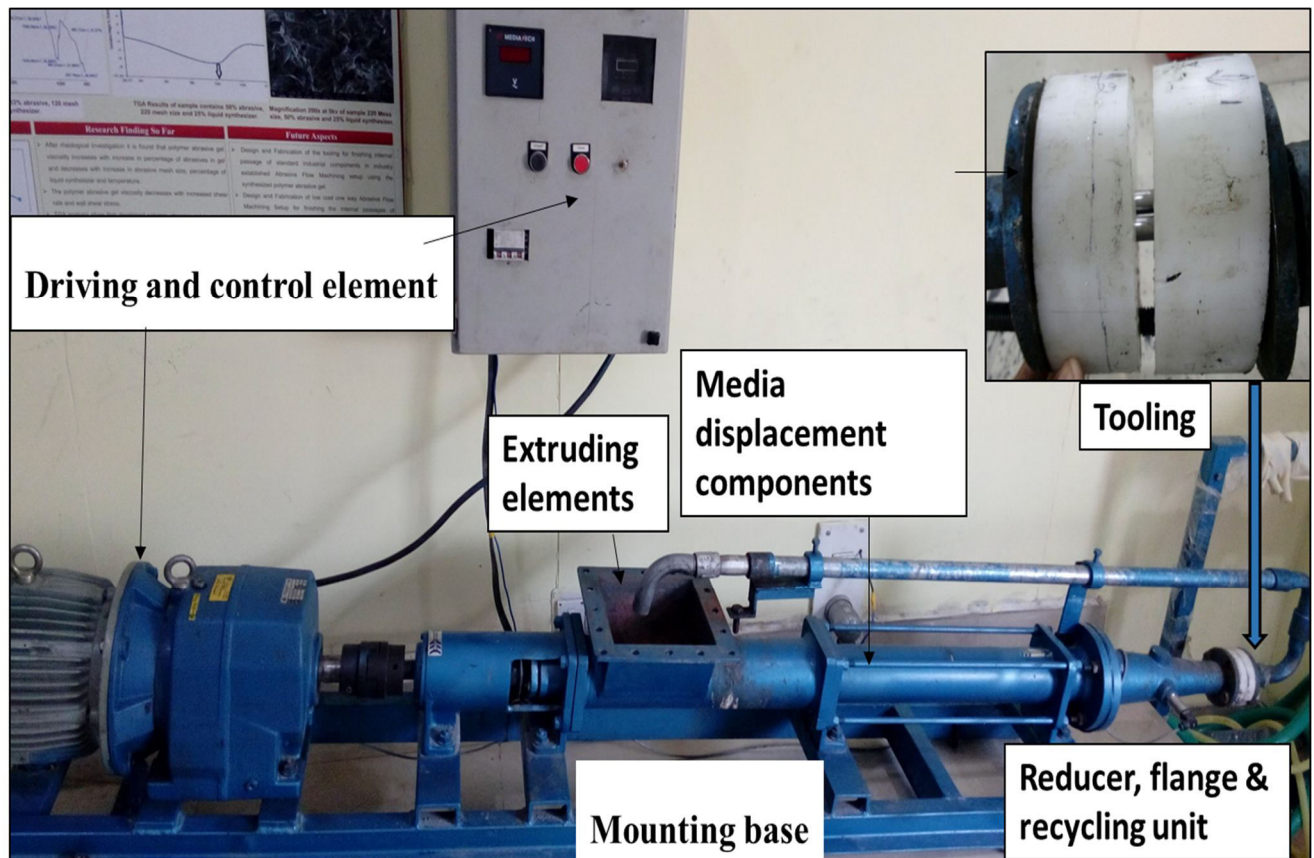


Figure 5.1 Fabricated unidirectional abrasive flow machine setup.

**Table 5.1 Specifications of UAFM**

|                                    |                                   |
|------------------------------------|-----------------------------------|
| Control Speed                      | Variable Frequency Drive Unit     |
| Media cylinder diameter            | 0.1 meter                         |
| Media Stroke Length                | 0.140 meter                       |
| Media flow rate                    | 0.0008166667 m <sup>3</sup> /sec. |
| Media Pressure                     | 0-3.2 * 10 <sup>6</sup> Pascal    |
| Media capacity                     | 6-10 kg                           |
| Max. Viscosity of fluid can handle | 2710 pa-sec.                      |

For holding the component, fixture and tooling was fabricated using nylon material. Fabricated fixtures with slot are explained in last chapter. Nylon material is easy to machine and slot can be made easily as per work piece geometry. During machining of AFM tooling the flow passage was progressively reduced letting smooth flow of media and minimum restrictions. The workpiece with tooling and fixture is detached and a new component is positioned using tooling and fixture slots after the fix number of finishing time, as design of experiment table. For avoiding the leakage of media, the fixture is tightened with two set of bolts.

### **5.1.2 Bidirectional abrasive flow machine (Micro Technica BL 100 D)**

Commercial bidirectional AFM (Micro Technica BL 100 D) was used to study the comparative performance analysis of PAG media and commercial AFM media (streamer). The photograph of the AFM is shown in Figure 5.2. The specifications of BL 100 D are given in Table 5.2 below.

**Table 5.2 Specifications of Bidirectional AFM-BL 100 D**

|                         |  |
|-------------------------|--|
| <b>Control System</b>   | <b>PLC controlled with Siemens TP177</b> |
| Media cylinder diameter | 0.1 meter                                |
| Media Stroke Length     | 0.280 meter                              |
| Media flow rate         | 0.0001 m <sup>3</sup> /sec.              |
| Media Pressure          | 0-10 <sup>7</sup> Pascal                 |
| Media capacity          | 6-10 kg                                  |
| Hydraulic Tank capacity | 75 Ltr.                                  |



**Figure 5.2 Bidirectional abrasive flow machine (Micro Technica BL100D)**

For holding the component, fixture and tooling is fabricated using nylon material. Fabricated fixtures with slot are explained in last chapter. The workpiece with tooling and fixture are detached and a new component is positioned using the working table attached in AFM.

### **5.1.3 Workpiece material**

For finishing experiments, the trim die and stamping die components are selected from a die industry (Push Up Tools Udhyog Ltd. Rohtak) as shown in Figure 4.20 (a) and Figure 4.23 (a). The components material are high speed steel (HSS) for trim die and stamping die. The composition of die material is determined using an optical spectrometer (LECO GDS500A). The percentage proportions of basic elements are presented in Table 5.3 and Table 5.4.

**Table 5.3 Percentage proportions of basic elements in trim die workpiece material**

| Basic Elements | C    | Si   | P    | Cr   | Al   | As   | Co   | Cu   | Nb   | Mn   | Mo   | Ti   | V    | W    | Ni   | Fe |
|----------------|------|------|------|------|------|------|------|------|------|------|------|------|------|------|------|----|
| Weight %       | 0.75 | 0.39 | 0.02 | 6.02 | 0.01 | 0.01 | 0.09 | 0.17 | 0.10 | 0.14 | 3.99 | 0.03 | 1.59 | 7.32 | 0.58 | 74 |

**Table 5.4 Percentage proportions of basic elements in stamping die workpiece material**

| Basic Elements | C    | SiC  | Mn   | P    | Cr   | Mo   | Ni   | Al    | As    | Sn   | V    | W    | Fe   |
|----------------|------|------|------|------|------|------|------|-------|-------|------|------|------|------|
| Weight %       | 1.21 | 0.28 | 0.11 | 0.01 | 13.8 | 0.84 | 0.24 | 0.008 | 0.016 | 0.01 | 0.26 | 0.03 | 83.1 |

#### 5.1.4 AFM media

For experimentation as per design of experiment three type of PAG media at different viscosity were synthesized. The viscosity of media was changed by varying percentage composition of liquid synthesizer. The synthesization procedure is already explained in chapter 3. The Silicon carbide (SiC) abrasives of 220 mesh size were used in PAG media. Also percentage of abrasives in PAG media was 50% throughout all experimentation.

### 5.2 Measuring instruments

The field emission scanning electron microscopy (Nova NanoSEM 450) is used to capture the surface quality before finishing and after finishing the components. Wensar Electronic weighing machine is used for measurement of weight of the workpiece during experimentations. Rotational Rheometer (Temperature control) of Anton Paar make is used for rheological study of developed PAG media. Surface roughness value of finished and unfinished workpiece is measured using Taylor hobson (Surtronic 100 series) surface roughness measuring instrument

The specifications of instrument used for measuring the surface roughness of finished surface given below:-

|                     |                       |
|---------------------|-----------------------|
| Manufacturer        | Taylor Hobson Limited |
| Serial number       | 001324                |
| Working temperature | 20 °C + 2 °C          |
| Least count         | 6nm                   |
| Stylus radius-      | 5µm                   |
| Evolution length-   | 4.0mm                 |
| Cut off value-      | 0.8mm                 |

### **5.3 Design of experiment**

To validate the developed UAFM process for finishing the industrial components, it is very important to search and select an economic and capable technique. UAFM setup and PAG media has been developed for the purpose and explained in chapter 3 and chapter 4. Now it is very essential to select process variables and their levels of developed UAFM setup for successful experimental analysis. A set of experiments have been performed in a pre-planned way to study the influence of various parameters of developed UAFM setup during finishing of Stamping die and trim die components.

Design of experiment is considered to be very beneficial technique for accomplishing these tasks. The advantage of using the design of experiment are significant reduction in number of trials, finding out optimal parametric setting and determination of experimental errors [102][103]. The detailed planning and design of experiments considered for present experimental investigation are briefly explained in this chapter.

### **5.4 Scheme of experimentation**

The experiments are planned in two stages, preliminary and detailed study. The basic motive of preliminary study is to test the fabricated UAFM setup with PAG media (explained in chapter 3). Also PAG media is used to identify the utility and effectiveness of developed UAFM setup for finishing industrial components. The objective of preliminary study is also to identify the trend of developed AFM process variables comparative with previous studies.

The main objective of detailed experimentation is to test the suitability of developed UAFM setup for finishing the industrial components, to study the parametric effect on performance measure responses, and to optimize the process variables for achieving the better surface improvement during the AFF process.

## 5.5 Preliminary study

As outlined in last section, the objective of preliminary experimentation is to test the fabricated UAFM setup using the PAG media (explained in chapter 2), and to identify the utility and effectiveness of developed UAFM setup for finishing industrial components. For preliminary test, improvement in surface roughness and material removal are considered as response characteristics.

### 5.5.1 Control factors and their range

The effect of three controllable factors namely finishing time, extrusion pressure and viscosity of PAG media are studied in the preliminary experiment. These control factors and their ranges were decided based on literature, pilot experimentation, and machine competence. The independent control factors and their levels in coded and actual values are shown in Table 5.5.

**Table 5.5 Experimental control factors and their levels**

| Sr. No. | Levels | Variables          | Levels |    |    | Unit    |
|---------|--------|--------------------|--------|----|----|---------|
|         |        |                    | 1      | 2  | 3  |         |
| 1       | A      | Extrusion Pressure | 12     | 22 | 32 | Bar     |
| 2       | B      | Finishing Time     | 30     | 40 | 50 | Minutes |
| 3       | C      | Viscosity          | L      | M  | H  | Pa-sec. |

### Other experimental conditions

|                           |   |                    |
|---------------------------|---|--------------------|
| Abrasive mesh size        | : | 220                |
| Abrasive concentration    | : | 66 %               |
| Media flow rate           | : | 48 L/min.          |
| Temperature of media      | : | 32 °C +-2 °C       |
| Initial surface roughness | : | 1.5 +- 0.2 $\mu$ m |
| Passage length            | : | 11mm               |

### 5.5.2 Taguchi based experimental design

Experimental design is mainly used for searching out optimal setting of control factors to make process insensitive to noise factors. Keep in view; the trial experimentation has been carried out using Taguchi experimental design technique for optimal parametric combinations of AFM process which can ensure the quality of the finishing through effective control over the process characteristic. In Taguchi technique, signal to noise ratio is used to measure the quality and orthogonal array is constructed for studying the design parameters simultaneously. The Signal to Noise ratio is of three types as Smaller-the-better, Normal-the- best and larger-the-better. During experiment, improvement in surface roughness and material removal can be considered as quality characteristics based on higher-the-better. The higher-the-better performance characteristic is expressed as follows:

$$\eta_{ij} = -10 \log(L_{ij}) \quad \dots 5.1$$

$$L_{HB} = \frac{1}{n} \sum_{i=1}^n \frac{1}{y_i^2} \quad \dots 5.2$$

The S/N ratio for improvement in surface roughness ( $\Delta Ra$ ) and material removal (MR) are calculated utilizing the above mathematical relation. Considering the various process variables in Table 5.5 i.e. extrusion pressure, finishing time and viscosity of PAG media; preliminary experiments are carried out based on Taguchi orthogonal array. The PAG media is converted into three viscosity grades levels by uniformly mixing the abrasive with polymer base and liquid synthesizer with low to high viscous in range of 50 pa-sec. to 300 pa-sec. (explained in appendix- D). Table 5.6 represents the Taguchi experimental design of  $L_9$  orthogonal array for conducting the preliminary experiments.

**Table 5.6 Taguchi experimental design of L<sub>9</sub> orthogonal array**

| Exp. No. | AFM parameters |   |   | UAFM parameters     |                          |                     |
|----------|----------------|---|---|---------------------|--------------------------|---------------------|
|          | A              | B | C | Ext. Pressure (bar) | Finishing Time (Minutes) | Viscosity (Pa-sec.) |
| 1        | 1              | 1 | 1 | 30                  | 35                       | L                   |
| 2        | 1              | 2 | 2 | 30                  | 45                       | M                   |
| 3        | 1              | 3 | 3 | 30                  | 55                       | H                   |
| 4        | 2              | 1 | 2 | 40                  | 35                       | M                   |
| 5        | 2              | 2 | 3 | 40                  | 45                       | H                   |
| 6        | 2              | 3 | 1 | 40                  | 55                       | L                   |
| 7        | 3              | 1 | 3 | 50                  | 35                       | H                   |
| 8        | 3              | 2 | 1 | 50                  | 45                       | L                   |
| 9        | 3              | 3 | 2 | 50                  | 55                       | M                   |

## 5.6 Detailed experiments

The objective of detailed experimentation is to utilize the fabricated UAFM setup using the PAG media (explained in chapter 2), and to identify the utility and effectiveness of developed UAFM setup for finishing industrial components. For detailed experiment, improvement in surface roughness ( $\Delta R_a$ ) and material removal (MR) are considered as response characteristics. The improvement is defined as difference in Ra before and after AFM of components. It has been referred as improvement in arithmetic mean value of surface roughness. Utilizing the test results improvement in surface roughness (improvement in SR) is calculated as follows,

$$\text{Improvement in SR} = [\text{SR (Initial value before finish)} - \text{SR (After finishing)}] \mu\text{m} \dots(5.3)$$



For measurement of surface roughness value, Taylor Hobson Surtronic 100 series instrument is used before and after every experiment.

### 5.6.1 Control factors and their range

From the basic working principle and characteristic feature of UAFM process for internal finishing, it has been observed that the machining variables such as extrusion pressure, finishing time, and viscosity of polymer abrasive gel (PAG) media are the most important controllable process parameters or variables of UAFM process. On the outcomes of trial investigation and an extensive literature survey, the variables implemented and each variables level are presented in Table 5.7.

**Table 5.7 Input variables and their levels**

| Sr. No. | Levels | Variables          | Levels |      |      | Unit    |
|---------|--------|--------------------|--------|------|------|---------|
|         |        |                    | -1     | 0    | 1    |         |
| 1       | A      | Extrusion Pressure | 12     | 22   | 32   | Bar     |
| 2       | B      | Finishing Time     | 30     | 40   | 50   | Minutes |
| 3       | C      | Viscosity          | (-1)L  | (0)M | (1)H | Pa-sec. |

#### Constant variables:

|                           |   |               |
|---------------------------|---|---------------|
| Abrasive mesh size        | : | 220           |
| Abrasive concentration    | : | 66 %          |
| Media flow rate           | : | 48 L/min.     |
| Temperature of media      | : | 32 °C +-2 °C  |
| Initial surface roughness | : | 1.5 +- 0.2 μm |
| Passage length            | : | 11mm          |

In detailed study, three major parameters namely extrusion pressure (A), finishing time (B) and viscosity of PAG media (C) are considered for investigation. Each considered variable has three different levels and accordingly design of experiment has been setup before conducting the details study during AFM of industrial components.

The abrasive mesh sizes are kept constant at 220 for preparation of PAG media and same was used for detailed experimentation. PAG media is synthesized by uniformly mixing (SiC) abrasives in the polymer base with weight ratio of 66%. The PAG media is converted into three viscosity grades levels by uniformly mixing the abrasive with polymer base and liquid synthesizer with low to high viscous in range of 50 pa-sec. to 300 pa-sec. (explained in appendix-D). Finishing time is varied from 30-50 minutes in step of 10 minutes with varying extrusion pressure from 12 bar to 32 bar. Other experimental condition are considered as stroke length 500 mm, media flow rate as 3 m<sup>3</sup>/hr.

### 5.6.2 Response surface method based experimental design

In present work, response surface method (RSM) was applied to observe influence of finishing process variables on finishing performance variables during experiments. RSM is based on a synergistic combination of mathematics and statistics. The performance of the process is described by the second order polynomial regression model known as a quadratic model. In this study Design expert 8.1 software is used to evaluate the coefficient of regression based on the experimental results. Therefore, a set of 17 experiments are constructed on central composite rotatable design of response surface method [90]. Response parameters (MR and ΔRa) for trim die are presented in Tables 5.8. RSM fits polynomial models for the existing data into following equation:

$$y = \beta_0 + \sum_{i=1}^k \beta_{ii}x_i^2 + \sum_i \sum_j \beta_{ij}x_ix_j \quad \dots 5.4$$

Where,  $y$  is the predicted response;  $\beta_0$  is a constant;  $\beta_i$  is the linear coefficient;  $\beta_{ii}$  is the squared coefficient;  $\beta_{ij}$  is the cross product coefficient, and  $k$  is the number of factors [104].

In this study, the experiments were based on the central composite design (CCD) method. The factorial portion of CCD is a full factorial design with all groupings of the factors at two levels (high, +1 and low, -1) and consisting of eight-star points and six central points (coded level 0) which are mid-point between high and low levels. The star points are at the face of the cube portion of the design that corresponds to  $\alpha = \pm 2$ , and this type of design is commonly called the ‘face-centered CCD.’ The face-centered CCD includes 17 experimental runs at three independent control factors [105]. The experimental design matrix with a combination of control factors and corresponding performance measure values obtained from experimentation are listed in Table 5.8.

**Table 5.8 Experimental design matrix and observed performance measures in**

| Std | Run | Block   | Ext. pressure (Bar) | Finishing time (Minutes) | Viscosity (pa-sec.) |
|-----|-----|---------|---------------------|--------------------------|---------------------|
| 1   | 1   | Block 1 | 12.00               | 30.00                    | 0.00                |
| 15  | 2   | Block 1 | 22.00               | 40.00                    | 0.00                |
| 9   | 3   | Block 1 | 22.00               | 30.00                    | -1.00               |
| 12  | 4   | Block 1 | 22.00               | 50.00                    | 1.00                |
| 7   | 5   | Block 1 | 12.00               | 40.00                    | 1.00                |
| 8   | 6   | Block 1 | 32.00               | 40.00                    | 1.00                |
| 3   | 7   | Block 1 | 12.00               | 50.00                    | 0.00                |
| 17  | 8   | Block 1 | 22.00               | 40.00                    | 0.00                |
| 11  | 9   | Block 1 | 22.00               | 30.00                    | 1.00                |
| 10  | 10  | Block 1 | 22.00               | 50.00                    | -1.00               |
| 4   | 11  | Block 1 | 32.00               | 50.00                    | 0.00                |
| 13  | 12  | Block 1 | 22.00               | 40.00                    | 0.00                |
| 14  | 13  | Block 1 | 22.00               | 40.00                    | 0.00                |
| 5   | 14  | Block 1 | 12.00               | 40.00                    | -1.00               |
| 2   | 15  | Block 1 | 32.00               | 30.00                    | 0.00                |
| 6   | 16  | Block 1 | 32.00               | 40.00                    | -1.00               |
| 16  | 17  | Block 1 | 22.00               | 40.00                    | 0.00                |



## Chapter 6 Experimentation, Results and Discussion

Experiments are performed in two stages as per scheme of experiment in chapter 5. The preliminary experimentation is carried out to test the fabricated UAFM setup with PAG media. Also PAG is used to identify the utility and effectiveness of developed UAFM setup for finishing industrial components. The objective of preliminary study is also to identify the trend of developed AFM process variables and comparative with previous studies. Thereafter detailed experimentations are carried out for finishing two different industrial components.

### **6.1 Preliminary experiments**

Preliminary experiment is carried out utilizing the design and fabricated UAFM setup (explained in chapter 4) and for identifying the various process parameters which affect the surface quality during finishing of internal surface in a pre-planned way is explained in section 5.5.2 of chapter 5.

These experiments also help to check the suitability of developed alternative PAG media for finishing the internal surfaces. Considering various process variables such as extrusion pressure (parameter, A), finishing time (parameter, B) and viscosity of PAG media (parameter, C) experiments were performed based on Taguchi experimental design concept L<sub>9</sub> orthogonal array shown in Table 6.1.

#### **6.1.1 Preliminary experimental results**

Using the experimental data, improvement in surface roughness is derived by a relation as follow:

$$\text{Improvement in SR} = [\text{SR (Initial value before finish)} - \text{SR (After finishing)}] \mu\text{m} \quad \dots$$

(6.1)

To study the parametric effect on AFM performance variable, results obtained from nine experiments are used for various graphs.

**Table 6.1 Parametric level setting as per L<sub>9</sub> orthogonal array with experimental outcomes**

| Exp. No. | AFM parameters |   |   | Surface roughness value                 |  |                                       | MR(mg) |
|----------|----------------|---|---|---|--|---------------------------------------|--------|
|          | A              | B | C | Before finishing<br>Avg. R <sub>a</sub> | After finishing<br>Avg. R <sub>a</sub> | Improvement in SR<br>( $\Delta R_a$ ) |        |
| 1        | 1              | 1 | 1 | 0.70 $\mu$ m                            | 0.40 $\mu$ m                           | 0.30                                  | 5.25   |
| 2        | 1              | 2 | 2 | 0.62 $\mu$ m                            | 0.30 $\mu$ m                           | 0.32                                  | 7.55   |
| 3        | 1              | 3 | 3 | 0.65 $\mu$ m                            | 0.30 $\mu$ m                           | 0.35                                  | 8.75   |
| 4        | 2              | 1 | 2 | 0.60 $\mu$ m                            | 0.26 $\mu$ m                           | 0.34                                  | 8.95   |
| 5        | 2              | 2 | 3 | 0.85 $\mu$ m                            | 0.46 $\mu$ m                           | 0.39                                  | 9.68   |
| 6        | 2              | 3 | 1 | 0.73 $\mu$ m                            | 0.36 $\mu$ m                           | 0.37                                  | 8.35   |
| 7        | 3              | 1 | 3 | 0.88 $\mu$ m                            | 0.50 $\mu$ m                           | 0.38                                  | 11.12  |
| 8        | 3              | 2 | 1 | 0.95 $\mu$ m                            | 0.56 $\mu$ m                           | 0.39                                  | 11.22  |
| 9        | 3              | 3 | 2 | 0.60 $\mu$ m                            | 0.18 $\mu$ m                           | 0.42                                  | 12.25  |

### 6.1.2 Discussion on preliminary results

Based on experimental results shown in Table 6.1, SN ratio graphs are calculated for the optimum levels of the AFM parameters. Figure 6.1 shows signal to noise ratio value of extrusion pressure at 32 bar, finishing time at 50 and viscosity at H grade media for improvement in surface roughness ( $\Delta R_a$ ).

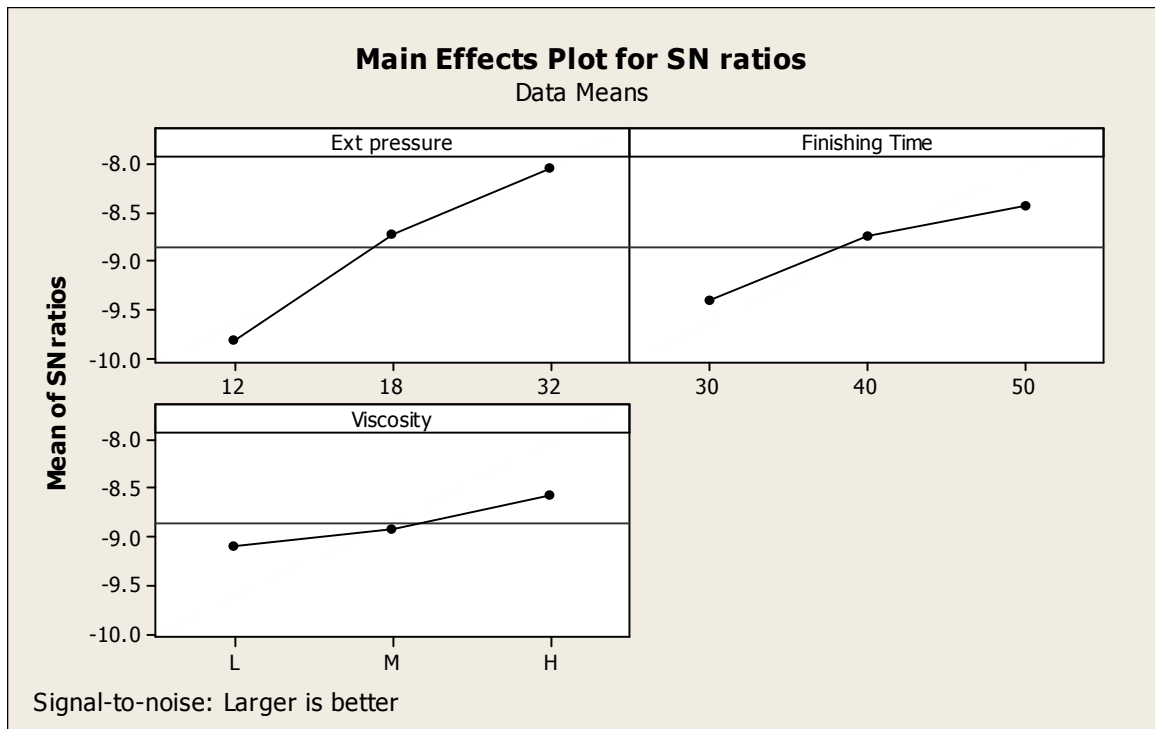


**Figure 6.1** Signal to Noise ratio graphs for improvement in surface roughness ( $\Delta Ra$ ).

Table 6.2 shows the rank of considered AFM process variables, which variables have most significant effect on improvement in surface roughness ( $\Delta Ra$ ). In this case extrusion pressure has most significant effect on improvement in surface roughness ( $\Delta Ra$ ).

**Table 6.2** Rank of AFM variable for improvement in surface roughness ( $\Delta Ra$ ).

| Level/Variables | Ext. Pressure | Finishing Time | Viscosity |
|-----------------|---------------|----------------|-----------|
| 1               | 0.3233        | 0.3400         | 0.3533    |
| 2               | 0.3667        | 0.3667         | 0.3600    |
| 3               | 0.3967        | 0.3800         | 0.3733    |
| Delta           | 0.0733        | 0.0400         | 0.0200    |
| Rank            | 1             | 3              | 2         |

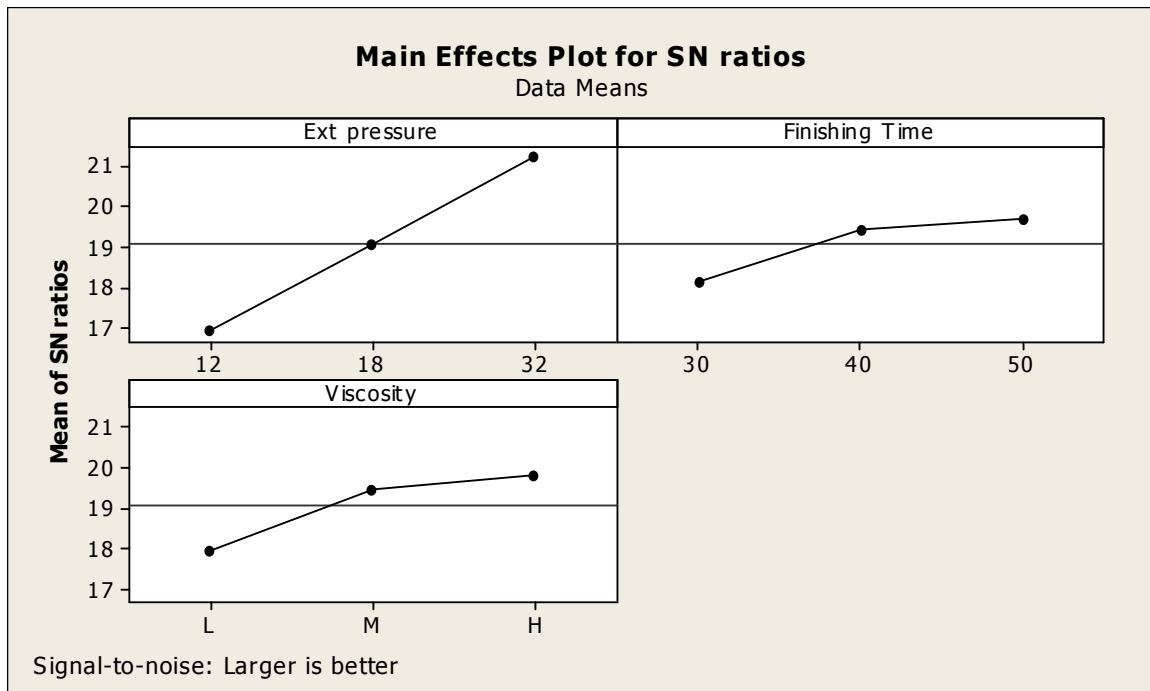


**Figure 6.2 Signal to Noise ratio graphs for material removal (MR)**

Figure 6.2 shows signal to noise ratio value of extrusion pressure at 32 bar, finishing time at 50 minutes and viscosity at H grade media for material removal (MR). Table 6.3 shows the rank of considered AFM process variables, which variables have most significant effect on material removal (MR). In this case also, extrusion pressure has most significant effect on material removal (MR).

**Table 6.3 Rank of AFM variable for Material removal (MR)**

| Level/Variables | Ext. pressure | Finishing Time | Viscosity |
|-----------------|---------------|----------------|-----------|
| 1               | 16.93         | 18.12          | 17.95     |
| 2               | 19.06         | 19.43          | 19.45     |
| 3               | 21.23         | 19.68          | 19.83     |
| Delta           | 4.29          | 1.56           | 1.88      |
| Rank            | 1             | 3              | 2         |



### 6.1.3 Parametric effect on response variables

This section explains the effect of different process parameters on performance parameters of AFM. Effect of variation in extrusion pressure (A), finishing time (B) and viscosity of PAF media (C) on developed UAFM response characteristics during finishing of internal surfaces using fabricated setup and PAG media are studied and explained through different graphs.

#### 6.1.3.1 Improvement in surface roughness ( $\Delta R_a$ )

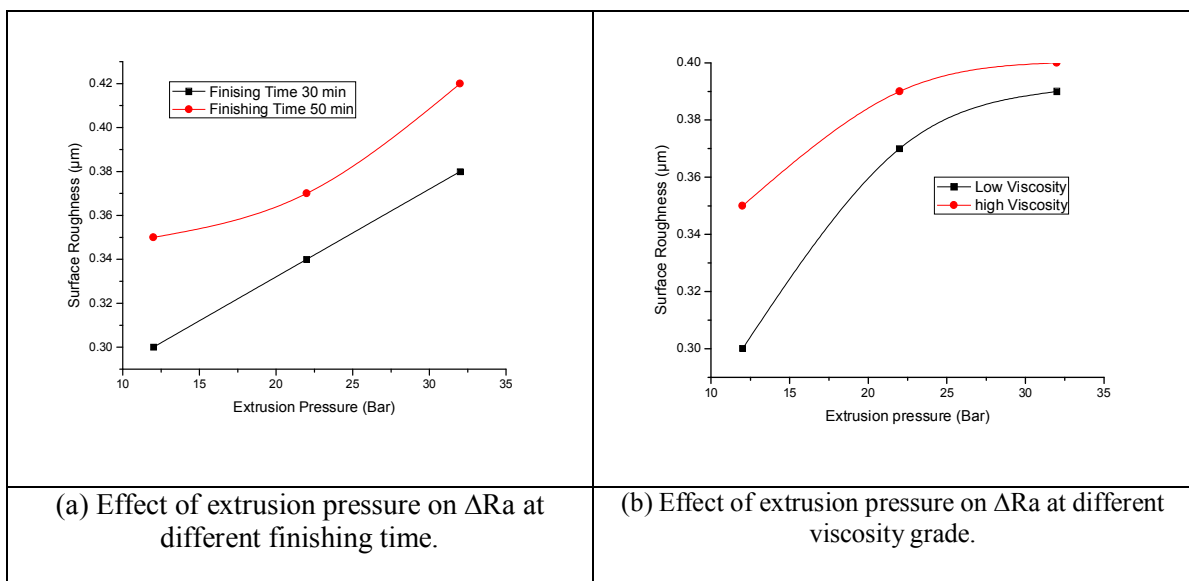
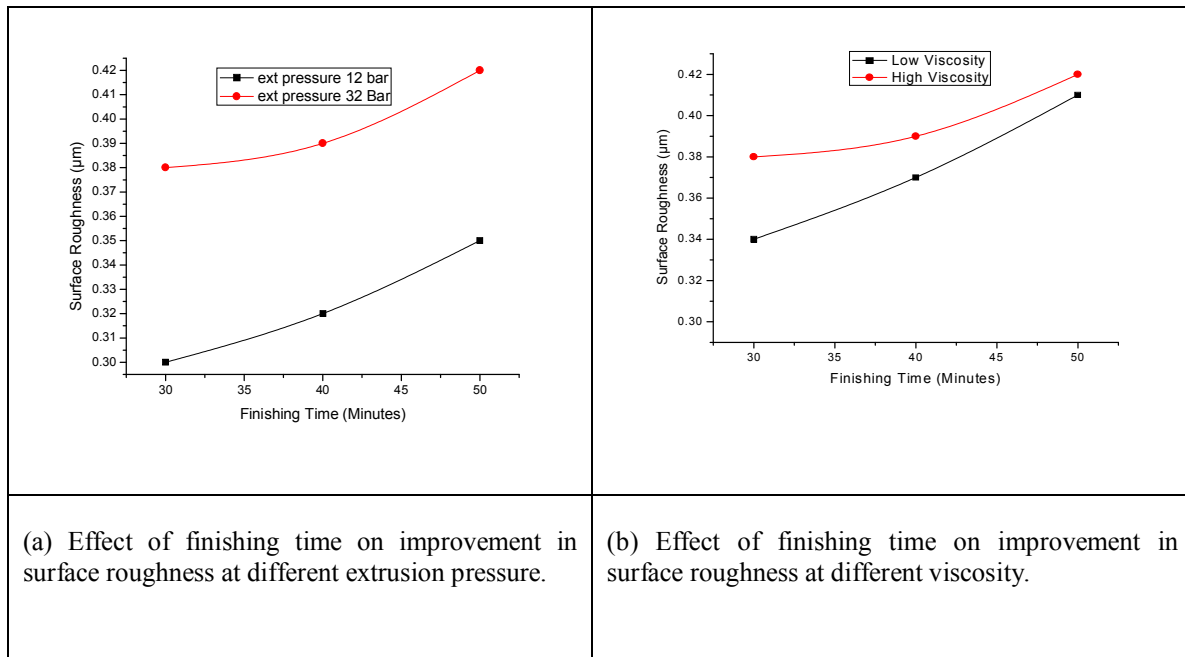


Figure 6.3 Effect of extrusion pressure

Figure 6.3 (a) shows the effect of extrusion pressure on improvement in surface roughness at different finishing time when viscosity is constant (Medium grade). From graphs shown in Figure 6.3 (a) it reveals that as extrusion pressure increases improvement in surface roughness increases. This is due to when extrusion pressure increases, normal force performing on each abrasive also increases that consequence in cavernous indentation on surface. At higher extrusion pressure, the material removal take place at deeper indentations in less finishing time results in more improvement in surface finishing. Figure 6.3 (b) shows the effect of extrusion pressure on improvement in surface roughness at different viscosity and finishing time is constant (40 minute). From graph it

reveals that improvement in surface roughness increased with higher extrusion pressure and higher viscosity.

Because of stiffer media, higher depth of penetration of abrasive grains is possible which would enhance the surface finish quality.



**Figure 6.4 Effect of finishing time**

Figure 6.4 (a) shows the effect of finishing time on improvement in surface roughness at different extrusion pressure when viscosity is constant (Medium grade). Graphs show that as the finishing time increases improvement in surface finishing  $\Delta Ra$  increases, at higher extrusion pressure. This is due to increases in time of indentation of abrasives particles on workpiece surface increases results in higher  $\Delta Ra$ . Figure 6.4 (b) Shows the effect of finishing time on improvement in surface roughness at different viscosity and extrusion pressure is constant (22 bar). In graphs, after certain finishing time (40 minutes),  $\Delta Ra$  decreases. This is due to fact that in initial finishing time, the peaks over the surface get removed and after certain finishing time,  $\Delta Ra$  decreases. But using higher viscosity

media,  $\Delta R_a$  increases due to more stiffed media extrudes the workpiece surface results in more improvement in surface roughness.

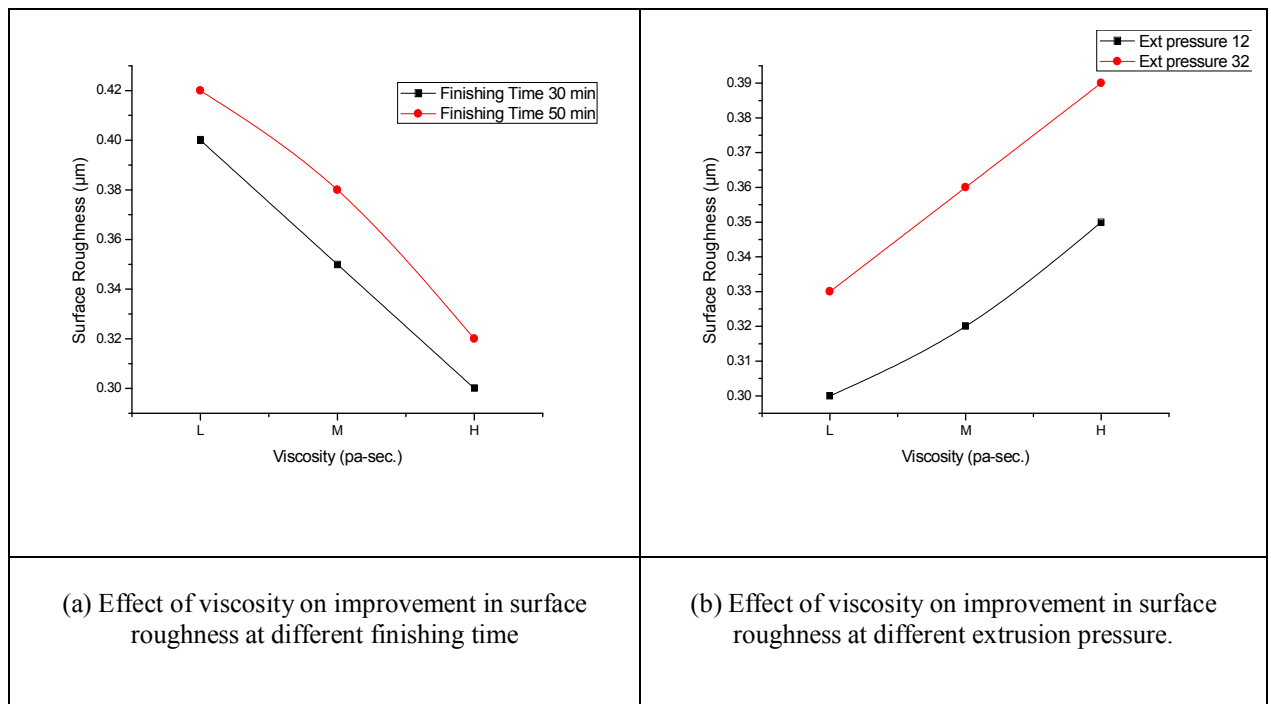


**Figure 6.5 Effect of viscosity on improvement in surface roughness**

Figure 6.5 (a) shows the effect of viscosity on improvement in surface roughness at different finishing time and extrusion pressure is constant (22 bar). In graphs, low finishing time affects the surface improvement quality by increasing  $\Delta R_a$  with increase in viscosity. But for higher finishing time it starts decreasing, due to same reason as stated in last section. Figure 6.5 (b) shows the effect of viscosity on improvement in surface roughness at different extrusion pressure and finishing time is constant (40 minute). Results in graph show that increase in extrusion pressure results in increase in  $\Delta R_a$  value with different viscosity media. This is due to the reason that at higher pressure media finishes higher penetration depth, so improvement in high but at higher viscosity improvement in surface roughness increase.

### 6.1.3.2 Material removal

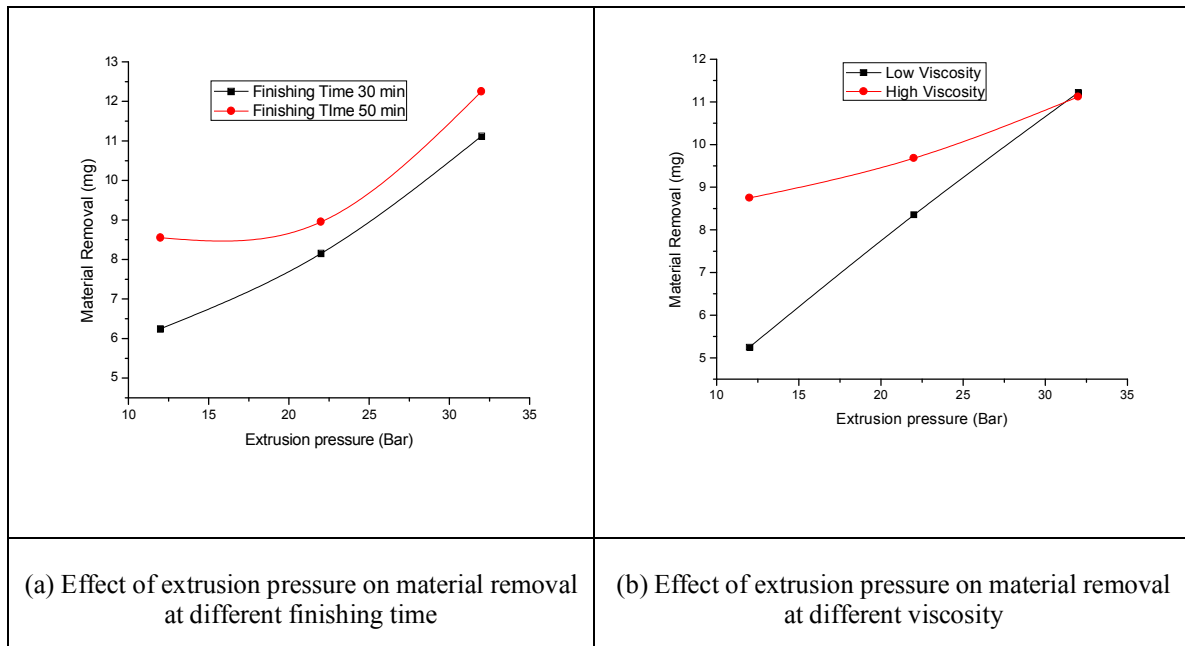


**Figure 6.6 Effect of extrusion pressure on material removal**

Figure 6.6 (a) shows the effect extrusion pressure on material removal at different finishing time when viscosity is constant (Medium grade). It is clear from graphs that effect of extrusion pressure at different finishing time is substantial on material removal. So the increase in material removal is due to increase in normal force acting on abrasive grits which results in increase in depth of cut and therefore results in increase in material removal. For higher finishing time material removal will be more due to increase in time of flowing the abrasive particles over the finishing surfaces. Figure 6.6 (b) shows the effect extrusion pressure on material removal at different viscosity when finishing time is constant. (40 minute). In this graph, material removal will increase with extrusion pressure and high viscosity media. It is due to fact that high viscous media having more resistance to the flow of medium.). Due to this higher resistance, more abrasion takes place and hence higher material removal take place compared to a lower viscous media.

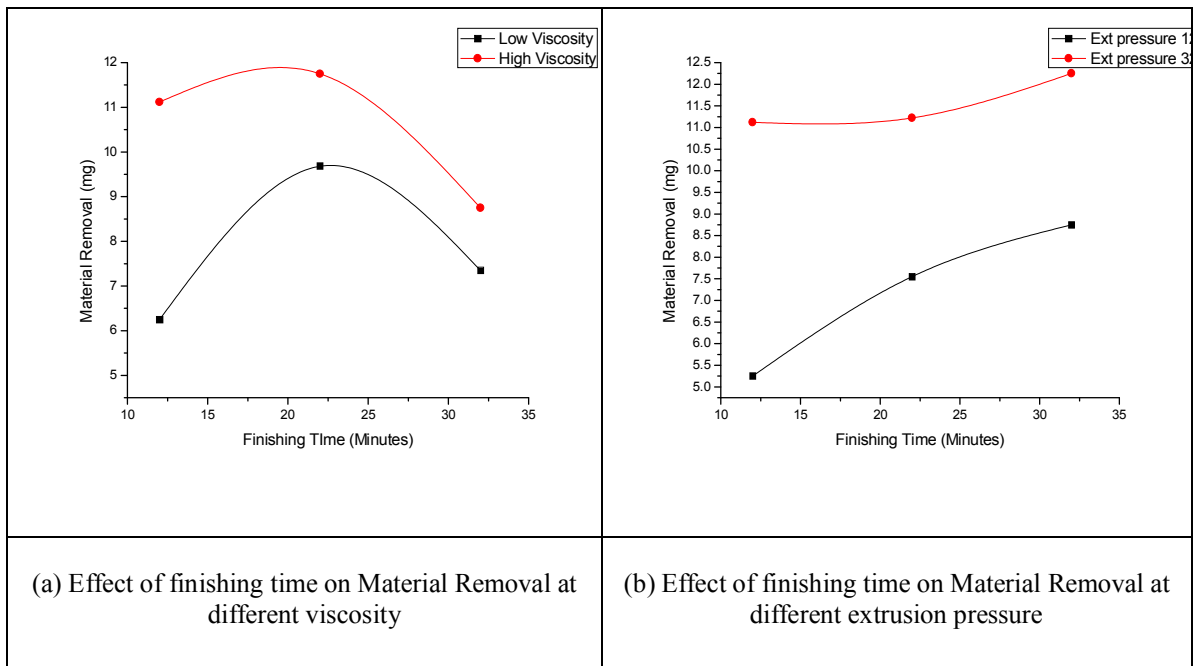


**Figure 6.7 Effect of finishing time on material removal**

Figure 6.7 (a) shows the effect of finishing time on material removal at different viscosity and extrusion pressure is constant (22 bar). From Figure 6.7 (a), it reveals that as finishing time increases material removal increases. In initial finishing time the material removal is high due to workpiece surface having large number of peaks and indentation. After some finishing time, the surface become flat (peak height reduces) and at higher finishing time the media just stream over the workpiece surface results in decreased in material removal. During finishing process, material removal is high when high viscosity and low finishing time is applied but at low viscosity and less finishing time results in low material removal because viscosity is more dominant variable than finishing time. Figure 6.7 (b) shows the effect of finishing time on material removal at different extrusion pressure when viscosity is constant (Medium grade). Graphs show the increases in material removal with finishing time at different extrusion pressure. At higher extrusion pressure, material removal is high at less finishing time due to reason as stated in last section.

Figure 6.8 (a) shows the effect of viscosity on material removal at different finishing time with constant extrusion pressure (22 bar). Graphs show the increase in material removal with increase in viscosity of media. This is due to fact that high viscosity media having higher confrontation so more material extrude out from surface which results in high material removal. For more finishing time, material removal will be higher at low and medium viscous media and material removal decreases at higher viscosity. Figure 6.8 (b) shows the effect of viscosity on material removal at different extrusion pressure and finishing time is constant. (40 minutes). Graphs show the higher material removal for increasing in viscosity when extrusion pressure is high. This is due to extrusion pressure having higher impact than other variable.

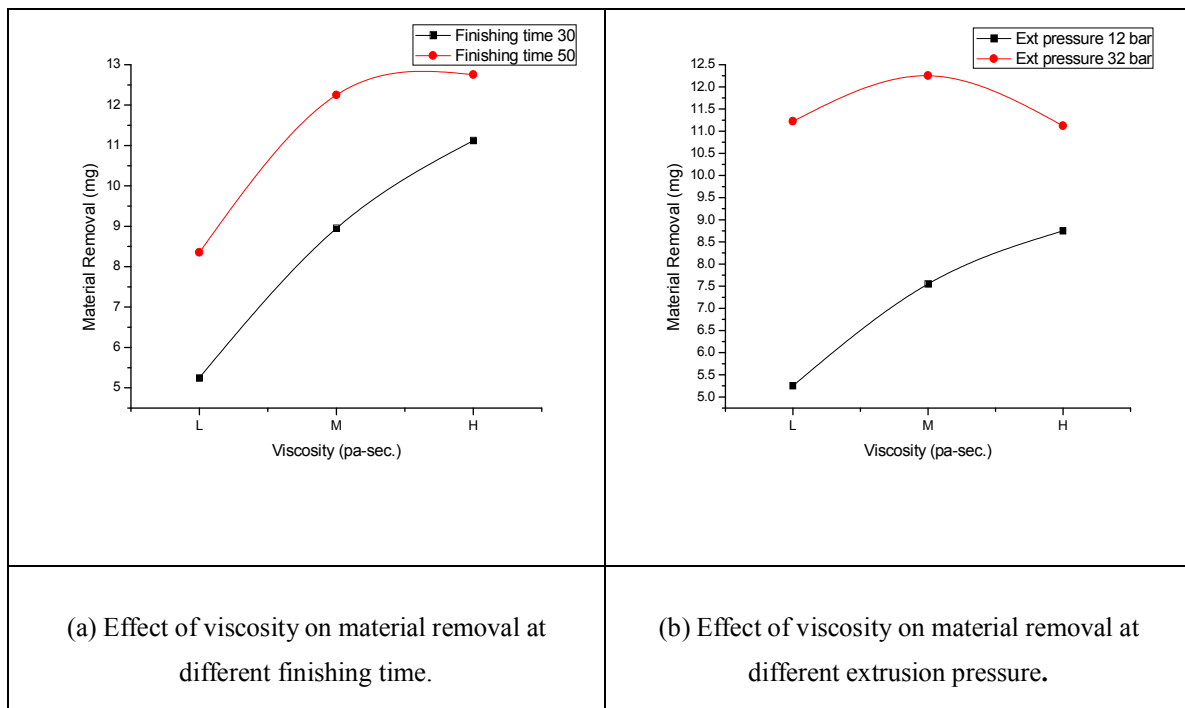


**Figure 6.8 Effect of viscosity on material removal**

## 6.2 Detailed experimentations

As per scheme of experimentation, the present work for detailed experimental investigation is performed in a pre-planned way during AFF of internal finishing of industrial components. The outcomes of the detailed experiments are explained in successive subsections.

### 6.2.1 Abrasive flow finishing of trim die components

In this section, experiments are performed for finishing the trim die components using the developed UAFM and PAG media. RSM technique is used for systematic experimental design as explained in section 5.6.1.

#### 6.2.1.1 Experimental results for RSM design

The experiments are performed for finishing of trim die components on UAFM setup as per experimental design shown in Table 5.7, chapter 5. Table 6.4 represent the experimental design matrix and observed performance measures for improvement in surface roughness ( $\Delta Ra$ ) and material removal (MR) in AFM of trim die components.

**Table 6.4 Experimental design matrix and observed performance measures in AFM of trim die**

| Run | Ext. pressure (Bar) | Finishing time (Minutes) | Viscosity (Pa-sec.) | $\Delta Ra$ ( $\mu m$ ) | MR (mg) |
|-----|---------------------|--------------------------|---------------------|-------------------------|---------|
| 1   | 12.00               | 30.00                    | 0.00                | 0.25                    | 6.95    |
| 2   | 22.00               | 40.00                    | 0.00                | 0.55                    | 10.46   |
| 3   | 22.00               | 30.00                    | -1.00               | 0.31                    | 6.25    |
| 4   | 22.00               | 50.00                    | 1.00                | 0.25                    | 13.22   |
| 5   | 12.00               | 40.00                    | 1.00                | 0.21                    | 10.65   |
| 6   | 32.00               | 40.00                    | 1.00                | 0.17                    | 13.28   |
| 7   | 12.00               | 50.00                    | 0.00                | 0.39                    | 10.98   |
| 8   | 22.00               | 40.00                    | 0.00                | 0.49                    | 10.35   |
| 9   | 22.00               | 30.00                    | 1.00                | 0.28                    | 10.78   |
| 10  | 22.00               | 50.00                    | -1.00               | 0.63                    | 10.63   |
| 11  | 32.00               | 50.00                    | 0.00                | 0.42                    | 12.96   |
| 12  | 22.00               | 40.00                    | 0.00                | 0.59                    | 10.41   |
| 13  | 22.00               | 40.00                    | 0.00                | 0.51                    | 10.43   |
| 14  | 12.00               | 40.00                    | -1.00               | 0.35                    | 7.15    |
| 15  | 32.00               | 30.00                    | 0.00                | 0.24                    | 10.32   |
| 16  | 32.00               | 40.00                    | -1.00               | 0.26                    | 10.42   |
| 17  | 22.00               | 40.00                    | 0.00                | 0.49                    | 10.54   |

### 6.2.1.2 Analysis of variance (ANOVA)

Analysis of variance (ANOVA) is executed to statistically investigate the results of the selected model. Significant control factors are recognized and interaction effects of these control factors on performance measures are studied using response surface graphs. In Table 6.5, the model F value of 20.74 with its Prob>F value less than 0.0003 directs that model is significant for  $\Delta Ra$  as it validates that the terms in the model have a significant effect on the response. The values of Prob>F less than 0.05 indicates the significance of model. The terms, A, B, C, AC, BC,  $A^2$ ,  $B^2$  and  $C^2$  are significant model terms for  $\Delta Ra$  with their percentage contribution of 21.67, 14.00, 24.3, 2.4, 4.81, 2.81, 9.60, 11.31 and 8.80 respectively. The determination coefficient for  $\Delta Ra$  is found to be 0.9638 suggesting the established model is accomplished of explaining the variation on  $\Delta Ra$  up to 96.38 % and model is adequate in demonstrating the process.

The other  $R^2$  statistics, the Pred.  $R^2$  (0.6626) is in good agreement with the Adj.  $R^2$  (0.9174). The smaller value (6.72) of CV % shows enhanced accuracy and consistency of the performed experiments [106]. Adeq. Precision found for the model is 14.77, which is well more than desired value of 4 and thus specifies a sufficient signal for the model. Hence, this model may be used to navigate the design space and forecast the values of the  $\Delta Ra$  within the limits of the factors studied.



**Table 6.5 ANOVA outcomes for fitted RSM model for improvement in surface roughness**

| Source                     | Sum of Squares (SS) | Degree of freedom (DF) | Mean Square (MS)         | F-Value  | p-value Prob > F |                 |
|----------------------------|---------------------|------------------------|--------------------------|----------|------------------|-----------------|
| Model                      | 0.154842            | 9                      | 0.017205                 | 20.74638 | 0.0003           | significant     |
| A-Ext pressure             | 0.032513            | 1                      | 0.032513                 | 39.20543 | 0.0004           |                 |
| B-Finishing Time           | 0.021013            | 1                      | 0.021013                 | 25.33807 | 0.0015           |                 |
| C-Viscosity                | 0.03645             | 1                      | 0.03645                  | 43.95349 | 0.0003           |                 |
| AB                         | 0.0036              | 1                      | 0.0036                   | 4.341085 | 0.0757           |                 |
| AC                         | 0.007225            | 1                      | 0.007225                 | 8.712317 | 0.0214           |                 |
| BC                         | 0.004225            | 1                      | 0.004225                 | 5.094746 | 0.0586           |                 |
| A <sup>2</sup>             | 0.014409            | 1                      | 0.014409                 | 17.37576 | 0.0042           |                 |
| B <sup>2</sup>             | 0.016978            | 1                      | 0.016978                 | 20.47291 | 0.0027           |                 |
| C <sup>2</sup>             | 0.013204            | 1                      | 0.013204                 | 15.92239 | 0.0053           |                 |
| Residual                   | 0.005805            | 7                      | 0.000829                 |          |                  |                 |
| Lack of Fit                | 0.003125            | 3                      | 0.001042                 | 1.554726 | 0.3315           | not significant |
| Pure Error                 | 0.00268             | 4                      | 0.00067                  |          |                  |                 |
| Cor Total                  | 0.160647            | 16                     |                          |          |                  |                 |
| Standard Deviation         | 0.028797            |                        | R <sup>2</sup>           | 0.963865 |                  |                 |
| Mean                       | 0.428235            |                        | Adjusted R <sup>2</sup>  | 0.917405 |                  |                 |
| coefficient of variation % | 6.724649            |                        | Predicted R <sup>2</sup> | 0.662692 |                  |                 |
| PRESS                      | 0.054188            |                        | Adequate Precision       | 14.77144 |                  |                 |

**Table 6.6 ANOVA outcomes for fitted RSM model for material removal**

| Source                     | Sum of Squares (SS) | Degree of freedom (DF) | Mean Square (MS)         | F Value  | p-value Prob > F |                 |
|----------------------------|---------------------|------------------------|--------------------------|----------|------------------|-----------------|
| Model                      | 62.90166            | 7                      | 8.985952                 | 522.6501 | < 0.0001         | significant     |
| A-Ext pressure             | 15.82031            | 1                      | 15.82031                 | 920.1571 | < 0.0001         |                 |
| B-Finishing time           | 22.74751            | 1                      | 22.74751                 | 1323.064 | < 0.0001         |                 |
| C-Viscosity                | 22.7138             | 1                      | 22.7138                  | 1321.103 | < 0.0001         |                 |
| AB                         | 0.483025            | 1                      | 0.483025                 | 28.09419 | 0.0005           |                 |
| AC                         | 0.1024              | 1                      | 0.1024                   | 5.955893 | 0.0373           |                 |
| BC                         | 0.9409              | 1                      | 0.9409                   | 54.72558 | < 0.0001         |                 |
| B <sup>2</sup>             | 0.093713            | 1                      | 0.093713                 | 5.450602 | 0.0444           |                 |
| Residual                   | 0.154738            | 9                      | 0.017193                 |          |                  |                 |
| Lack of Fit                | 0.135258            | 5                      | 0.027052                 | 5.554723 | 0.0608           | not significant |
| Pure Error                 | 0.01948             | 4                      | 0.00487                  |          |                  |                 |
| Correlation Total          | 63.0564             | 16                     |                          |          |                  |                 |
| Std. Dev.                  | 0.131122            |                        | R <sup>2</sup>           | 0.997546 |                  |                 |
| Mean                       | 10.34               |                        | Adjusted R <sup>2</sup>  | 0.995637 |                  |                 |
| coefficient of variation % | 1.268107            |                        | Predicted R <sup>2</sup> | 0.985193 |                  |                 |
| PRESS                      | 0.933686            |                        | Adequate Precision       | 77.11301 |                  |                 |

As shown in Table 6.6, for the material removal model terms, A, B, C, AB, AC, BC, B<sup>2</sup> are significant for material removal with their percentage contribution of 25.15, 36.16, 36.11, 0.76, 0.16, 1.49, and 0.14 respectively. The value of determination coefficient (R<sup>2</sup>) is 0.9975. It illustrates that the quadratic model can explain up to 99.75% variation in the material removal. The Pred. R<sup>2</sup> value of 0.9851 is in reasonable agreement with the Adj. R<sup>2</sup> of 0.9956.

The smaller value (1.26) of the coefficient of variation discloses enhanced precision and reliability of the executed experiments. A value of 77.11 for Adeq. Precision states an adequate signal for the model as a ratio greater than 4 is desirable. Therefore, this quadratic model can be used to navigate the design space and considered substantial for fitting and predicting the experimental results.

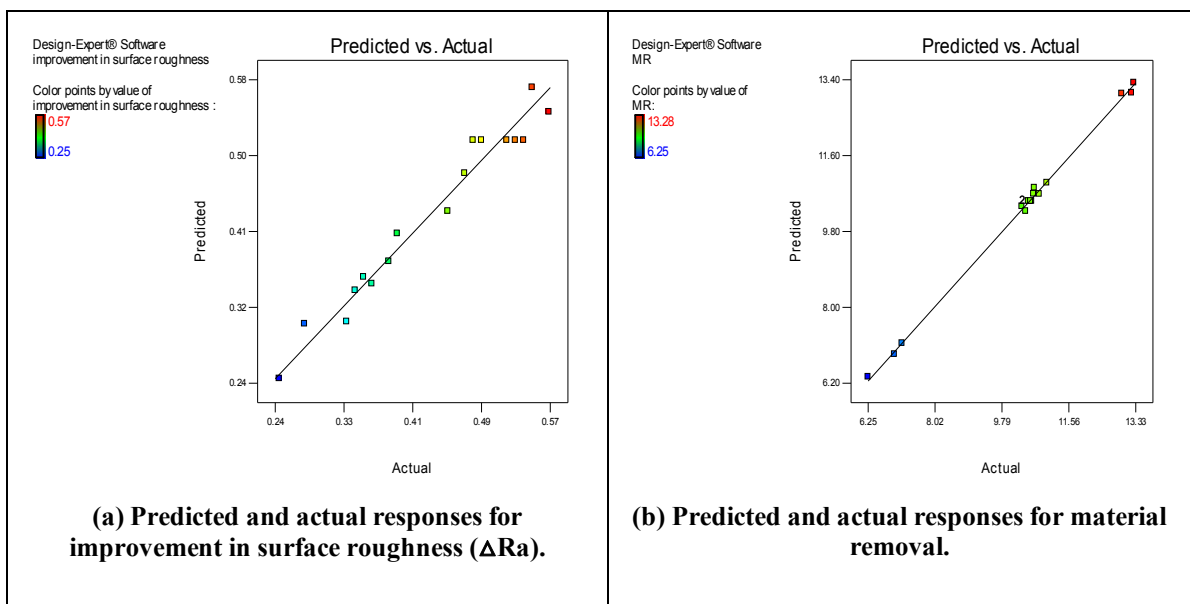


**Figure 6.9 Predicted and actual responses for improvement in surface roughness and material removal**

Figure 6.9 (a) and 6.9 (b) demonstrate the plot of predicted and actual responses [107]. It is perceived that outcomes between the predicted and actual are very near for both  $\Delta R_a$  and MR. This confirms that predicted model is acceptable; prediction further supports in machine setting directly in industry applications. Also it was perceived that MR and  $\Delta R_a$  were most influenced by the extrusion pressure as presented in Table 6.5 and Table 6.6.

Adjusted and predicted results plotted in Figure 6.9 (a) and 6.9 (b) are well inside the range. The regression equation of respective response variable as function of  $\Delta R_a$  and MR in terms of coded value is presented in Table 6.7.

**Table 6.7 Regression relations for improvement in surface roughness and material removal**

| Responses                        | R-square | Adjusted R-square | Regression Model  |
|----------------------------------|----------|-------------------|---|
| Improvement in surface roughness | 0.9638   | 0.9174            | Improvement in surface roughness=<br>$1.28839+0.037740*EP+0.057650*FT+1.20000E-004*Vis-$<br>$3.00000E-004* EP*FT+4.25000E-005*EP$<br>$*Vis+3.25000E-005* FT* Vis-5.85000E-004* EP^2-$<br>$6.35000E-004* FT^2-5.60000E-006* Vis^2$ |
| Material Removal                 | 0.9975   | 0.9956            | MR= $-4.86675+0.27962*EP+0.36407* FT+3.97700* Vis-$<br>$3.47500E-003* EP * FT-0.016000* EP* Vis-0.048500* FT$<br>$* Vis-1.48750E-003* FT^2$   |

\*EP-Extrusion pressure, bar: FT-Finishing time, minute: Viscosity- Vis, pa-sec.

### 6.2.1.3 Influence of control factors on performance variables

In next part, three-dimensional response curves and perturbation graphs are explained to observe the influence of individual AFM variables and their interactions on the performance variables. The perturbation graph in Figure 6.10 illustrates the relative influence of significant AFM finishing variables on the improvement in surface roughness. The midpoint of levels (coded value 0) is always defined by Design-Expert tool to fix the reference point of all variables. A sudden slope for extrusion pressure (A), finishing time (B), and viscosity (C), illustrations that  $\Delta Ra$  is highly susceptible to these process variables. The motives for these inclinations have been deliberated while enlightening the interaction effects of variables. Table 6.5 and Table 6.6 show that the interactions which subsidize the most to the model are among the finishing time and viscosity (BC), extrusion pressure and viscosity (AC), finishing time (B), viscosity (C) and extrusion pressure (A) for  $\Delta Ra$ . Also interactions of extrusion pressure and viscosity (AC), extrusion pressure and finishing time (AB) and finishing time and viscosity (BC),

Finishing time (B), viscosity (C) and extrusion pressure (A) significantly affect the MR. The interaction graphs equivalent for above interactions are presented in Figure 6.11 and 6.12 and Figure 6.14, 6.15, 6.16.

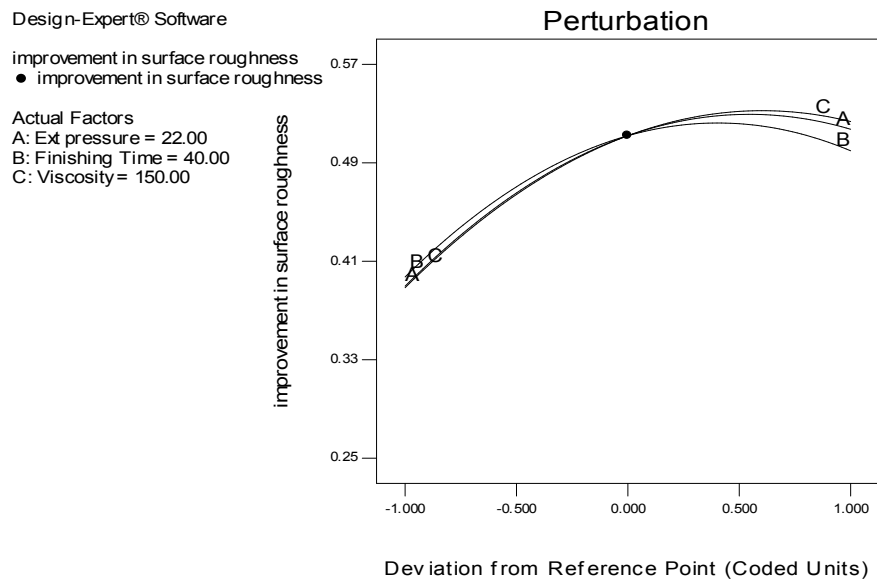


Figure 6.10 Perturbation plots for  $\Delta Ra$

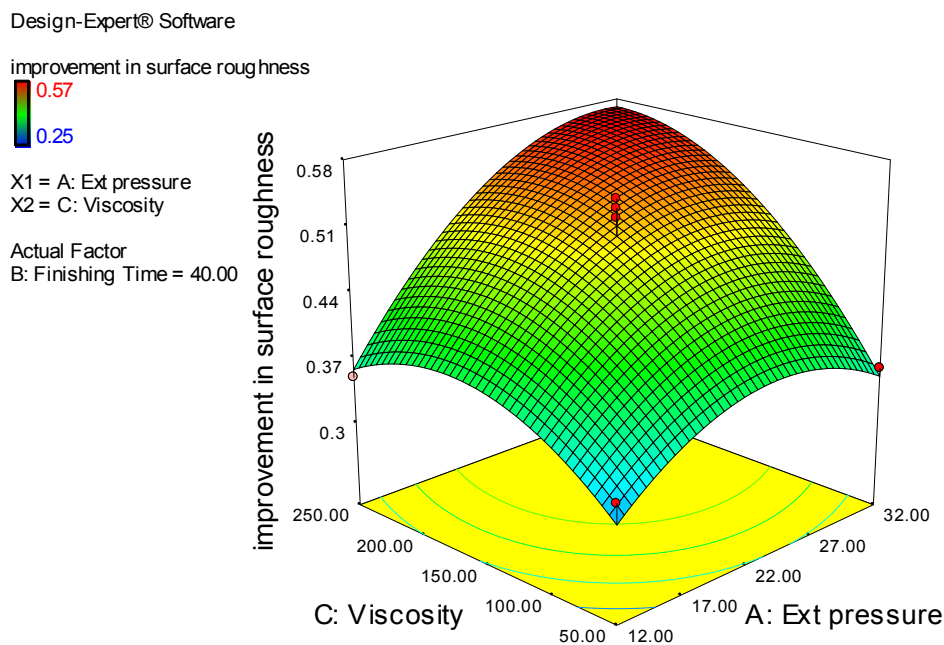
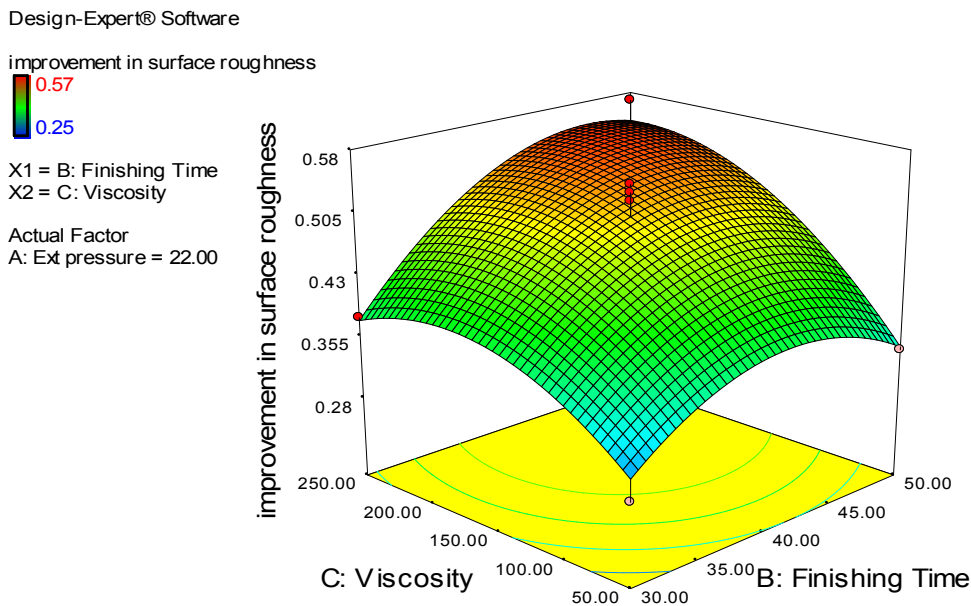


Figure 6.11 Response 3D surface plot demonstrating the interactive influence of finishing time and extrusion pressure for  $\Delta Ra$ .



**Figure 6.12 Response 3D surface plot demonstrating the interactive influence of finishing time and viscosity for  $\Delta Ra$**

Figure 6.11 illustrates the influence of extrusion pressure and viscosity on  $\Delta Ra$  at constant finishing time. It shows that initially with increase in extrusion pressure,  $\Delta Ra$  value increase but at the end it starts decreasing. This is due fact that when extrusion pressure escalates, normal force performing on each grain also increases that consequence in cavernous indentation on surface. At higher extrusion pressure, the material removal take place at deeper indentations in less finishing time results in more improvement in surface finishing. Figure 6.11 also shows that  $\Delta Ra$  increases with increase in viscosity. This is owing to high viscous media, more deep penetration of abrasive particles is conceivable, and it results increase in the surface finishing quality. Figure 6.12 also show that  $\Delta Ra$  increases in initial finishing time and decrease in after certain finishing time. This is due to in initial finishing time the peaks over the surface get removed and after certain finishing time,  $\Delta Ra$  decreases. Minimum improvement in surface roughness was observed at viscosity (50 pa-sec.) and finishing time (30 minute).

Design-Expert® Software

MR  
● MR

Actual Factors  
A: Ext pressure = 22.00  
B: Finishing Time = 40.00  
C: Viscosity = 150.00

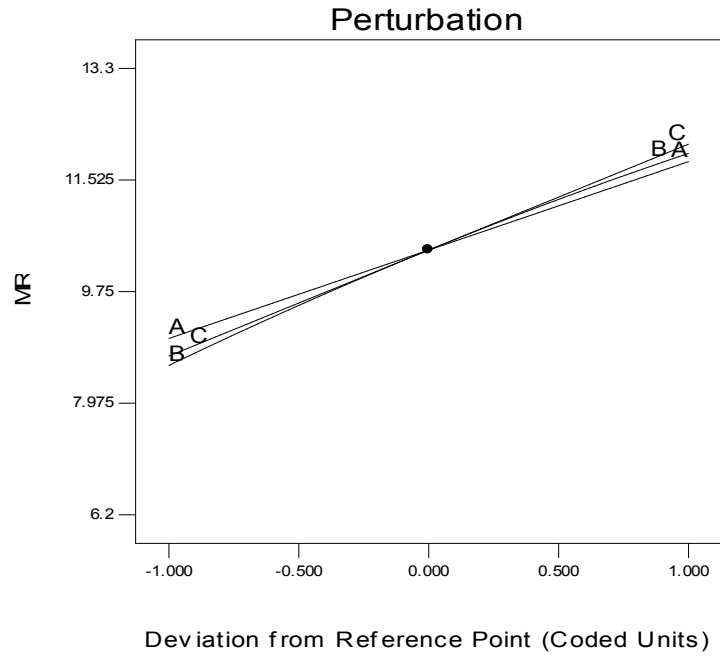


Figure 6.13 Perturbation graph for MR

Design-Expert® Software

MR  
13.28  
6.25

X1 = A: Ext pressure  
X2 = B: Finishing Time

Actual Factor  
C: Viscosity = 150.00

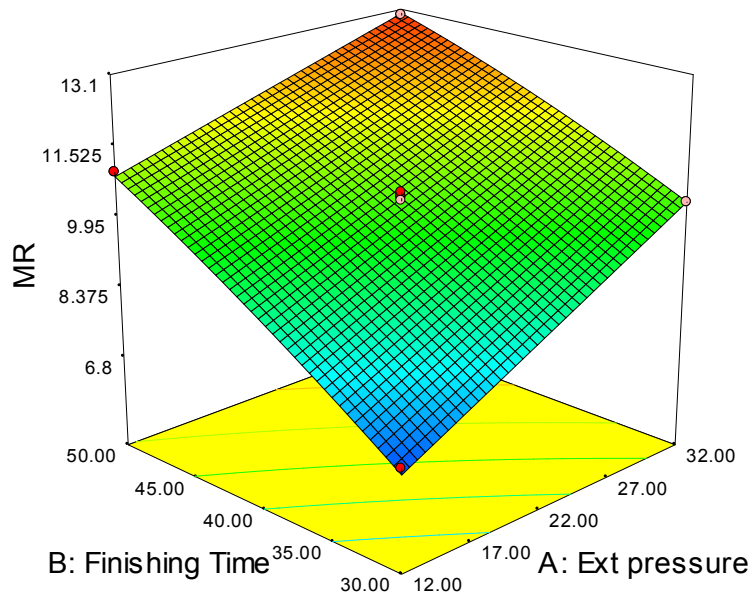
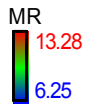


Figure 6.14 Response 3D surface plot demonstrating the interactive influence of finishing time and extrusion pressure for MR

Design-Expert® Software



X1 = A: Ext pressure  
X2 = C: Viscosity

Actual Factor  
B: Finishing Time = 40.00

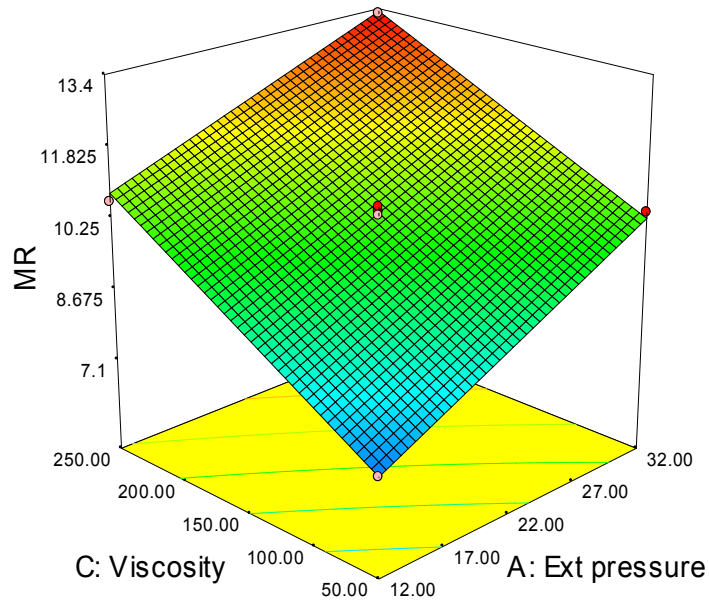
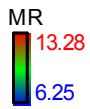


Figure 6.15 Response 3D surface plot demonstrating the interactive influence of viscosity and extrusion pressure for MR

Design-Expert® Software



X1 = B: Finishing Time  
X2 = C: Viscosity

Actual Factor  
A: Ext pressure = 22.00

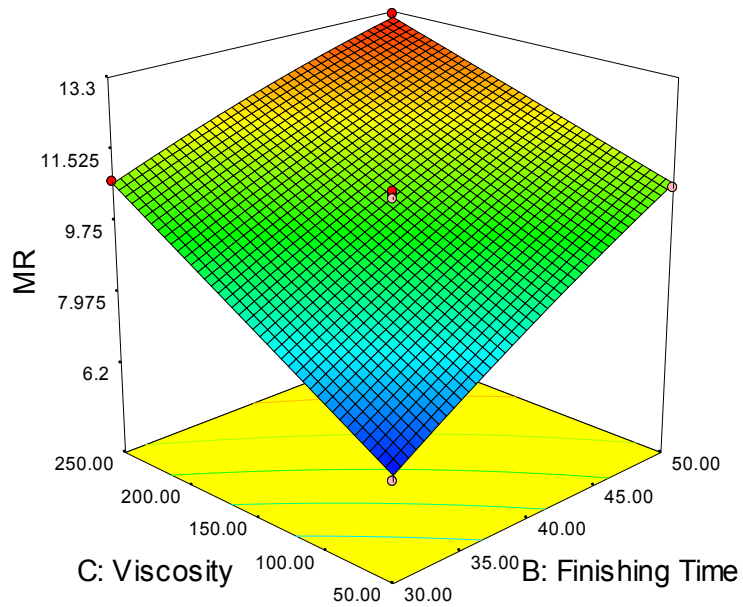


Figure 6.16 Response 3D surface plot demonstrating the interactive influence of viscosity and finishing time for MR

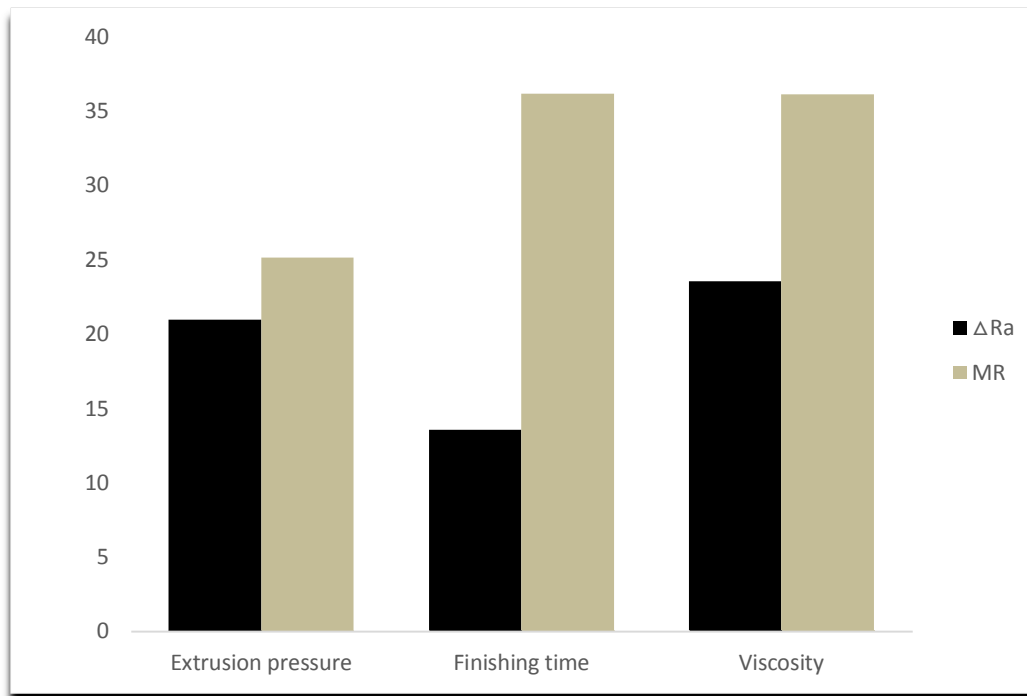


Figure 6.14 illustrates the influence of extrusion pressure and finishing time on MR while keeping viscosity of media constant. It shows that with increase in extrusion pressure, MR increase. This is due to an increase in normal force acting on abrasive grits, which results in increase in deep penetration and more material removal over the finishing surface. Figure 6.14 illustrate that with rise in finishing time, material removal decreases, due to in initial finishing time the material removal is high due to workpiece surface having large number of peaks and indentation. After some finishing time, the surface becomes flat (peak height reduces) and at higher finishing time the media just stream over the workpiece surface results in decreased in material removal.

Figure 6.15 shows effect of extrusion pressure and viscosity on MR while keeping finishing time constant. It shows that with rise in viscosity, the MR will also increase, due to high viscosity media having higher confrontation so more material extrudes out from surface consequences in high MR. Figure 6.15 also indicates that low value of viscosity (50 pa-sec.) and extrusion pressure (12 bar) cause low MR. Also Figure 6.16 indicates, low values of viscosity (50 pa-sec.) and low finishing time (30 minute) also cause low material removal.

#### **6.2.1.4 Optimization**

Optimization was performed to maximize  $\Delta Ra$  and maximize MR of finished component surface subject to working limit of three factors shown in Table 5.7. Figure 6.17 represents the percentage contribution of each factor which is derived by dividing the “specific (model) value “sum of squares by “model” sum of squares (SS) from Table 6.5 and Table 6.6 for  $\Delta Ra$  and MR respectively. It is observed that viscosity (highest % contribution 23.54) is most important factor for improvement in surface roughness, whereas finishing time (highest % contribution 36.16) is most important factor for material removal.



**Figure 6.17 Percentage contribution of AFM variables on MR and  $\Delta Ra$**

The parametric optimization is performed using the design expert software. This technique consists of desirability factor, which is derived by converting a predictable factor into a scale free term. Desirability factor have ranges from 0 to 1 in which least value stands for less desirable factor [105]. The process variable values with extreme desirability are meant to be the optimal variable settings. The combinations owning uppermost desirability value is designated as an optimum state for the preferred responses [105][108][109]

Optimum values for input variables and the equivalent responses are calculated using software and details are presented in Table 6.8. In single factor optimization, the other factors are discounted but for multi-variable optimization, all responses are deliberated and given equivalent significance. For validation of optimized outcomes, confirmation experiments have been achieved (Table 6.8.) and output results observed from experimental study are near to the predicted values.

**Table 6.8 Single factor and multi-factor optimization and comparative study of optimized outcomes and experimental facts**

| Optimization type | Objective                                     | Optimum process variables |           |              | Response (predicted)      | Response (experimental)   | Desirability |
|-------------------|---|---------------------------|-----------|--------------|---------------------------|---------------------------|--------------|
|                   |   | EP (bar)                  | FT (min.) | Vis (pa-sec) |                           |                           |              |
| Single response   | To maximize the $\Delta Ra$                   | 26.72                     | 45.70     | 218.68       | 0.5760 $\mu m$            | 0.5520 $\mu m$            | 1            |
| Single response   | To maximize the MR                            | 31.95                     | 46.37     | 224.02       | 13.50 mg                  | 14.20mg                   | 1            |
| Multi-response    | To maximize $\Delta Ra$ and MR simultaneously | 31.77                     | 47.85     | 242.38       | 0.5730 $\mu m$ & 13.80 mg | 0.5620 $\mu m$ & 14.50 mg | 1            |

#### 6.2.1.5 SEM images of trim die before and after finishing

After finishing by AFM process, the components are analyzed using scanning electron microscopy (SEM). SEM analysis is accomplished to perceive the microstructure of finished workpiece profile at 1000X magnification. Figure 6.18 illustrates microstructure image of finished work piece before AFM and after AFM. The surface imperfections such as recast layers and blows can be seen on unfinished surface as revealed in Figure 6.18 (a). SEM images displayed in Figure 6.18 (b), 6.18 (c), and 6.18 (d) demonstrate visibly that surface structure is considerably enhanced after finishing process. At higher magnification, no cracks are observed, although entrenching of abrasive particles is observed infrequently. In consequences images smoother surface is perceived. Figure 6.18 (c) and Figure 6.18(d) shows better surface qualities on finished work pieces due to high extrusion pressure, high finishing time and high viscosity of media.

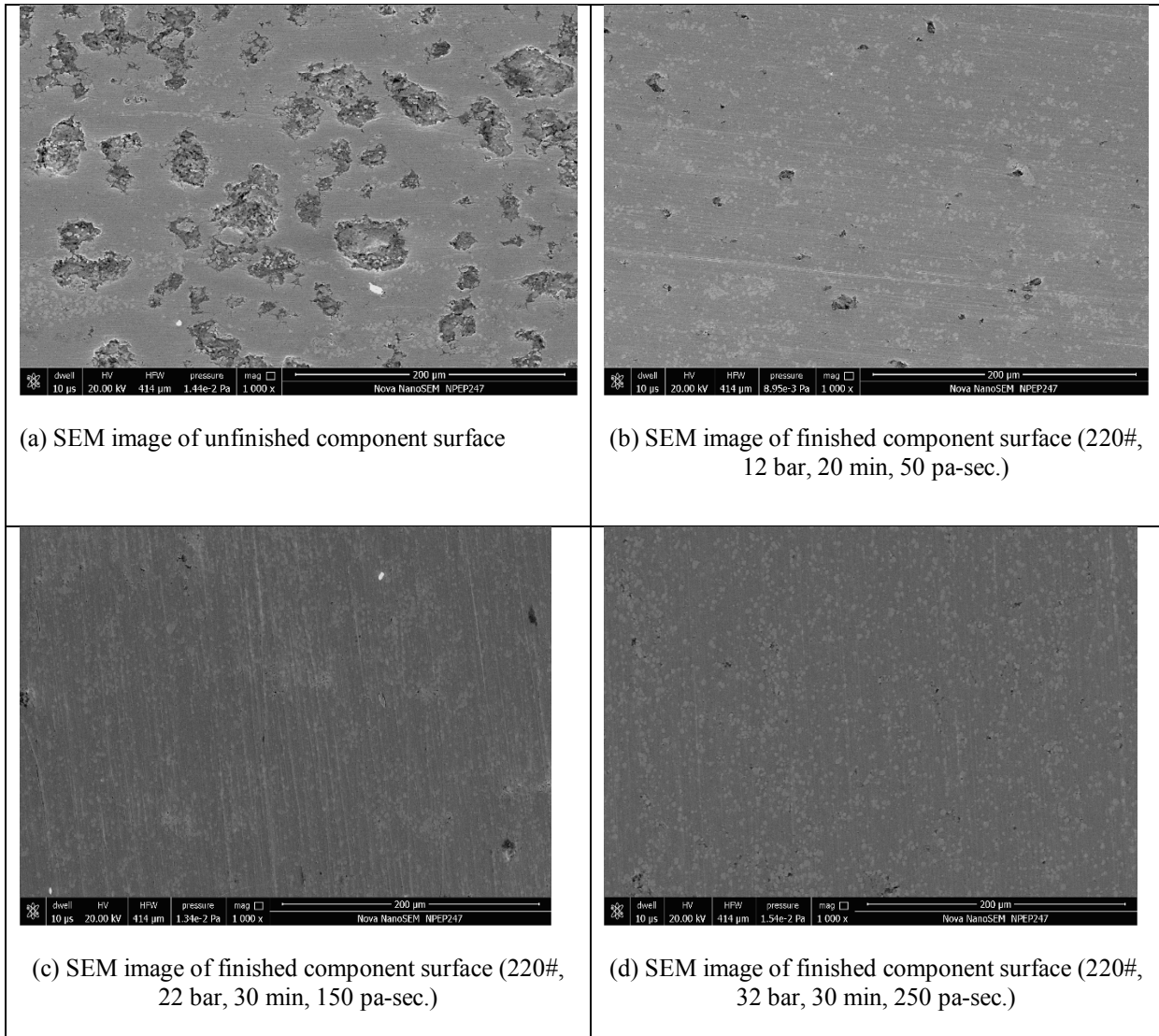


**Figure 6.18 SEM images of trim die before and after finishing**

### 6.2.1.6 XRD analysis

XRD analysis of finished work pieces has been performed on a software tool (X'Pert High Score). XRD graph of HSS trim dies are presented in Figure 6.19. From XRD graphs, it is observed that maximum peaks are identified for Fe, Ni and Cr groups at 2ThetaF value of 44.39. Also some more peaks are identified for Cr at 2ThetaF value of 39.71, Ni at 2ThetaF value of 44.39. Some groups with lower peaks have been discounted.

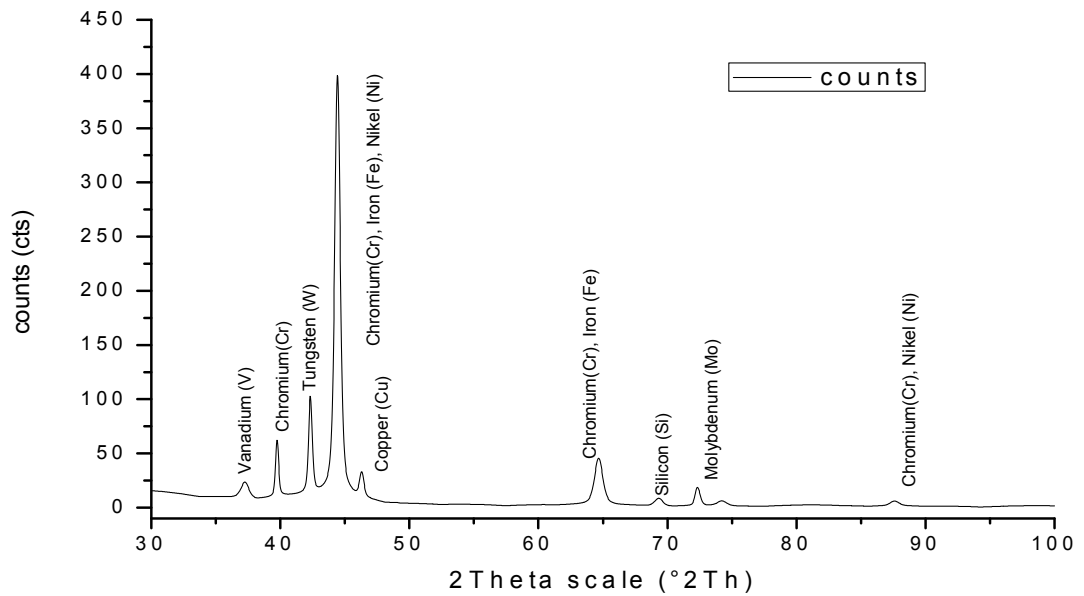


**Figure 6.19 XRD results of finished workpiece**

## **6.2.2 Abrasive flow finishing of stamping die components**

In this section, experiments are performed for finishing the stamping die components using the developed UAFM and PAG media. RSM technique is used for systematic experimental design as explained in section 5.6.1.

### **6.2.2.1 Experimental results as per RSM design**

The experiments are performed for finishing of stamping die components on UAFM setup as per experimental design shown in, chapter 5.

Table 6.9 represents the experimental design matrix and observed performance measures for improvement in surface roughness ( $\Delta Ra$ ) and material removal (MR) in AFM of stamping die components

**Table 6.9 Experimental design matrix and observed performance measures in AFM of stamping die**

| Std | Run | Block   | Ext. pressure(Bar) | Finishing time (Minutes) | Viscosity(pa-sec.) | SR ( $\Delta Ra$ ) | MR (mg) |
|-----|-----|---------|--------------------|--------------------------|--------------------|--------------------|---------|
| 15  | 1   | Block 1 | 22.00              | 40.00                    | 0.00               | 0.52               | 12.50   |
| 9   | 2   | Block 1 | 22.00              | 30.00                    | -1.00              | 0.42               | 10.25   |
| 12  | 3   | Block 1 | 22.00              | 50.00                    | 1.00               | 0.48               | 10.85   |
| 10  | 4   | Block 1 | 22.00              | 50.00                    | -1.00              | 0.57               | 12.20   |
| 17  | 5   | Block 1 | 22.00              | 40.00                    | 0.00               | 0.46               | 10.60   |
| 4   | 6   | Block 1 | 32.00              | 50.00                    | 0.00               | 0.32               | 7.5     |
| 3   | 7   | Block 1 | 12.00              | 50.00                    | 0.00               | 0.82               | 17.8    |
| 6   | 8   | Block 1 | 32.00              | 40.00                    | -1.00              | 0.55               | 12      |
| 1   | 9   | Block 1 | 12.00              | 30.00                    | 0.00               | 0.28               | 7.2     |
| 13  | 10  | Block 1 | 22.00              | 40.00                    | 0.00               | 0.85               | 17.65   |
| 11  | 11  | Block 1 | 22.00              | 30.00                    | 1.00               | 0.50               | 12.65   |
| 8   | 12  | Block 1 | 32.00              | 40.00                    | 1.00               | 0.30               | 7.35    |
| 5   | 13  | Block 1 | 12.00              | 40.00                    | -1.00              | 0.45               | 10.55   |
| 14  | 14  | Block 1 | 22.00              | 40.00                    | 0.00               | 0.42               | 10.65   |
| 16  | 15  | Block 1 | 22.00              | 40.00                    | 0.00               | 0.44               | 10.75   |
| 7   | 16  | Block 1 | 12.00              | 40.00                    | 1.00               | 0.78               | 17.35   |
| 2   | 17  | Block 1 | 32.00              | 30.00                    | 0.00               | 0.48               | 10.95   |

**6.2.2.2 Analysis of variance (ANOVA)**

Analysis of variance (ANOVA) is executed to statistically investigate the results of the selected model. Significant control factors are recognized and interaction effects of these control factors on performance measures are studied using response surface graphs. In Table 6.10, the model F value of 102.78 with its Prob>F value less than 0.0001 directs that the model is significant for  $\Delta Ra$  as it validates that the terms in the model have a significant effect on the response. The values of Prob>F less than 0.05 indicates the significance of model. The terms, A, B, C, AB, AC, BC and A2 are significant model terms for  $\Delta Ra$  with their percentage contribution of 28.22, 31.67, 28.78, 4.33, 1.59, 2.92, and 1.26 respectively. The determination coefficient for  $\Delta Ra$  is found to be 0.987646 suggesting the established model is accomplished of explaining the variation on  $\Delta Ra$  up

to 98.76 % and the model is adequate in demonstrating the process.

The other  $R^2$  statistics, the Pred.  $R^2$  (0.9811) is in good agreement with the Adj.  $R^2$  (0.9780). The smaller value (4.90) of CV % shows enhanced accuracy and consistency of the performed experiments [28]. Adeq. Precision found for the model is 33.16 which is quite more than desired value of 4 and thus specifies a sufficient signal for the model. Hence, this model may be used to navigate the design space and forecast the values for improvement in surface roughness ( $\Delta R_a$ ) within the limits of the factors studied.

**Table 6.10 ANOVA outcomes for fitted RSM model for improvement in surface roughness**

| Source               | Sum of Square (SS) | Degree of Freedom (DF) | Mean Square    | F Value  | p-value Prob > F |                 |
|----------------------|--------------------|------------------------|----------------|----------|------------------|-----------------|
| Model                | 0.446462           | 7                      | 0.06378        | 102.7845 | < 0.0001         | significant     |
| A-Extrusion Pressure | 0.127513           | 1                      | 0.127513       | 205.4914 | < 0.0001         |                 |
| B-Finishing Time     | 0.143113           | 1                      | 0.143113       | 230.6314 | < 0.0001         |                 |
| C-Viscosity          | 0.13005            | 1                      | 0.13005        | 209.5807 | < 0.0001         |                 |
| AB                   | 0.0196             | 1                      | 0.0196         | 31.58617 | 0.0003           |                 |
| AC                   | 0.007225           | 1                      | 0.007225       | 11.64337 | 0.0077           |                 |
| BC                   | 0.013225           | 1                      | 0.013225       | 21.31261 | 0.0013           |                 |
| A <sup>2</sup>       | 0.005737           | 1                      | 0.005737       | 9.245944 | 0.0140           |                 |
| Residual             | 0.005585           | 9                      | 0.000621       |          |                  |                 |
| Lack of Fit          | 0.000265           | 5                      | 5.29E-05       | 0.039808 | 0.9983           | not significant |
| Pure Error           | 0.00532            | 4                      | 0.00133        |          |                  |                 |
| Cor Total            | 0.452047           | 16                     |                |          |                  |                 |
| Std. Dev.            | 0.02491            |                        | R-Squared      | 0.987646 |                  |                 |
| Mean                 | 0.508235           |                        | Adj R-Squared  | 0.978037 |                  |                 |
| C.V. %               | 4.901339           |                        | Pred R-Squared | 0.981176 |                  |                 |
| PRESS                | 0.008509           |                        | Adeq Precision | 33.16913 |                  |                 |

**Table 6.11 ANOVA outcomes for fitted RSM model for material removal**

| Source               | Sum of Square (SS) | Degree of Freedom (DF) | Mean Square     | F Value  | p-value Prob > F |                 |
|----------------------|--------------------|------------------------|-----------------|----------|------------------|-----------------|
| Model                | 168.2869           | 6                      | 28.04781        | 97.81152 | < 0.0001         | significant     |
| A-Extrusion Pressure | 56.18              | 1                      | 56.18           | 195.9173 | < 0.0001         |                 |
| B-Finishing Time     | 52.27531           | 1                      | 52.27531        | 182.3004 | < 0.0001         |                 |
| C-Viscosity          | 49.25281           | 1                      | 49.25281        | 171.76   | < 0.0001         |                 |
| AB                   | 4.515625           | 1                      | 4.515625        | 15.7474  | 0.0027           |                 |
| AC                   | 2.640625           | 1                      | 2.640625        | 9.208688 | 0.0126           |                 |
| BC                   | 3.4225             | 1                      | 3.4225          | 11.93533 | 0.0062           |                 |
| Residual             | 2.867537           | 10                     | 0.286754        |          |                  |                 |
| Lack of Fit          | 1.070537           | 6                      | 0.178423        | 0.397157 | 0.8501           | not significant |
| Pure Error           | 1.797              | 4                      | 0.44925         |          |                  |                 |
| Cor Total            | 171.1544           | 16                     |                 |          |                  |                 |
| Std. Dev.            | 0.535494           |                        | R-Squared       | 0.983246 |                  |                 |
| Mean                 | 11.69412           |                        | Adj R-Squared   | 0.973193 |                  |                 |
| C.V. %               | 4.579173           |                        | Pred R-Squared  | 0.971689 |                  |                 |
| PRESS                | 4.845488           |                        | Adeq. Precision | 30.81161 |                  |                 |

As shown in Table 6.11, the material removal model terms A, B, C, AB, AC and BC are significant for material removal with their percentage contribution of 33.03, 30.73, 28.95, 2.65, 1.55, and 2.01 respectively. The value of determination coefficient ( $R^2$ ) is 0.9832 which illustrates that the quadratic model can explain up to 98.32% variation in the material removal. The Pred.  $R^2$  value of 0.9716 is in reasonable agreement with the Adj.  $R^2$  of 0.9731. The smaller value (4.57) of the coefficient of variation discloses enhanced precision and reliability of the executed experiments. A value of 30.81 for Adeq. Precision states an adequate signal for the model as a ratio greater than 4 is desirable.



Therefore, this quadratic model can be used to navigate the design space and considered substantial for fitting and predicting the experimental results.

Figure 6.20 (a) and 6.20 (b) demonstrate the plot of predicted and actual responses. It is perceived that outcomes between the predicted and actual are very near for both  $\Delta R_a$  and MR. Adjusted and predicted results plotted in Figure 6.20 (a) and 6.20 (b) are well inside the range. This confirms that predicted model is acceptable; prediction further supports in machine setting directly in industry applications.

The regression equations of respective response variable as function of  $\Delta R_a$  and MR in terms of coded value are presented in Table 6.12.

**Table 6.12 Regression relations for improvement in surface roughness and material removal**

| Responses                        | R-square | Adjusted R-square | Regression Model  |
|----------------------------------|----------|-------------------|---|
| Improvement in surface roughness | 0.9878   | 0.9780            | Improvement in surface roughness=-<br>1.28497+0.019978*EP-0.039125*FT+1.50000E-003 * EP*<br>FT-1.64722E-003*EP <sup>2</sup>                     |
| Material Removal                 | 0.9832   | 0.9732            | MR=-4.86675+0.27962*EP+0.36407* FT+3.97700* Vis-<br>3.47500E-003* EP * FT-0.016000* EP* Vis-0.048500* FT<br>* Vis-1.48750E-003* FT <sup>2</sup> |

EP-Extrusion pressure, bar: FT-Finishing time, minute: Viscosity- Vis, pa-sec.

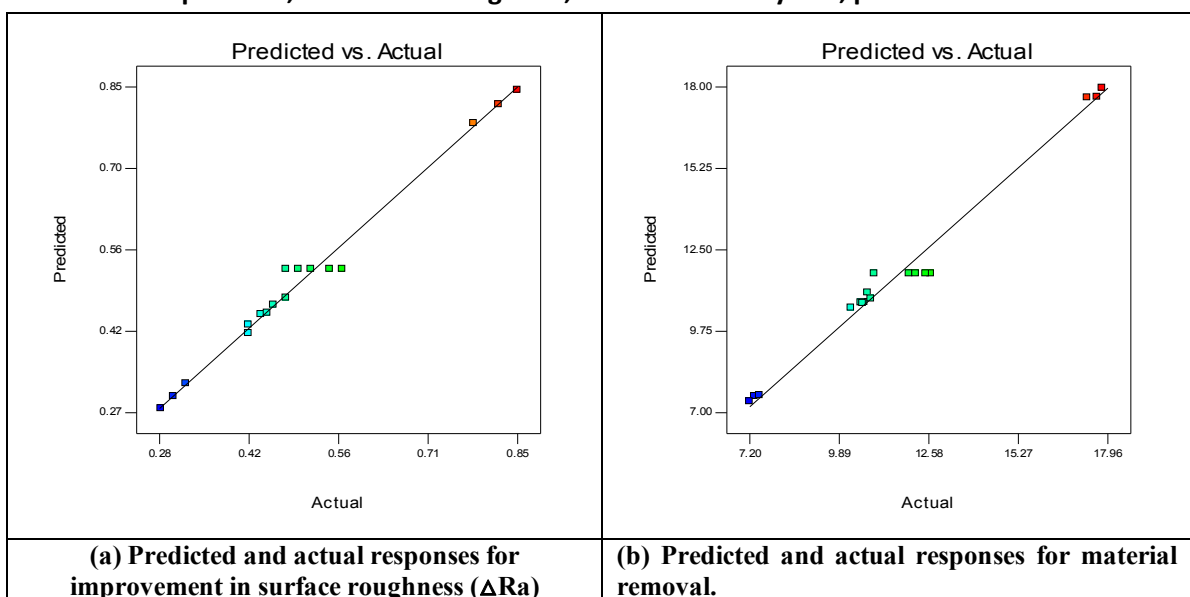


**Figure 6.20 Predicted and actual responses for improvement in surface roughness and material removal**

### 6.2.2.3 Influence of control factors on performance variables

In next part, three-dimensional response curves and perturbation graphs are explained to observe the influence of individual AFM variables and their interactions on the performance variables. The perturbation graph in Figure 6.21 illustrates the relative influence of significant AFM finishing variables on the improvement in surface roughness. The midpoint of levels (coded value 0) is always defined by Design-Expert tool to fix the reference point of all variables. A sudden slope for extrusion pressure (A), finishing time (B), and viscosity (C), illustrations that  $\Delta Ra$  is highly subtle to these process variables. The motives for these inclinations have been deliberated while enlightening the interaction effects of variables. Table 6.10 and Table 6.11 shows that the interactions which subsidize the most to the model are among the finishing time and viscosity (BC), extrusion pressure and viscosity (AC), Extrusion pressure and finishing time (AB), finishing time (B), viscosity (C) and extrusion pressure (A) for  $\Delta Ra$ . Also interactions of extrusion pressure and viscosity (AC), extrusion pressure and finishing time (AB) and finishing time and viscosity (BC), Finishing time (B), viscosity (C) and extrusion pressure (A) significantly effects the MR. The interaction graphs equivalent for improvement in surface roughness and material removal of above interactions are presented in Figure 6.22, 6.23 and 6.24, Figure 6.26, 6.27 and 6.28 respectively.

Design-Expert® Software

Surface Roughness  
● Surface Roughness

Actual Factors  
A: Extrusion Pressure = 22.00  
B: Finishing Time = 40.00  
C: Viscosity = 150.00

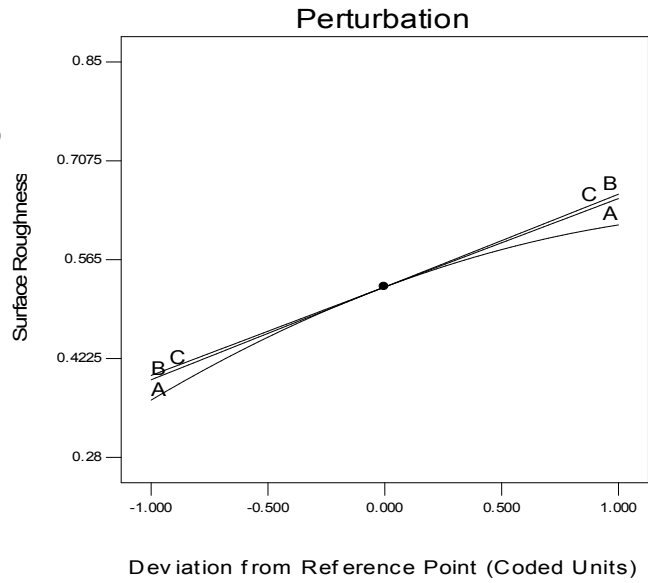


Figure 6.21 Perturbation plots for  $\Delta Ra$

Design-Expert® Software

Surface Roughness



X1 = A: Extrusion Pressure  
X2 = B: Finishing Time

Actual Factor  
C: Viscosity = 150.00

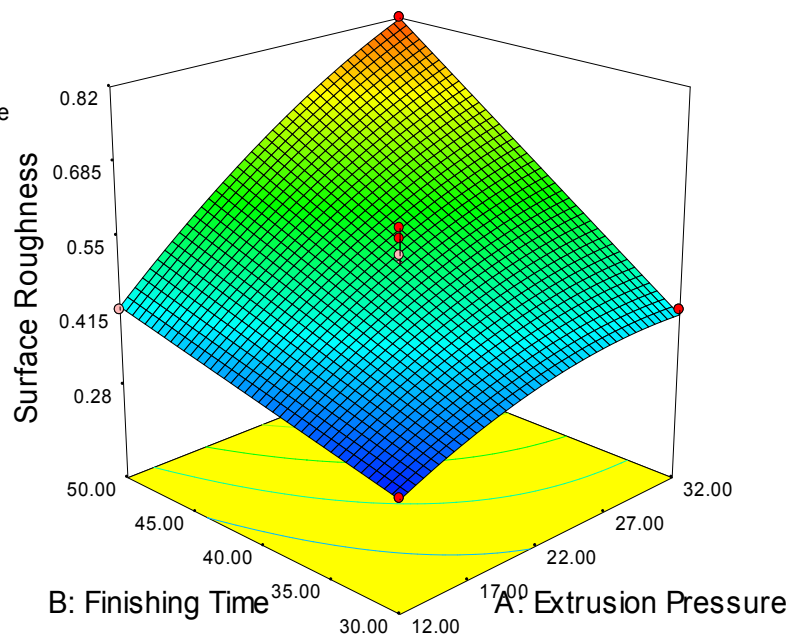


Figure 6.22 Response 3D surface plot demonstrating the interactive influence of finishing time and extrusion pressure for  $\Delta Ra$

Design-Expert® Software

Surface Roughness



X1 = A: Extrusion Pressure  
X2 = C: Viscosity

Actual Factor  
B: Finishing Time = 40.00

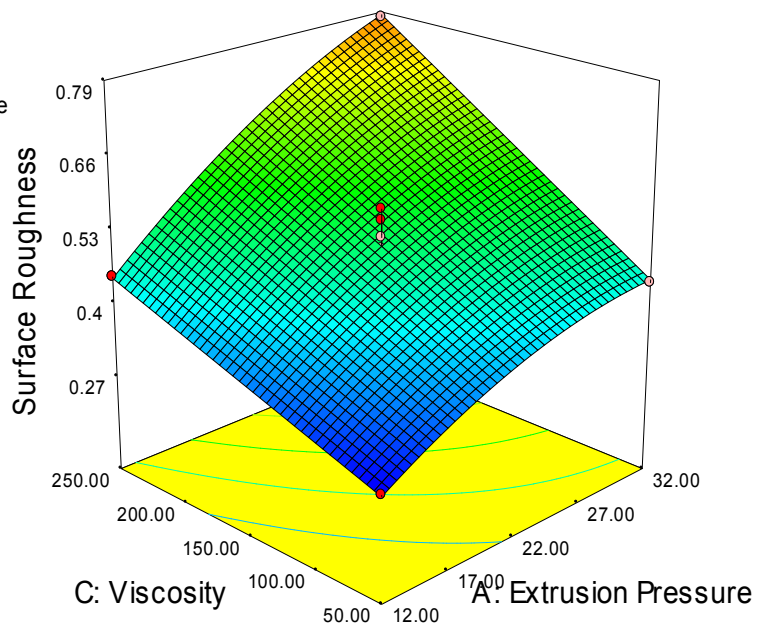


Figure 6.23 Response 3D surface plot demonstrating the interactive influence of extrusion pressure and viscosity for  $\Delta Ra$

Design-Expert® Software

Surface Roughness



X1 = B: Finishing Time  
X2 = C: Viscosity

Actual Factor  
A: Extrusion Pressure = 22.00

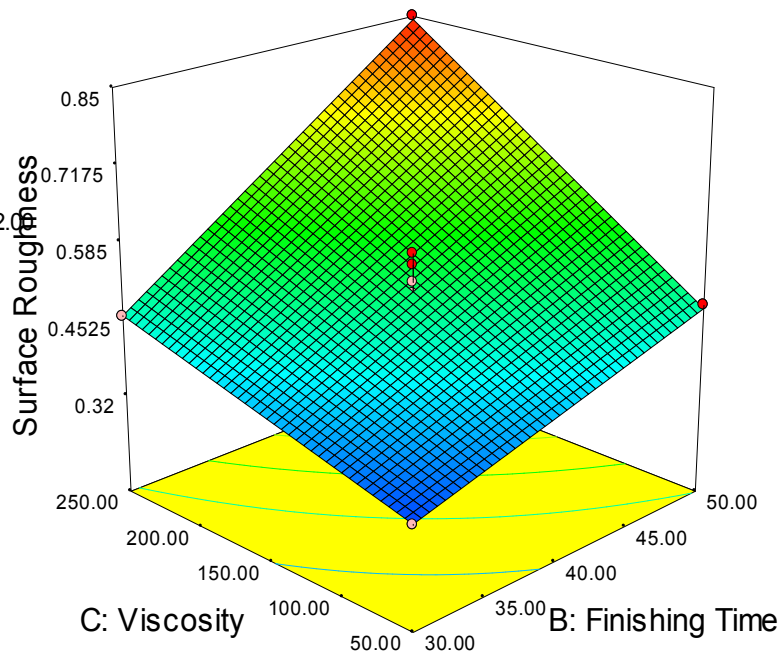


Figure 6.24 Response 3D surface plot demonstrating the interactive influence of extrusion pressure and viscosity for  $\Delta Ra$

Figure 6.22 illustrates the influence of extrusion pressure and finishing time on  $\Delta Ra$  while keeping viscosity constant. It shows that initially with increase in extrusion pressure,  $\Delta Ra$  value increase. This is due fact that when extrusion pressure escalates, normal force performing on each grain also increases that consequences in cavernous indentation on surface. At higher extrusion pressure, the material removal take place at deeper indentations in less finishing time results in more improvement in surface finishing. Figure 6.22 also shows that  $\Delta Ra$  increases in initial finishing time and decreases after certain finishing time. This is due to fact that in initial finishing time the peaks over the surface get removed and after certain finishing time,  $\Delta Ra$  decreases. Figure 6.23 also shows that  $\Delta Ra$  increases with increase in viscosity. This is owing to high viscous media, more deep penetration of abrasive particles is conceivable, and it results in increase in the surface finishing quality. Figure 6.23 shows the interactive influence of extrusion pressure and viscosity for  $\Delta Ra$ .

Figure 6.24 also shows that  $\Delta Ra$  increases in initial finishing time and decreases after certain finishing time. This is due to fact that in initial finishing time the peaks over the surface get removed and after certain finishing time,  $\Delta Ra$  decreases.

Design-Expert® Software

Material Removal  
● Material Removal

Actual Factors  
A: Extrusion Pressure = 22.00  
B: Finishing Time = 40.00  
C: Viscosity = 150.00

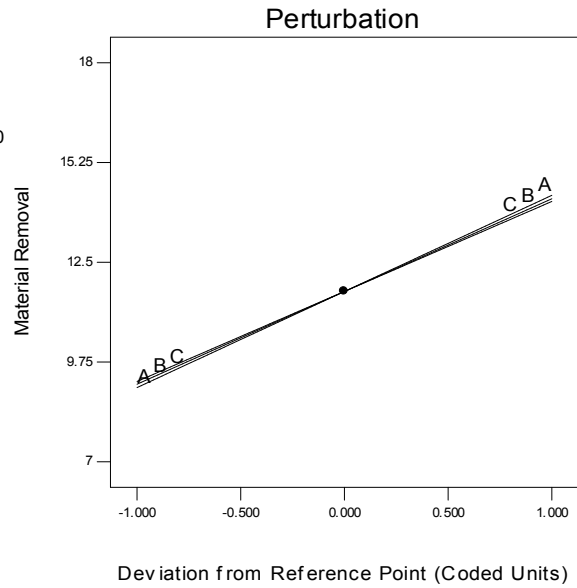


Figure 6.25 Perturbation graph for MR

Design-Expert® Software

Material Removal  
17.8  
7.2

X1 = A: Extrusion Pressure  
X2 = B: Finishing Time

Actual Factor  
C: Viscosity = 150.00

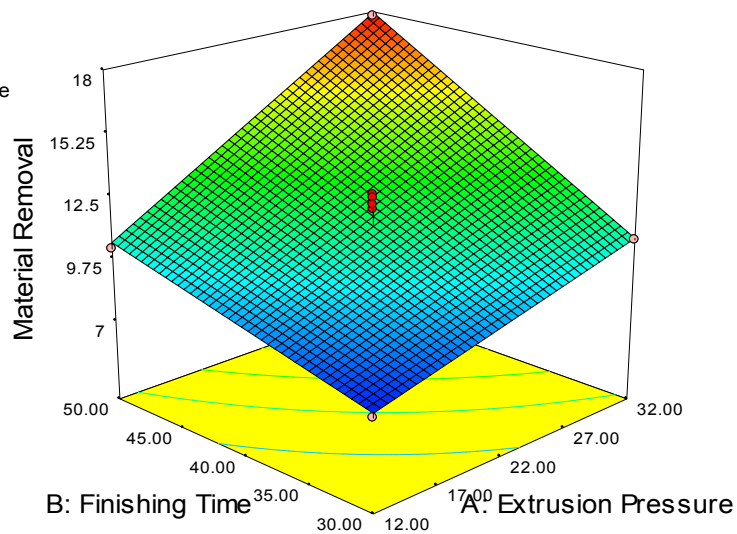


Figure 6.26 Response 3D surface plot demonstrating the interactive influence of finishing time and extrusion pressure for MR

Design-Expert® Software

Material Removal



X1 = A: Extrusion Pressure  
X2 = C: Viscosity

Actual Factor  
B: Finishing Time = 40.00

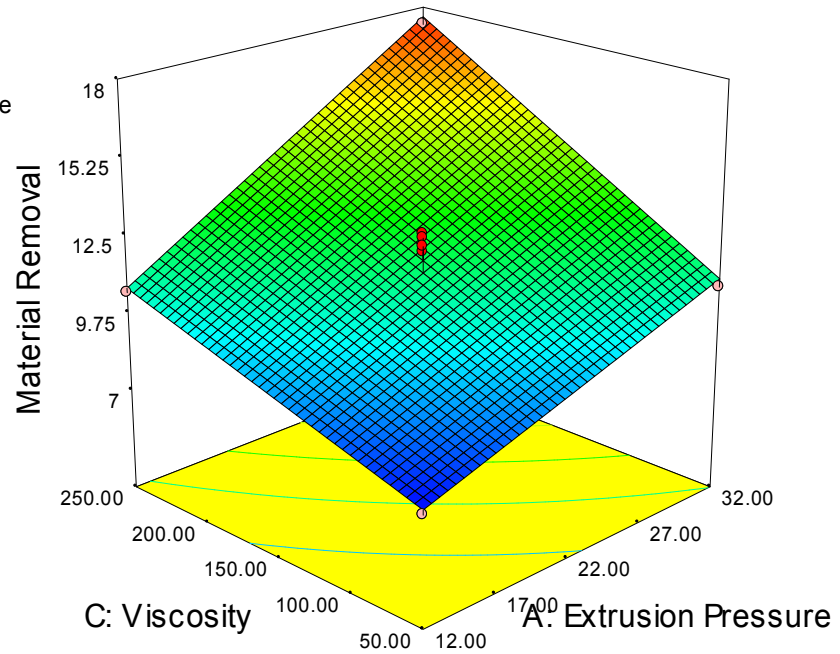


Figure 6.27 Response 3D surface plot demonstrating the interactive influence of viscosity and extrusion pressure for MR

Design-Expert® Software

Material Removal



X1 = B: Finishing Time  
X2 = C: Viscosity

Actual Factor  
A: Extrusion Pressure = 22.00

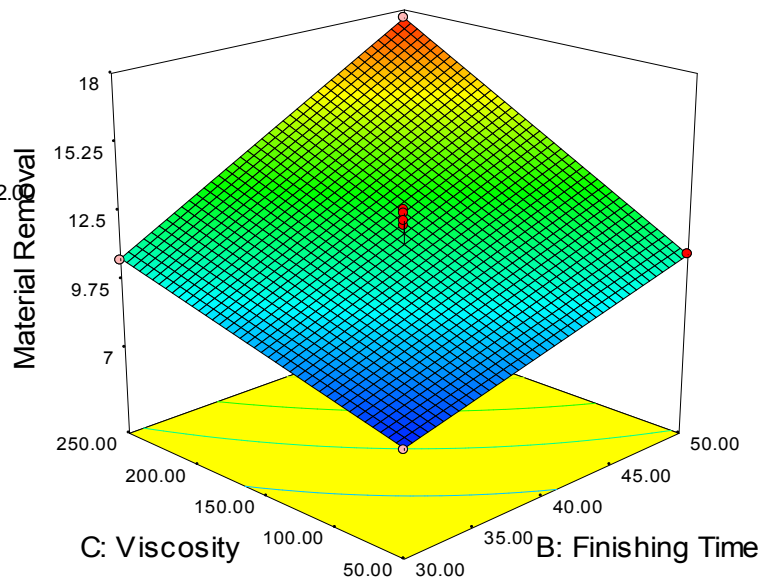


Figure 6.28 Response 3D surface plot demonstrating the interactive influence of viscosity and finishing time for MR

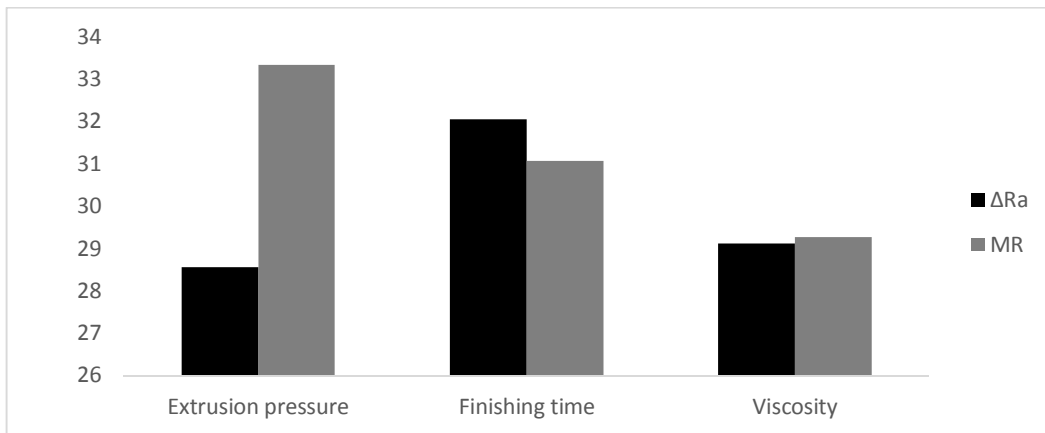
Figure 6.26 illustrates the influence of extrusion pressure and finishing time on MR while keeping viscosity of media constant. It shows that with increase in extrusion pressure, MR increase. This is due to fact that increase in normal force acting on abrasive grits, results in increase in deep penetration and results more material removal over the finishing surface. Figure 6.26 illustrates that with rise in finishing time, material removal decreases, because of in initial finishing time the material removal is high due to workpiece surface have large number of peaks and indentation. After some finishing time, the surface becomes flat (peak height reduces) and at higher finishing time the media just stream over the workpiece surface results in decreased material removal.

Figure 6.27 shows effect of extrusion pressure and viscosity on MR while keeping finishing time constant. It shows that with rise in viscosity, the MR will also increase, due to high viscosity media have higher confrontation so more material extrude out from surface consequences in high MR. Also Figure 6.28 indicates, low values of viscosity (50 pa-sec.) and low finishing time (30 minute) also cause low material removal.

#### **6.2.2.4 Optimization**

Optimization was performed to maximize  $\Delta Ra$  and maximize MR of finished component surface subject to working limit of three factors shown in Table 5.6. Figure 6.29 represents the percentage contribution of each factor which is derived by dividing the “specific (model) value “sum of squares by “model” sum of squares (SS) from Table 6.10 and Table 6.11 for  $\Delta Ra$  and MR respectively. It was observed that finishing time (highest % contribution 32.05) is most important factor for improvement in surface roughness, whereas extrusion pressure (highest % contribution 33.33) is most important factor for material removal.





**Figure 6.29 Percentage contribution of AFM variables on MR and ΔRa**

The parametric optimization is performed using the design expert software. This technique consists of desirability factor, which is derived by converting a predictable factor into a scale free term. Desirability factor have ranges from 0 to 1 in which least value stands for less desirable factor. The process variable values with extreme desirability are meant to be the optimal variable settings.

Optimum values for input variables and the equivalent responses are calculated using software and detailed are presented in Table 6.13. In single factor optimization, the other factors are discounted but for multi-variable optimization, all responses are deliberated and give equivalent significance. For validation of optimized outcomes, confirmation experiments have been achieved (Table 6.13.) and output results observed from experimental study are near to the predicted values.

**Table 6.13 Single factor and multi-factor optimization and comparative study of optimized outcomes and experimental facts**

| Optimization type | Objective                             | Optimum process variables |             |              | Response (predicted) | Response (experimental) | Desirability |
|-------------------|---------------------------------------|---------------------------|-------------|--------------|----------------------|-------------------------|--------------|
|                   |                                       | EP (bar)                  | FT (minute) | Vis (pa-sec) |                      |                         |              |
| Single response   | To maximize the ΔRa                   | 26.72                     | 45.70       | 218.68       | 0.5760 μm            | 0.5520 μm               | 1            |
| Single response   | To maximize the MR                    | 31.95                     | 46.37       | 224.02       | 13.50 mg             | 14.20 mg                | 1            |
| Multi-response    | To maximize ΔRa and MR simultaneously | 31.77                     | 47.85       | 242.38       | 0.5730 μm & 13.80 mg | 0.5620 μm & 14.50 mg    | 1            |

### 6.2.2.5 SEM Images of stamping die before and after finishing

After finishing by AFM process, the stamping die component surfaces are analyzed using scanning electron microscopy (SEM). SEM analysis is accomplished to perceive the microstructure of finished workpiece profile at 1000X magnification. Figure 6.30 illustrates microstructure image of finished work piece before AFM and after AFM. The surface imperfections such as recast layers and blows can be seen on unfinished surface as revealed in Figure 6.30 (a) and Figure 6.30 (c). SEM images displayed in Figure 6.30 (b), 6.30 (d) demonstrate visibly that surface structure is considerably enhanced after finishing process. At higher magnification, no cracks are observed, although entrenching of abrasive particles is observed infrequently. In consequences images smoother surface is perceived.

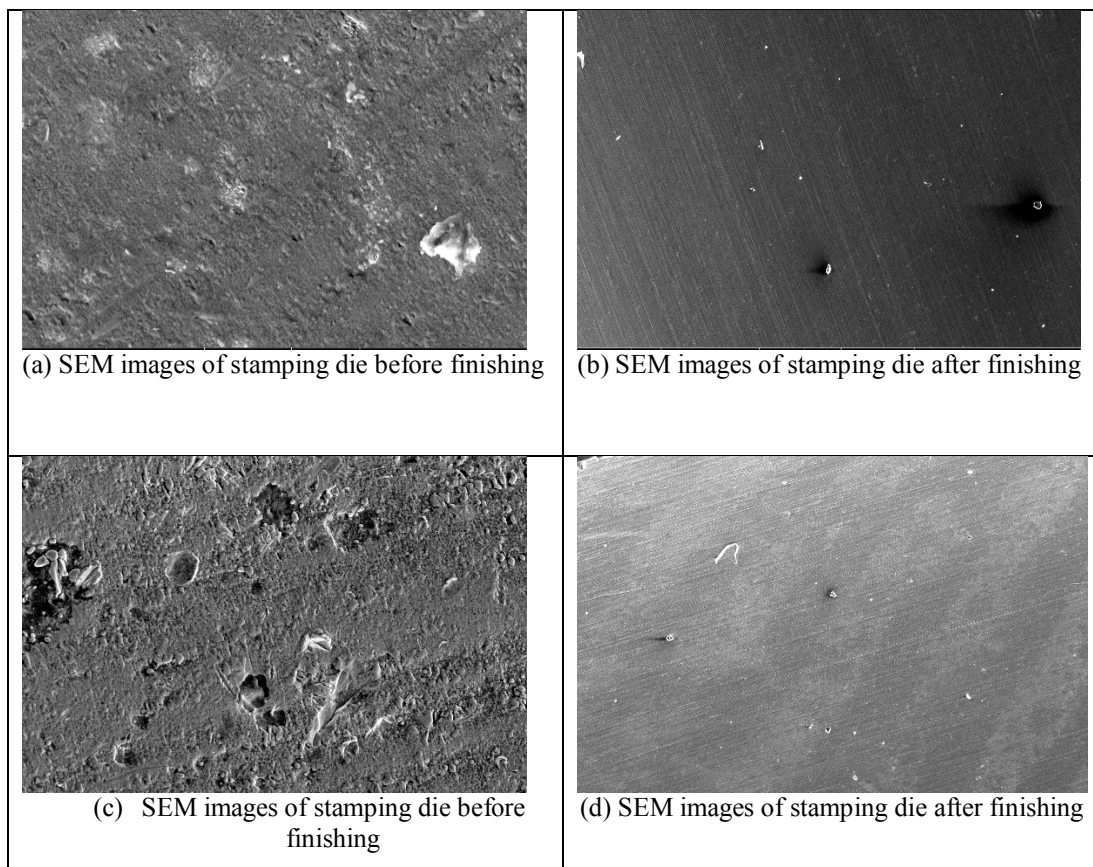


**Figure 6.30 SEM images of stamping die surface before and after finishing**

### 6.2.2.6 XRD results for stamping die

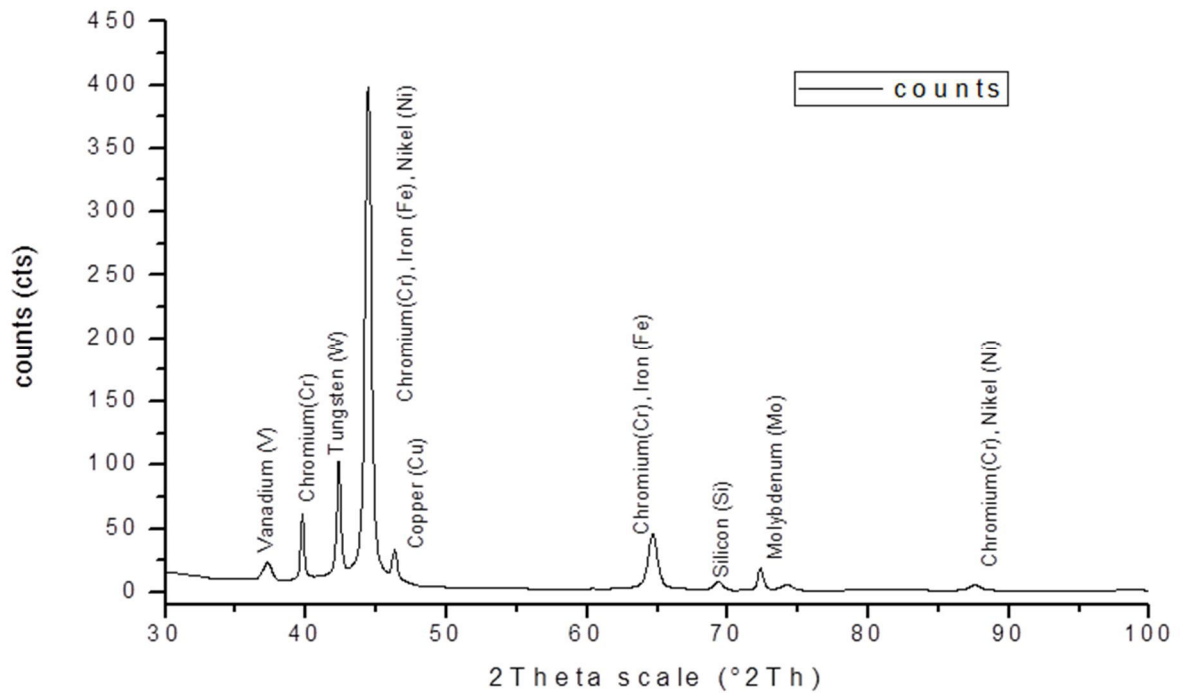


**Figure 6.31 XRD results of finished stamping die surface**

XRD analysis of finished work pieces has been performed on a software tool (X'Pert High Score). XRD graph of HSS stamping dies are presented in Figure 6.31. From XRD graphs, it is observed that maximum peaks are identified for Fe, Ni and Cr groups at 2ThetaF value of 44.39. Also some more peaks were identified for Cr at 2ThetaF value of 39.11, Ni at 2ThetaF value of 64.70. Some groups with lower peaks have been discounted. From XRD graphs different peaks were identified for Cr, Fe, Ni at various 2ThetaF value. The analysis shows that Cr, Fe, Ni are the common major phases invariably present in S.S. before and after processing the workpieces. During finishing process does not affect the surface micro-layer during processing under the conditions used for the present study.

## **Chapter 7 Mathematical Modelling and Validation**

---

### **7.1 Introduction**

This chapter explains the model developed for predicting the material removal during finishing the internal geometry surface in AFM. In earlier stage some researcher developed models for understanding the mechanism of material removal rate and flow behavior of media during finishing process. Williams et al. [8] developed a modelling and analysis technique called data dependent system (DDS) to observe the surface roughness value with and without AFM. Also a set of polynomials equation was derived to study the effect of different AFM variables on material removal and surface roughness [6]. Media flow behaviour during abrasive flow machining was characterized by Rajeshwar et al. [110] and developed a simulation model using finite difference methodology. R.K Jain et al. [24] used finite element modelling technique to calculate the stresses and forces generated during finishing process. Also they compared theoretical results obtained from FEM analysis with the experimental data existing in literature. V.K.Gorana et al. [27] predicted the surface roughness for two-way AFM and they found increase in active grain density with increases in abrasive concentration in media and this results in increase the reduction in average surface roughness ( $R_a$ ) value. G. Venketash et al. [78] constructed 3-D model to simulate the flow using CFD approach for Ultrasonic Assisted Abrasive flow Machining (UAAF) of bevel gears. After experimental study they compared the result of UAAF with conventional AFM and found this process superior for bevel gear finishing. The finishing time and improvement in surface roughness was relatively better than AFM.

In this chapter, model for material removal is developed for validation of experimental outcomes drawn from developed UAAF setup. The material removal for UAAF is derived theoretically using developed mathematical model and then compared with

experimental fact observed with experimental study. The experiments are performed using Taguchi experimental design using extrusion pressure, finishing time and viscosity of media as the process parameters. These models are based on assumptions of homogeneous medium flowing through the workpiece. Whereas abrasive particles act as dispersed phase in carrier medium.

## 7.2 Modelling of material removal

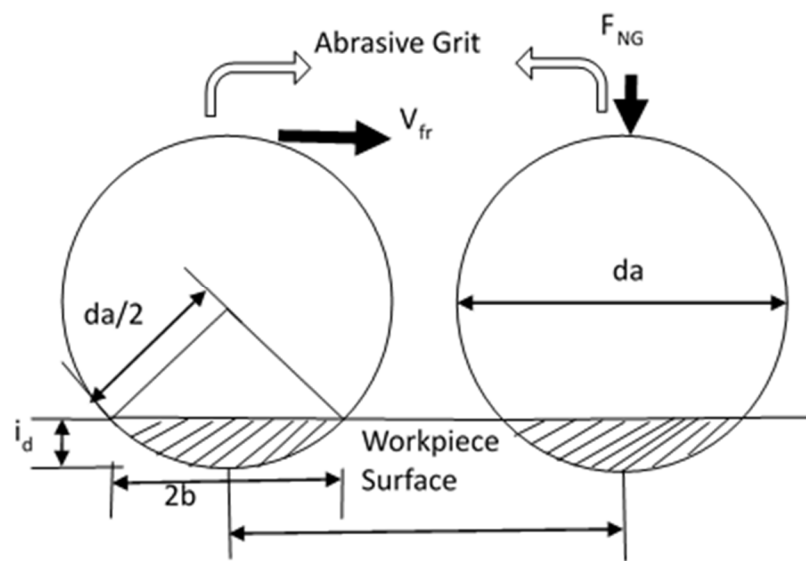


**Figure 7.1 Schematic diagram of spherical geometry of abrasive grit during material removal process in AFM**

Relevant literature on simulation and modelling shows that most of the researchers [23] used finite element method (FEM) for modelling of AFM process. Jain et al. [24] used FEM to determine normal stress on the workpiece surface which is then used to estimate material removal rate.

In AFM process material removal takes place due to rubbing action of particles on the target surface in the AFM media. Depending upon applied extrusion pressure the hard abrasive particle tends to cause indentation and roughness elements are removed as the abrasive particles flow along the target surface. The material removal rate is complex function of workpiece hardness, abrasive concentration, extrusion pressure, transport

properties of carrier media and workpiece geometry. Using classical indentation model as shown in figure 7.1 the amount of material removed by an individual abrasive particle during its contact with target surface can be derived, provided the velocity of particle is known. Given the carrier medium is highly viscous, it is reasonable to assume inertial forces to be negligible compared to viscous forces and velocity profile for Stokes flow in a given geometry can be used to estimate particle velocity.

### **Assumptions**

The subsequent assumptions are used for study of material removal in AFM process.

1. Most of the abrasive grits in AFM media may be estimated spherical in profile [20]. In AFM media, each grit contains single active cutting edge. More than one cutting edges in single grit, results in lacks of space among cutting edges to accumulate the produced chip during finishing process [111].
2. Load on individually abrasive particle is supposed to be constant and that is equivalent to the average load of abrasive particles.
3. It is assumed that all active abrasive grits are equal in mesh size, which is equal to the average of given range of mesh size.
4. It is assumed that each abrasive grain attain the same penetration depth and that subject to the functional normal force for a given work-piece's material hardness.
5. Abrasive grits are not supposed to be wearing and fracture during finishing action and in finishing area there is no comparative displacement between the abrasive grits in the AFM media.
6. Abrasive particles are homogeneously distributed in the carrier media.
7. The number of active grits per unit area remains constants for fixed concentration (it should be independent of flow rate).

### 7.2.1 Material Removal

For a given area of indentation and particle flow velocity, the material removal rate by each active abrasive particle is given as:

$$\dot{V}_{grit} = A' \cdot v_{grit} \quad \dots(7.1)$$

$v_{grit}$  is average grit velocity at machining surface,  $A'$  is cross sectional area of groove formed on the workpiece due to abrasive indentation.

Now, if  $N_a$  is number of active grits per unit machining area,

$$\text{Total number of active grits } N = N_a \cdot A_m \quad \dots(7.2)$$

Where,  $A_m$  is area to be finished

Using equation 7.1 and 7.2, the overall material removal rate is given as

$$\dot{V} = \dot{V}_{grit} \cdot N \quad \dots(7.3)$$

By putting the value of  $N$  and  $\dot{V}_{grit}$  in equation 7.3

$$\dot{V} = A' \cdot v_{grit} \cdot N_a \cdot A_m \quad \dots(7.4)$$

Assuming the uniform distribution of abrasive particles in the carrier medium.

The number of active abrasive particles for a given workpiece geometry is calculated as follows :

$$V_{cm} [m^3] = \frac{m_{cm}}{\rho_{cm}} \left[ \frac{kg}{m^3} \right] \quad \dots (7.5)$$

$$V_{ab} [m^3] = \frac{m_{ab}}{\rho_{ab}} [m^3] \quad \dots (7.6)$$

Where,

$m_{cm}$  - total mass of carrier medium,  $\rho_{cm}$  - density of carrier medium

$m_{ab}$  - total mass of abrasive,  $\rho_{ab}$  - density of carrier abrasive

$$V_{\text{total}} = V_{\text{cm}} + V_{\text{ab}} \quad \dots (7.7)$$

Given the average abrasive size of abrasive particles

$$\text{The total number of particles in the medium } N = V_{\text{ab}} / \frac{4}{3} \pi r^3 \quad \dots (7.8)$$

Where  $r$  is the radius of abrasive particle.

Specific number of abrasive particles per unit volume of media is given by

$$N_{\text{sp}} = N / V_{\text{T}} \quad \dots (7.9)$$

At any time during the machining the active abrasive particles are those, which are in contact with machining surface.

In case of cylindrical workpiece the number of active abrasive particle is given by

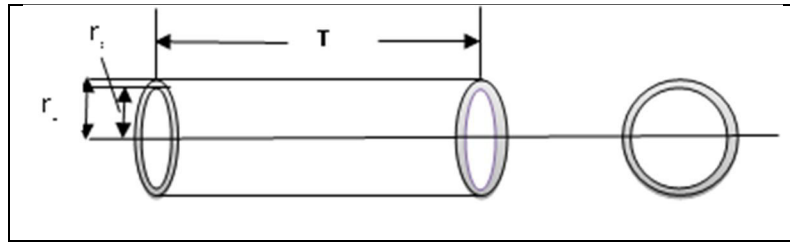


Figure 7.2 Cylindrical shape work piece.

$$N_{\text{a}} = N_{\text{sp}} * V_{\text{act}} \quad \dots (7.10)$$

Where  $V_{\text{act}}$  is active volume of media as shown in Figure 7.2

$$\text{Active volume } V_{\text{act}} = \pi (r_o^2 - r_i^2) L \quad \dots (7.11)$$

$L$  = Length of cylinder,  $r_o$  - outer radius of cylinder,  $r_i$  - inner radius of cylinder

The grit velocity  $v_{\text{grit}}$  at the workpiece surface is calculated assuming parabolic velocity profile for Stokes flow of highly viscous fluid medium,

$$\text{Velocity } u(r) = - \left( \frac{R^2 - r^2}{4\mu} \right) \left( \frac{dP}{dx} \right) \quad \dots (7.12)$$

Profile will be parabolic in nature for fully developed case.



However the use of developed velocity profile is not recommended if the workpiece length is short. The entrance length may be long enough for high viscosity carrier fluid. Therefore the media flow close to the entrance is almost uniform, while it develops along the flow direction. The use of plug flow velocity profile can be considered for a workpiece of short length

The indentation model for calculation of cross section area of groove due to abrasive particle is given next

$$\text{Normal Force } F_{NG} = \sigma_N \cdot \pi \cdot \frac{d_a^2}{4} \quad \dots(7.13)$$

Where  $\sigma_N$  = Normal stress acting on the abrasive grit.

Projected indentation area  $\nabla A$  i.e.  $\nabla A = \pi b^2$ , where  $b$  is the radius of projected indentation,  $i_d$  is depth of indentation

$$F_{NG} = H_w \cdot \nabla A \quad \dots(7.14)$$

$$F_{NG} = H_w \cdot \pi b^2 \quad \dots(7.15)$$

$$F_{NG} = H_w \cdot \pi i_d (d_a - i_d) \quad \dots(7.16)$$

Here,  $H_w$  is the work-piece hardness.

Now radius of projected indentation area ' $b$ ' and depth of indentation ' $i_d$ ' can be obtained as below by using Geometric relations,

$$b = \sqrt{i_d(i_d - b)} \quad \dots (7.17)$$

$$i_d = \left(\frac{d_a}{2}\right) - \sqrt{\left(\frac{d_a^2}{4} - b^2\right)} \quad \dots(7.18)$$

By substituting value of  $b^2$  from equation (3)

$$b^2 = \frac{F_{NG}}{H_w \pi} \quad \dots(7.19)$$

$$i_d = \left(\frac{d_a}{2}\right) - \sqrt{\left(\frac{d_a^2}{4} - \frac{F_{NG}}{H_w \pi}\right)} \quad \dots(7.20)$$

Cross section area  $A'$  of groove generated (Shaded portion in figure) can be derived by geometry as,

$$A' = \frac{d_a^2}{4} \sin^{-1} \frac{2\sqrt{i_d(d_a - i_d)}}{d_a} - \sqrt{i_d(d_a - i_d)} \left(\frac{d_a}{2} - i_d\right) \quad \dots(7.21)$$

For calculation of  $A'$ , major input are grain diameter, surface hardness  $H_w$  and normal force  $F_{NG}$ .  $F_{NG}$  value can be obtained from below equation

$$F_{NG} = P \cdot \pi \cdot \frac{d_a^2}{4} \quad \dots (7.22)$$

Where P is extrusion pressure value maintained during finishing experiment inside the work piece profile. After calculation of  $F_{NG}$  value of  $A'$  can be derived.

After substituting the value of  $A'$  in equation 7.4

Material removal will be

$$\dot{V} = \frac{d_a^2}{4} \sin^{-1} \frac{2\sqrt{i_d(d_a - i_d)}}{d_a} - \sqrt{i_d(d_a - i_d)} \left(\frac{d_a}{2} - i_d\right) V_{grit} \cdot N_a \cdot A_m \quad \dots(7.23)$$

Equation 7.23 proposes that material removal in AFM process depends mainly on  $A_m$  - area to be finished,  $N_a$  - number of active grits per unit machining area,  $H_w$ -work-piece hardness, p - average pressure of media and  $d_a$ -grit size. Theoretical material removal is derived using the variables of equation 7.23

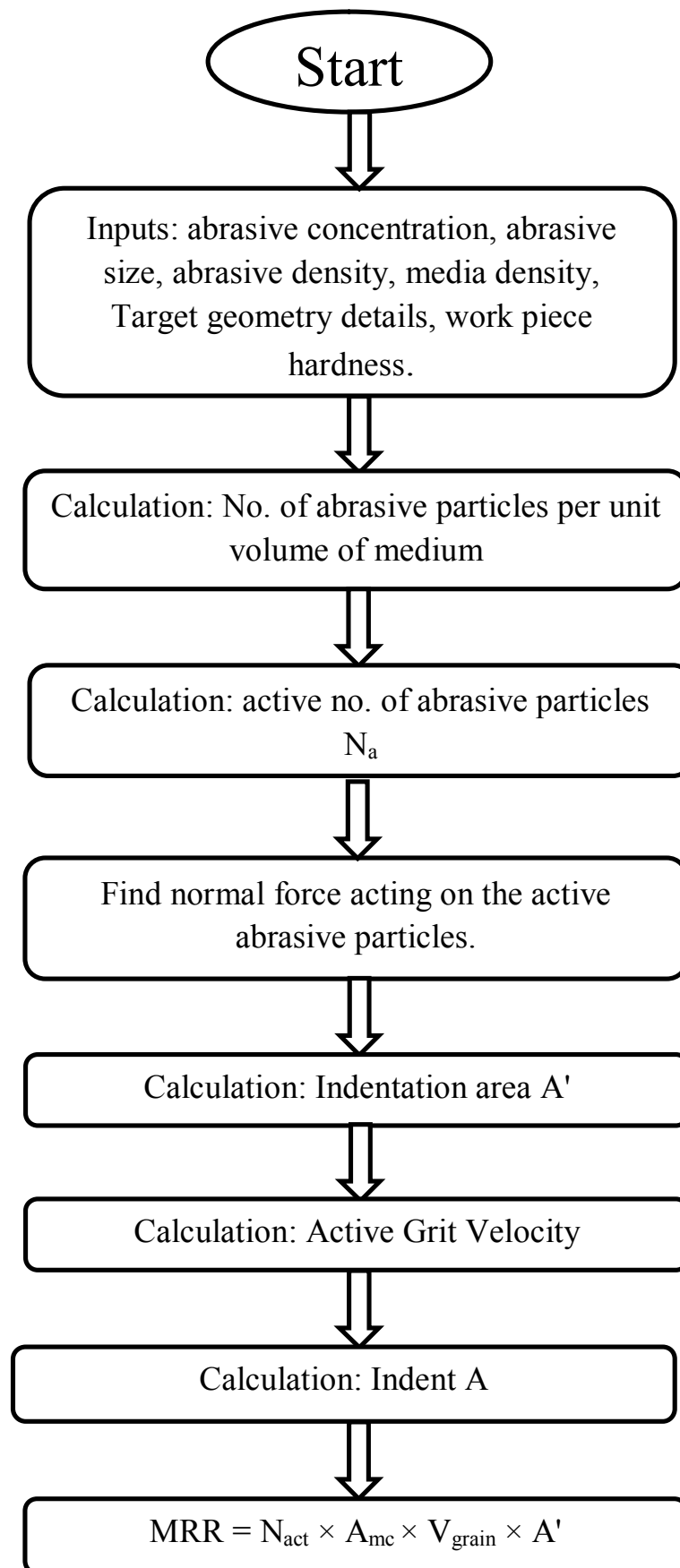


Figure 7.3 Flow chart for Material Removal

### 7.3 Control factors and their range

Experiments are conducted using Taguchi L<sub>9</sub> orthogonal experimental design as given in Table 7.1.

**Table 7.1 Coded levels and corresponding actual values of process parameters**

| Symbols | AFM Parameters     | Unit    | Levels                   |                           |                            |
|---------|--------------------|---------|--------------------------|---------------------------|----------------------------|
|         |                    |         | 1                        | 2                         | 3                          |
| A       | Extrusion Pressure | Bar     | 12                       | 22                        | 32                         |
| B       | Finishing Time     | Minute  | 30                       | 40                        | 50                         |
| C       | Viscosity          | Pa-sec. | L<br>(50-100<br>pa-sec.) | M<br>(150-200<br>pa-sec.) | H<br>(250-300 pa-<br>sec.) |

The workpiece material used is cylindrical bush of stainless steel (Fe 83%, Cr 13.8% and C 1.21%) of hardness 55 HRC. Silicon carbide (abrasive mesh size 220, 66% w/w abrasive concentration) is used as abrasive and it is mixed with natural polymer base and gel to make media for finishing process. By using taguchi technique, three independent variables are chosen viz. extrusion pressure (A), finishing time (B) and viscosity (C) and their selected values as in shown in Table 7.1. Table 7.1 shows the experiment and levels of each variable. Viscosity of media is measured using Rotational Rheometer and graded in low viscosity (50-100 pa-sec.), medium viscosity (150-200 pa-sec.) and high viscosity (250-300 pa-sec.) according to range of viscosity of media synthesized.

### 7.4 Comparison of theoretical and experimental results

Normal force and velocity of abrasive grit are calculated theoretically using the developed mathematical model in MATLAB® software. The normal stress derived from model is applied to calculate the material removal. In simulation, response variables is MR and

process variables are extrusion pressure, finishing time and viscosity of media and their values are selected as given Table 7.1.

Based on experimental study, results obtained in terms of effect of extrusion pressure, finishing time and viscosity have been calculated and discussed based on experimental and theoretical results. In current work, modelling of the process, and the experiments are conducted to validate the proposed mathematical model. This study includes the comparative results of the experimental and theoretical relationships between the AFM variables and material removal.

From modelling analysis the normal force exerted on each grain is calculated by multiply the cross sectional area of grain. Weight removal rate is derived using equation (7.22). Material removal mainly depends on area to be finished ( $A_m$ ), number of active grits per unit machining area ( $N_a$ ), work-piece hardness ( $H_w$ ), avg. pressure of media ( $P$ ) and grit size.

## **Material Removal**

### **7.4.1 Effect of extrusion pressure on material removal**

Figure 7.4 shows comparison of theoretical and experimental material removal with extrusion pressure at low viscosity and high viscosity keeping finishing time constant (40 minute). From graphs it is clear that tendency of theoretical material removal is closer to experimental material removal. As extrusion pressure is increasing material removal is increasing. The inconsistency between the graphs of experimental and theoretical is may be due fixture and tooling design or may be due to basic assumption made in theoretical model.

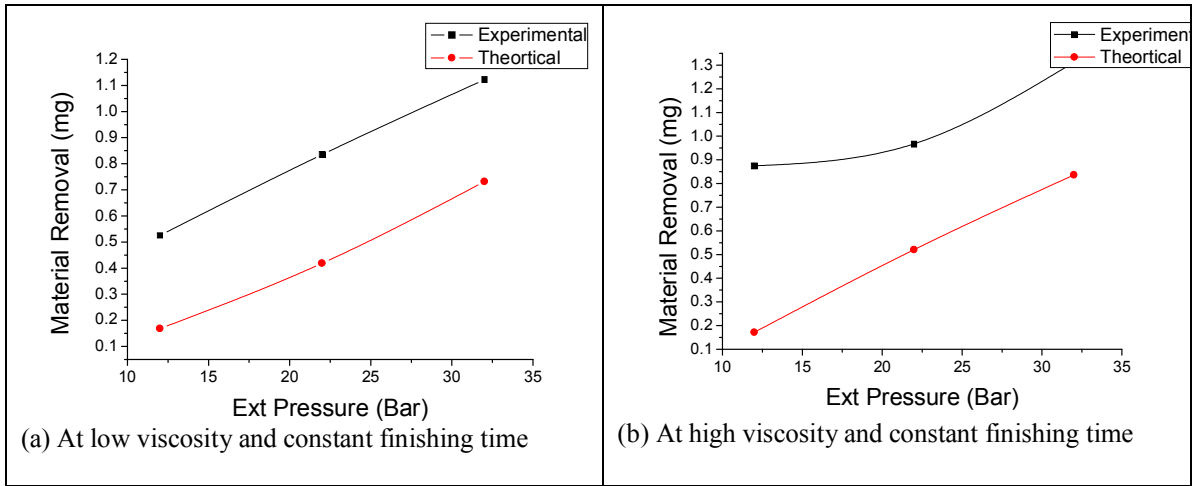


**Figure 7.4 Comparison of theoretical and experimental material removal with extrusion pressure at finishing time constant (40 minute)**

Figure 7.5 shows the comparison of theoretical and experimental material removal with extrusion pressure at 30 minute finishing time and 50 minute finishing time keeping viscosity constant (medium grade).

In this graph, material removal will also increase with extrusion pressure but at higher viscosity media and low extrusion pressure the inconsistency is more compared to Figure 7.4. This is due to high viscosity of media will be responsible for higher material removal rate.

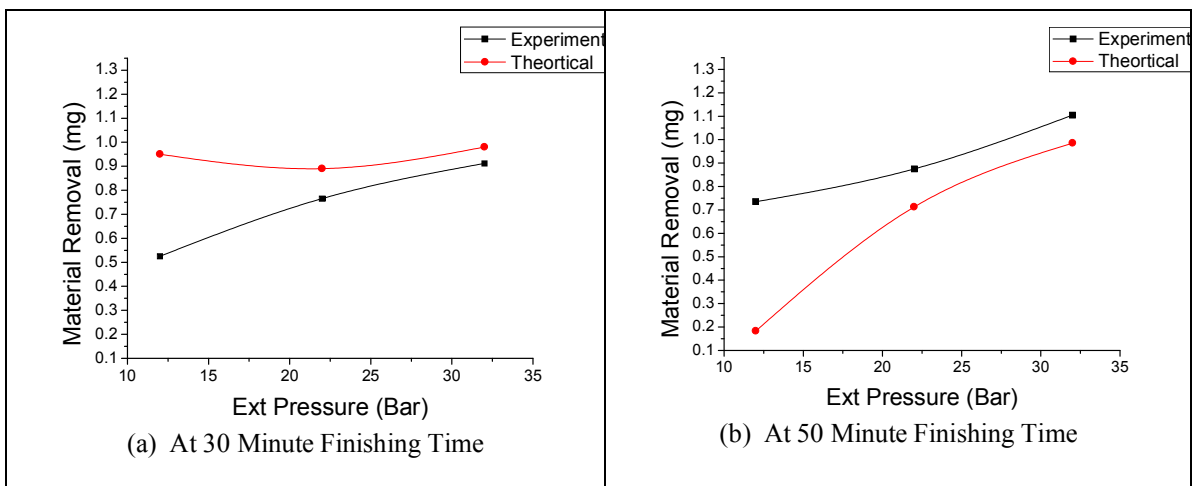


**Figure 7.5 Comparison of theoretical and experimental material removal with extrusion pressure keeping viscosity constant (Medium Grade)**

#### 7.4.2 Effect of finishing time on material removal

In Figure 7.6 (a) and (b), theoretical and experimental material removal is linearly changing with finishing time. Material removal is higher at low finishing time at high viscosity media due to removal of high peaks over the workpiece surfaces. After some finishing time, surface converts into flat, results in decrease in material removal. The inconsistency in theoretical and graphical results is due to assumption that equal material is removed on each finishing time. Also the abrasive shape is assumed as spherical but its irregular in shape and size.

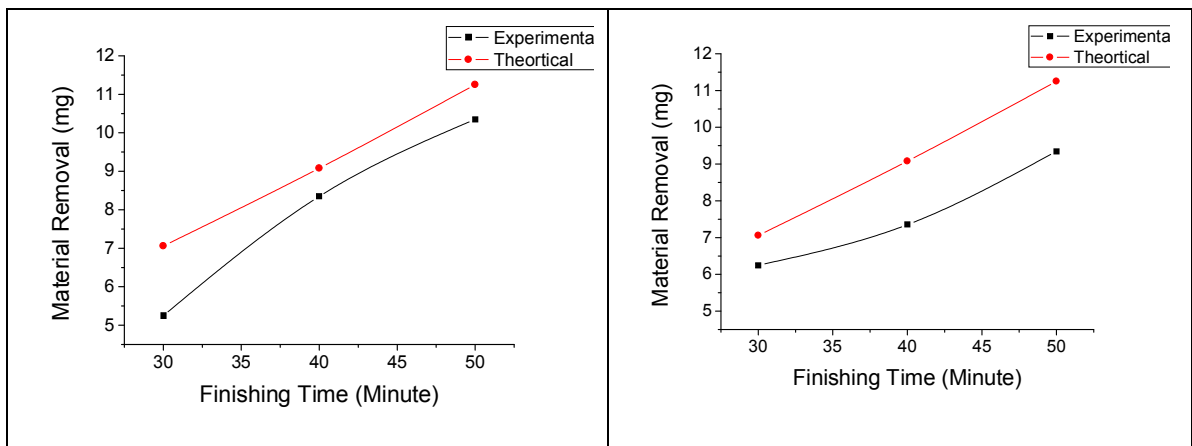


**Figure 7.6 Comparison of theoretical and experimental material removal with finishing time keeping extrusion pressure constant (22 bar).**

Figure 7.7 shows the comparison of theoretical and experimental material removal with finishing time at extrusion pressure 12 bar and extrusion pressure 32 bar keeping viscosity constant (medium grade). Graphs show same increase in material removal with finishing time but at higher extrusion pressure (Figure 7.7 (b)), material removal is more than at lower extrusion pressure. This is due to higher extrusion pressure, help to remove more material from workpieces surface.

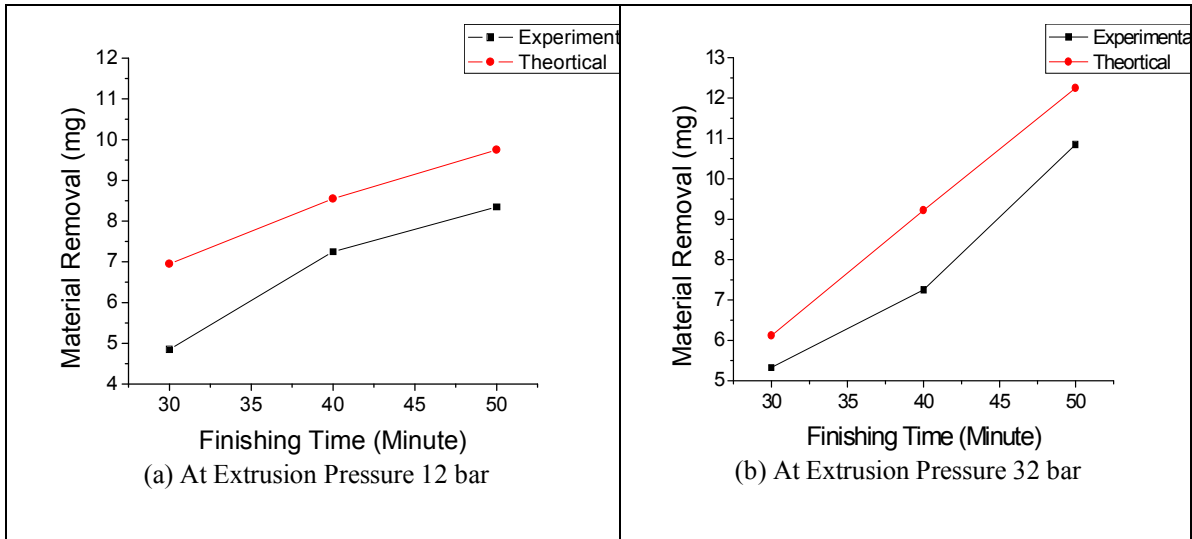


**Figure 7.7 Comparison of theoretical and experimental material removal with finishing time keeping viscosity constant (medium grade)**

### 7.4.3 Effect of viscosity on material removal

In Figure 7.8 (a) and (b), theoretical and experimental material removal is linearly changing with viscosity. Material removal is higher at high viscosity media due more stiff media provide more resistance to flow over the surface results in higher material removal. The inconsistency in theoretical and graphical results are due to assumption that abrasive sin media are equal in mesh size and all are not in same grit size but irregular in shape and size.

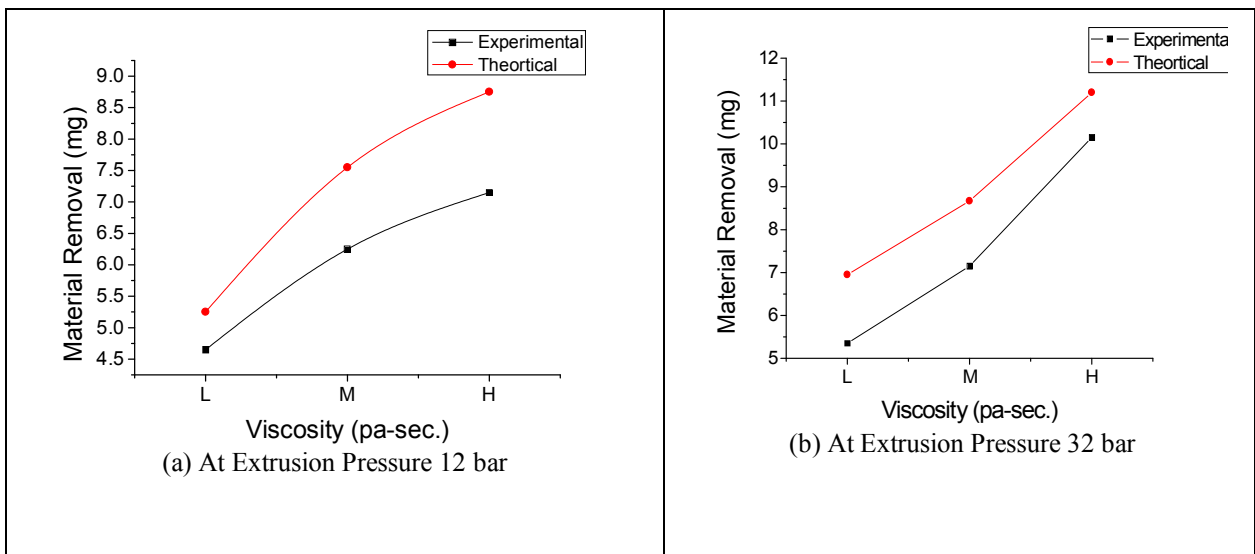


**Figure 7.8 Comparison of theoretical and experimental material removal with viscosity keeping finishing time constant (40 minute).**



Also in Figure 7.9 (a) and (b), theoretical and experimental material removal is linearly changing with viscosity, but at varying finishing time the trend of material removal is different. In 30 minute finishing time material removal is higher but for 50 minutes material removal is less due to as stated in last section.

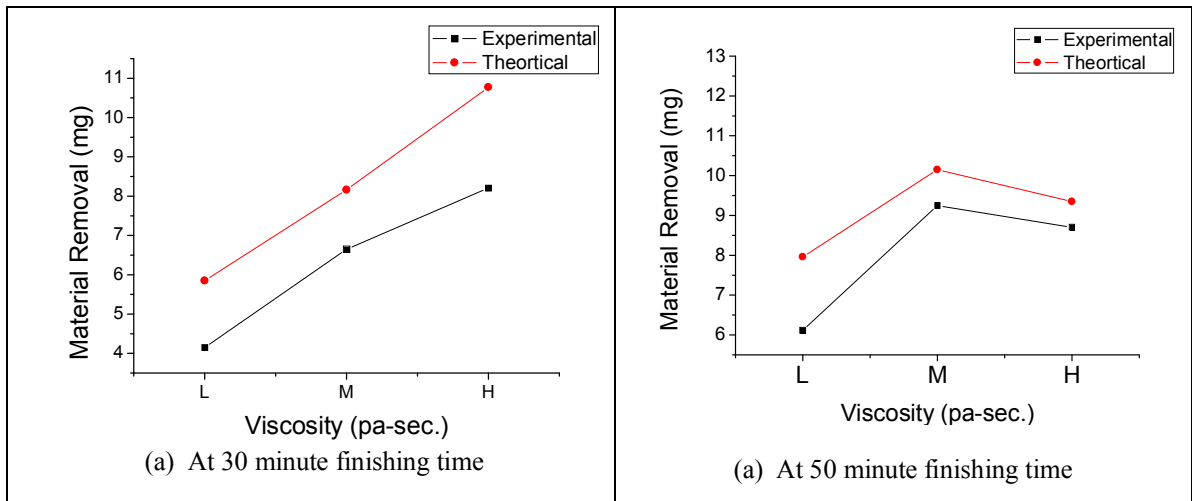


**Figure 7.9 Comparison of theoretical and experimental material removal with viscosity keeping extrusion pressure constant (22 bar)**



## Chapter 8 Conclusions and Future Scope

### 8.1 Conclusion

#### Characterization and rheology study of PAG

- Low cost and environmental friendly AFM media has been synthesized and same AFM media is utilized for finishing application.
- FTIR results show that alkenes, esters, amines and aromatic are more dominating which provides the elastic nature, thermal stability and tensile strength to the media.
- The percentage of liquid synthesizer, abrasive concentration, and abrasive mesh size were found to be significant parameters for thermal stability of media contributing 35.62%, 29.82%, 17.73% respectively on critical temp.
- SEM results show the interface between the constituents of the additives polymeric base and abrasive particles.
- The percentage of liquid synthesizer is found to be significant parameter of media contributing 35.77 % on viscosity of media.
- ANOVA analysis for yield stress shows that abrasive concentration is most significant parameter which affects the yield stress of polymer abrasive gel.

#### Performance study of PAG and commercial media (Streamer)

- An alternatively developed media (PAG) and commercial media (streamer) are characterized through rheological as well as by FTIR and TGA analysis.
- Rheological study for both media shows that as apparent viscosity decreases with shear rate, it shows the shear thinning behaviour (Power law) of AFM media.

- Experimental studies show material removal increases with increase in extrusion pressure, viscosity of media and finishing time. Extrusion pressure has most impact compared to other variable on material removal as well as on improvement in surface roughness value. Also improvement in surface roughness value increased with increase in extrusion pressure, viscosity and finishing time. But finishing time has lowest impact on finishing quality as compared to other variables.

### **Design and fabrication UAFM setup**

- Micro UAFM setup has been developed and validated for finishing wire draw die.
- Based on successive experimental outcomes of MUAFM, a production grade low cost UAFM setup has been designed and fabricated.
- For finishing price sensitive industrial components, nylon material tooling has been designed and developed.

### **Experimental investigation on developed UAFM setup for finishing internal passage of industrial components**

- Maximum improvement in surface finishing observed  $\Delta Ra$  0.6  $\mu m$  and  $\Delta R_t$  4  $\mu m$ .
- Results of trial experiment show the optimum levels of variable for response parameters i.e. extrusion pressure 32 bar, finishing time 50 minute, viscosity High.
- Trial experiment shows maximum improvement in surface roughness as 0.42  $\mu m$ .
- RSM results show that finishing time, viscosity and extrusion pressure has significant effect on response variable (Improvement in surface roughness ( $\Delta Ra$ ) and material removal).

- Improvement in surface roughness value increased with increase in extrusion pressure, viscosity and finishing time. But finishing time has low impact on finishing quality as compared to other variables.
- Industrial component (trim die and stamping die) was finished utilizing alternative developed unidirectional AFM setup and alternative PAG media which is low cost and environmental sustainable.
- Finishing time and viscosity of media have largest effect on finishing performance than other variables of the AFM process.
- The process had capability to remove craters and cracks of workpiece surface, at higher values of variables more glazed quality was observed while finishing with AFM process.

#### **Comparison of experimental and analytical results for material removal**

- Theoretical material removal deliberate from the model established is related with the experimental outcomes. Graphs on theoretical and experimental follow same trend but overall they have deviation in graphs.

#### **Component specific finishing consultancy for tool & die industry**

- Studies are performed for finishing Glass mold component of cast iron material using UAFM setup and PAG media.
- Alternative PAG media is used and tooling and fixture unit for holding the workpiece was designed and fabricated in the laboratory.
- For glass mold finishing, lowest surface roughness value obtained was  $0.61 \mu\text{m}$  and maximum material removal was 4gm.
- Maximum improvement in surface roughness ( $\Delta\text{Ra}$ ) observed is  $1.26 \mu\text{m}$  at 22 bar

pressure, 50% abrasive concentration, medium viscosity, and 40 minutes of finishing time.

- For finishing 3D printer nozzle of 3mm diameter, PAG media and UAFM setup is utilized and images of finished surface show significant improvement.
- For 3D printer nozzle, results show the maximum improvement in surface roughness achieved and material removal is 0.92  $\mu\text{m}$  and 136 mg respectively

### **8.1.1 Contribution in AFF technology**

The contributions from this research in the field of AFF technology and its practical application are provided below from the manufacturing perspective of price sensitive industrial components:

- An alternative to conventional, which is low cost and environment friendly media, is characterized to serve the industries for finishing.
- A low cost modular setup has been designed and developed for finishing internal surfaces of price sensitive industrial components, which are currently finished manually.
- Exhaustive experimentation has been carried out on the developed setup using the low cost and environment friendly AFM media for performance analysis of setup and media.
- The performance of developed UAFM setup has been further demonstrated for finishing the price sensitive industrial components.
- The developed media and UAFM setup has been used for finishing 3D printer nozzle and glass mold, which cannot be consistently finished manually or any other conventional technology other than Abrasive Flow Machining which was beyond the reach of these plants.

## **8.2 Future work**

- This work can be extended for finishing of biomaterial components and medical implants with enhanced AFM media properties.
- For monitoring the finishing process, current AFM setup could be equipped with online line acoustic based conditioning monitoring system, to measure the forces over the finishing surface.
- Finishing of miniaturized components like micro-channels made out of hard materials like carbides and ceramics could be taken up.
- For further more improvement of material removal rate this process can be hybridized with other processes.

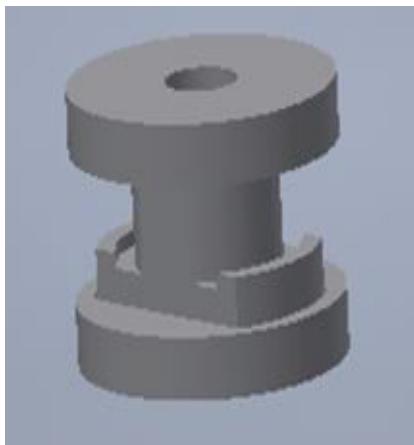
### **Additional experiments for validation of UAFM**

#### **8.2.1 Glass mold finishing**

Additional experimentation were performed for finishing the internal surface of industrial components for finishing glass molds (shown in Figure 8.2 (a)) using the developed UAFM setup and PAG media. Quality of surfaces in glass molds have wide role in quality products manufactured. So for improvement of glass mold internal surface at low cost, the developed UAFM setup and PAG media is used for finishing.

##### **8.2.1.1 Tooling design**

Initially, tooling and fixture are designed as shown in Figure 8.2 (b) using nylon material for the glass mold shown in Figure 8.2. Nylon tooling is designed for easy mounting of components and provides smooth flow of PAG media to the work piece surface to be finished. Tooling is designed using Autodesk inventor 2015 software. Nylon material is used as raw material and CNC milling machine is used for machining process and fabricated as shown in Figure 8.1.



(a) CAD model of designed



(b) Nylon raw material



(c) CNC milling used for machining the tooling.



(d) Fabricated Tooling for Glass mold.

**Figure 8.1 Steps for tooling design and fabrication**

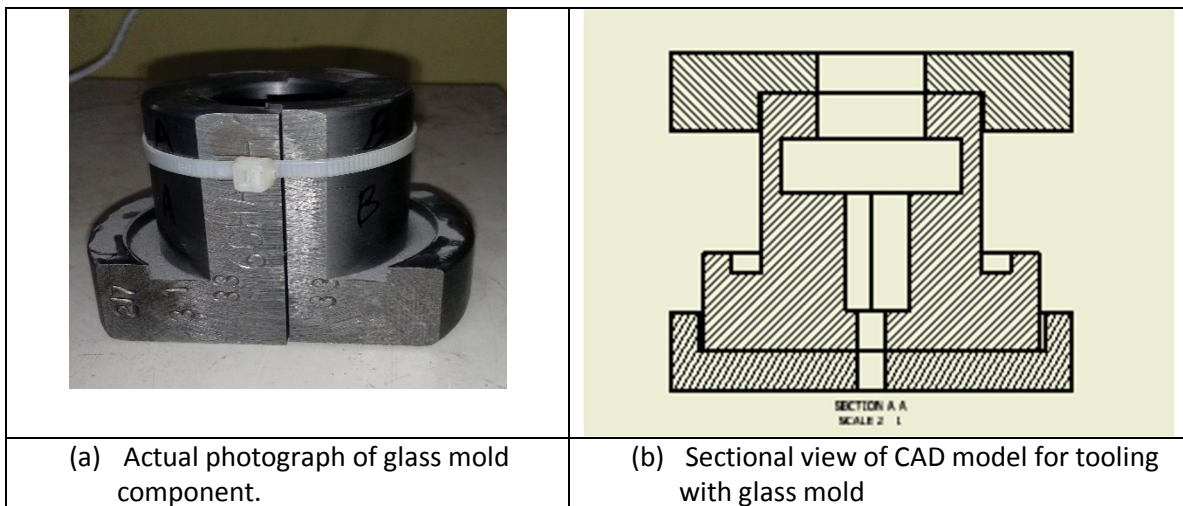


**Figure 8.2 Actual photograph and schematic view.**



### 8.2.1.2 Experiment results



**Figure 8.3 Photograph of UAFM setup with tooling holding the glass mold**

The component is fixed in UAFM setup using the developed tooling as shown in Figure 8.3.

During experimentation, process variables are selected as extrusion pressure (12 bar to 32 bar), finishing time (30 minute to 50 minute) and viscosity (50 pa-sec. to 250 pa-sec.). The performance variables are improvement in surface roughness ( $\Delta Ra$  in  $\mu m$ ) and material removal (mg). Other constant variables are 220 abrasive mesh size and 66% abrasive concentration in PAG media.

**Table 8.1 Weight and dimensional changes**

|                 | Mold (M1)        |                 |                     | Mold (M2)        |                 |                     |
|-----------------|------------------|-----------------|---------------------|------------------|-----------------|---------------------|
|                 | Before finishing | After Finishing | MR Dimension change | Before Finishing | After Finishing | MR Dimension change |
| <b>Weight</b>   | 1125gm           | 1122gm          | 3 gm                | 1133 gm          | 1129 gm         | 4 gm                |
| <b>Entry id</b> | 28.56 mm         | 28.56 mm        | -                   | 28.50 mm         | 28.57 mm        | 0.07 mm             |
| <b>Exit id</b>  | 11.36 mm         | 11.50 mm        | 0.14 mm             | 11.59 mm         | 11.62 mm        | 0.03 mm             |

**Table 8.2 Improvement in surface roughness value for Mold (M1) and Mold (M2)**

| <b>Finishing parameters</b>                        | <b>Mold (M1)<br/>Initial Ra and<br/>Final Ra value</b> | <b>Imp. in surface<br/>roughness (<math>\Delta R_a</math>) for<br/>M1</b> | <b>Mold (M2)<br/>Initial Ra and Final<br/>Ra value</b> | <b>Imp. in surface<br/>roughness (<math>\Delta R_a</math>)<br/>for M2</b> |
|--|--|---|--|---|
| EP 12 bar, 33% Ab.<br>Conc., M vis., FT-40<br>min. | 3.01-2.40 $\mu\text{m}$                                | 0.61 $\mu\text{m}$  | 3.05-2.52 $\mu\text{m}$                                | 0.53 $\mu\text{m}$  |
| EP 22 bar, 50% ab.<br>Conc., M vis., FT 40<br>min. | 2.40-1.65 $\mu\text{m}$                                | 0.75 $\mu\text{m}$  | 2.52-1.52 $\mu\text{m}$                                | 1.0 $\mu\text{m}$   |
| EP 32 bar, 66% ab.<br>Conc., M vis., FT 40<br>min. | 1.65-0.79 $\mu\text{m}$                                | 0.86 $\mu\text{m}$  | 1.52-0.76 $\mu\text{m}$                                | 0.76 $\mu\text{m}$  |

Table 8.1 and Table 8.2 results show the lowest surface roughness value obtained after finishing is 0.61  $\mu\text{m}$  and maximum material removal is as high as 4 gm. After finishing glass mold, the maximum improvement in surface roughness ( $\Delta R_a$ ) observed was 1.26  $\mu\text{m}$  at 22 bar pressure, 50% abrasive concentration, medium viscosity, and 40 minutes of finishing time.

### **8.2.1.3 Images of glass mold:**

Figure 8.5 and Figure 8.6 shows the images of glass mold M1 and Mold M2 before finishing at various locations. After finishing with AFM, at same location the images was recorded and improvement in surface quality can be clearly seen in below images in Figure 8.4 and Figure 8.5.

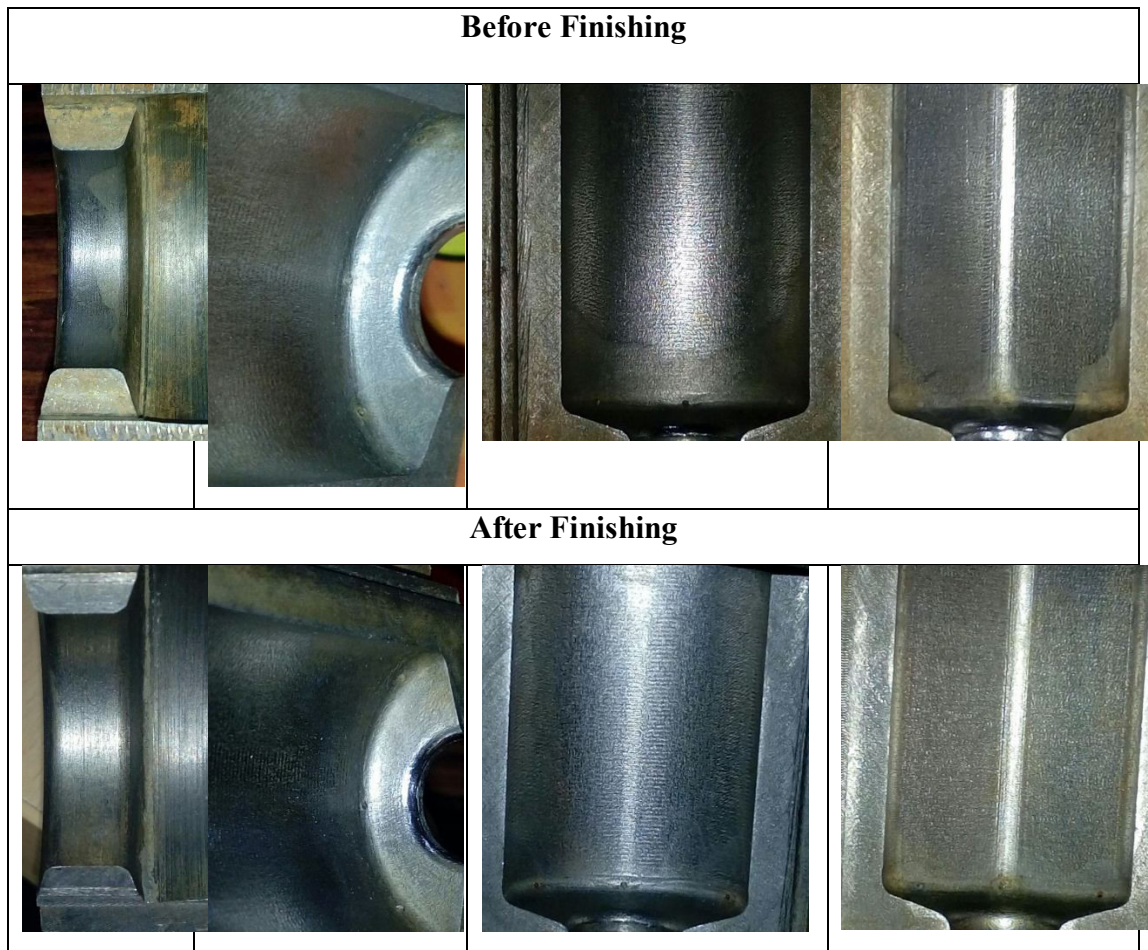


**Figure 8.4 Images of glass mold M1 before AFM and after AFM**

### **8.2.2 3D Printer nozzle finishing**

In this study, components are 3D printer nozzle as shown in Figure 8.7 (3 mm internal diameter). The need of finishing arises due to rough internal surface of nozzle; ABS material is sticking inside the nozzle while printing the parts. So problem is resolved by finishing the internal surface of nozzle using developed UAFM setup and PAG media.

#### **8.2.2.1 Tooling design**

Initially, tooling and fixture are designed as shown in Figure 8.6 and fabricated using nylon material and CNC milling machines. Nylon tooling is designed for easy mounting of components and one time three nozzle can be finished. Tooling is designed using Autodesk<sup>®</sup> Inventor 2015 software. Figure 8.8 shows the sectional view of tooling holding three nozzles at one time.

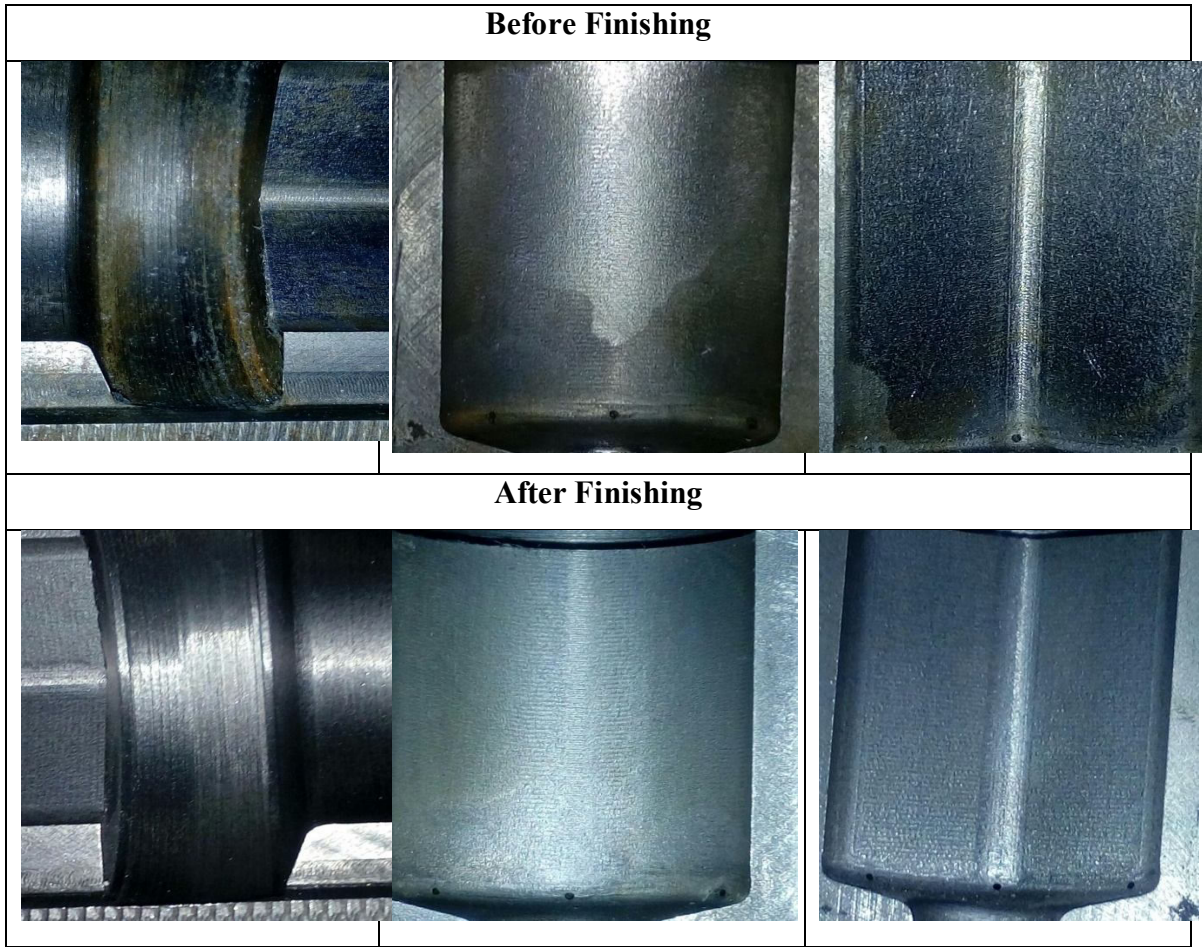


**Figure 8.5 Images of glass mold M2 before AFM and after AFM**

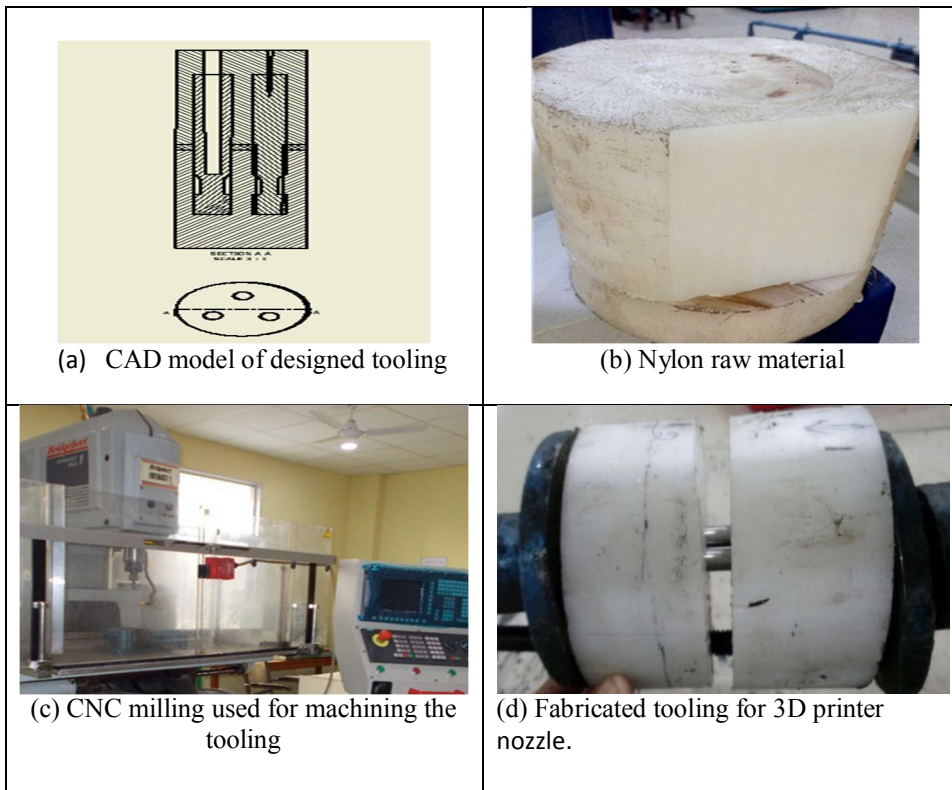


**Figure 8.6 Steps for tooling design and fabrication**

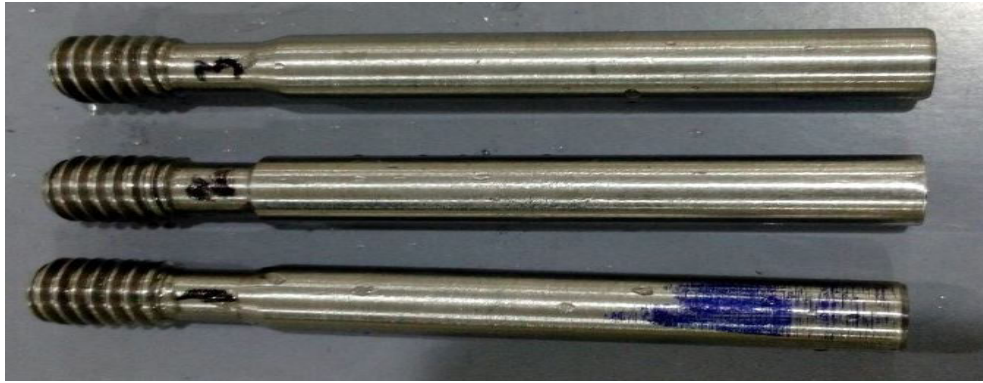


Figure 8.7 3D printer nozzle component

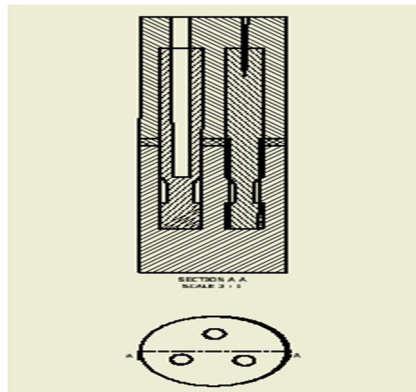


Figure 8.8 Sectional view of CAD model for tooling

### 8.2.2.2 Experiment Results

Experiments are performed using L<sub>9</sub> Taguchi experimental design. The process parameter used and their levels selected are shown in Table 8.3.

Table 8.3 Design of experiment

| Sr. No. | Levels | Variables          | Levels |    |    | Unit    |
|---------|--------|--------------------|--------|----|----|---------|
|         |        |                    | 1      | 2  | 3  |         |
| 1       | A      | Extrusion Pressure | 12     | 22 | 32 | Bar     |
| 2       | B      | Finishing Time     | 30     | 40 | 50 | Minute  |
| 3       | C      | Viscosity          | L      | M  | H  | Pa-sec. |

Same developed PAG media and UAFM setup was utilized for finishing experimentation. During experimentation, process variable were extrusion pressure (12-32 bar), finishing time (30-50 minute) and viscosity (50-250 pa-sec.) and performance variable were improvement in surface roughness ( $\Delta R_a$ ) and material removal. Other constant variables were 220 abrasive mesh size and 66% abrasive concentration.

### Response variable

Improvement in surface roughness ( $\Delta R_a$ ) =  $\mu\text{m}$

Material removal = Initial weight – Final weight (mg)

**Table 8.4 Parametric level setting as per  $L_9$  orthogonal array with experimental outcomes**

| Exp. No. | AFM parameters |    |     | Response variable                     |         |
|----------|----------------|----|-----|---------------------------------------|---------|
|          | EP             | FT | Vis | Improvement in SR<br>( $\Delta R_a$ ) | MR (mg) |
| 1        | 12             | 30 | L   | 0.30                                  | 42      |
| 2        | 12             | 40 | M   | 0.56                                  | 78      |
| 3        | 12             | 50 | H   | 0.86                                  | 128     |
| 4        | 22             | 30 | M   | 0.58                                  | 90      |
| 5        | 22             | 40 | H   | 0.66                                  | 88      |
| 6        | 22             | 50 | L   | 0.59                                  | 90      |
| 7        | 32             | 30 | H   | 0.88                                  | 132     |
| 8        | 32             | 40 | L   | 0.62                                  | 94      |
| 9        | 32             | 50 | M   | 0.92                                  | 136     |

Based on experimental results shown in Table 8.4, SN ratio graphs are calculated for the optimum levels of the AFM parameters. Figure 8.9 and Figure 8.10 show signal to noise ratio for improvement in surface roughness ( $\Delta R_a$ ) and material removal (MR).

For improvement in surface roughness ( $\Delta R_a$ ) the optimum level of parameters are 50 minutes finishing time, 32 bar extrusion pressure and H viscosity level as per Figure 8.9.

For material removal the optimum level of parameters are 50 minutes finishing time, 32 bar extrusion pressure and H viscosity level as per Figure 8.10.

After experimentation, results show the maximum improvement in surface roughness achieved and material removal was  $0.92 \mu\text{m}$  and  $136 \text{ mg}$  respectively.

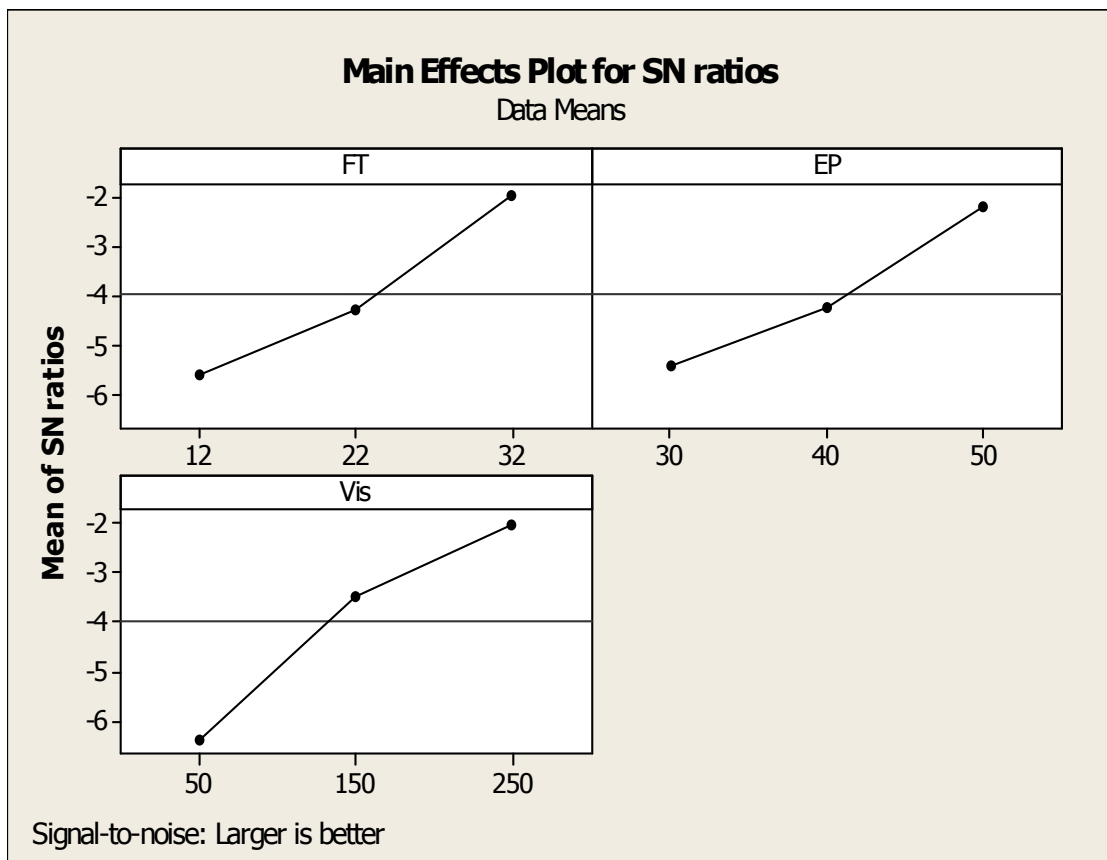


Figure 8.9 Signal to noise ratio for improvement in surface roughness ( $\Delta R_a$ )

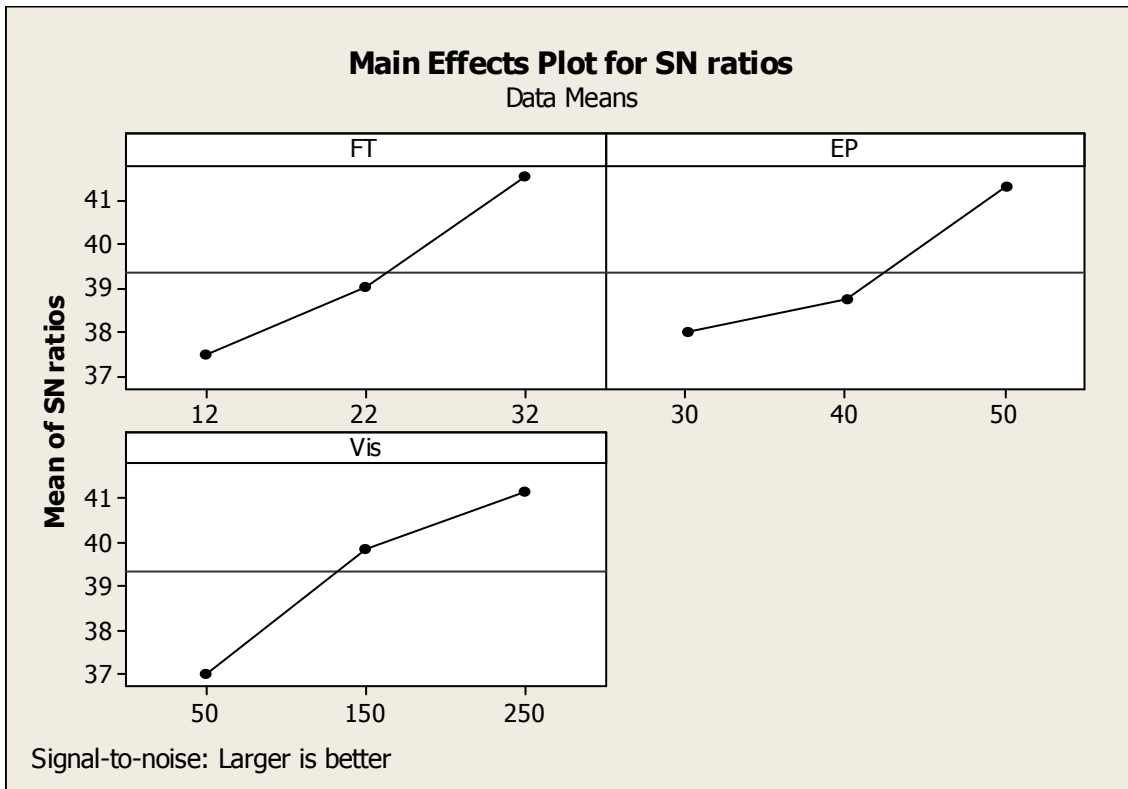


Figure 8.10 Signal to noise ratio for material removal (MR)

Table 8.5 Rank of AFM variable for material removal (MR)

| Level | FT     | EP    | Vis    |
|-------|--------|-------|--------|
| 1     | 82.67  | 88.00 | 75.33  |
| 2     | 89.33  | 86.67 | 101.33 |
| 3     | 120.67 | 118.0 | 116    |
| Rank  | 2      | 3     | 1      |

Table 8.6 Rank of AFM variable for improvement in surface roughness ( $\Delta Ra$ ).

| Level | FT     | EP     | Vis    |
|-------|--------|--------|--------|
| 1     | 0.5733 | 0.5867 | 0.5033 |
| 2     | 0.61   | .6133  | 0.6887 |
| 3     | 0.8067 | 0.7900 | 0.80   |
| Rank  | 2      | 3      | 1      |



Table 8.5 shows the rank of considered AFM process variables, which variables have most significant effect on material removal (MR). In this case viscosity of PAG media have most significant effect on material removal (MR). Table 8.6 shows the rank of considered AFM process variables, which variables have most significant effect on improvement in surface roughness ( $\Delta Ra$ ). In this case viscosity of PAG media have most significant effect on improvement in surface roughness ( $\Delta Ra$ ).

### 8.2.2.3 Images of nozzle surfaces

Figure 8.11 shows the images of nozzle surfaces before finishing at various locations. After finishing with AFM, at same location the images is recorded and improvement in surface quality can be clearly seen in below images.

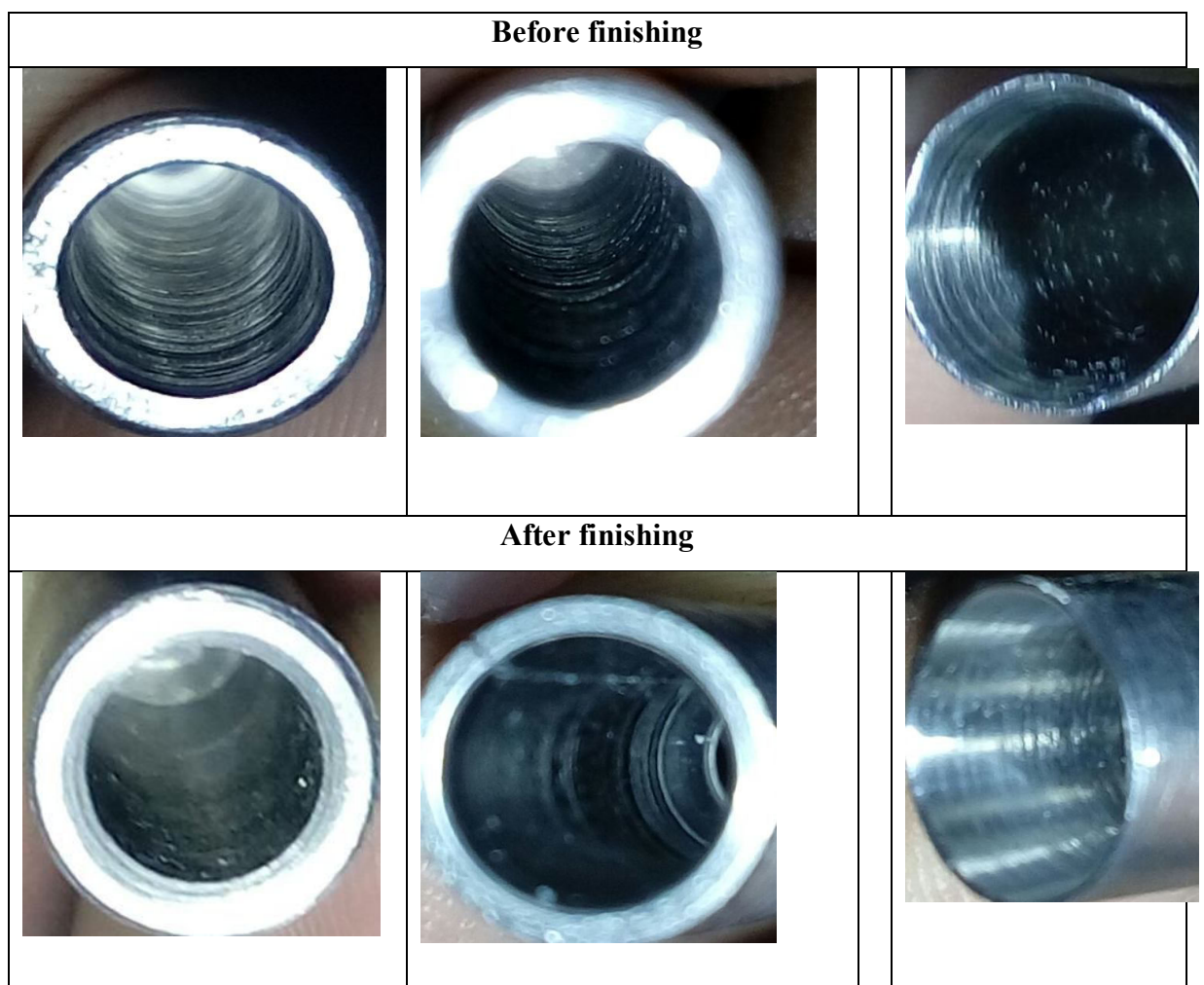


Figure 8.11 Images of nozzle surfaces



## References

---

- [1] M. C. Shaw, “Principles of abrasive processing,” *Clarendon Press*, 1996.
- [2] V. K. Jain, “Abrasive-Based Nano-Finishing Techniques: An Overview,” *Mach. Sci. Technol.*, vol. 12, no. 3, pp. 257–294, 2008.
- [3] L.J.Rhoades, “Abrasive flow machining : A review,” *Manuf. Eng.*, vol. 75–78, 1988.
- [4] L. J. Rhoades, T. A. Kohut, N. P. Nokovich, and D. W. Yanda, “Unidirectional abrasive flow machining,” US Patent 5,367,833, 1994.
- [5] R. Lawrence J., “Orbital and/or Reciprocal Machining with a Viscous Plastic Medium,” WO 90/05044, 1990.
- [6] V. K. Jain and S. G. Adsul, “Experimental investigations into abrasive flow machining (AFM),” *Int. J. Mach. Tools Manuf.*, vol. 40, no. 7, pp. 1003–1021, 2000.
- [7] L. Rhoades, “Abrasive flow machining: a case study,” *J. Mater. Process. Technol.*, vol. 28, no. 1–2, pp. 107–116, 1991.
- [8] R. E. Williams, “Stochastic Modeling and Analysis of Abrasive Flow Machining,” *Trans. ASME*, vol. 114, no. February, pp. 74–81, 1992.
- [9] V. K. Gorana, V. K. Jain, and G. K. Lal, “Experimental investigation into cutting forces and active grain density during abrasive flow machining,” *Int. J. Mach. Tools Manuf.*, vol. 44, no. 2–3, pp. 201–211, 2004.
- [10] T. R. Loveless, R. E. Williams, and K. P. Rajurkar, “A study of the effects of abrasive-flow finishing on various machined surfaces,” *J. Mater. Process.*

- Technol.*, vol. 47, no. 1–2, pp. 133–151, 1994.
- [11] L. Fang, J. Zhao, B. Li, and K. Sun, “Movement patterns of ellipsoidal particle in abrasive flow machining,” *J. Mater. Process. Technol.*, vol. 209, no. 20, pp. 6048–6056, 2009.
- [12] K. Gov, O. Eyercioglu, and M. V. Cakir, “Hardness effects on abrasive flow machining,” *Stroj. Vestnik/Journal Mech. Eng.*, vol. 59, no. 10, pp. 626–631, 2013.
- [13] J. Du Kim and K. D. Kim, “Deburring of burrs in spring collets by abrasive flow machining,” *Int. J. Adv. Manuf. Technol.*, vol. 24, no. 7–8, pp. 469–473, 2004.
- [14] K. Gov and O. Eyercioglu, “Effects of abrasive types on the surface integrity of abrasive-flow-machined surfaces,” *Proc. Inst. Mech. Eng. Part B J. Eng. Manuf.*, pp. 1–10, 2016.
- [15] V. K. Gorana, V. K. Jain, and G. K. Lal, “Forces prediction during material deformation in abrasive flow machining,” *Wear*, vol. 260, no. 1–2, pp. 128–139, 2006.
- [16] M. R. Sankar, J. Ramkumar, and V. K. Jain, “Experimental investigation and mechanism of material removal in nano finishing of MMCs using abrasive flow finishing (AFF) process,” *Wear*, vol. 266, no. 7–8, pp. 688–698, 2009.
- [17] L. Yin, E. Y. J. Vancoille, K. Ramesh, and H. Huang, “Surface characterization of 6H-SiC (0001) substrates in indentation and abrasive machining,” *Int. J. Mach. Tools Manuf.*, vol. 44, no. 6, pp. 607–615, 2004.
- [18] J. Kenda, F. Pusavec, G. Kermouche, and J. Kopac, “Surface integrity in abrasive flow machining of hardened tool steel AISI D2,” *Procedia Eng.*, vol. 19, pp. 172–

- 177, 2011.
- [19] A. C. Wang, K. C. Cheng, K. Y. Chen, and S. H. Chou, “Enhancing the surface precision for the helical passageways in abrasive flow ma - chining.”
- [20] Z. Dong, G. Ya, and J. Liu, “Study on machining mechanism of high viscoelastic abrasive flowing machining ( AFM ) for surface finishing,” no. 79, pp. 1–24, 2015.
- [21] R. K. Jain and V. K. Jain, “Specific energy and temperature determination in abrasive flow machining process,” *Int. J. Mach. Tools Manuf.*, vol. 41, no. 12, pp. 1689–1704, 2001.
- [22] V. K. Jain, S. C. Jayswal, and P. M. Dixit, “Modeling and Simulation of Surface Roughness in Magnetic Abrasive Finishing Using Non-Uniform Surface Profiles,” *Mater. Manuf. Process.*, vol. 22, no. 2, pp. 256–270, 2007.
- [23] V. K. Jain, R. Kumar, P. M. Dixit, and A. Sidpara, “Investigations into abrasive flow finishing of complex workpieces using FEM,” *Wear*, vol. 267, no. 1–4, pp. 71–80, 2009.
- [24] R. K. Jain, V. K. Jain, and P. M. Dixit, “Modeling of material removal and surface roughness in abrasive flow machining process,” *Int. J. Mach. Tools Manuf.*, vol. 39, no. 12, pp. 1903–1923, 1999.
- [25] R. K. Jain and V. K. Jain, “Stochastic simulation of active grain density in abrasive flow machining,” *J. Mater. Process. Technol.*, vol. 152, no. 1, pp. 17–22, 2004.
- [26] R. Kumar Jain and V. K. Jain, “Simulation of surface generated in abrasive flow machining process,” *Robot. Comput. Integr. Manuf.*, vol. 15, no. 5, pp. 403–412, 1999.

- [27] V. K. Gorana, V. K. Jain, and G. K. Lal, "Prediction of surface roughness during abrasive flow machining," *Int. J. Adv. Manuf. Technol.*, vol. 31, no. 3–4, pp. 258–267, 2006.
- [28] A. C. Wang, C. H. Liu, K. Z. Liang, and S. H. Pai, "Study of the rheological properties and the finishing behavior of abrasive gels in abrasive flow machining," *J. Mech. Sci. Technol.*, vol. 21, no. 10, pp. 1593–1598, 2007.
- [29] L. Fang, J. Zhao, K. Sun, D. Zheng, and D. Ma, "Temperature as sensitive monitor for efficiency of work in abrasive flow machining," *Wear*, vol. 266, no. 7–8, pp. 678–687, 2009.
- [30] A. C. Wang, L. Tsai, K. Z. Liang, C. H. Liu, and S. H. Weng, "Uniform surface polished method of complex holes in abrasive flow machining," *Trans. Nonferrous Met. Soc. China (English Ed.)*, vol. 19, no. SUPPL. 1, 2009.
- [31] S. Wan, Y. J. Ang, T. Sato, and G. C. Lim, "Process modeling and CFD simulation of two-way abrasive flow machining," *Int. J. Adv. Manuf. Technol.*, vol. 71, no. 5–8, pp. 1077–1086, 2014.
- [32] M. Howard and K. Cheng, "An industrially feasible approach to process optimisation of abrasive flow machining and its implementation perspectives," *Proc. Inst. Mech. Eng. Part B J. Eng. Manuf.*, vol. 227, no. 11, pp. 1748–1752, 2013.
- [33] E. Uhlmann, V. Mihotovic, and A. Coenen, "Modelling the abrasive flow machining process on advanced ceramic materials," *J. Mater. Process. Technol.*, vol. 209, no. 20, pp. 6062–6066, 2009.
- [34] R. K. Jain, V. K. Jain, and P. K. Kalra, "Modelling of abrasive flow machining

- process: A neural network approach,” *Wear*, vol. 231, no. 2, pp. 242–248, 1999.
- [35] H. S. Mali and A. Manna, “Simulation of surface generated during abrasive flow finishing of Al/SiCp-MMC using neural networks,” *Int. J. Adv. Manuf. Technol.*, vol. 61, no. 9–12, pp. 1263–1268, 2012.
- [36] K. L. Petri, R. E. Billo, and B. Bidanda, “A neural network process model for abrasive flow machining operations,” *J. Manuf. Syst.*, vol. 17, no. 1, pp. 52–64, 1998.
- [37] N. K. Jain, V. K. Jain, and K. Deb, “Optimization of process parameters of mechanical type advanced machining processes using genetic algorithms,” *Int. J. Mach. Tools Manuf.*, vol. 47, no. 6, pp. 900–919, 2007.
- [38] H. S. Mali and A. Manna, “Optimum selection of abrasive flow machining conditions during fine finishing of Al/15 wt% SiC-MMC using Taguchi method,” *Int. J. Adv. Manuf. Technol.*, vol. 50, no. 9–12, pp. 1013–1024, 2010.
- [39] R. K. Jain and V. K. Jain, “Optimum selection of machining conditions in abrasive flow machining using neural network,” *J. Mater. Process. Technol.*, vol. 108, pp. 62–67, 2000.
- [40] N. K. Jain, V. K. Jain, and S. Jha, “Parametric optimization of advanced fine-finishing processes,” *Int. J. Adv. Manuf. Technol.*, vol. 34, no. 11–12, pp. 1191–1213, 2007.
- [41] R. S. Walia, H. S. Shan, and P. Kumar, “Parametric Optimization of Centrifugal Force-Assisted Abrasive Flow Machining (CFAAFM) by the Taguchi Method,” *Mater. Manuf. Process.*, vol. 21, no. 4, pp. 375–382, 2006.

- [42] D. K. Singh, V. K. Jain, and V. Raghuram, "Parametric study of magnetic abrasive finishing process," *J. Mater. Process. Technol.*, vol. 149, no. 1–3, pp. 22–29, 2004.
- [43] P. Davies and A. Fletcher, "The Assessment of the Rheological Characteristics of Various Polyborosiloxane/Grit Mixtures as Utilized in the Abrasive Flow Machining Process," *Proc. Inst. Mech. Eng. Part C J. Mech. Eng. Sci.*, vol. 209, no. 6, pp. 409–418, 1995.
- [44] A. C. Wang and S. H. Weng, "Developing the polymer abrasive gels in AFM processs," *J. Mater. Process. Technol.*, vol. 192–193, pp. 486–490, 2007.
- [45] M. Ravi Sankar, V. K. Jain, J. Ramkumar, and Y. M. Joshi, "Rheological characterization of styrene-butadiene based medium and its finishing performance using rotational abrasive flow finishing process," *Int. J. Mach. Tools Manuf.*, vol. 51, no. 12, pp. 947–957, 2011.
- [46] K. K. Kar, N. L. Ravikumar, P. B. Tailor, J. Ramkumar, and D. Sathiyamoorthy, "Performance evaluation and rheological characterization of newly developed butyl rubber based media for abrasive flow machining process," *J. Mater. Process. Technol.*, vol. 209, no. 4, pp. 2212–2221, 2009.
- [47] K. K. Kar, N. L. Ravikumar, P. B. Tailor, J. Ramkumar, and D. Sathiyamoorthy, "Preferential Media for Abrasive Flow Machining," *J. Manuf. Sci. Eng.*, vol. 131, no. 1, p. 11009, 2009.
- [48] L. Dabrowski, M. Marciniak, and T. Szewczyk, "Analysis of Abrasive Flow Machining with an Electrochemical Process Aid," *Proc. Inst. Mech. Eng. Part B J. Eng. Manuf.*, vol. 220, no. 3, pp. 397–403, 2006.
- [49] S. Rajesha, G. Venkatesh, a. K. Sharma, and P. Kumar, "Performance study of a



- natural polymer based media for abrasive flow machining,” *Indian J. Eng. Mater. Sci.*, vol. 17, no. 6, pp. 407–413, 2010.
- [50] JaiKishan Sambharia and Harlal Singh Mali, “Characterisation and performance evaluation of developed alternative polymer abrasive gels for abrasive flow finishing process,” *Int. J. Precis. Technol.*, vol. 5, pp. 185–200, 2015.
- [51] V. K. Jain, C. Ranganatha, and K. Muralidhar, “Rheological properties of medium for AFM process evaluation of rheological properties of medium for AFM process,” *Mach. Sci. Technol. An Int. J.*, vol. 5, no. 2, pp. 151–170, 2001.
- [52] H. J. Tzeng, B. H. Yan, R. T. Hsu, and Y. C. Lin, “Self-modulating abrasive medium and its application to abrasive flow machining for finishing micro channel surfaces,” *Int. J. Adv. Manuf. Technol.*, vol. 32, no. 11–12, pp. 1163–1169, 2007.
- [53] H. S. Mali and Jaikishan, “Developing alternative polymer abrasive gels for abrasive flow finishing process,” in *5 th International & 26 th All India Manufacturing Technology, Design and Research Conference (AIMTDR 2014)*, 2014, pp. 1–8.
- [54] A. Sidpara, M. Das, and V. K. Jain, “Rheological Characterization of Magnetorheological Finishing Fluid,” *Mater. Manuf. Process.*, vol. 24, no. 12, pp. 1467–1478, 2009.
- [55] K. Saraswathamma, S. Jha, and P. V. Rao, “Rheological Characterization of MR Polishing Fluid Used for Silicon Polishing in BEMRF Process,” *Mater. Manuf. Process.*, vol. 30, no. 5, pp. 661–668, 2015.
- [56] M. Ravi Sankar, V. K. Jain, J. Ramkumar, and Y. M. Joshi, “Rheological characterization of styrene-butadiene based medium and its finishing performance

- using rotational abrasive flow finishing process,” *Int. J. Mach. Tools Manuf.*, vol. 51, no. 12, pp. 947–957, 2011.
- [57] G. Zhang, Y. Zhao, D. Zhao, D. Zuo, and F. Yin, “New iron-based SiC spherical composite magnetic abrasive for magnetic abrasive finishing,” *Chinese J. Mech. Eng.*, vol. 26, no. 2, pp. 377–383, 2013.
- [58] D. R. Unune and H. S. Mali, “Current status and applications of hybrid micro-machining processes: A review,” *Proc. Inst. Mech. Eng. Part B J. Eng. Manuf.*, no. August, 2014.
- [59] M. R. Sankar, V. K. Jain, and J. Ramkumar, “Experimental investigations into rotating workpiece abrasive flow finishing,” *Wear*, vol. 267, no. 1–4, pp. 43–51, 2009.
- [60] S. Jha and V. K. Jain, “Nanofinishing of silicon nitride workpieces using magnetorheological abrasive flow finishing,” *Int. J. Nanomanuf.*, vol. 1, no. 1, p. 17, 2006.
- [61] S. Singh and H. S. Shan, “Development of magneto abrasive flow machining process,” *Int. J. Mach. Tools Manuf.*, vol. 42, no. 8, pp. 953–959, 2002.
- [62] R. S. Walia, H. S. Shan, and P. Kumar, “Determining dynamically active abrasive particles in the media used in centrifugal force assisted abrasive flow machining process,” *Int. J. Adv. Manuf. Technol.*, vol. 38, no. 11–12, pp. 1157–1164, 2008.
- [63] M. R. Sankar, S. Mondal, J. Ramkumar, and V. K. Jain, “Experimental investigations and modeling of drill bit-guided abrasive flow finishing (DBG-AFF) process,” *Int. J. Adv. Manuf. Technol.*, vol. 42, no. 7–8, pp. 678–688, 2009.

- [64] S. Singh, H. S. Shan, and P. Kumar, "Wear behavior of materials in magnetically assisted abrasive flow machining," *J. Mater. Process. Technol.*, vol. 128, no. 1–3, pp. 155–161, 2002.
- [65] S. Jha and V. K. Jain, "Design and development of the magnetorheological abrasive flow finishing (MRAFF) process," *Int. J. Mach. Tools Manuf.*, vol. 44, no. 10, pp. 1019–1029, 2004.
- [66] S. Jha and V. K. Jain, "Modeling and simulation of surface roughness in magnetorheological abrasive flow finishing (MRAFF) process," *Wear*, vol. 261, no. 7–8, pp. 856–866, 2006.
- [67] S. Jha, V. K. Jain, and R. Komanduri, "Effect of extrusion pressure and number of finishing cycles on surface roughness in magnetorheological abrasive flow finishing (MRAFF) process," *Int. J. Adv. Manuf. Technol.*, vol. 33, no. 7–8, pp. 725–729, 2007.
- [68] R. S. Walia, H. S. Shan, and P. Kumar, "Abrasive Flow Machining With Additional Centrifugal Force Applied To the Media," *Mach. Sci. Technol.*, vol. 10, no. 3, pp. 341–354, 2006.
- [69] R. S. Walia, H. S. Shan, and P. Kumar, "Finite element analysis of media used in the centrifugal force assisted abrasive flow machining process," *Proc IMechE Part B J Eng. Manuf.*, vol. 220, pp. 1775–1785, 2006.
- [70] R. S. Walia, H. S. Shan, and P. Kumar, "Morphology and integrity of surfaces finished by centrifugal force assisted abrasive flow machining," *Int. J. Adv. Manuf. Technol.*, vol. 39, pp. 1301–1308, 2007.
- [71] R. S. Walia, H. S. Shan, and P. Kumar, "Multiresponse optimization of CFAAFM

- process through Taguchi method and utility concept,” *Mater. Manuf. Process.*, vol. 21, pp. 907–914, 2006.
- [72] M. K. Reddy, A. K. Sharma, and P. Kumar, “Some aspects of centrifugal force assisted abrasive flow machining of 2014 Al alloy,” *Proc. Inst. Mech. Eng. Part B J. Eng. Manuf.*, vol. 222, pp. 773–783, 2010.
- [73] M. Ravi Sankar, V. K. Jain, and J. Ramkumar, “Rotational abrasive flow finishing (R-AFF) process and its effects on finished surface topography,” *Int. J. Mach. Tools Manuf.*, vol. 50, no. 7, pp. 637–650, 2010.
- [74] A. R. Jones and J. B. Hull, “Ultrasonic flow polishing,” *Ultrasonics*, vol. 36, no. 1–5, pp. 97–101, 1998.
- [75] R. S. Mulik and P. M. Pandey, “Ultrasonic assisted magnetic abrasive finishing of hardened AISI 52100 steel using unbonded SiC abrasives,” *Int. J. Refract. Met. Hard Mater.*, vol. 29, no. 1, pp. 68–77, 2010.
- [76] R. S. Mulik and P. M. Pandey, “Mechanism of Surface Finishing in Ultrasonic-Assisted Magnetic Abrasive Finishing Process,” *Mater. Manuf. Process.*, vol. 25, no. 12, pp. 1418–1427, 2010.
- [77] R. S. Mulik and P. M. Pandey, “Experimental Investigations and Modeling of Finishing Force and Torque in Ultrasonic Assisted Magnetic Abrasive Finishing,” *J. Manuf. Sci. Eng.*, vol. 134, no. 5, p. 51008, 2012.
- [78] G. Venkatesh, A. K. Sharma, and P. Kumar, “On ultrasonic assisted abrasive flow finishing of bevel gears,” *Int. J. Mach. Tools Manuf.*, vol. 89, pp. 29–38, 2015.
- [79] P. Kala and P. M. Pandey, “Comparison of finishing characteristics of two

- paramagnetic materials using double disc magnetic abrasive finishing,” *J. Manuf. Process.*, vol. 17, pp. 63–70, 2015.
- [80] L. Dabrowski, M. Marciniak, and A. Zygmunt, “Advancement of Abrasive Flow Machining Using an Anodic Solution,” vol. 445, pp. 439–445, 2006.
- [81] B. S. Brar, R. S. Walia, and V. P. Singh, “Electrochemical-aided abrasive flow machining (ECA&lt;sup&gt;2&lt;/sup&gt;FM) process: a hybrid machining process,” *Int. J. Adv. Manuf. Technol.*, vol. 79, no. 1–4, pp. 329–342, 2015.
- [82] B. S. Brar, R. S. Walia, and V. P. Singh, “Regression Model for Electro-Chemical Aided Abrasive Flow Machining ( Eca 2 Fm ) Process,” no. Aimtdr, pp. 1–8, 2014.
- [83] R. E. Williams, D. F. Walczyk, and H. T. Dang, “Using abrasive flow machining to seal and finish conformal channels in laminated tooling,” *Rapid Prototyp. J.*, vol. 13, no. 2, pp. 64–75, 2007.
- [84] N. L. Ravikumar, K. K. Kar, D. Sathiyamoorthy, A. Kumar, and R. Devi, “Surface Finishing of Carbon-Carbon Composites Using Abrasive Flow Machining,” *Fullerenes, Nanotub. Carbon Nanostructures*, vol. 20, no. 2, pp. 170–182, 2012.
- [85] M. Sushil, K. Vinod, and K. Harmesh, “Experimental Investigation and Optimization of Process Parameters of Al/Sic MMCs Finished by Abrasive Flow Machining,” *Mater. Manuf. Process.*, no. August, p. 150202232731002, 2015.
- [86] V. K. Jain and a. M. Sidpara, “Nanofinishing of freeform surfaces of prosthetic knee joint implant,” *Proc. Inst. Mech. Eng. Part B J. Eng. Manuf.*, vol. 226, no. 11, pp. 1833–1846, 2012.
- [87] K. B. Judal and Y. Yadava, “Experimental Investigations into Electrochemical

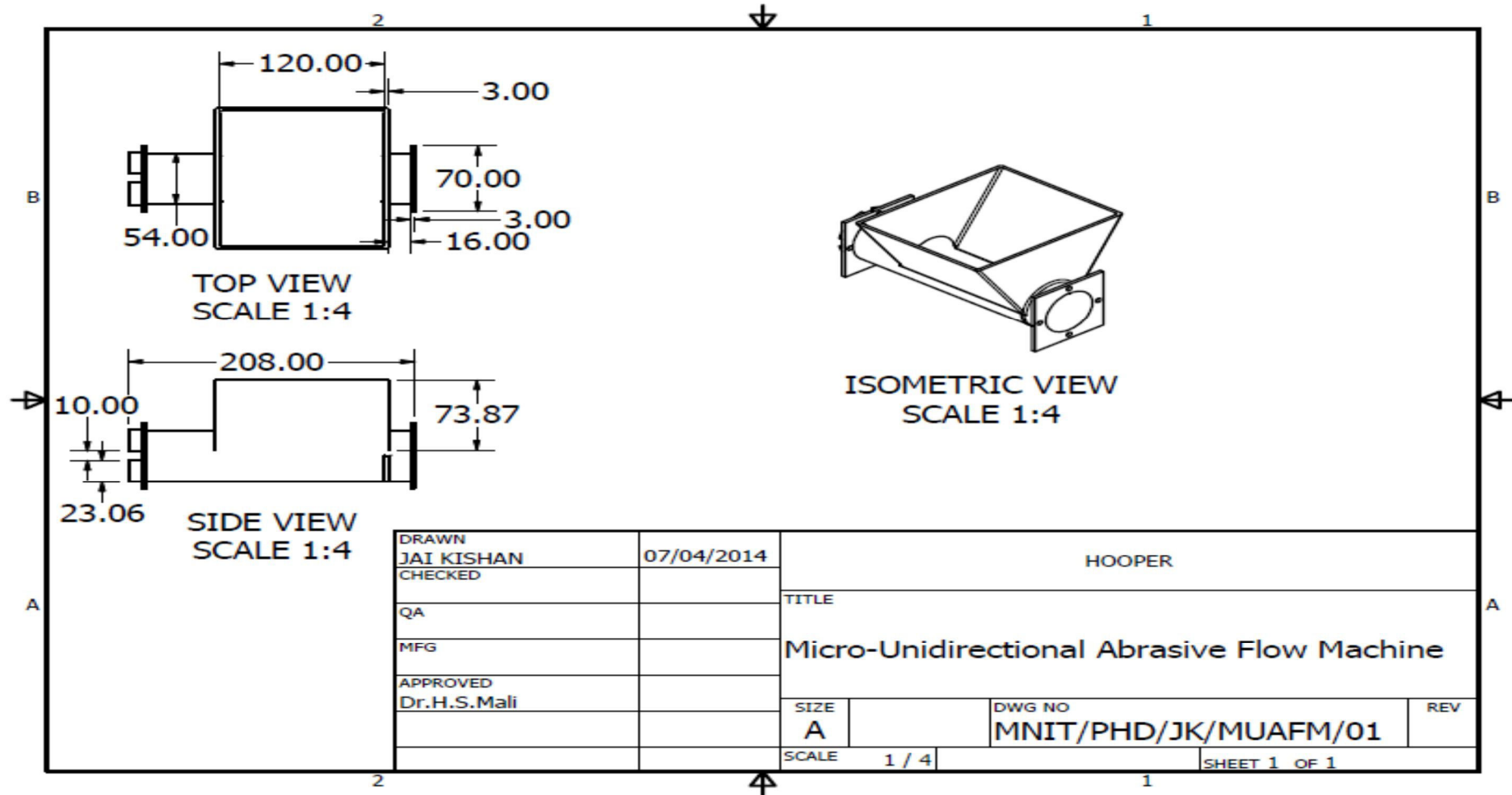
- Magnetic Abrasive Machining of Cylindrical Shaped Nonmagnetic Stainless Steel Workpiece,” *Mater. Manuf. Process.*, vol. 28, no. 10, pp. 1095–1101, 2013.
- [88] J. Kenda, J. Duhovnik, J. Tavčar, and J. Kopač, “Abrasive flow machining applied to plastic gear matrix polishing,” *Int. J. Adv. Manuf. Technol.*, vol. 71, no. 1–4, pp. 141–151, 2014.
- [89] M. Howard and K. Cheng, “An integrated systematic investigation of the process variables on surface generation in abrasive flow machining of titanium alloy 6Al4V,” *Proc. Inst. Mech. Eng. Part B J. Eng. Manuf.*, vol. 228, no. 11, pp. 1419–1431, 2014.
- [90] Douglas C. Montgomery, *Design and Analysis of Experiments, 5th Edition*, 5th ed. Arizona state university: John Wiley & Sons, 2001.
- [91] A. Rao, *Rheology of Fluid, Semisolid, and Solid Foods*. Springer US, 2014.
- [92] H. S. Mali and A. Manna, “An experimental investigation during finishing of particulate reinforced Al / 10 wt % SiC p -MMC on developed AFF setup,” *Int. J. Manuf. Manag.*, vol. 28, no. 1/2/3, pp. 114–131, 2014.
- [93] L. J. Rhoades, “Abrasive Flow Machining and Its Use,” in *Proceeding of Non Traditional Machining Conference*, 1985, pp. 111–120.
- [94] H. S. Mali and a Manna, “Current status and application of abrasive flow finishing processes: a review,” *Proc. Inst. Mech. Eng. Part B J. Eng. Manuf.*, vol. 223, no. 7, pp. 809–820, 2009.
- [95] A. Fletcher and F. A., “Polishing and honing processes : an investigation of the thermal properties of mixtures of polyborosiloxane and silicon carbide abrasive,”

- Proc. Inst. Mech. Eng.*, vol. 210, pp. 255–266, 1996.
- [96] H. S. Mali, “A base material and a system for finishing work-piece(s),” 2369/Del/2010, 2010.
- [97] S. Jha and V. K. Jain, “8 Nanofinishing Techniques,” no. Taniguchi 1983, 2000.
- [98] H. El-Hofy, “Fundamental of machining processes,” T. and Francis, Ed. Newyork, 2007.
- [99] V. K. Jain, *Advanced Machining Processes*. Delhi: Allied Publishers Pvt. Ltd, 2002.
- [100] G. Vetter and R. Kozmiensky, “Pulsation and NPSHA in rotary positive displacement pumps,” *World Pumps*, vol. 1999, no. 389, pp. 37–42, 1999.
- [101] G. Gode, “Positive displacement pump drive selection and operation,” *World Pumps*, vol. 2000, no. 411, pp. 36–37, 2000.
- [102] A. Y.P., M. E.V., and G. Y.V., “The design of experimentd to find optimal conditions,” in *Mir Publishers*, 1975.
- [103] R. H. Nilesn, “Proc. Joint Conf. on Neural Networks,” vol. 1, pp. 593–617, 1989.
- [104] S. Youssefi, Z. Emam-Djomeh, and S. M. Mousavi, “Comparison of Artificial Neural Network (ANN) and Response Surface Methodology (RSM) in the Prediction of Quality Parameters of Spray-Dried Pomegranate Juice,” *Dry. Technol.*, vol. 27, pp. 910–917, 2009.
- [105] V. Aggarwal, S. S. Khangura, and R. K. Garg, “Parametric modeling and optimization for wire electrical discharge machining of Inconel 718 using response surface methodology,” *Int. J. Adv. Manuf. Technol.*, vol. 79, pp. 31–47, 2015.

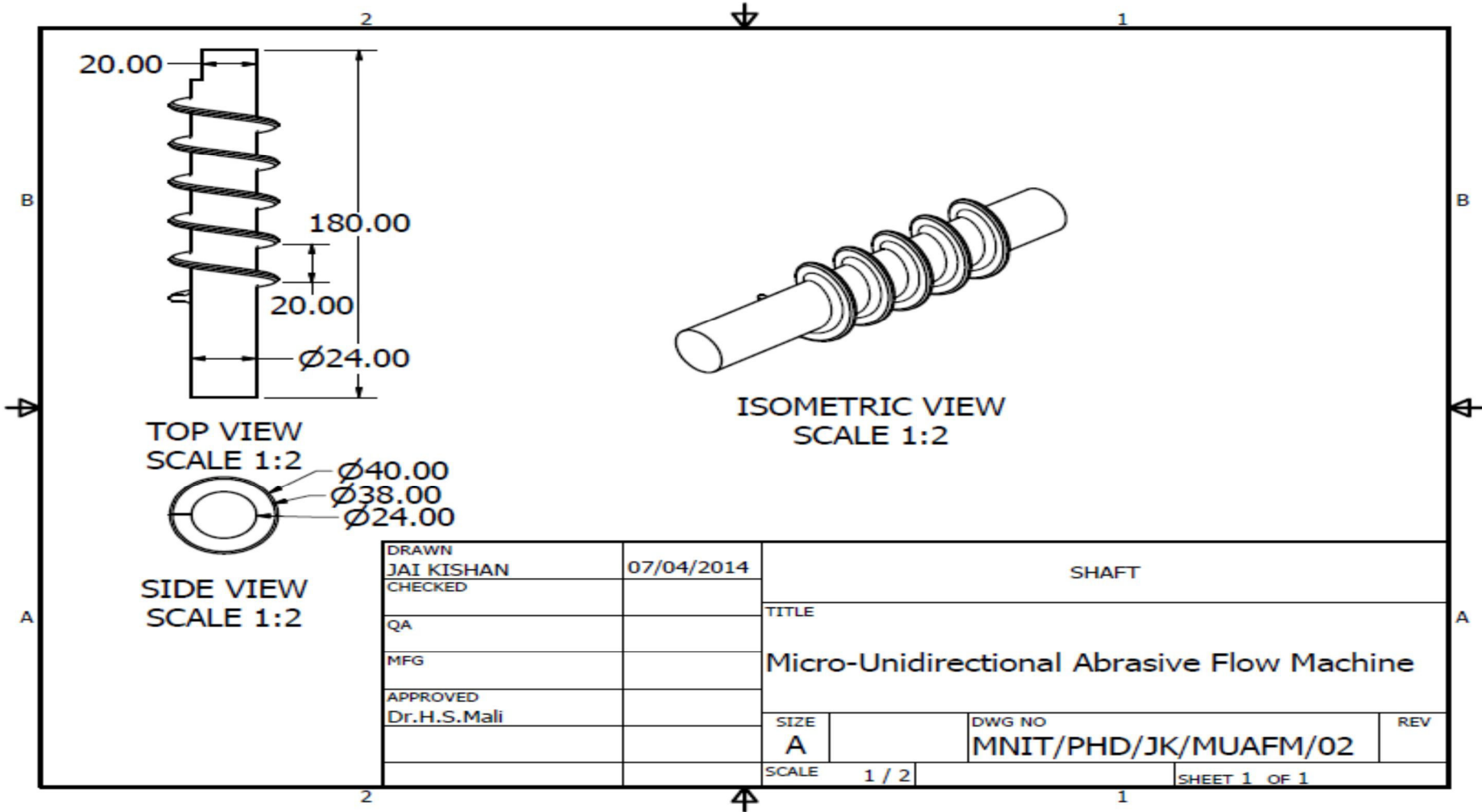
- [106] S. S. Mahapatra and A. Patnaik, "Optimization of wire electrical discharge machining (WEDM) process parameters using Taguchi method," *Int. J. Adv. Manuf. Technol.*, vol. 34, no. 9–10, pp. 911–925, 2007.
- [107] D. C. Montgomery, "Design and Analysis of Experiments," 8 ed., New York: John Wiley & Sons, Inc., 2013.
- [108] A. Kumar, V. Kumar, and J. Kumar, "Multi-response optimization of process parameters based on response surface methodology for pure titanium using WEDM process," *Int. J. Adv. Manuf. Technol.*, vol. 68, pp. 2645–2668, 2013.
- [109] T. A. El-Taweel and S. A. Gouda, "'Performance analysis of wire electrochemical turning process—RSM approach," *Int. J. Adv. Manuf. Technol.*, vol. 53, pp. 181–190, 2010.
- [110] G. Rajeshwar, J. Kozak, and K. Rajurkar, "Modeling and computer simulation of media flow in abrasive flow machining process," in *Proceedings of the International Mechanical Engineering Congress and Exposition*, 1994.
- [111] M. Shaw, "A new Theory of Grinding," in *Proc. of the Institution's Conference on Production Society in Industry*, 1971, pp. 73–78.



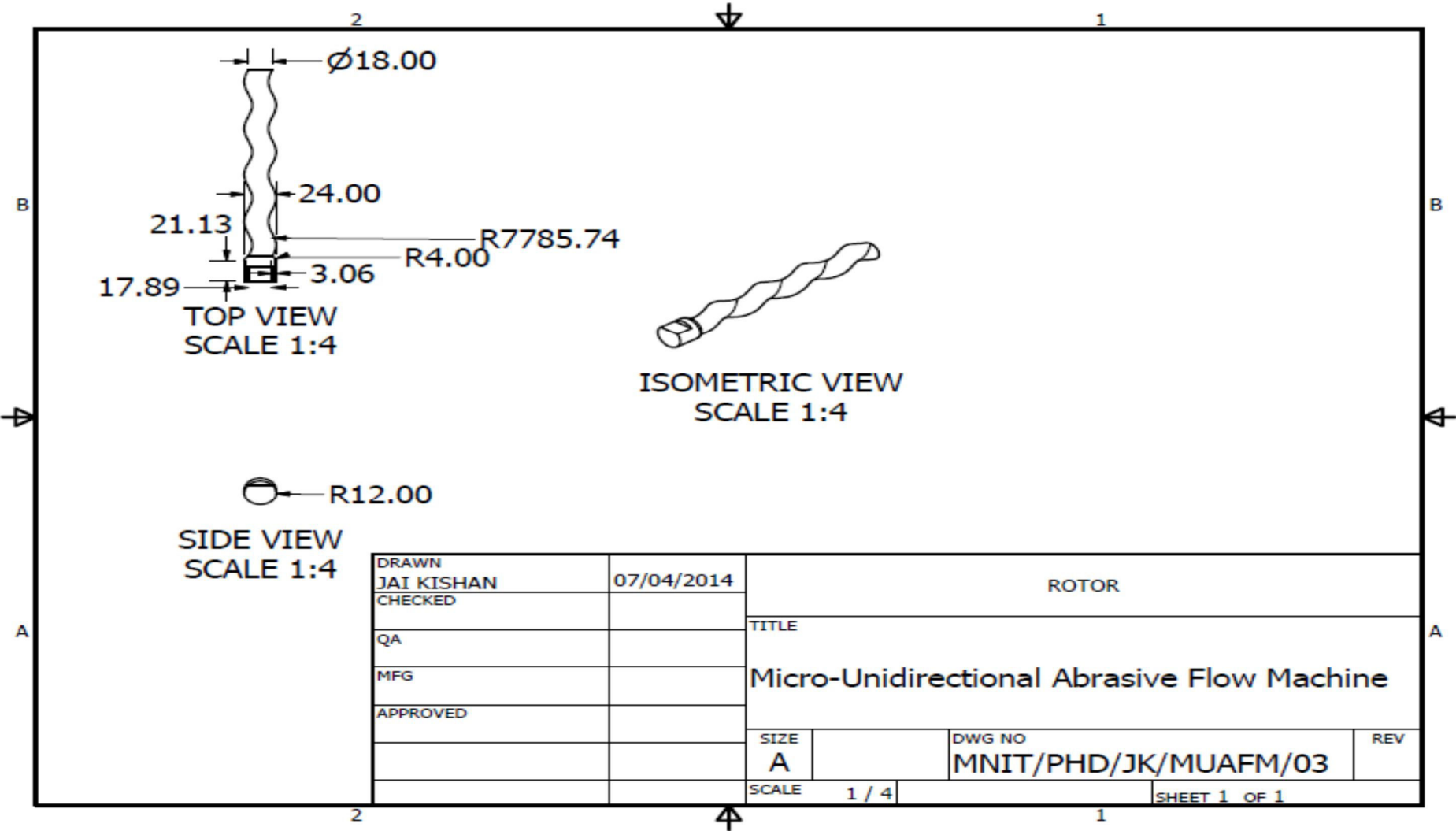
## Appendix-A (1) Extruding element



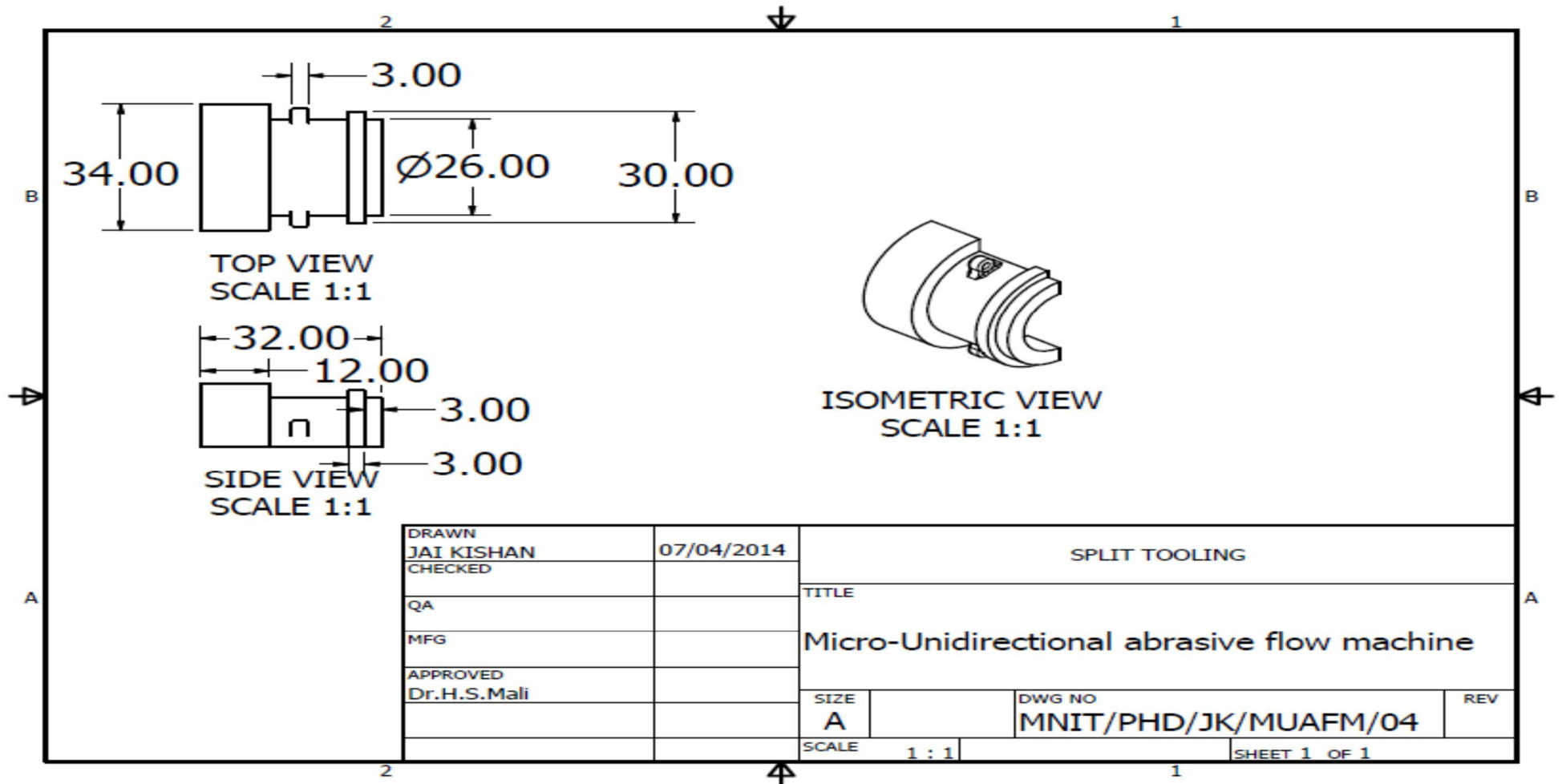
Appendix-A (2) Screw feeder



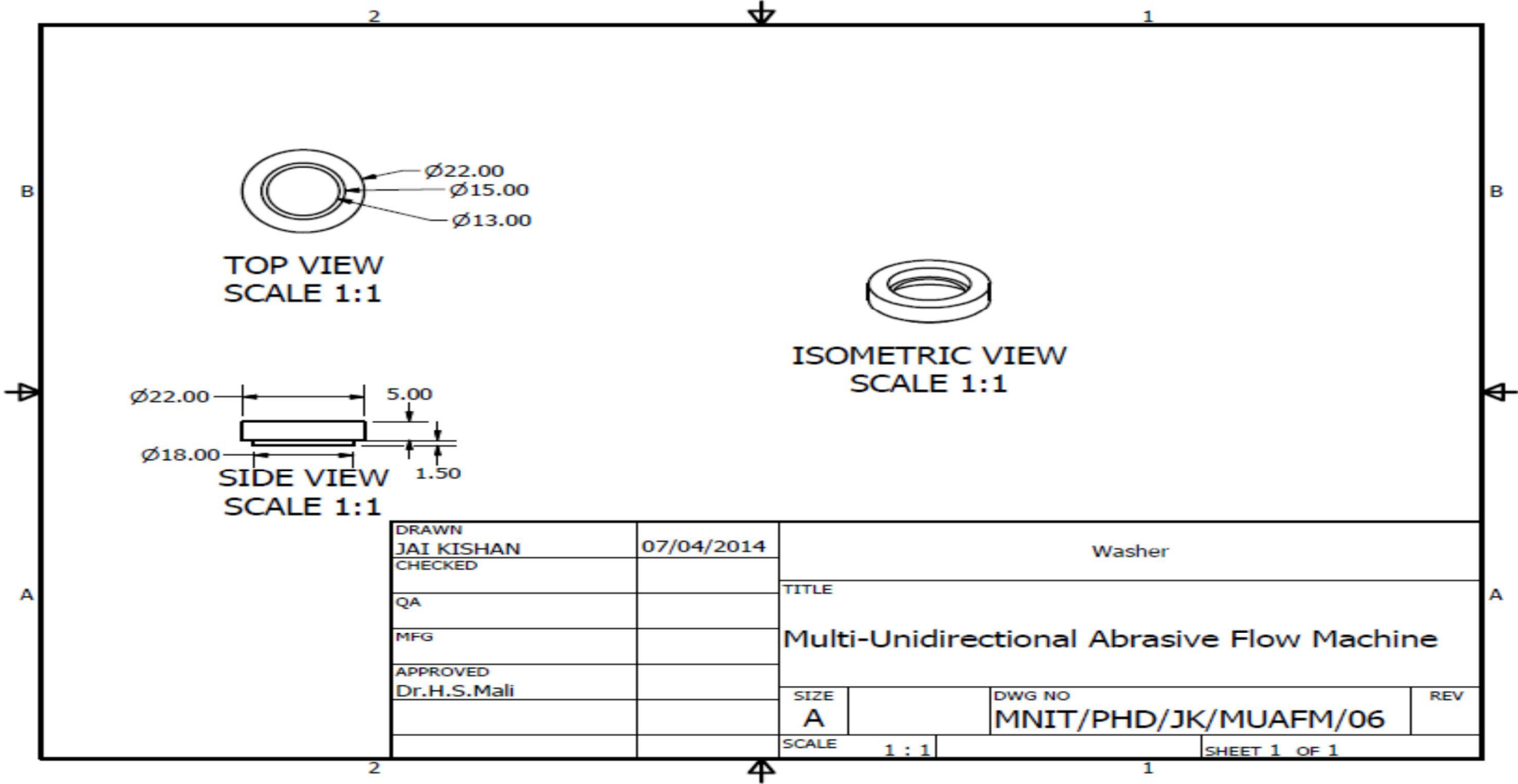
Appendix-A (3) Rotor



## Appendix-A (4) Split tooling

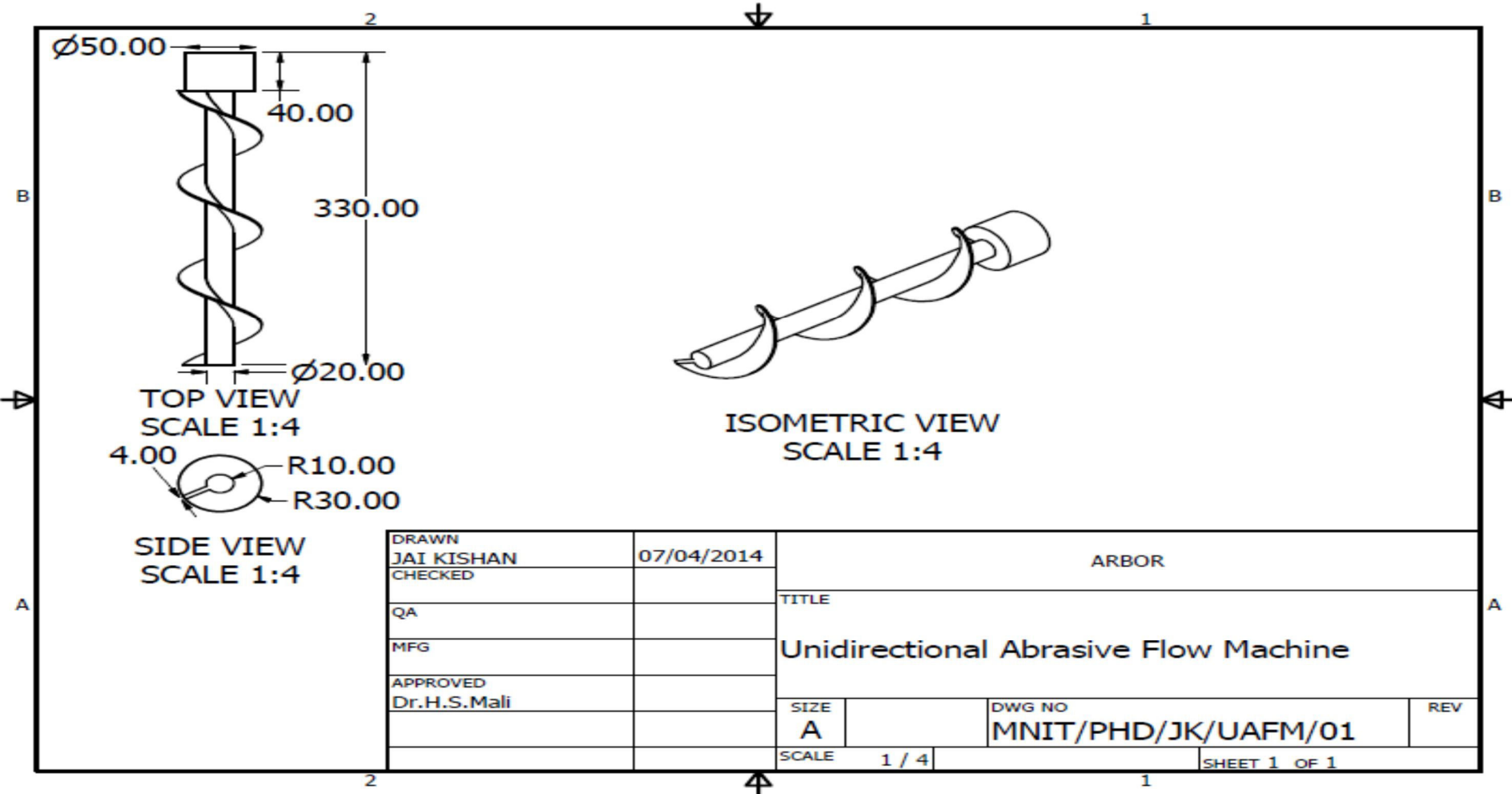


Appendix-A (5) Tooling washer

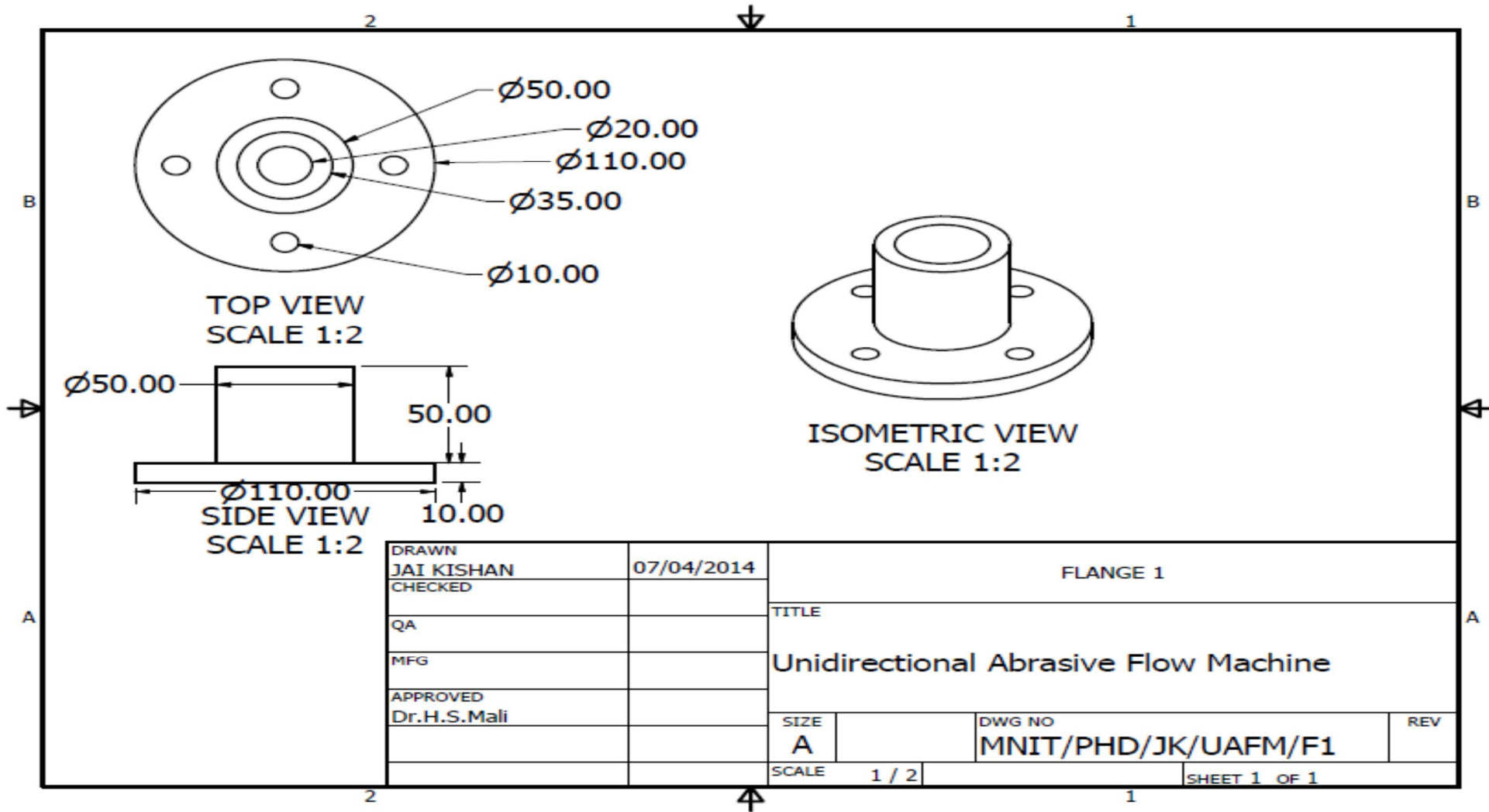




Appendix-B (1) UAFM-Screw feeder

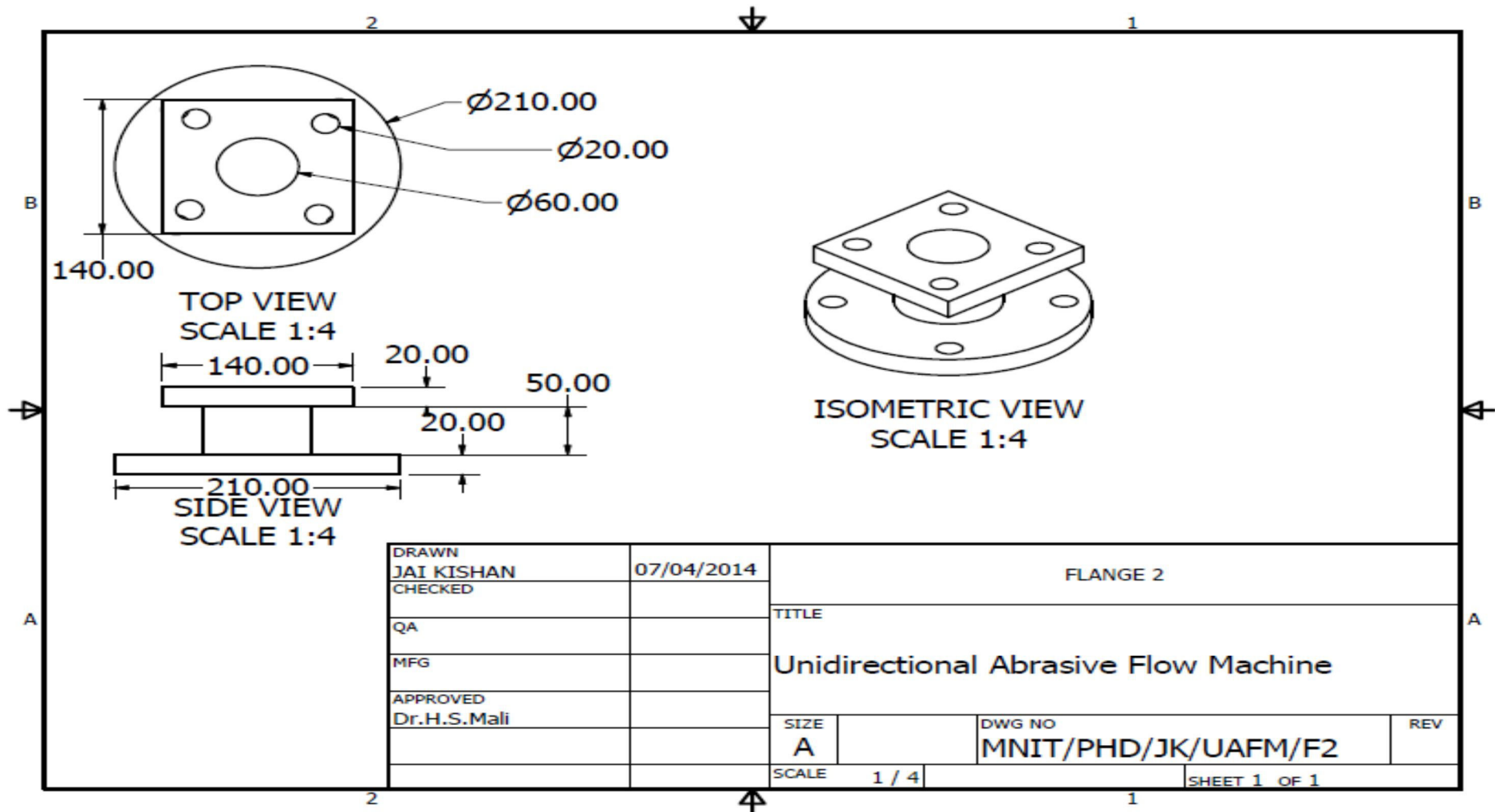


Appendix-B (2) Flange -Tooling

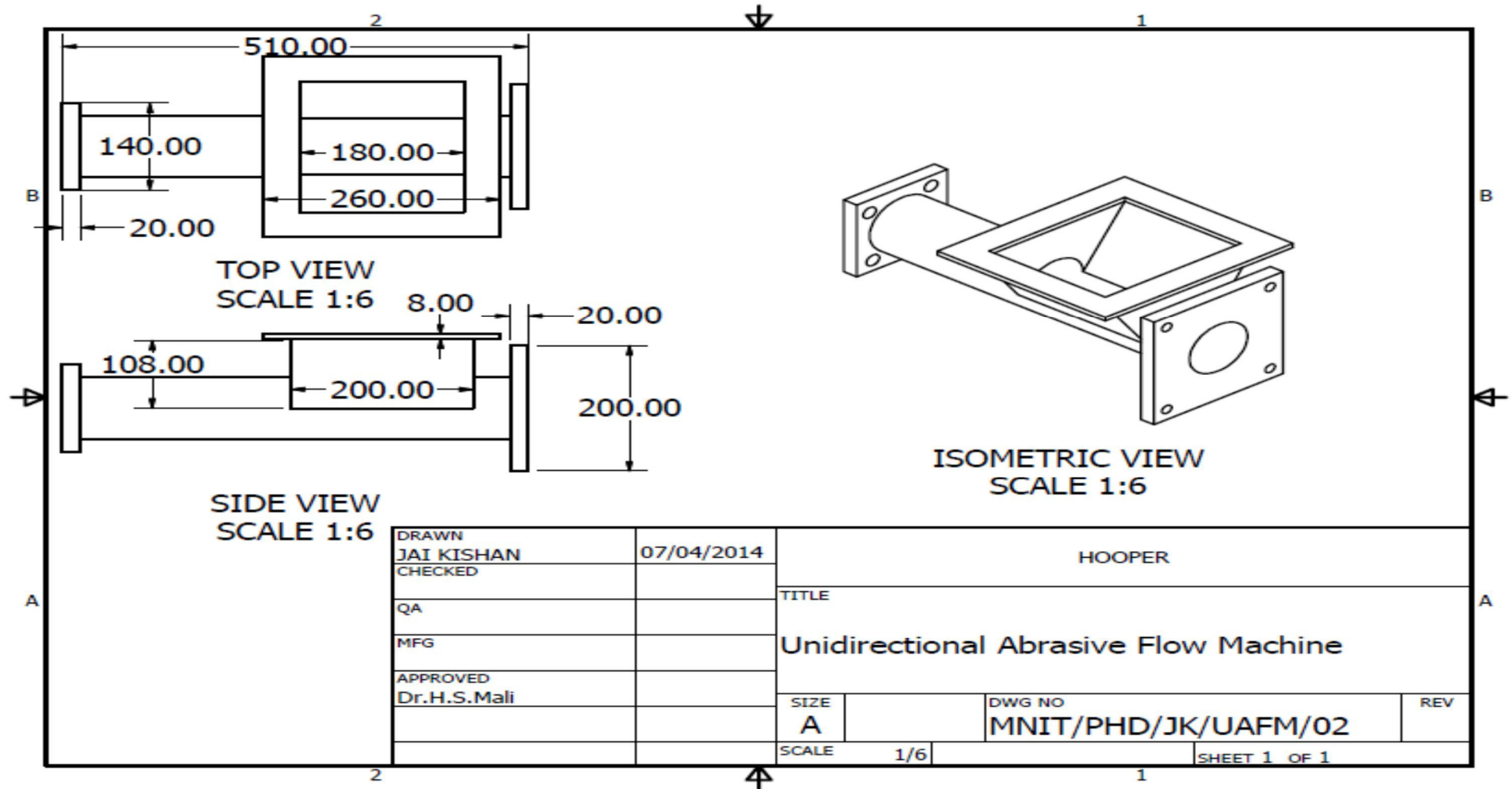




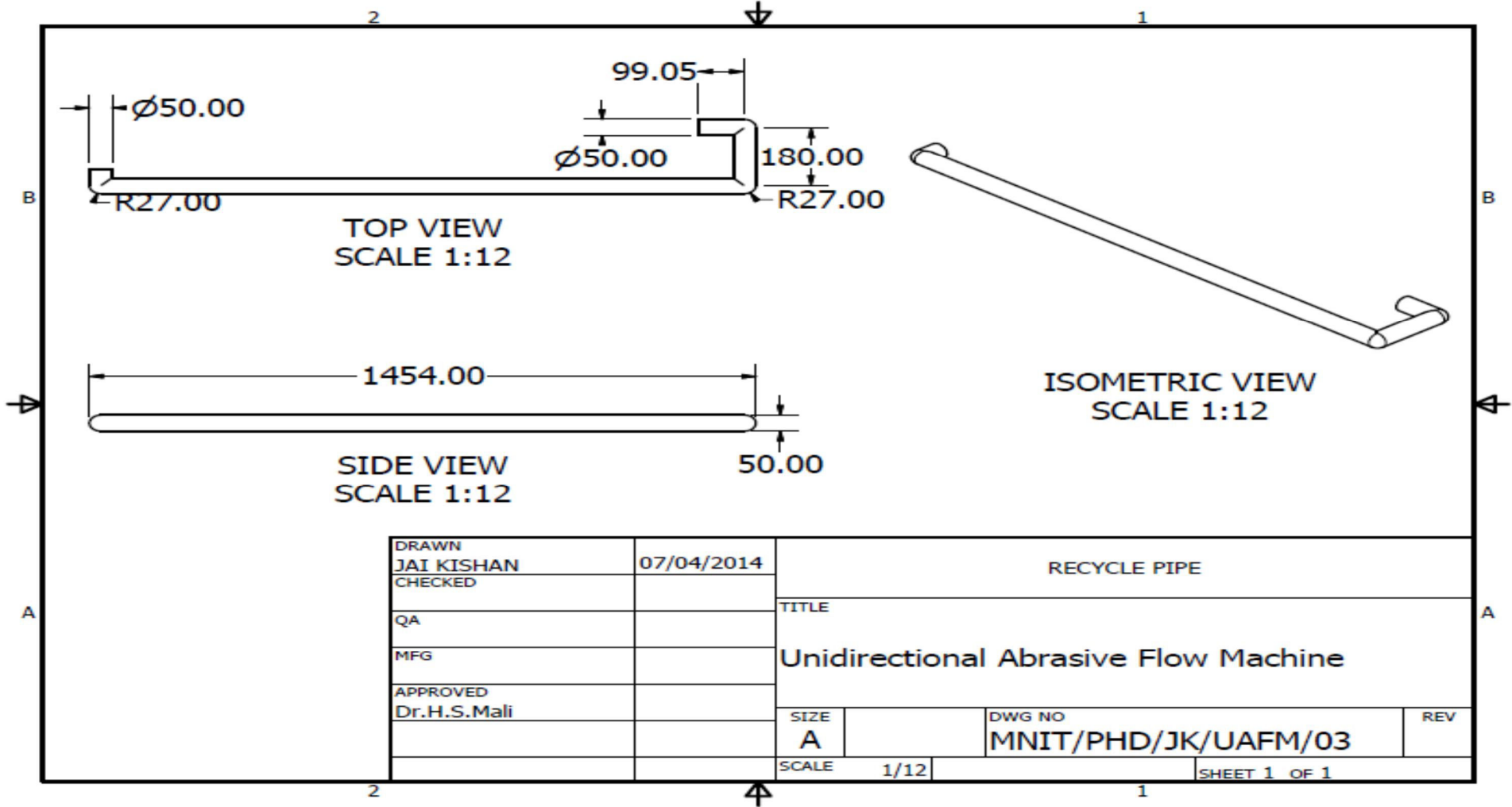
## Appendix-B (3) Flange-Reducer



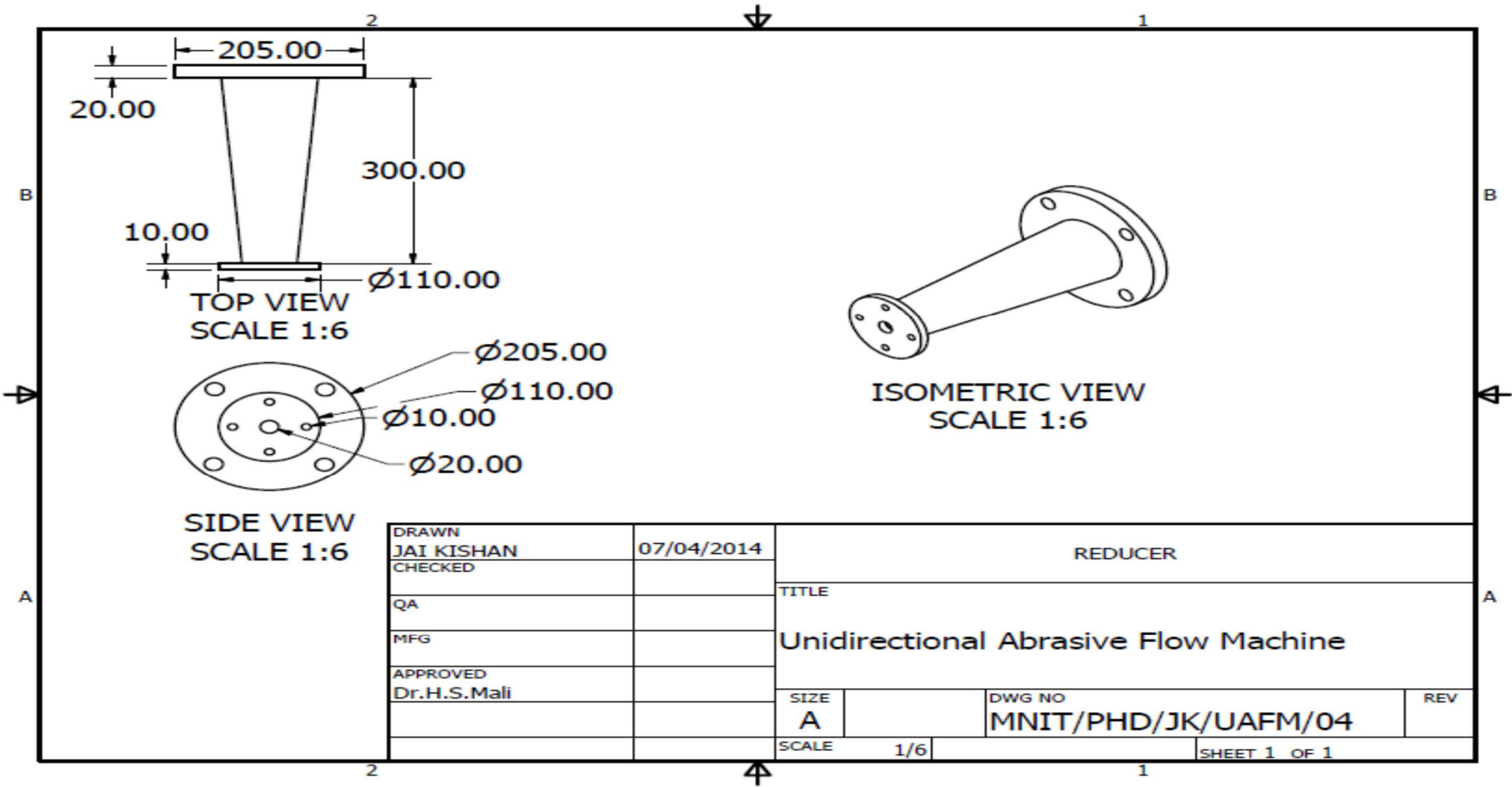
## Appendix-B (4) Extruding element



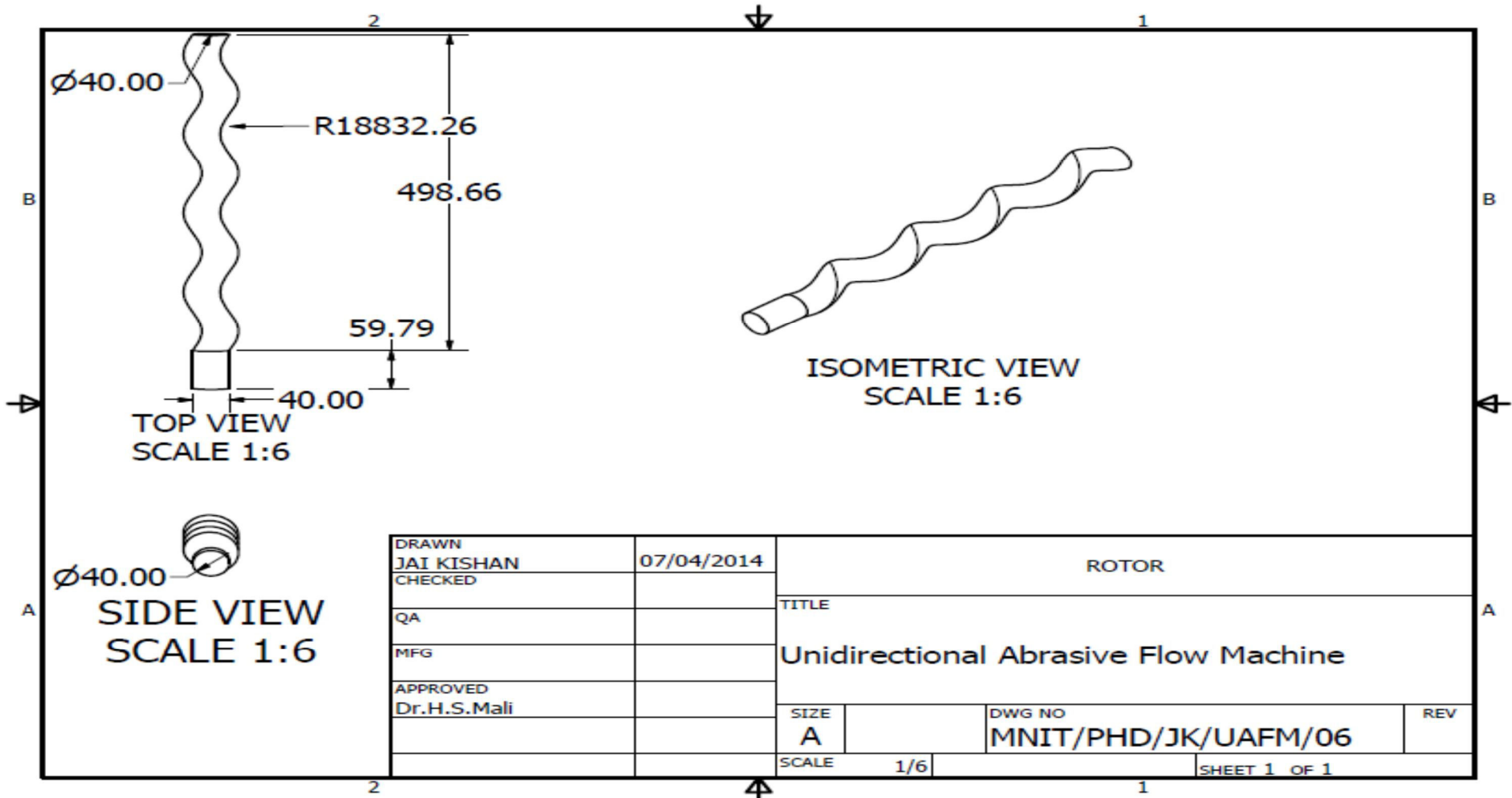
Appendix-B (5) Recycling pipe



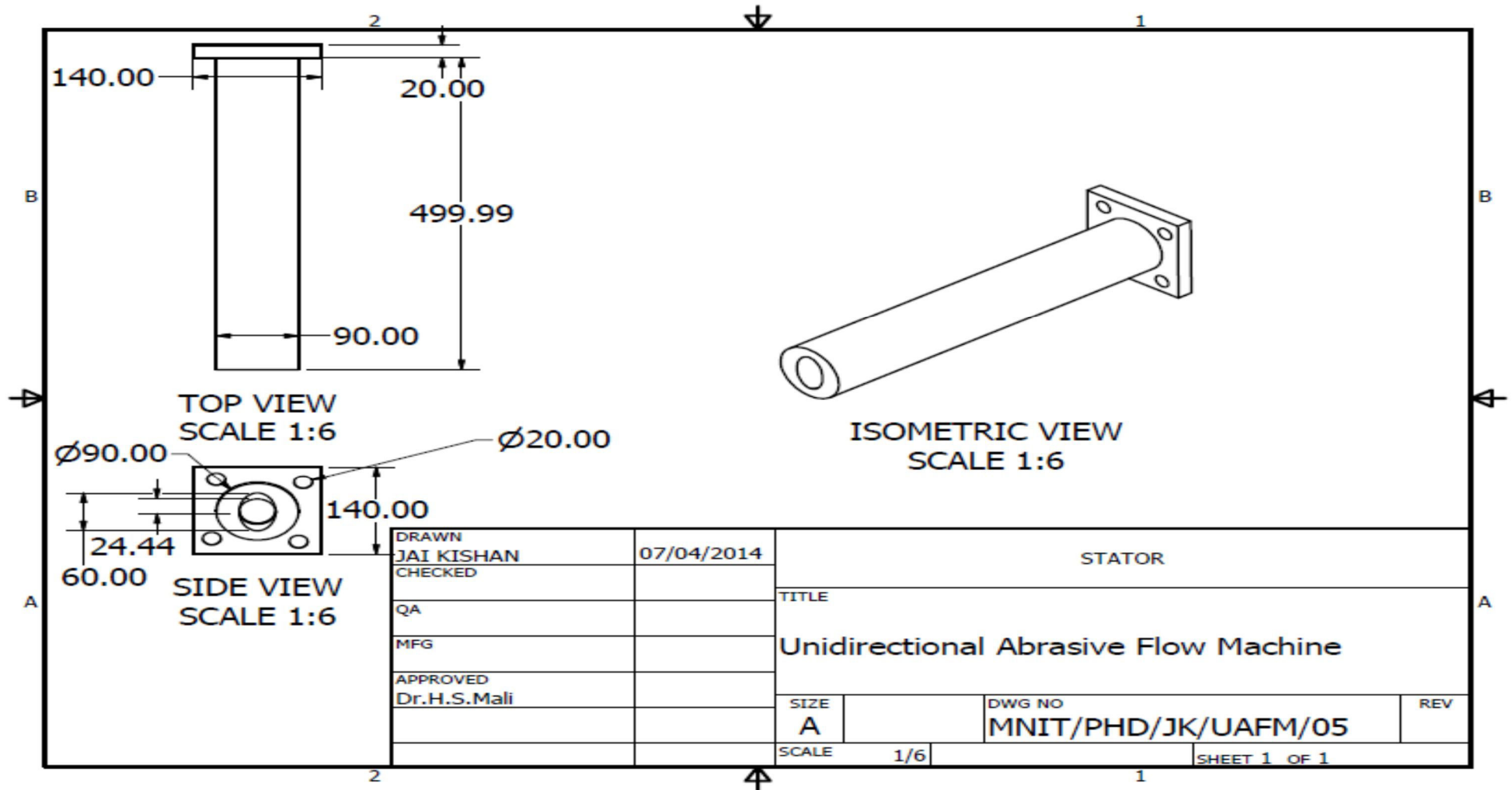
Appendix-B (6) Reducer



Appendix-B (7) Rotor



## Appendix-B (8) Stator



### **Appendix-C Design specification of UAFM system**

| Components | Details raw materials        | Mathematical relation used   | Calculated size  | Designed size  |
|------------|------------------------------|--|--|--|
| Stator     | Ethylene-Propylene<br>Rubber | For media flow rate $V_{th} = 3.195 \text{ m}^3/\text{hr}$<br>For maximum extrusion pressure = 3.2 MPa | Stator O.D.<br>88.9 mm<br>Stator I.D.<br>40.27 mm<br>Pitch of stator 500 mm  | Stator O.D.<br>91.44 mm<br>Stator I.D.<br>42.27 mm                           |
| Rotor      | Cr Ni-Steel 1.4301           | For media flow rate $V_{th} = 3.195 \text{ m}^3/\text{hr}$<br>For maximum extrusion pressure = 3.2 MPa | Rotor dia.<br>40.64 mm<br>Angular velocity- 285 rpm<br>Eccentricity- 2.46 mm | Rotor dia.<br>41.85 mm<br>Angular velocity- 285 rpm<br>Eccentricity- 2.52 mm |

|                            |                  |  |   |   |
|----------------------------|------------------|--|---|---|
| Media displacement element | Rotor and Stator | <p style="text-align: center;">Clearance (C) = <math>\frac{R_d - R_s}{2}</math></p> <p style="text-align: center;">Displacement D = <math>(4 \cdot e \cdot R_d - 8 \cdot e \cdot C - \pi(R_d \cdot C - C^2) + 2 \left\{ \frac{R_d^2}{4} \times \sin^{-1} \frac{2\sqrt{R_d C - C^2}}{R_d} - \sqrt{R_d C - C^2} \times \left( \frac{R_d}{2} - C \right) \right\})</math></p> <p>CASE (1) C &gt; 0</p> <p style="text-align: center;">Slip (s) = <math>V_{th} - V_{actual}</math></p> <p style="text-align: center;"><math>V_{th} = 3.195 \text{ m}^3/\text{hr}</math></p> <p>CASE (2) C &lt; 0</p> <p style="text-align: center;">Slip (s) = <math>V_{th} - V_{actual}</math></p> <p style="text-align: center;"><math>V_{th} = 3.186 \text{ m}^3/\text{hr}</math></p> | <p>Clearance<br/>0.185 mm</p> <p>D = <math>0.186878 \times 10^{-3} \text{ m}^3</math></p> <p>S = <math>0.255 \text{ m}^3/\text{hr}</math></p> <p>D = <math>0.186372 \times 10^{-3} \text{ m}^3</math></p> <p>S = <math>0.246 \text{ m}^3/\text{hr}</math></p> | <p style="text-align: center;">Clearance<br/>0.197 mm</p> |
|----------------------------|------------------|--|---|---|



## Appendix-D Viscosity grade and cost comparison

Table D.1 Grading of PAG media based on apparent viscosity for Taguchi orthogonal L<sub>9</sub> experiment.

| Sr. No. | Apparent Viscosity | Media Viscosity Grade |
|---------|--------------------|-----------------------|
| 1       | 50-100 pa-sec.     | L                     |
| 2       | 150-250 pa-sec.    | M                     |
| 3       | 250-300 pa-sec.    | H                     |

Table D.2 Grading of PAG media based on apparent viscosity for RSM experimental design.

| Sr. No. | Apparent Viscosity | Media Viscosity Grade |
|---------|--------------------|-----------------------|
| 1       | 50-100 pa-sec.     | L (-1)                |
| 2       | 150-250 pa-sec.    | M (0)                 |
| 3       | 250-300 pa-sec.    | H (1)                 |

Table D.3 Cost Comparison of Developed Polymer abrasive Gel and Commercial available AFM Media.

| Media Ingredients                                    | Polymer Abrasive Gel    | Commercial Available AFM Media   |
|--|-------------------------|--|
| Abrasive (50%) Aluminium oxide of 24 Grit Size       | \$42                    | Total cost of media for \$200 per 10 gallons, 24 Grit Aluminium Oxide in a Polymer Slurry (STUTZ Company, US). |
| Additive polymer base (50%)                          | \$23                    |  |
| Liquid synthesizer (3%)                              | \$2                     |  |
| Total cost of Developed Media (For 10 gallons media) | \$67 (Approximate cost) |  |



## Appendix-E TGA graphs for PAG samples

---

Sample 1

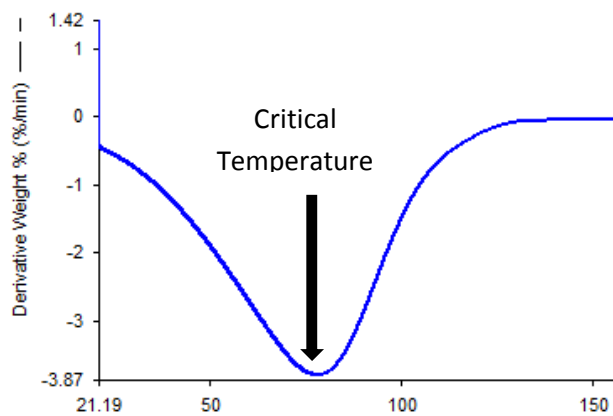


Figure E.1 TGA analysis for PAG 30SiC120-LS-11.

Sample 2

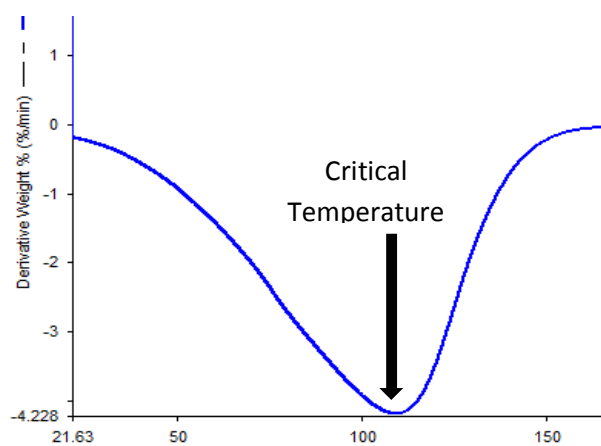


Figure E.2 TGA analysis for PAG 30SiC170-LS-15.

Sample 3

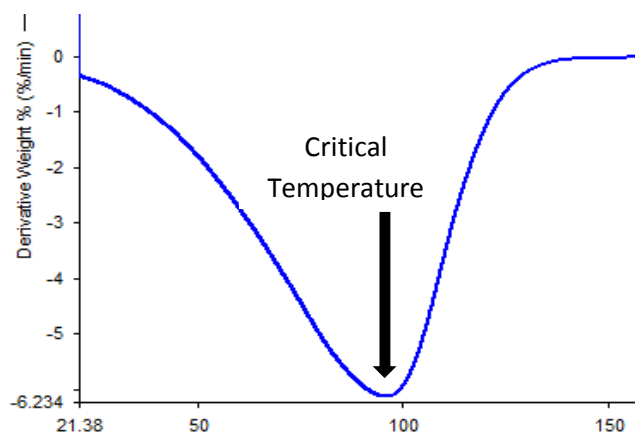


Figure E.3 TGA analysis for PAG 30SiC220-LS-19.

Sample 4

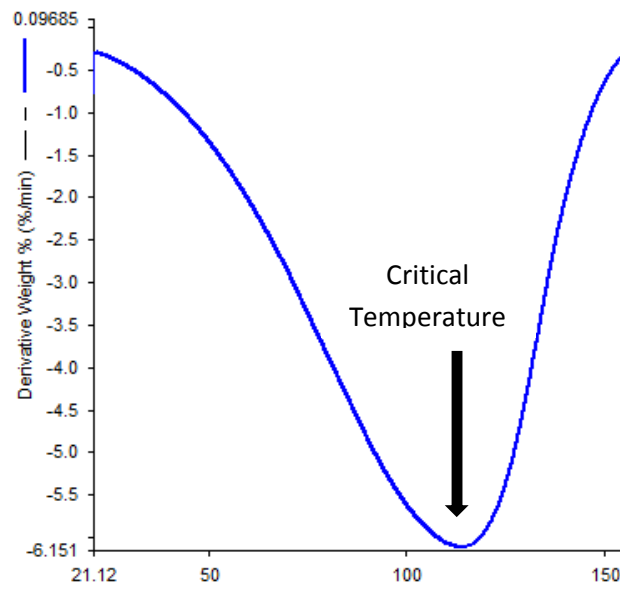


Figure E.4 TGA analysis for PAG 30SiC270-LS-23

Sample 5

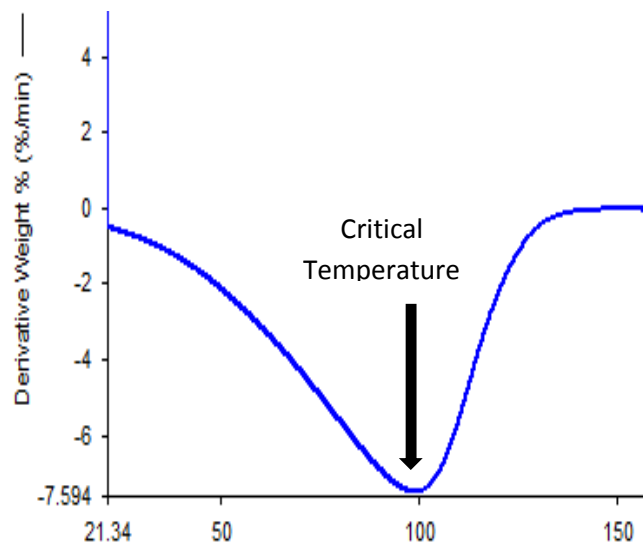


Figure E.5 TGA analysis for PAG 30SiC320-LS-27

Sample 6

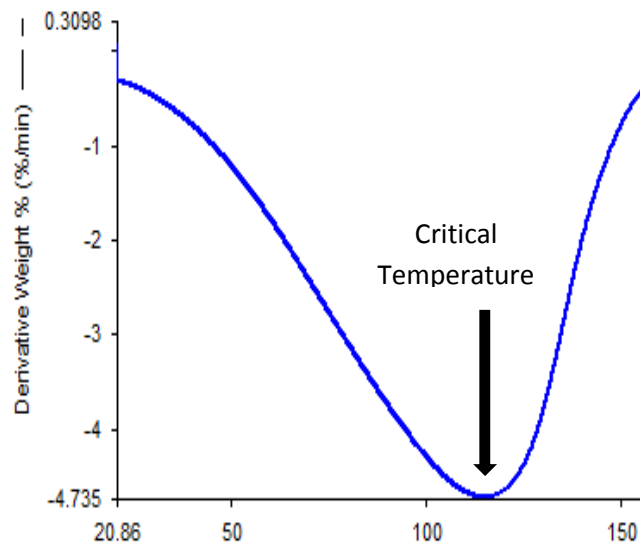


Figure E.6 TGA analysis for PAG 40SiC120-LS-15

Sample 7

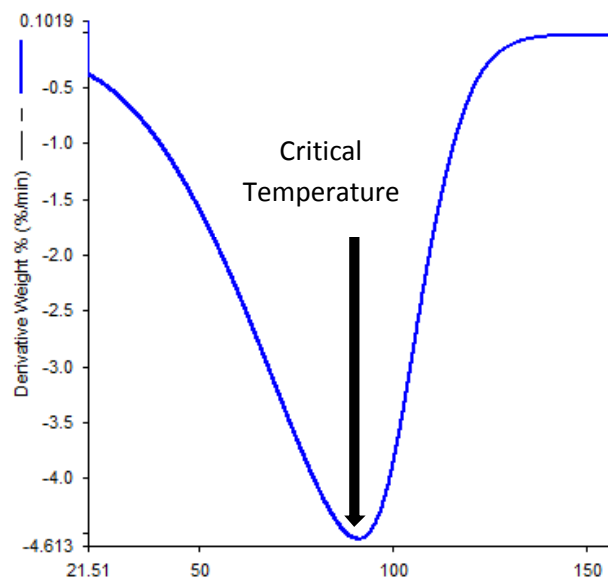


Figure E.7 TGA analysis for PAG 40SiC170-LS-19

Sample 8

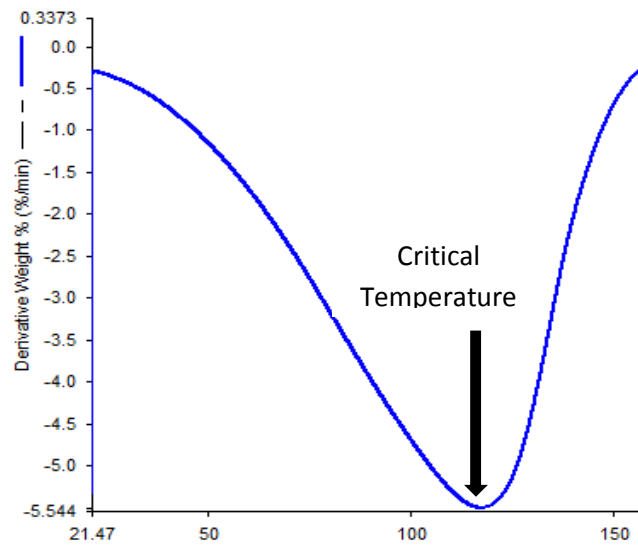


Figure E.8 TGA analysis for PAG 40SiC220-LS-23

Sample 9

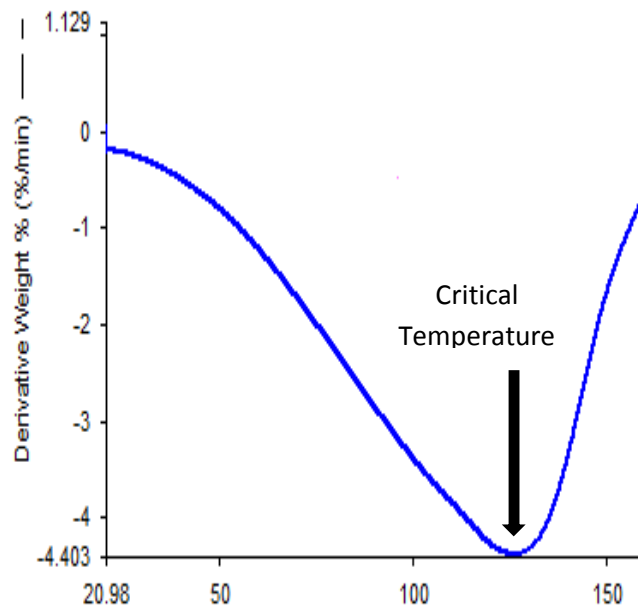


Figure E.9 TGA analysis for PAG 40SiC270-LS-27

Sample 10

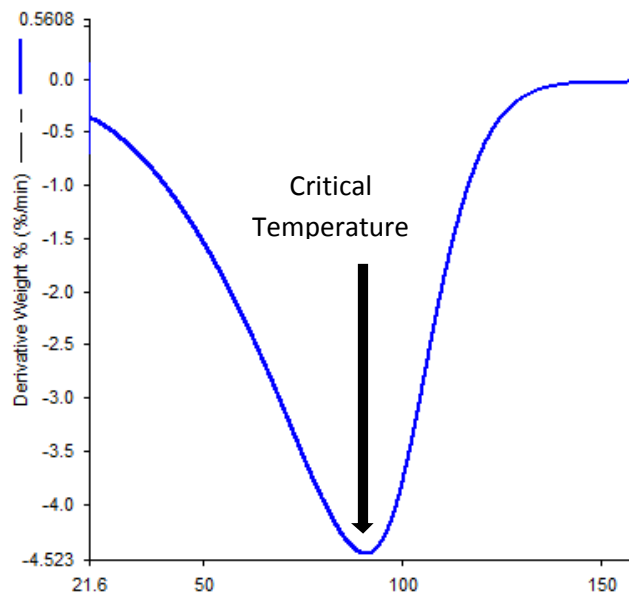


Figure E.10 TGA analysis for PAG 40SiC320-LS-11

Sample 11

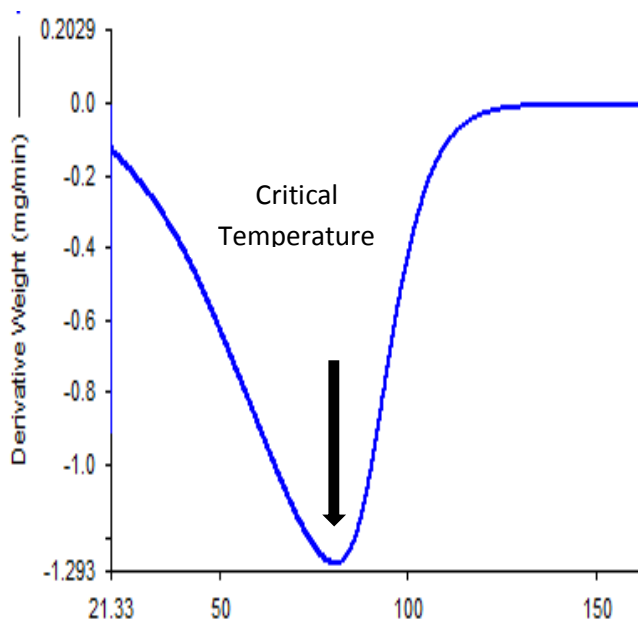


Figure E.11 TGA analysis for PAG 50SiC120-LS-19

Sample 12

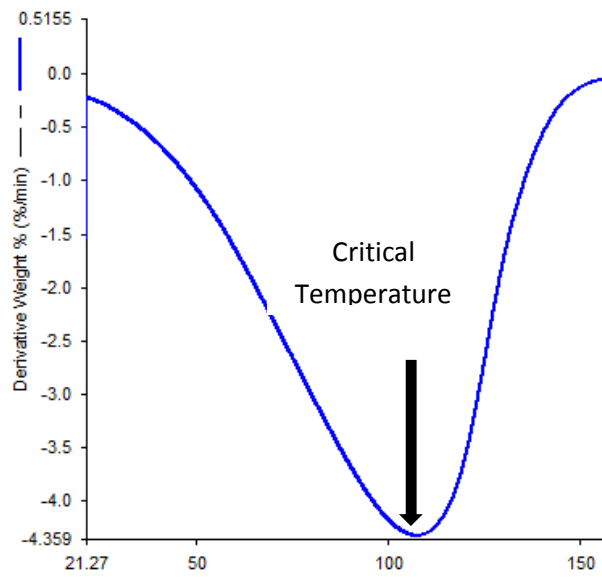


Figure E.12 TGA analysis for PAG 50SiC170-LS-23

Sample 13

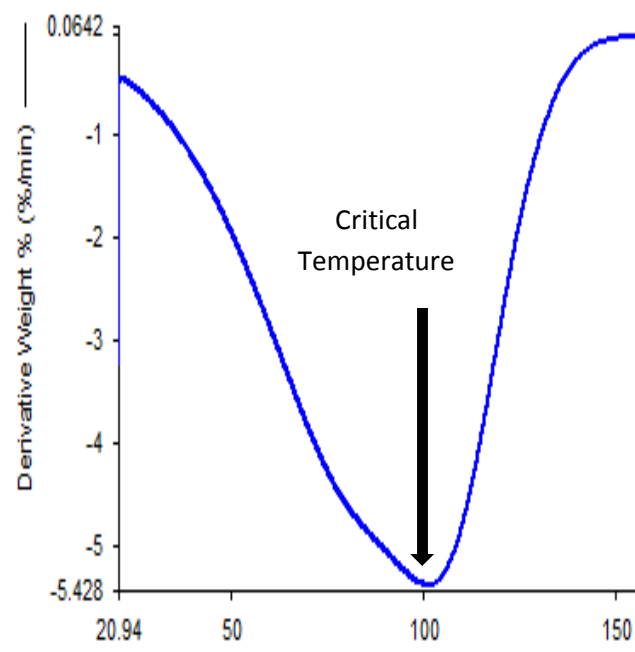


Figure E.13 TGA analysis for PAG 50SiC220-LS-27



Sample 14

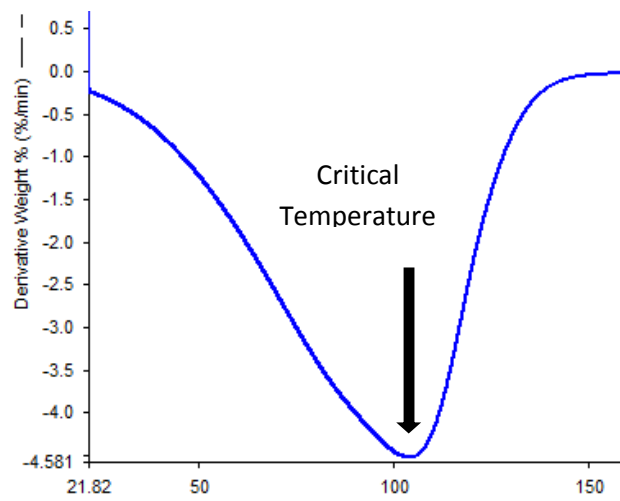


Figure E.14 TGA analysis for PAG 50SiC270-LS-11

Sample 15

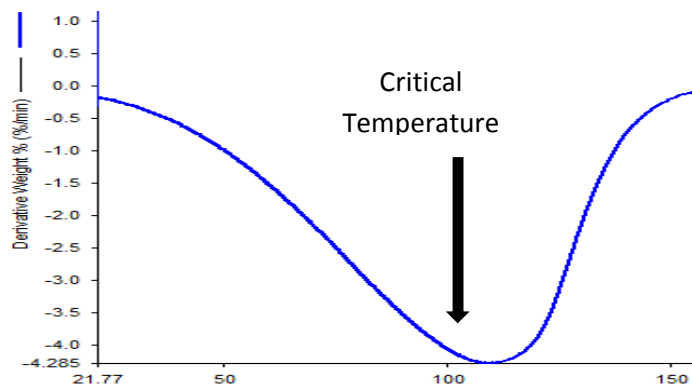


Figure E.15 TGA analysis for PAG 50SiC320-LS-15

Sample 16

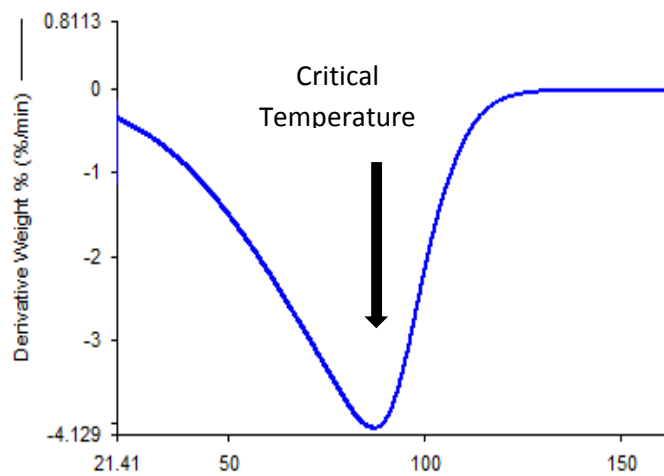


Figure E.16 TGA analysis for PAG 60SiC120-LS-23

Sample 17

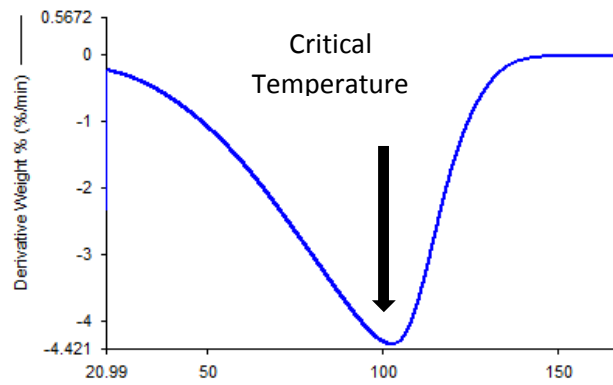


Figure E.17 TGA analysis for PAG 60SiC170-LS-27

Sample 18

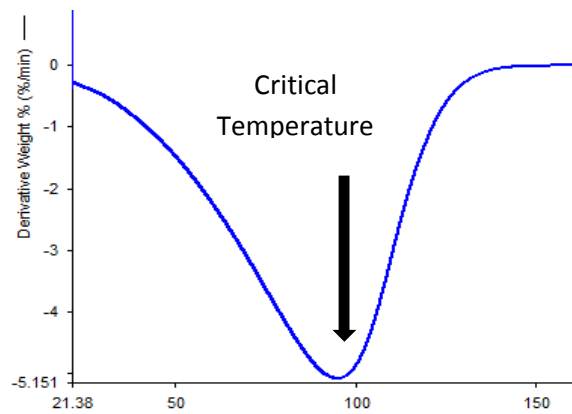


Figure E.18 TGA analysis for PAG 60SiC220-LS-11

Sample 19

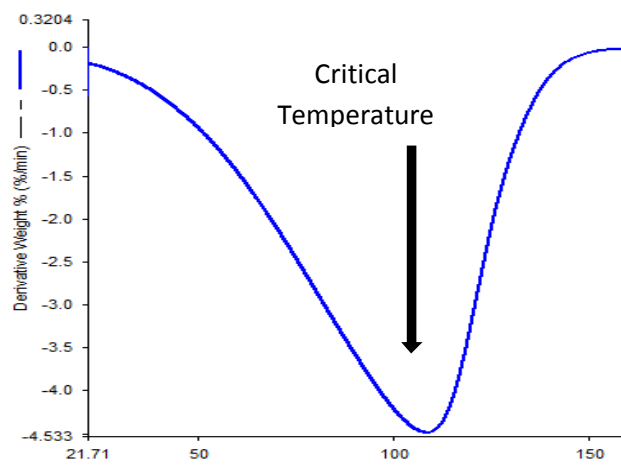


Figure E.19 TGA analysis for PAG 60SiC270-LS-15

Sample 20

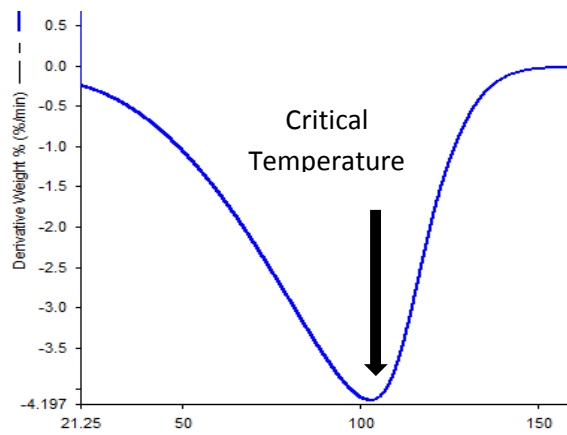


Figure E.20 TGA analysis for PAG 60SiC320-LS-19

Sample 21

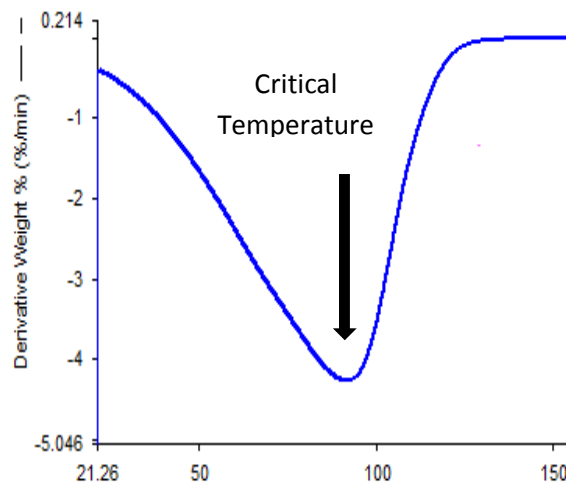


Figure E.21 TGA analysis for PAG 70SiC120-LS-27

Sample 22

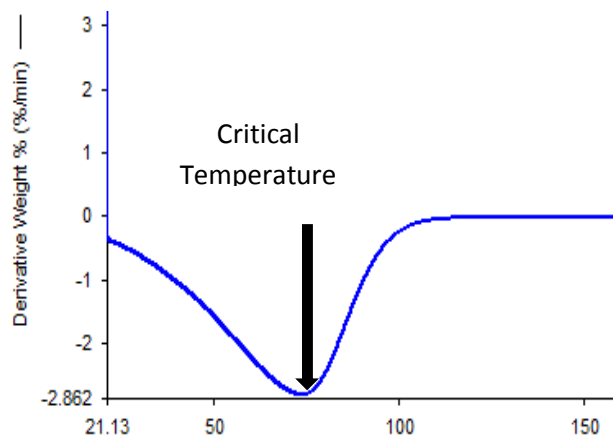


Figure E.22 TGA analysis for PAG 70SiC170-LS-11

Sample 23

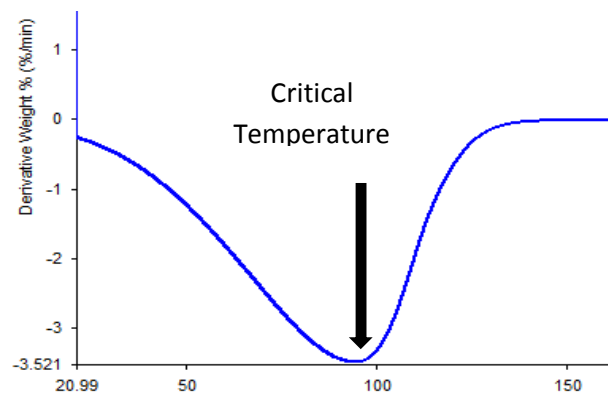


Figure E.23 TGA analysis for PAG 70SiC220-LS-15

Sample 24

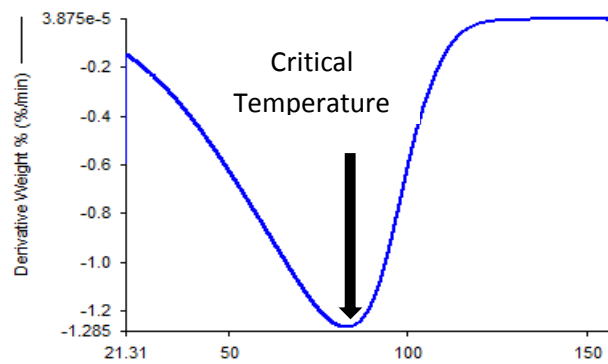


Figure E.24 TGA analysis for PAG 70SiC270-LS-19

Sample 25

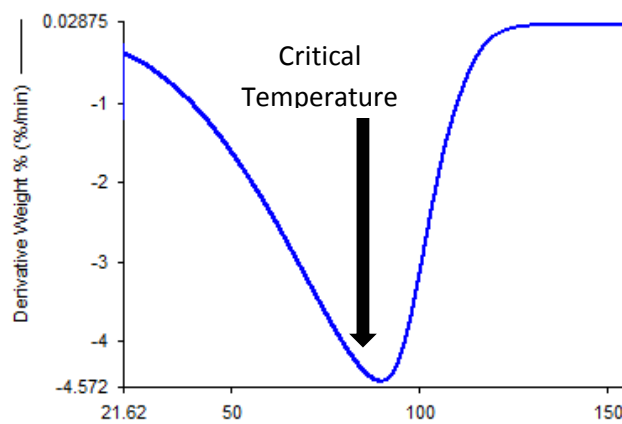
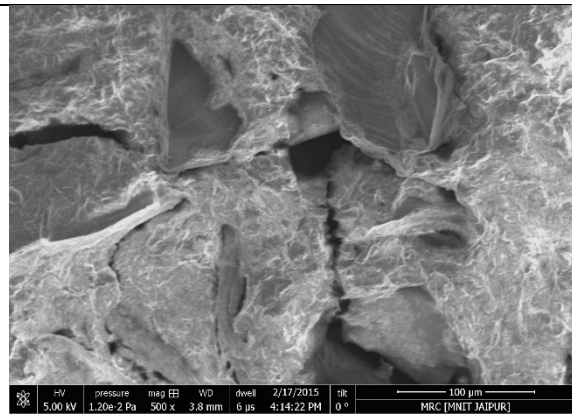
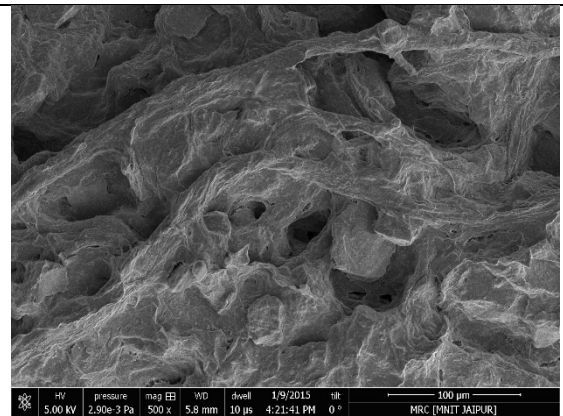


Figure E.25 TGA analysis for PAG 70SiC320-LS-23.

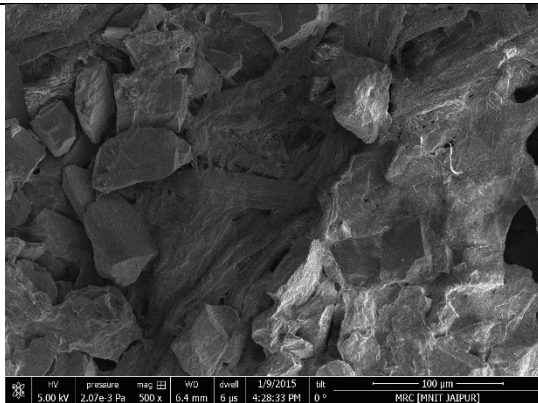
## Appendix-F SEM images of PAG samples



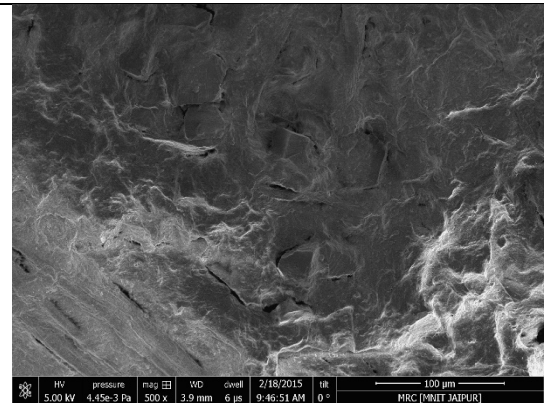
PAG-30SiC120-LS-11



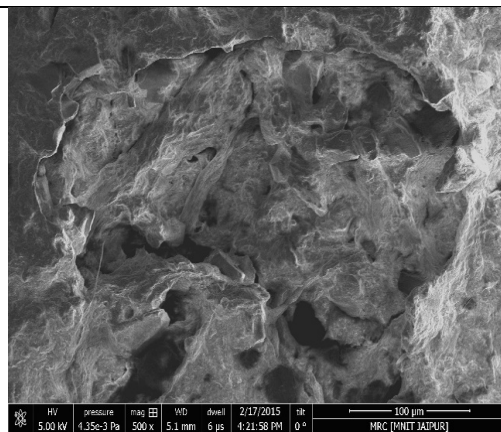
PAG-30SiC170-LS-15



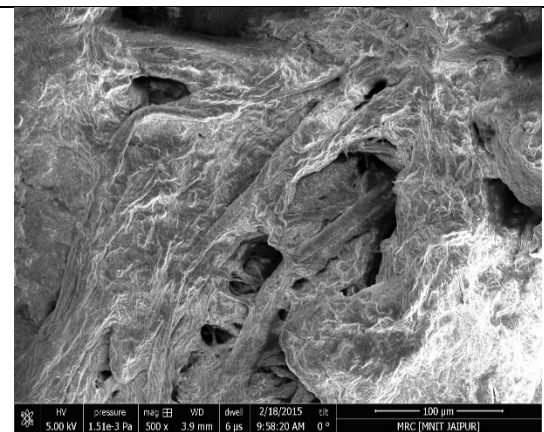
PAG-30SiC220-LS-19



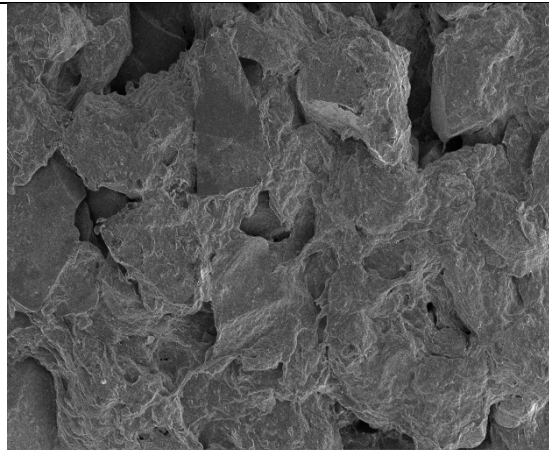
PAG-30SiC270-LS-23



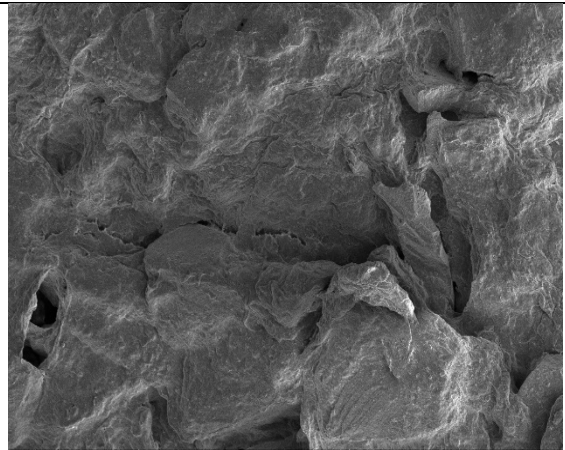
PAG-30SiC320-LS-27



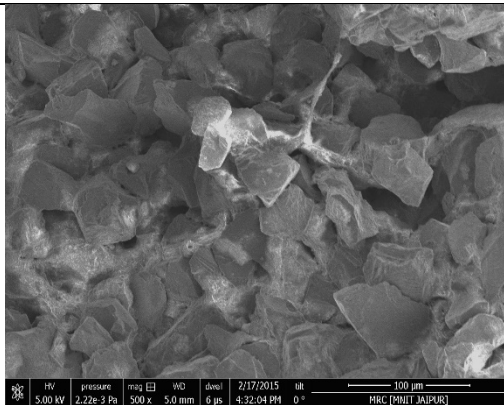
PAG-40SiC120-LS-15



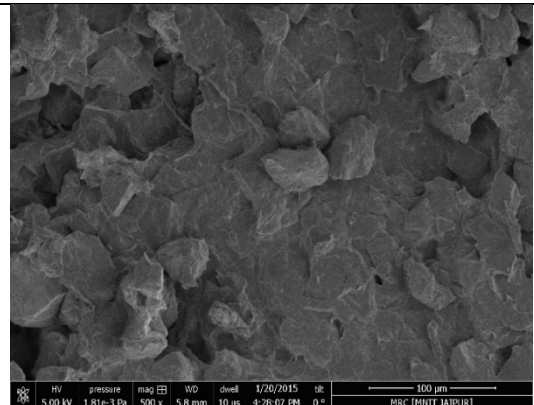
PAG-40SiC170-LS-19



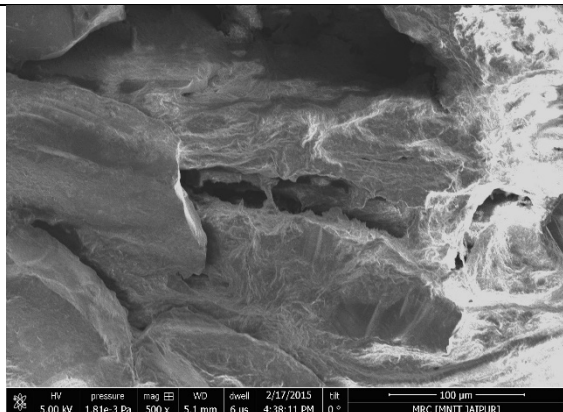
PAG-40SiC220-LS-23



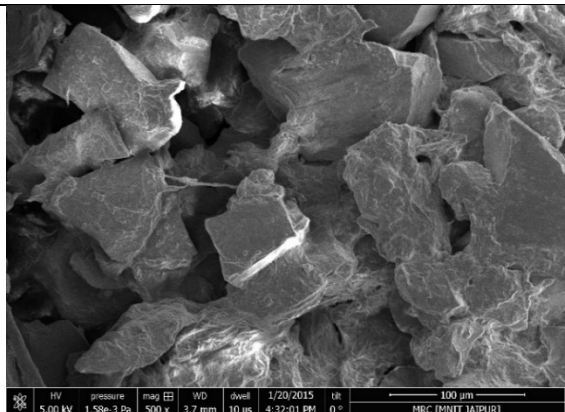
PAG-40SiC270-LS-27



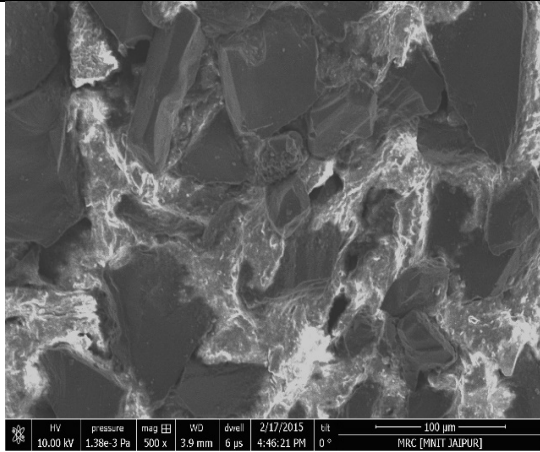
PAG-40SiC320-LS-11



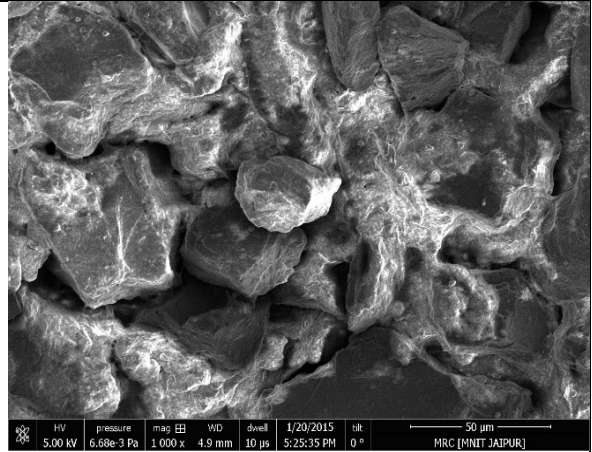
PAG-50SiC120-LS-19



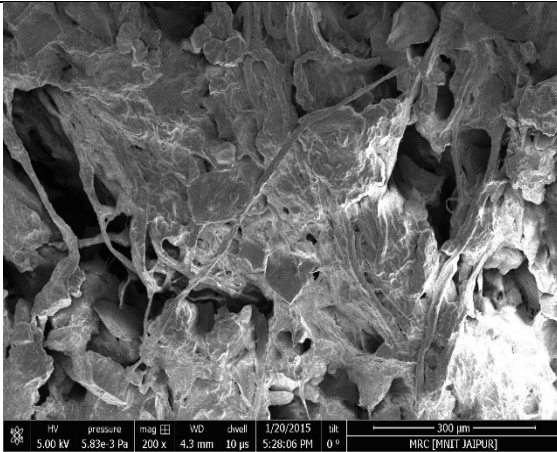
PAG-50SiC170-LS-23



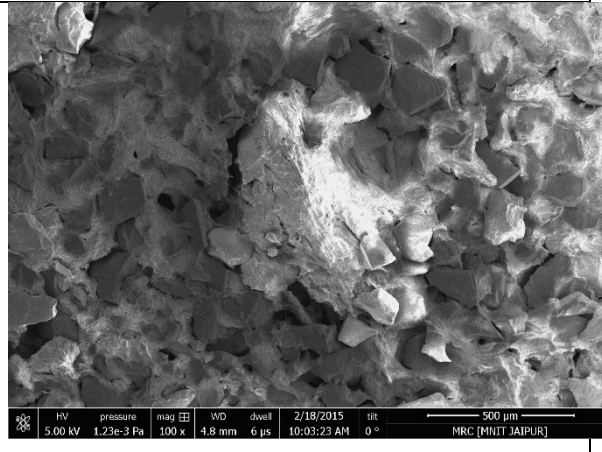
PAG-50SiC220-LS-27



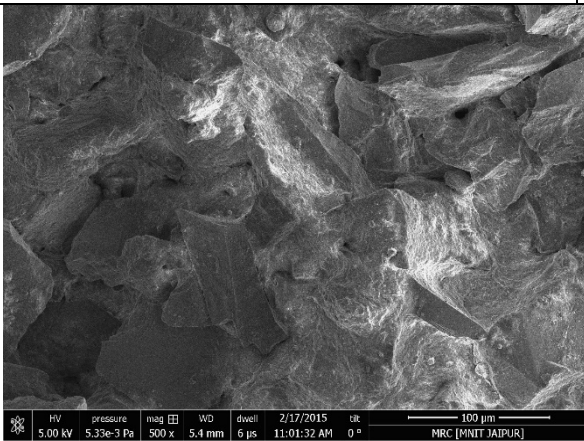
PAG-50SiC270-LS-11



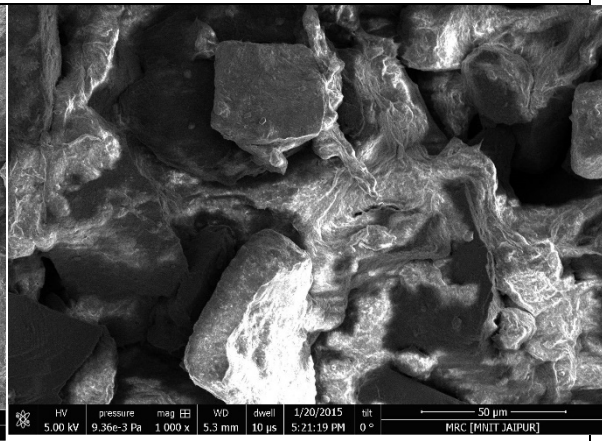
PAG-50SiC320-LS-15



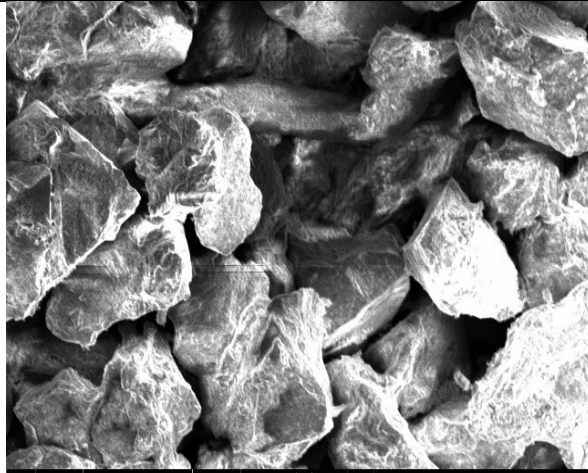
PAG-60SiC120-LS-23



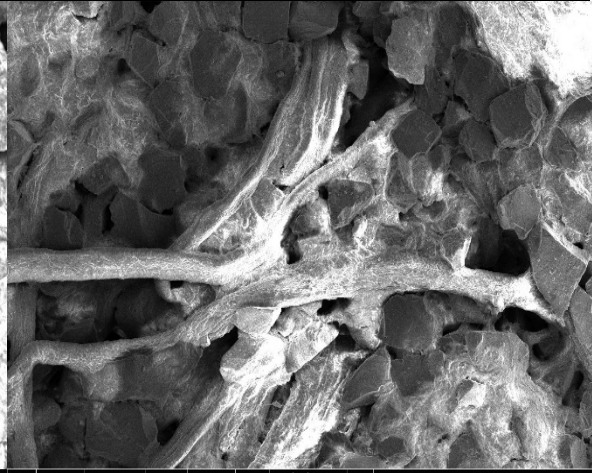
PAG-60SiC170-LS-27



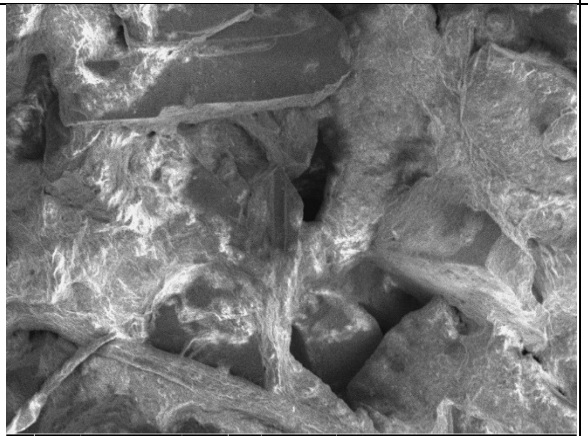
PAG-60SiC220-LS-11



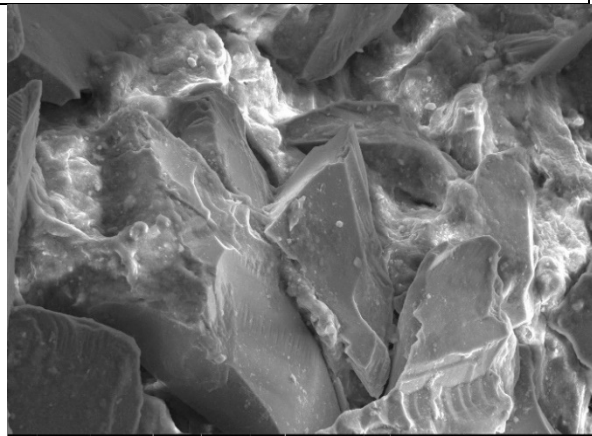
PAG-60SiC270-LS-15



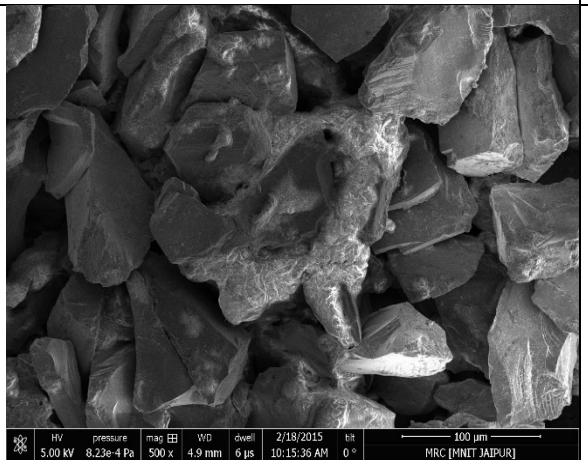
PAG-60SiC320-LS-19



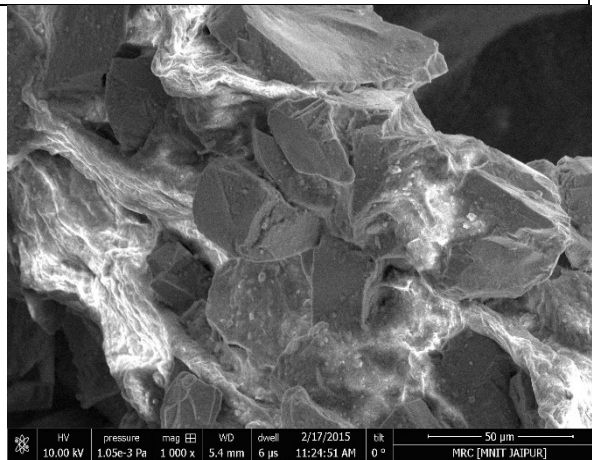
PAG-70SiC120-LS-27



PAG-70SiC170-LS-11

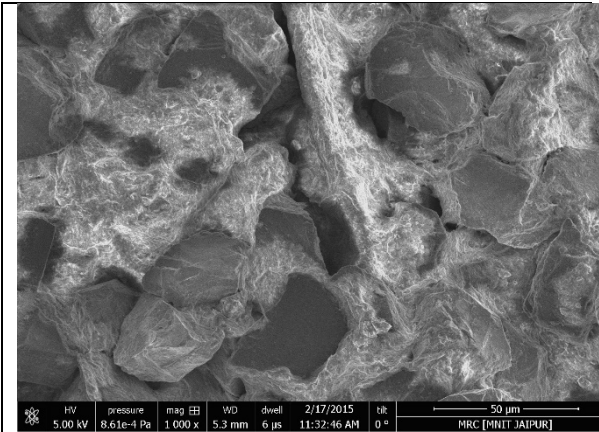


PAG-70SiC220-LS-15



PAG-70SiC270-LS-19





PAG-70SiC320-LS-23



## Appendix-G Experiments on MUAFM

### Experiments on Micro unidirectional abrasive flow machine

This research is mainly aimed to experimental investigation about abrasive flow machining of internal surface of wire drawing die by different technological parameters of abrasive concentration, percentage of liquid synthesizer, speed, extrusion pressure, and cycle time.

#### G.1 Design of experiment

Table G.1 Control factors with their levels.

| Factor                   | Level 1 | Level 2 | Level 3 | Level 5 | Level 5 |
|--------------------------|---------|---------|---------|---------|---------|
| % Abrasive Concentration | 30      | 40      | 50      | 60      | 70      |
| % Liquid Synthesizer     | 15      | 25      | 35      | 45      | 55      |
| Speed (rpm)              | 50      | 60      | 70      | 80      | 90      |
| Extrusion Pressure(bar)  | 3       | 5       | 7       | 9       | 11      |
| Cycle Time (minute)      | 5       | 7       | 9       | 11      | 13      |

The effects of variation in abrasive concentration, percentage of liquid synthesizer, speed, extrusion pressure, and cycle time (Table G.1) are studied on average surface roughness (Ra value).

A wire drawing die of tungsten carbide material has been selected for finishing using the fabricated MUAFM setup. Initially the surface roughness (Ra) is measured at five randomly selected positions in the central area (A) to get an average surface roughness. Taylor Hobson surface analyzer is used for measuring the average surface roughness (Ra) value before and after finishing the work piece.

Change in Ra value is defined as:

$$\text{Change in Ra } (\Delta R_a) = \text{Initial } R_a - \text{Final } R_a$$

For finishing the wire drawing die, CBN abrasives are used in polymer abrasive gel media. Major constituents of media are polymer base, abrasive particle and liquid synthesizer. The mixture of polymer base and gel is mixed with abrasive particles in certain proportion to attain the desired percentage concentration by weight. The weight percentage of an ingredient is evaluated as:

$$\text{Weight percentage of an ingredient} = \frac{\text{Weight of ingredient}}{\text{total weight of media}} \times 100 \quad \dots(G.1)$$

The liquid synthesizer percentage content is varied from 15% to 55% and abrasive concentration is varied from 30% to 70%. Synthesis process of polymer abrasive gel is already explained in chapter 3.

## G.2 Results and discussion

For finishing, the wire drawing die component is fixed in two half tooling and fixture unit as shown in Figure 4.6. The experiments are conducted for observing the effect of finishing variables on change in surface roughness value.

### G.2.1 Surface roughness

**Effects of abrasive concentration on change in surface roughness:**

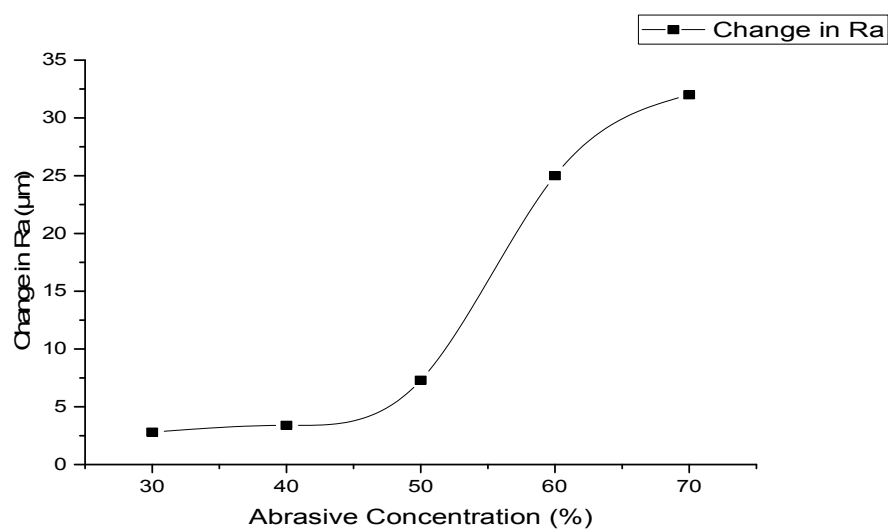


Figure G.1 Effect of percentage in abrasive concentration on change in surface roughness

Ra.

Figure G.1 shows the effect of abrasive concentration on change in surface roughness at 9 minute cycle time, 35% liquid synthesizer, 220 abrasive mesh size and 70 rpm speed. For 50% increase in abrasive concentration, the improvement in Ra is very low. But there is rapid improvement in Ra after 50% weight percentage abrasive concentration due to higher abrasive concentration, more abrasive grains come in contact with the workpiece finishing surface resulting in more abrasion, hence higher change in Ra.

### Effect of extrusion pressure on change in surface roughness

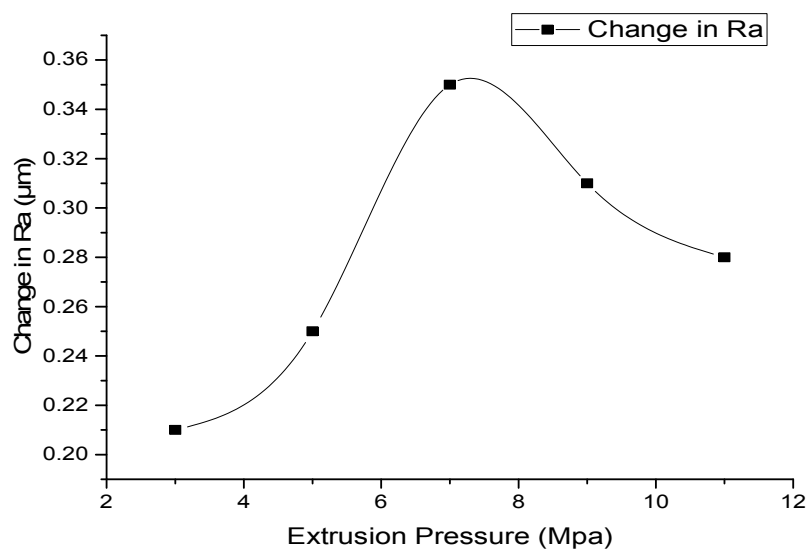


Figure G.2 Effect of extrusion pressure on change in roughness (Ra)

Figure G.2 shows the effects of extrusion pressure on change in surface roughness at cycle time 9 minute, liquid synthesizer 35%, abrasive concentration 50 %, abrasive mesh size 220 and speed 70 rpm. Results show that as the extrusion pressure increases from 3 to 7 bar, change in surface roughness will increase, due to increase in axial force ( $F_a$ ) and radial force ( $F_r$ ), so the shearing of peaks increases up to certain level of extrusion pressure (7 bar). After further increase in extrusion pressure, abrasive particles start indenting along with shearing of surface peaks that results in decrease in change in Ra value.

### Effect of increase in percentage liquid synthesizer on change in surface roughness.

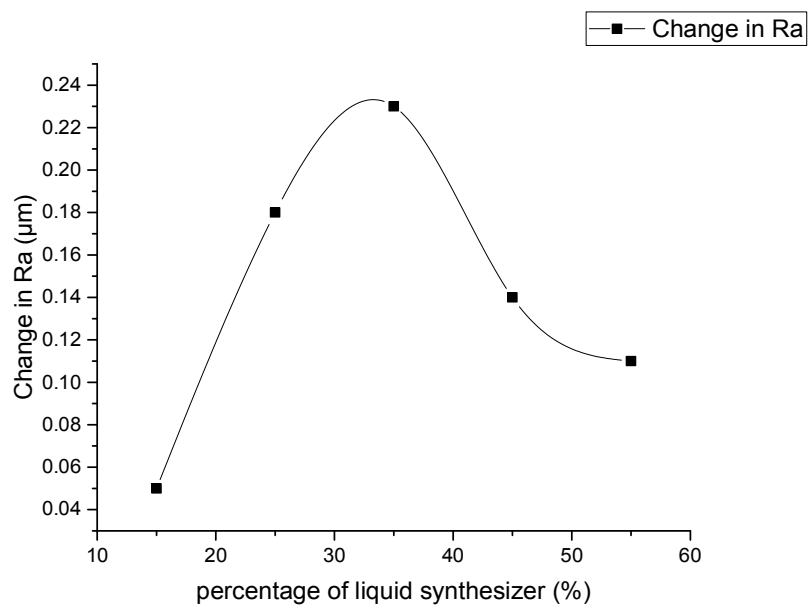
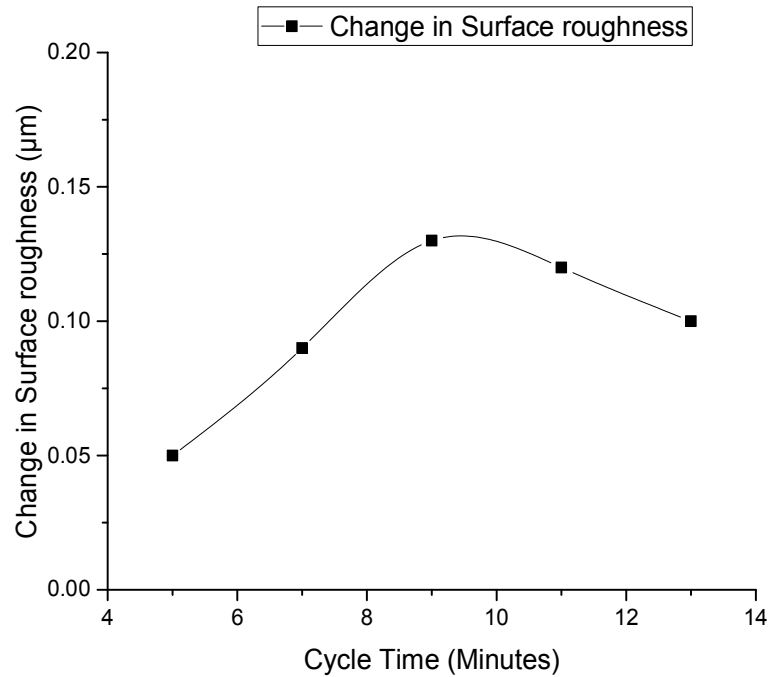


Figure G.3 Effect of percentage of liquid synthesizer on change of surface roughness.

Figure G.3 shows the effect of percentage increase in liquid synthesizer on change in surface roughness. In this experimentation, AFM medium properties are varied by changing the synthesized processing oil content (i.e., 15-55 %) while abrasive concentration (50wt%), abrasive mesh size (#220), extrusion pressure (7 bar), speed (70 rpm) and cycle time (9 minutes) are kept constant. As the liquid synthesizer in abrasive media increases, there will increase in change in Ra up to some extent because of increase in bonding strength in abrasive and polymer base. During finishing process, polymer base will provide strength to active abrasive particle that will shear off the peaks of surface of work piece to be finished. So surface roughness will improves with increase in percentage of liquid synthesizer. But when quantity of liquid synthesizer increases, the quantity of polymer base will decrease. So abrasive bonding capability of polymer base will decreased which results in decrease in improvement in surface roughness.

### Effect of cycle time on change in surface roughness (Ra)



**Figure G.4 Effect of cycle time on change of surface roughness**

Figure G.4 shows the effect of increase in cycle time on change in surface roughness. During experimentation, cycle time is varied as per the design of experiment table (from 5 to 13 minutes) and extrusion pressure 7 bar is used to see the effect on change in surface roughness Ra. Change in Ra varies nonlinearly with increase in cycle time, As the cycle time increases, times period of contact of the abrasive present in media increases with the workpiece increases, so the Ra increases.

## Effect of flow rate on change in surface roughness

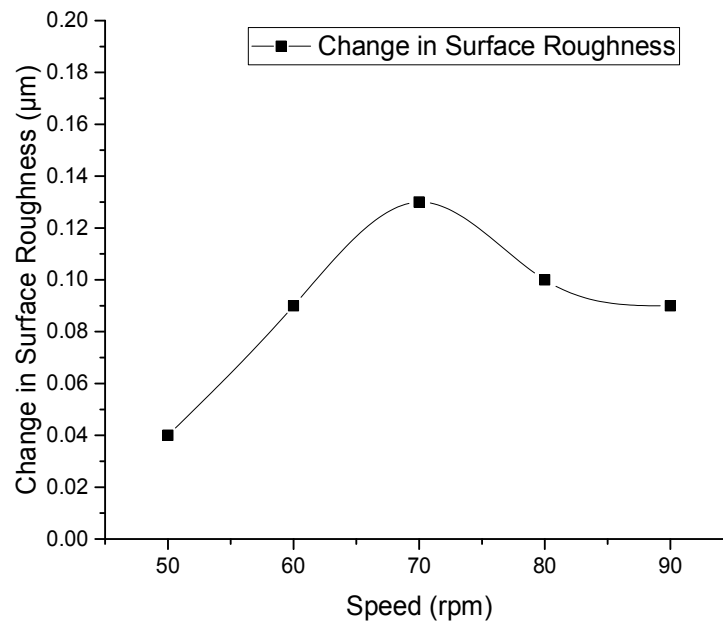


Figure G.5 Effect of flow rate on change in surface roughness (Ra)

Figure G.5 shows that change in surface roughness increase as the speed (rpm) of machine increases from 50 to 70 after that it will decrease till 90 rpm. As the rpm increases, rubbing speed also increase which results in improvement in surface finishing. Due to increase in rubbing speed the abrasive particle present in media will high axial and radial force on the surface of work piece that is to be finished.

### G.3 Conclusion

In this study an experimental setup for finishing wire drawing die, micro unidirectional abrasive flow machining (MUAFM) has been designed and fabricated. Experiments are performed to study the effects of different machining variables on change in surface roughness. The following conclusions are drawn:

1. Designed and fabricated MUAFM setup is used for finishing tungsten carbide wire drawing die using highly stiffed media with CBN abrasives. The finished component



shows the significant surface improvement in average surface roughness ( $R_a$ ). Sudden improvement in surface roughness is observed when abrasive concentration increases 50 to 70.

2. Higher extrusion pressure leads to faster the improvement in surface roughness.
3. During finishing best surface finish is observed at 35% liquid synthesizer in abrasive media used for finishing.
4. During finishing it is observed that as the cycle times increases,  $\Delta R_a$  increases.



## Appendix H Results for Modelling and Validation

---

**Table H.1 Parametric level setting as per L<sub>9</sub> orthogonal array with experimental and theoretical outcome for surface roughness**

| Sr. No. | Ext. Pressure<br>(bar) | Finishing Time<br>(Minutes) | Viscosity<br>(Pa-sec.) | SR(Ra)<br>μm | MR(mg) |
|---------|------------------------|-----------------------------|------------------------|--------------|--------|
| 1       | 12                     | 30                          | L                      | 0.3          | 5.25   |
| 2       | 12                     | 40                          | M                      | 0.32         | 7.55   |
| 3       | 12                     | 50                          | H                      | 0.35         | 8.75   |
| 4       | 22                     | 30                          | M                      | 0.34         | 8.95   |
| 5       | 22                     | 40                          | H                      | 0.39         | 9.68   |
| 6       | 22                     | 50                          | L                      | 0.37         | 8.35   |
| 7       | 32                     | 30                          | H                      | 0.38         | 11.12  |
| 8       | 32                     | 40                          | L                      | 0.39         | 11.22  |
| 9       | 32                     | 50                          | M                      | 0.42         | 12.25  |



## List of the publications based on this research

---

### Patent:

1. Jai Kishan Sambharia, Jitendra Kumar, Dr. Harlal Singh Mali, "Design of a System for Finishing Complicated Workpiece(s) using Abrasive Laden Base Material", No. 201611008902.

### Consultancies:

1. 3D printer Nozzles Finishing (Aha 3D Innovations Pvt Ltd. Jaipur) Duration: 11.06.2016 to 23.07.2016.
2. Glass Mold Finishing (Piramal Glass Ltd, Gujrat) Duration: 20.06.2016 to 26.11.2016.

### International Journals:

1. Sambharia J., Mali, H.S. (2017) "Recent Developments in Abrasive Flow Finishing Process-A Review of Current Research and Future Prospects", Proceedings of the Institution of Mechanical Engineers, Part B: Journal of Engineering Manufacture, SAGE. **(SCI-Indexed) Accepted**.
2. Sambharia J., Mali, H.S. (2017) "Experimental Investigation into Unidirectional Abrasive Flow Machining of Trim Die", Materials and Manufacturing Processes, **Springer (SCI-Indexed)**, doi.org/10.1080/10426914.2017.1364847.
3. Sambharia J., Mali, H.S. (2015) "Characterization and Performance Evaluation of Developed Alternative Polymer Abrasive Gels for Abrasive Flow Finishing Process", International Journal of Precision Technology, 2015, Vol.5, No.3/4, pp. 185-200. Inderscience **(Peer Reviewed, Scopus)**.
4. Sambharia J., Mali, H.S. (2017) "Characterization and Optimization of Rheological Parameters of Developed Alternative Polymer Abrasive Gels for Abrasive Flow Machine", Journal of Materials Science and Surface Engineering **(Peer Reviewed, Scopus)**, Vol 5(3), 549-555.

### International Conferences:

1. Mali, HS, Jai Kishan (2014) "Developing Alternative Polymer Abrasive Gels for Abrasive Flow Finishing Process", 5th International & 26th All India Manufacturing Technology, Design and Research **(AIMTDR 2014) at IIT Guwahati**, India, 12-14th Dec. 2014.
2. Sambharia, J. Mali, H., Ram, J. (2015) "Rheological Investigation and Comparative Study on Synthesized Low Cost Consumables for Abrasive Flow Finishing Processes", International Conference on Precision, Meso, Micro and Nano Engineering **(COPEN-9) at IIT Bombay**, India, 10-12 Dec. 2015.
3. Sambharia, J., Mali, H. (2016) "Performance study of Developed Alternative Polymer Abrasive Gel and Commercial Media in Abrasive Flow Machining", 6th International & 27th All India Manufacturing Technology, Design and Research **(AIMTDR 2016) at COEP Pune**, India, 16-18 Dec 2016.
4. Sambharia, J., Gupta G., Mali, H. S. (2017) "Fine finishing of glass mold surfaces using low cost Unidirectional Abrasive Flow Machine", International Conference on Precision, Meso, Micro and Nano Engineering **(COPEN-10), 2017 (Accepted)**
5. Sambharia, J., Garg, V., Mali, H. S. (2017) "Experimental investigation on finishing of 3D printer nozzle using Unidirectional Abrasive Flow Machine",

International Conference on Precision, Meso, Micro and Nano Engineering (COPEN-10), 2017 (Accepted).

**National Conference:**

1. Jai Kishan, Mali, HS “Abrasive Flow Finishing Process – A sustainability Study”, Proceeding of National Conference on Sustainable Manufacturing (NCSM-2015) 2-3 Jan. 2015 at MNIT Jaipur, India.

**Brief bio-data of the author**

Mr. Jai Kishan, born on 14<sup>th</sup> Feb 1989, completed bachelors’ degree in Mechanical Engineering with first class with distinction from SITM, Rewari, Haryana, India and post graduate degree in Mechanical Engineering with first class from S.V. National Institute of Technology, Surat, Gujrat, India

Since Jan. 2013, he has been engaged in his Doctoral research in the area of Abrasive Flow Finishing Process, at Mechanical Engineering Department, Malaviya National Institute of Technology Jaipur, Rajasthan, India under the Institute Research Fellowship scheme by Ministry of Human Resource Development, Government of India. He has two research papers published in SCI indexed Journal and two papers in peer reviewed and Scopus journals and presented three research papers in international conferences in reputed institutes. He has one patent filed/published (current status is awaiting for examination) to his credit.